Michigan State University
Pavement Research Center of Excellence

Evaluation of MDOT's Long-Life Pilot Projects

RC-1722

FINAL REPORT

Michigan State University
Department of Civil and Environmental Engineering
428 S. Shaw Lane, 3546 Engineering Building, East Lansing, MI 48824

Hamad Muslim
Research Assistant
Michigan State University
muslimha@msu.edu

Mahdi Ghazavi
Research Assistant
Michigan State University
ghazavim@msu.edu

Muhammed Emin Kutay, PhD, PE (PI)
Professor
Michigan State University
kutay@egr.msu.edu

Syed Waqar Haider, PhD, PE (Co-PI)
Associate Professor
Michigan State University
syedwaqa@egr.msu.edu

Bora Cetin, PhD
Associate Professor
Michigan State University
cetinbor@msu.edu

Celso Santos
Research Assistant
Michigan State University
santosce@msu.edu

Neeraj Buch, PhD
Chairperson & Professor
Michigan State University
buch@egr.msu.edu

Will Hansen, PhD
Professor
University of Michigan
whansen@umich.edu

Haluk Sinan Coban, PhD, EIT
Research Associate
Michigan State University
cobanhal@msu.edu

Mike Lanotte, PhD
Assistant Professor
Michigan State University
mlanotte@egr.msu.edu

April 19, 2023

TECHNICAL REPORT DOCUMENTATION PAGE

1. Report No.	2. Government Accession No.	3. Recipient's Catalog No.
SPR - 1722	N/A	N/A

4. Title and Subtitle	5. Report Date
Evaluation of MDOT's Long-Life Pilot Projects	April 3, 2023
	6. Performing Organization Code N/A

7. Author(s)	8. Performing Organization Report No.
Hamad Muslim, Mahdi Ghazavi, M. Emin Kutay, Syed W. Haider, Bora Cetin, Celso Santos, Neeraj Buch, Will Hansen, Haluk S. Coban and Mike Lanotte.	N/A

9. Performing Organization Name and Address	10. Work Unit No.
Michigan State University Department of Civil and Environmental Engineering 228 S Shaw Lane, 3546 Engineering Building East Lansing, Michigan 48824	N/A
	11. Contract or Grant No. Contract 2019-0997

12. Sponsoring Agency Name and Address	13. Type of Report and Period Covered
Michigan Department of Transportation (MDOT) Research Administration 8885 Ricks Road P.O. Box 33049 Lansing, Michigan 48909	Final Report, 10/25/2019 - 12/31/2022
	14. Sponsoring Agency Code N/A

15. Supplementary Notes

Conducted in cooperation with the U.S. Department of Transportation, Federal Highway Administration. MDOT research reports are available at www.michigan.gov/mdotresearch.

16. Abstract

In Michigan, four pilot long-life pavement sections were constructed between 2017 and 2019; two rigid and two flexible pavements. Each pilot project included a long-life and an accompanying standard (control) section constructed on the same highway. Modifications to standard designs and materials were made to extend their service life. The scope of this project included as-built evaluation of these pilot long-life projects to determine their potential for meeting the intended design and service lives. MDOT performed numerous field tests and collected material samples from these projects. The project team performed extensive analyses of the field data and run numerous laboratory tests to characterize the material properties. As-constructed material properties were used in different mechanistic-empirical (ME) design software to estimate the expected performance of all the pilot projects. Based on the detailed laboratory and field testing and the mechanistic-empirical performance predictions, recommendations were made in structural design, material selection, construction, and quality control and quality assurance procedures.

17. Key Words	18. Distribution Statement
Long life pavements, perpetual pavements, flexible and rigid pavements, mechanistic-empirical pavement design	No restrictions. This document is also available to the public through the Michigan Department of Transportation.

19. Security Classif. (of this report)	20. Security Classif. (of this page)	21. No. of Pages	22. Price
Unclassified	Unclassified	146	N/A

Form DOT F 1700.7 (8-72) Reproduction of completed page authorized

TABLE OF CONTENTS

INTRODUCTION

The concept of perpetual or long-life pavements has been introduced in the USA and Europe in the last few decades [1-4]. Such roadways are defined as flexible or rigid pavement designed and built to last longer than 50 years without needing major structural rehabilitation or reconstruction and requiring only periodic surface renewal in response to distresses of the top surface. It is also recognized that many well-built and thick pavements categorized as to either 'full-depth' or 'deep-strength' had been in service for decades with only minor periodic surface rehabilitation to remove defects and improve ride quality. Therefore, it is reasonable to consider the long-life pavement concept, with primary advantages including [4-8]: (i) low life-cycle cost by avoiding deep pavement repairs or reconstruction, (ii) less frequent repair and rehabilitation and contribution to highway safety and congestion mitigation, (iii) low user-delay costs since minor surface rehabilitation of pavements only require short work windows that can avoid peak traffic hours, (iv) low environmental impact by reducing the construction materials amount over the pavement's life, (v) more relevance to a public-private partnership (PPP) because the longtime commitment typically favors the use of materials, design features, and construction techniques that result in long life and low maintenance.

A somewhat unified approach to designing long-life flexible pavements has been adopted by many experts [9, 10] based on mechanistic-empirical analysis and design concepts. The premise of this approach is that pavement distresses with deep pavement layer structure and appropriate materials can be avoided or delayed if pavement responses — stresses, strains, and deflections — are kept below critical values at the locations where the distresses initiate to occur. Thus, pavement can be designed for an indefinite structural life for heavy vehicle loads and repetitions without being too conservative.

Several states in the US have built long-life pavements by enhancing (i) structural design methods, (ii) materials evaluation and specification procedures, (iii) construction practices, and (iv) maintenance practices [5, 8, 11-14]. In Michigan, four long-life pavement sections were constructed as a result of the Public Act 175 (2015) and Roads Innovation Task Force (RITF) Report [15]: (i) 30-year (pavement design life) HMA on US-131 in the Grand Region (constructed in 2017), (ii) 30-year concrete on I-69 in the Bay Region (constructed in 2018), (iii) 50-year concrete on US-131 in the Grand Region (constructed in 2018) and (iv) 50-year HMA on I-475 in the Bay Region (construction completed in 2019). Locations of these long-life pilot projects are illustrated in Figure 1. As part of each project, several 'test sections' (that include long-life and standard control areas) were identified for sampling and testing, which are listed in

Table 1. Figure 2, Figure 3, Figure 4, and Figure 5 show the aerial view of the locations of each of these test sections for each pilot project.

Modifications to standard designs and materials were necessary to pursue the goal of extending the pavement structure design life (e.g., increased layer thicknesses, improved materials' properties, enhanced construction specifications, and upgraded design aspects), and their as-built evaluation will assist MDOT in determining their potential for meeting the intended design and services lives of 50 and 75 years. For this purpose, MDOT has collected material samples from the pilot projects to evaluate various engineering properties and compare the performance predictions of the standard and long-life pavement cross-sections. Such an evaluation will produce valuable information that will lead to adjustments to the engineering design aspects and specifications of standard pavement designs too. Therefore, this study will generate vital knowledge to establish the baseline for long-life pavements in Michigan.

Figure 1. Locations of the four long-life pilot projects

Table 1 List of MDOT's long-life pilot projects and standard and long-life test sections

Pavement type	Project	Test section	Location (Station)		Direction	Design life (years)
HMA	US-131	Test section 1	1090+00	1100+00	NB	30
		Test section 2	1127+52	1137+81	NB	30
		Test section 3	1170+00	1180+00	NB	30
		Test section 4	1210+10	1220+00	NB	20
	I-475	Test section 1	0650+00	0660+00	NB	50
		Test section 2	0745+00	0755+00	NB	50
		Test section 3	0770+00	0780+00	NB	50
		Test section 1	0650+00	0660+00	SB	20
		Test section 2	0745+00	0755+00	SB	20
		Test section 3	0770+00	0780+00	SB	20
JPCP (concrete)	I-69	Test section 1	0340+00	0350+00	EB	20
		Test section 2	0367+00	0377+00	EB	20
		Test section 3	0340+00	0350+00	WB	30
		Test section 4	0396+00	0406+00	WB	30
	US-131	Test section 1	0852+00	0862+00	NB	50
		Test section 2	0885+00	0895+00	NB	50
		Test section 3	0970+00	0980+00	NB	50
		Test section 1	0850+00	0860+00	SB	20
		Test section 2	0895+00	0905+00	SB	20
		Test section 3	0977+00	0987+00	SB	20

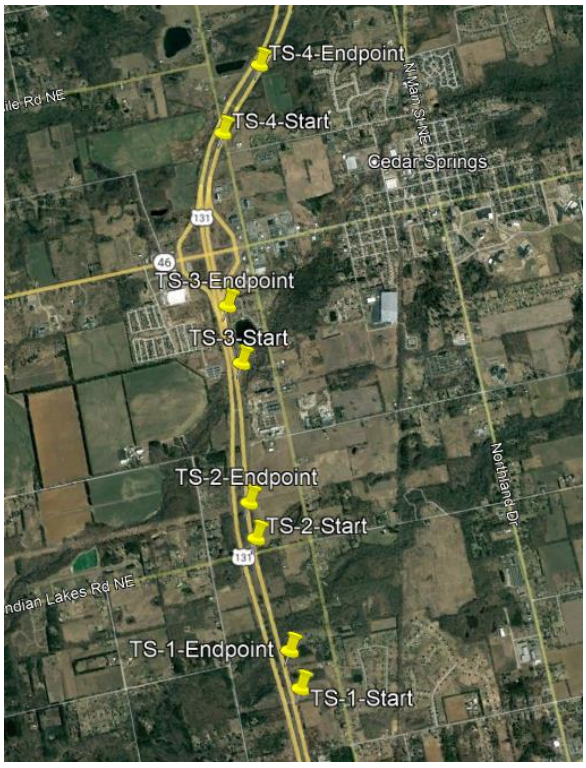

Figure 2. Locations of the test sections on the US-131 HMA 30-year project

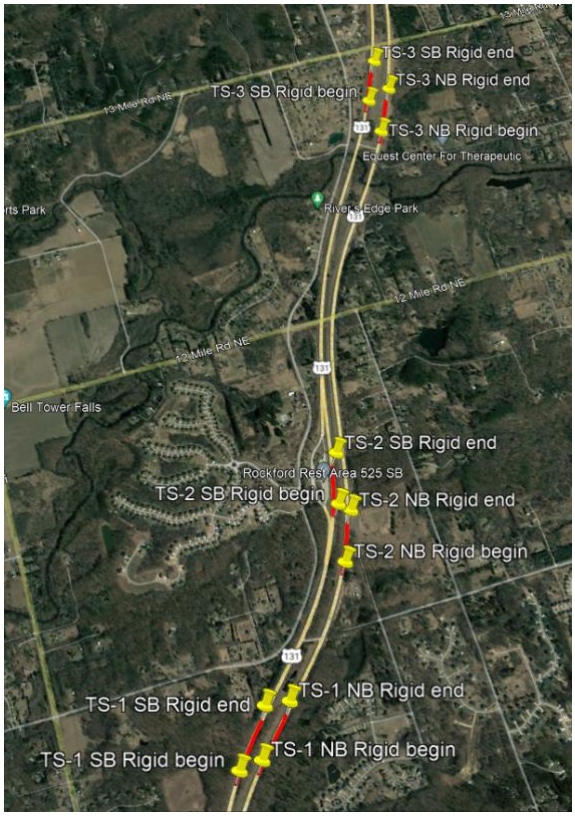

Figure 3. Locations of the test sections on the US-131 Rigid 50-year project

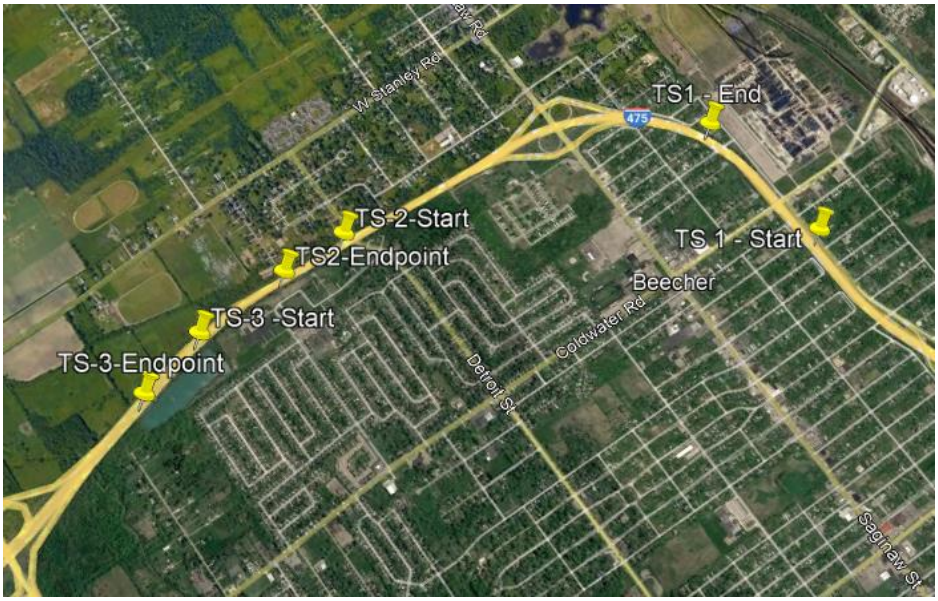

Figure 4. Locations of the test sections on the I-475 HMA 50-year project

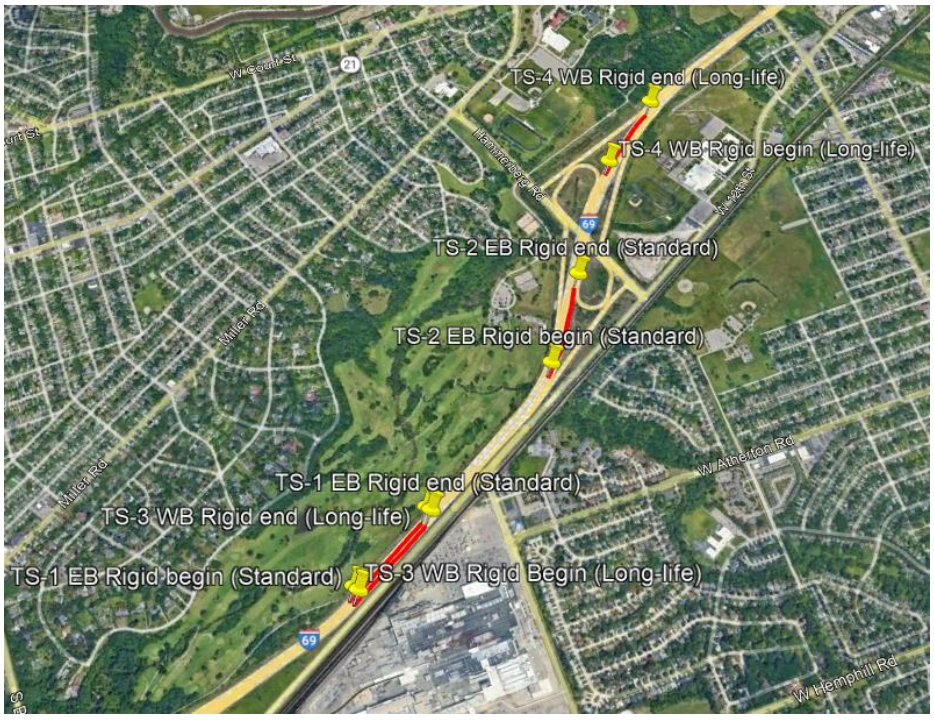

Figure 5. Locations of the test sections on the I-69 Rigid 30-year project

OBJECTIVES

The specific objectives of this study were to:

(1) Document and summarize project details related to design methods, construction practices, and materials for long-life pavements and compare them to those used in standard designs. The summary also includes plans subsequently modified during construction for various reasons.
(2) Evaluate materials' properties of samples collected from both standard and long-life sections of the four projects. The testing plan includes detailed laboratory and field testing. The as-constructed material properties are used in the mechanistic-empirical (ME) design software for evaluating the expected performance of all projects (see #4).
(3) Update the MDOT materials databases with laboratory test results.
(4) Analyze the expected performance of long-life and standard sections in the pilot projects through Pavement-ME and locally calibrated performance models.
(5) Assess whether the pilot projects will achieve the desired design and service life and project details that will contribute the most to the expected service life of the long-life sections.
(6) Suggest improvements for future long-life pavements (design, construction, materials, and performance monitoring).

CHAPTER 1: REVIEWING THE ROADS INNOVATION TASK FORCE REPORT AND GATHERING DESIGN DATA

As part of this task, the Roads Innovation Task Force (RITF) report, project plans, and available materials information was reviewed by the research team. The RITF report includes a comprehensive synthesis of the literature, inputs from other DOTs, county road associations (and county road departments), academia, industry, relevant associations, and pavement demonstration reports. A review of the RITF report revealed important information about potential enhancements to traditional pavement design and construction practices to achieve a longer structural life. A summary of the recommended enhancements listed in the RITF report to achieve long-life pavements is illustrated in Figure 6 and Figure 7, for flexible and rigid pavements, respectively. As shown, structural design, materials characteristics, construction practices, and QC/QA specifications are all thoroughly considered, and recommendations have been made.

Tables 2 to 5 summarize the recommended enhancements to HMA and PCC long-life projects and the information on whether these were or were not met (red shading) in the four pilot projects. It should be noted that the recommended enhancements shown in Figure 6 should be treated as wish list, not like a specification to be followed. Each project is different and some deviations from these recommendations is inevitable. The fact that there are some red shadings in Tables 2 to 5 does not necessarily mean that there should be a concern for potential poor performance in those pavement sections.

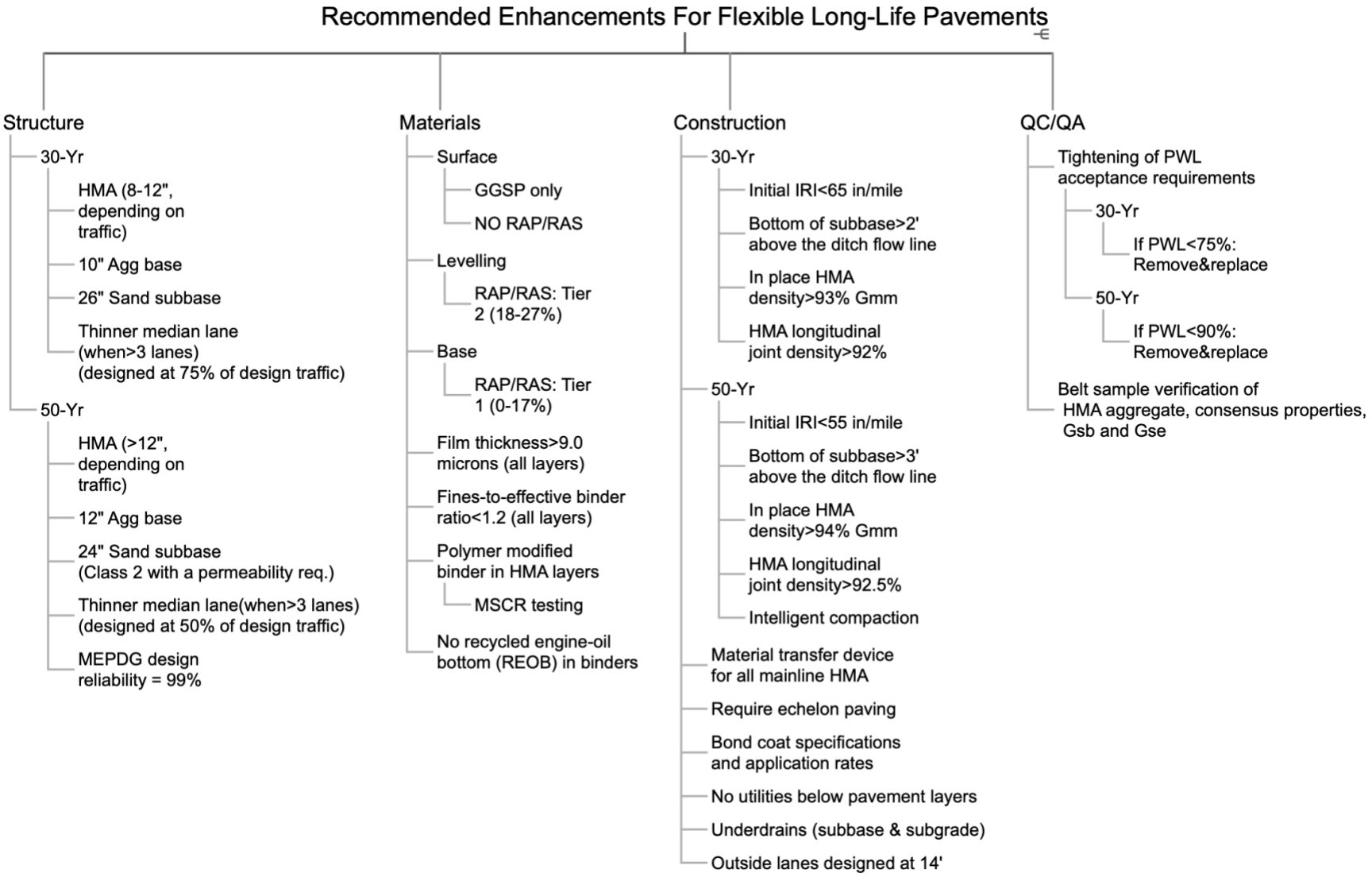

Figure 6. Potential enhancements to design long-life HMA pavements (based on reference: Roads Innovation Task Force Report, 2016)

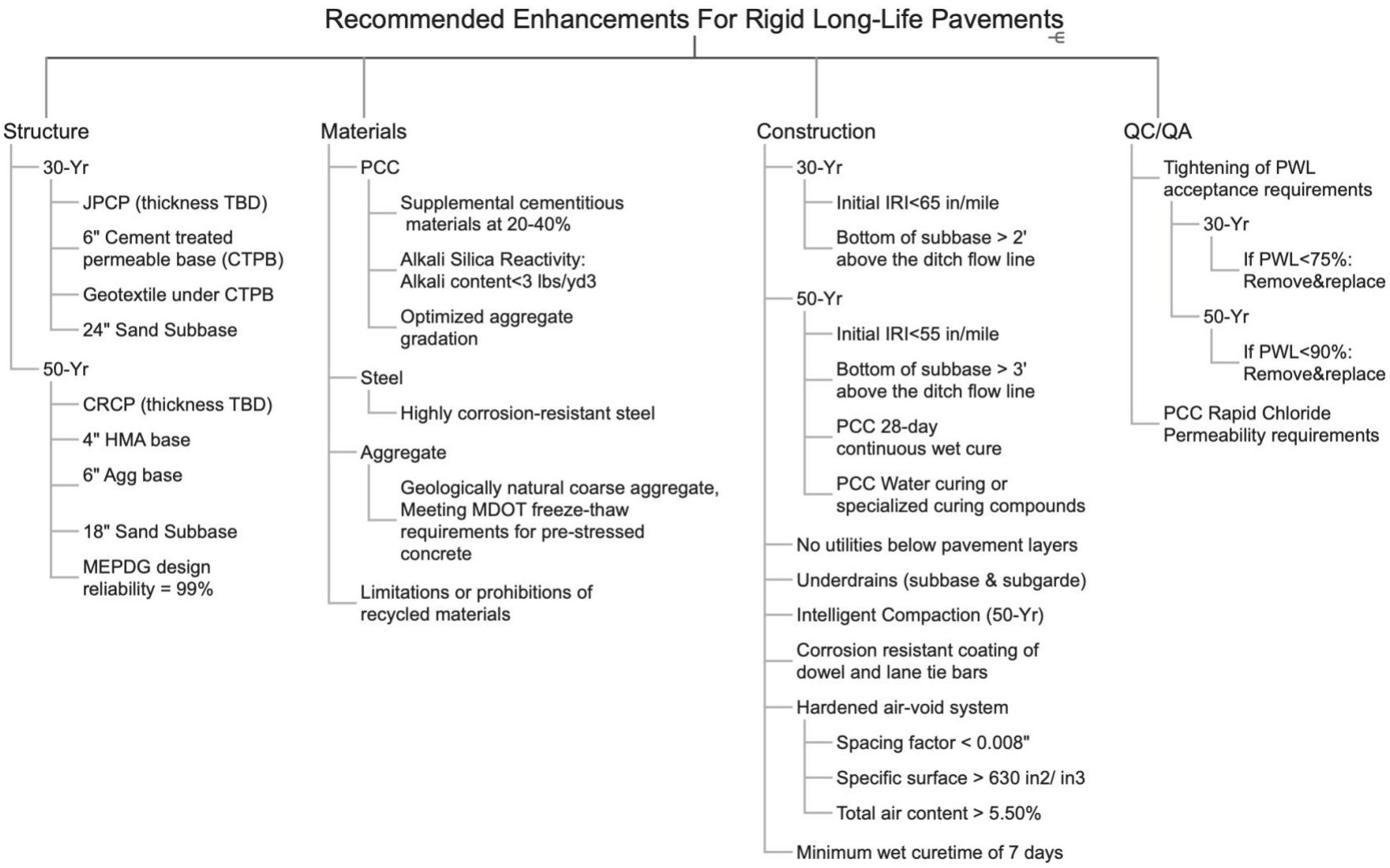

Figure 7. Potential enhancements to design long-life Rigid pavements (based on reference: Roads Innovation Task Force Report, 2016)

Table 2 RITF recommended enhancements and comparison with implementations on the US-131 HMA pavement project.

Pavement type and design life			Standard - 20 years	Long-life - 30 years		
Test section number			Test section 4 NB	Test section 1 NB	Test section 2 NB	Test section 3 NB
Structure		8-12" HMA	1.75"5E10	1.5" GGSP	1.5" GGSP	1.5" GGSP
			3" 3E10	2.5" 4E30	2.5" 4E30	2.5" 4E30
			4.5" 2E10	7.25" 3E30	7.25" 3E30	7.25" 3E30
		10" Agg base	6" Aggregate Base	12" Aggregate Base	12" Aggregate Base	12" Aggregate Base
		26" Sand subbase	18" Sand Subbase	24" Sand Subbase	24" Sand Subbase	24" Sand Subbase
		Thinner median lane (when > 3 lanes)	NA	Not applicable as it was a two-lane pavement.		
Materials	Surface	GGSP only	5E10	GGSP- No RAP/RAS	GGSP- No RAP/RAS	GGSP- No RAP/RAS
		No RAP/RAS	19%-Tier 2	GGSP- No RAP/RAS	GGSP- No RAP/RAS	GGSP- No RAP/RAS
	Leveling	RAP/RAS Tier 2:18-27%	16 %- Tier 1	9%- Tier 1	9%- Tier 1	9%- Tier 1
	Base	RAP/RAS Tier1: 0-17%	24 %- Tier 2	13 %- Tier 1	13 %- Tier 1	13 %- Tier 1
	Surface	Film thickness > 9.0 microns (all layers)	8.8	10	10	10
	Leveling		9.2	9.5	9.5	9.5
	Base		8.1	9.8	9.8	9.8
	Surface	Fines/effective binder ratio < 1.2 (all layers)	0.94	1.27	1.27	1.27
	Leveling		0.97	0.83	0.83	0.83
	Base		1.11	0.83	0.83	0.83
	Surface	Polymer modified binders in HMA Layers	64-28 (Virgin: PG 64-28)	70-28P (Virgin: PG 70-28P)	70-28P (Virgin: PG 70-28P)	70-28P (Virgin: PG 70-28P)
	Leveling		64-28 (Virgin: PG 64-28)	70-28P (Virgin: PG 70-28P)	70-28P (Virgin: PG 70-28P)	70-28P (Virgin: PG 70-28P)
	Base		58-22 (Virgin: PG58-28)	64-28 (Virgin: PG 64-28)	64-28 (Virgin: PG 64-28)	64-28 (Virgin: PG 64-28)
	All layers	MSCR testing	NA	No MSCR testing was required		
		No REOB in binders	NA	REOB not used		
		Limitations or prohibitions of recycled materials	NA	Recycled materials were used for unbound layers. (Recycled concrete aggregate base)		
Construction		Initial IRI < 65 in/mile	28.1 (in/mile)	29.2 (in/mile)		
		Bottom of subbase >2' above the ditch flow line	NA	Unknown		
		In place HMA density >93% Gmm	5E10 avg= 94.06%	GGSP avg= 91.60%		
			3E10 avg= 93.84%	4E30 avg= 95.30%		
			2E10 avg= 94.60%	3E30 avg=94.89%		
		HMA longitudinal joint density >92%	5E10 avg=92.27% 3E10 avg=92.44%	Echelon paving for the top layer. 4E30 avg= 93.36%		
		Material transfer device for all mainline HMA	NA	Unknown		
		Require echelon paving	NA	Only the top layer was paved using echelon paving.		
		Bond coat specifications and application rates	NA	Unknown		
		No utilities below pavement layers	NA	No utilities except a transverse gas line in a small area		
		Underdrains (subbase and subgrade)	NA	Unknown		
		Outside lanes designed at 14'	NA	Outside lanes designed at 12'		
QC/QA		Tightening of PWL acceptance requirements	NA	No change in PWL acceptance requirements.		
		If PWL<75% Remove & replace	NA	No change in PWL acceptance requirements		
		Belt sample verification of HMA aggregate consensus properties, Gsb and Gse	NA	Unknown		

Note: NA = Not applicable.

Table 3 RITF recommended enhancements and comparison with implementations on the I-475 HMA pavement project

Pavement type and design life			Standard - 20 years			Long-life - 50 years		
Test section number			TS-1 SB	TS-2 SB	TS-3 SB	TS-1 NB	TS-2 NB	TS-3 NB
Structure		Thickness >12" HMA	1.75” 5E10	1.75” 5E10	1.75” 5E10	2” GGSP	2” GGSP	2” GGSP
			2.5” 5E10	2.5” 5E10	2.5” 5E10	2.5” 4E30	2.5” 4E30	2.5” 4E30
			3.5” 3E10	3.5” 3E10	3.5” 3E10	6.5” 3E30	6.5” 3E30	6.5” 3E30
		12" Aggregate base	6” Agg. Base (RCA used)	6” Agg. Base	6” Agg. Base (RCA used)	12” Agg. Base (RCA used)	12” Agg. Base	12” Agg. Base
		24" Sand subbase (class 2 with a permeability req)	18” Sand Subbase	18” Sand Subbase	18” Sand Subbase	24” Sand Subbase	24” Sand Subbase	24” Sand Subbase
		Thinner median lane (when > 3 lanes)	NA			Not applicable as it was a two-lane project		
		MEPDG Design reliability= 99%	NA	NA	NA	95%	95%	95%
Materials	Surface	GGSP only	5E10	5E10	5E10	GGSP- No RAP/RAS	GGSP- No RAP/RAS	GGSP- No RAP/RAS
		No RAP/RAS	31%- Tier 3	31%- Tier 3	31%- Tier 3	GGSP- No RAP/RAS	GGSP- No RAP/RAS	GGSP- No RAP/RAS
	Leveling	RAP/RAS Tier 2:18-27%	31%- Tier 3	31%- Tier 3	31%- Tier 3	17%-Tier 1	17%-Tier 1	17%-Tier 1
	Base	RAP/RAS Tier1:0-17%	25%- Tier 2	25%- Tier 2	25%- Tier 2	19%-Tier 2	19%-Tier 2	19%-Tier 2
	Surface	Film thickness > 9.0 microns (all layers)	7.3	7.3	7.3	10	10	10
	Leveling		8.5	8.5	8.5	9.3	9.3	9.3
	Base		8.3	8.3	8.3	9.6	9.6	9.6
	Surface	Fines/effective binder ratio < 1.2 (all layers)	1.11	1.11	1.11	1.37	1.37	1.37
	Leveling		1.11	1.11	1.11	0.95	0.95	0.95
	Base		1.15	1.15	1.15	0.91	0.91	0.91
	Surface	Polymer modified binders in HMA Layers	PG 64-28 (Virgin: PG 58-34)	PG 64-28 (Virgin: PG 58-34)	PG 64-28 (Virgin: PG 58-34)	PG 70-28P (Virgin: 70-28P)	PG 70-28P (Virgin: 70-28P)	PG 70-28P (Virgin: 70-28P)
	Leveling		PG 64-28 (Virgin: PG 58-34)	PG 64-28 (Virgin: PG 58-34)	PG 64-28 (Virgin: PG 58-34)	PG 70-28P (Virgin: 70-28P)	PG 70-28P (Virgin: 70-28P)	PG 70-28P (Virgin: 70-28P)
	Base		PG 58-28 (Virgin: PG 52-34)	PG 58-28 (Virgin: PG 52-34)	PG 58-28 (Virgin: PG 52-34)	PG 64-28 (Virgin: PG 58-34)	PG 64-28 (Virgin: PG 58-34)	PG 64-28 (Virgin: PG 58-34)
	All layers	MSCR testing	NA			No MSCR testing was required		
		No REOB in binders	NA			No information		
		Limitations or prohibitions of recycled materials	NA			Recycled materials were used for unbound layers. (Recycled concrete aggregate base)		

Note: NA = Not applicable.

Table 3 RITF recommended enhancements and comparison with implementations on the I-475 HMA pavement project (continued…)

Construction	Initial IRI < 55 in/mile	49.3 (in/mile)	46.4 (in/mile)
	Bottom of subbase >3' above the ditch flow line	NA	
	In place HMA density >94% Gmm	5E10 avg=94.69% 3E10 avg=94.91%	GGSP avg=95.91% 4E30 avg=95.28% 3E30 avg=95.16%
	HMA longitudinal joint density >92.5%	5E10 avg=90.80%	GGSP avg=96.12%
	Material transfer device for all mainline HMA	NA	No information
	Require echelon paving	NA	Only the top layer was paved using echelon paving.
	Bond coat specifications and application rates	NA	No information
	No utilities below pavement layers	NA	Some utility lines crossing perpendicular to the road, but those are not significant for pavement performance.
	Underdrains (subbase and subgrade)	NA	No information
	Outside lanes designed at 14'	NA	Outside lanes designed at 12’
	Intelligent compaction (50-yr)	NA	Not used.
QC/QA	Tightening of PWL acceptance requirements	NA	No change in PWL acceptance requirements.
	If PWL<90% Remove & replace	NA	No change in PWL acceptance requirements
	Belt sample verification of HMA aggregate consensus properties, Gsb and Gse	NA	No information

Table 4 RITF recommended enhancements and comparison with implementations on the I-69 (Rigid Pavement)

Pavement type and design life		Standard - 20 years		Long-life - 30 years	
Test section number		Test section 1	Test section 2	Test section 3	Test section 4
Structure	JPCP	9.5" NRHP	9.5" NRHP	10.5" NRHP	10.5" NRHP
	6" CTPB	6" OGDC (RCA used)	6" OGDC (RCA used)	6" CTPB (RCA used)	6" CTPB (RCA used)
	Geotextile under CTPB	Geotextile under OGDC	Geotextile under OGDC	Geotextile under CTPB	Geotextile under CTPB
	24" Sand[1]	No	No	No	No

[1] Enhancement requirement

	Aggregate Base[2]		No base	No base	6" Agg. Base	6" Agg. Base
	Subbase		10" Sand Subbase	10" Sand Subbase	8" Sand Subbase	8" Sand Subbase
	Subgrade		Unstabilized	Unstabilized	12" Cement Stabilized	12" Cement Stabilized
Materials	PCC	SCM's (20-40 %)	30% (Slag)	30% (Slag)	30% (Slag)	30% (Slag was specified but Fly Ash was used)
		Alkali-Silica Reactivity: Alkali Content < 3 lb./yd³	Yes	Yes	Yes	Yes
		Optimized Aggregate Gradation	Yes	Yes	Yes	Yes
	Steel	Highly Corrosion-resistant Steel	NA	NA	NA	NA
	Agg.	Geologically natural CA, meeting MDOT F-T requirements for pre-stressed concrete	0.016	0.016	0.016	0.016
		Limitations or prohibitions of recycled materials	None	None	None	None
Construction	Initial IRI (in/mile) < 65 inches/mile		73 (in/mile)		71 (in/mile) Note: Specification was not changed to require IRI<65 in/mile	
	Bottom of subbase > 2' above the ditch flow line		Yes	Yes	Yes	Yes
	No utilities below pavement layers		Yes	Yes	Yes	Yes
	Underdrains (subbase and subgrade)		Yes	Yes	Yes	Yes
	Corrosion-resistant coating of dowel and lane tie bars (PCC)		Yes	Yes	Yes	Yes
	Hardened air-void system (PCC)					
	Spacing factor < 0.008"		SAM (0.26)	SAM (0.21)	SAM (0.26)	SAM (0.3)
	Specific Surface > 630 in²/in³					
	Total air content > 5.50 %		Yes	Yes	Yes	Yes
	A minimum wet cure time of 7 days (PCC)		No	No	No	No
QC/QA	Tightening of PWL acceptance requirements					
	If PWL< 75%, Remove & replace		Not followed		No change in PWL acceptance requirements	
	PCC Rapid Chloride Permeability requirements		No	No	No	No

Note: OGDC = Open-graded drainage course. RCA = Recycled concrete aggregate. CTP

Table 5 RITF recommended enhancements and comparison with implementations on the US-131 (Rigid Pavement)

Pavement type and design Life		US-131 SB (Standard) 20 years			US-131 NB (Long-life) 50 years		
Test section number		Test section 1	Test section 2	Test section 3	Test section 1	Test section 2	Test section 3
Stationing		850+00-860+00	895+00-905+00	977+00-987+00	852+00-862+00	885+00-895+00	970+00-980+00
Structure	CRCP	10.5" NRHP	10.5" NRHP	10.5" NRHP	10.5" NRHP	10.5" NRHP	10.5" NRHP
	4" HMA Base	No	No	No	6" CTPB (RCA used)	6" CTPB (RCA used)	6" CTPB
	Geotextile under CTPB[3]	No	No	No	Yes (woven)	Yes (woven)	Yes (non-woven)
	6" Aggregate Base	6" OGDC	6" OGDC	6" OGDC	6" Agg. Base	6" Agg. Base	6" OGDC, Special

[2] *Actual structure (as constructed)*

[3] Not an enhancement but provided in the pavement structure

Pavement type and design Life			US-131 SB (Standard) 20 years			US-131 NB (Long-life) 50 years		
Test section number			Test section 1	Test section 2	Test section 3	Test section 1	Test section 2	Test section 3
Stationing			850+00-860+00	895+00-905+00	977+00-987+00	852+00-862+00	885+00-895+00	970+00-980+00
			(RCA used)	(RCA used)	(RCA used)	(RCA used)	(RCA used)	
	18" Sand Subbase		10" Subbase	10" Subbase	10" Subbase	8", CIP	8", CIP	20", CIP
	Subgrade		Unstabilized	Unstabilized	Unstabilized	12" Cement Stab	12" Cement Stab	Unstabilized
	MEPDG design Reliability = 99%							
Materials	PCC	SCM's (20-40 %)	30% (Slag)	30% (Slag)	30% (Slag)	30% (Slag)	30% (Slag)	30% (Slag)
		Alkali-Silica Reactivity: Alkali Content < 3lbs/yd³	Yes	Yes	Yes	Yes	Yes	Yes
		Optimized Aggregate Gradation	Yes	Yes	Yes	Yes	Yes	Yes
	Steel	Highly Corrosion-resistant Steel	N/A	N/A	N/A	N/A	N/A	N/A
	Agg.	Geologically natural CA, meeting MDOT F-T requirements for pre-stressed concrete	0.006	0.006	0.006	0.006	0.006	0.006
		Limitations or prohibitions of recycled materials	None	None	None	None	None	None
Construction	Initial IRI < 55 in/mile		No (66.5 in/mi)			No (72 in/mi) Note: Specification was not changed to require IRI<55 in/mile		
	Bottom of subbase > 3' above the ditch flow line		Yes	Yes	Yes	Yes	Yes	Yes
	PCC 28-day continuous wet cure		No	No	No	No	No	No
	PCC Water curing or specialized curing compounds		Yes	Yes	Yes	Yes	Yes	Yes
	No utilities below pavement layers					Yes	Yes	Yes
	Underdrains (subbase and subgrade)					Yes	Yes	Yes
	Intelligent compaction		No	No	No	No	No	No
	Corrosion-resistant coating of dowel and lane tie bars		Yes	Yes	Yes	Yes	Yes	Yes
	Hardened air-void system							
	Spacing factor < 0.008"		NA			No information		
	Specific Surface > 630 in²/in³		NA			No information		
	Total air content > 5.50 %		Yes	Yes	Yes	Yes	Yes	Yes
	A minimum wet cure time of 7 days		No	No	No	No	No	No
QC/QA	Tightening of PWL acceptance requirements		NA			Spec not changed		
	If PWL< 90% Remove & replace		NA			Spec not changed		
	Rapid Chloride Permeability requirements		NA			No	No	No

Note: OGDC = Open-graded drainage course. RCA = Recycled concrete aggregate. CTPB = Cement-treated permeable base

CHAPTER 2: GATHERING POST-CONSTRUCTION DATA

The research team conducted interviews with the MDOT region personnel involved in the long-life pilot projects. Interviews identified special measures considered for improving construction quality of these pilot projects. Data relating to the acceptance of construction parameters was obtained from the construction staff. Moreover, the project team undertook data mining to gather different information from the database provided by MDOT for determining the performance of the long-life pilot projects. All data regarding these parameters have been organized and processed systematically to make its usage efficient.

Pavement Cross-Sections

The cross-sections of the standard and the long-life sections were obtained from the letting plans and verified with the MDOT engineers during the interviews. The structural properties were shown previously in Table 2 for US-131 HMA project, Table 3 for I-475 HMA pavement project, Table 4 for I-69 Rigid pavement project and Table 5 for US-131 Rigid pavement project.

Mix Designs

Job mix formulae (JMF) and concrete mix designs are critical information that can explain the behavior of the asphalt mixture and the concrete slab in the field and laboratory tests, respectively. Several concrete mix design documents were available, and their intended use was not always apparent. To identify the exact concrete mix designs used for the construction of the mainline pavement, it was necessary to summarize the mix design data. This activity allowed comparing the composition of the different mixes and knowing the w/cm ratios. Besides, the desired strength, F-T requirements, and other important information were summarized readily.

I-475 HMA Pavement Project

Table 6 presents the critical JMF details for all the mixes used in the different layers of both the standard and long-life sections of the project.

Table 6 I-475 Mixtures design characteristics

ID	PG	Layer	Pb (%)	NMAS (mm)	Design ESAL (Million)	Ndes	VMA (%)	VFA (%)
GGSP	70-28P	Top	6.27	19	10 to 100	109	17.79	83.14
4E30	70-28P	Leveling	5.58	12.5	50	109	14.87	79.82
3E30	58-34	Base	5.40	19	50	109	14.20	78.88
5E10-Top	58-34	Top	6.07	9.5	10	96	15.42	80.54
5E10-Lev	58-34	Leveling	6.07	9.5	10	96	15.42	80.54
3E10	52-34	Base	4.79	19	10	96	13.71	78.12
Notes: GGSP = Gap Graded Superpave, Ndes = number of design gyrations, Pb = Binder content, VMA = Voids in Mineral Aggregate, VFA = Voids Filled with Asphalt, PG = Performance Grade.								

US-131 HMA Pavement Project

Table 7 presents the critical JMF details for all the mixes used in the different layers of both the standard and long-life sections of the project.

Table 7 US-131 Mixtures design characteristics

ID	PG	Layer	P_b (%)	NMAS (mm)	Design ESAL (Million)	N_{des}	VMA (%)	VFA (%)
GGSP	70-28P	Top	6.39	9.5	10 to 100	109	18.28	83.59
4E30	70-28P	Leveling	5.21	12.5	30	109	15.21	80.28
3E30	64-28	Base	4.90	12.5	30	109	14.29	79.01
5E10	64-28	Top	5.90	9.5	10	96	16.14	81.41
3E10	64-28	Leveling	5.07	12.5	10	96	14.18	78.84
2E10	58-28	Base	4.48	19	10	96	13.08	77.06
Notes: GGSP = Gap Graded Superpave, N_{des} = number of design gyrations, Pb = Binder content, VMA = Voids in Mineral Aggregate, VFA = Voids Filled with Asphalt, PG = Performance Grade.								

I-69 JPCP Pavement Project

Several design mixes were identified from the data files for the project. Table 8 shows the mainline mixes information as confirmed by the MDOT Bay Region construction staff for the I-69 project. Mix no— 527-1 was a machine-work mix used primarily for the mainline construction (37 lots). Mix no—527-2, a handwork mix that was used at specific locations (3 lots). Mixes 87H and P1M-18 W/MRWR were also used in four and one lot, respectively. In addition, mix no— 527-0 was used for the construction of the cement-treated permeable base (CTPB) layer on the I-69 WB long-life pavement sections. Recycled concrete aggregates (RCA) were used in the construction of the CTPB as revealed during the interview with the Bay region construction staff. Concrete leaching from such aggregates can result in severe damage to the PCC layer due to its negative impact on the drainage ability of the base layer. However, in this project, the RCA was cement stabilized which has proven to practically eliminate leachate.

Table 8 Concrete mixes used in the construction of mainline I-69 JPCP project

Ser. no.	Mix design no.	Required strength (psi)	Design slump (inches)	Supplementary cementitious material (lbs.)	Cement (lbs.)	Water (lbs.)	w/cm ratio	Design air (%)
a.	527-1	3500	3	30% Slag (147)	343	206	0.42	6.5
b.	527-2	3500	5	30% Slag (158)	368	231	0.44	6.5
c.	87H	3500	5	25% Fly ash (125)	375	220	0.44	7
d.	P1M-18 W/MRWR	3500	6	20% Fly ash (105)	421	236	0.45	6
e	527-0*	700-1000	-	-	250	110	0.44	-

*"- "means "Nil" or "not a requirement". * RCA used.*

US-131 JPCP Pavement Project

Table 9 summarizes the major features of the concrete mixes used for the construction of the mainline pavement's PCC layer along with the CTPB layer on the NB long-life TS-1 and 2.

RCA was also used in the construction of the CTPB layer which may cause drainage problems due to concrete leaching. However, in this project, the RCA was cement stabilized which has proven to practically eliminate leachate.

Table 9 Concrete mixes used in the construction of mainline US-131 JPCP project

Ser. no.	Mix design no.	Required strength (psi)	Design slump (inches)	Supplementary cementitious material (lbs.)	Cement (lbs.)	Water (lbs.)	w/cm ratio	Design air (%)
a.	533-1	3500	3	30% Slag (147)	343	206	0.42	6.5
b.	533-2	3500	3	30% Slag (158)	368	231	0.44	6.5
c.	533-0*	750-1000	-	-	250	115	0.46	-

*"- "means "Nil" or "not a requirement". * RCA used.*

Quality Control and Quality Assurance (QC/QA) Tests

This section presents a summary of the different construction quality control and quality assurance (QC/QA) tests conducted by the MDOT. The tests include the concrete durability tests (i.e., concrete resistivity tests, super air meter (SAM) tests, air content measurement) and Magnetic Imaging Tools (MIT) scans for dowel bar alignment.

Concrete Durability

One of the major distresses in concrete pavements is joint spalling due to deicer frost deterioration of the cement matrix combined with internal cracking in saturated concrete from insufficient air-void-related properties (i.e., total air content in fresh concrete, spacing factor, and specific surface area in the hardened concrete). Permeability requirements are also essential for concrete durability, and it is commonly measured in terms of its ability to resist chloride ion penetration (AASHTO T 277 and ASTM C1202), known as the rapid chloride permeability test (RCPT). However, research has shown that the surface resistivity (SR) test (AASHTO TP 95) is a promising alternative to the RCPT [16]. The SR test results conducted by the MDOT on both the I-69 and US-131 JPCP projects have been evaluated, and Table 10 shows the relationship between the chloride ion penetrability and the SR test (AASHTO TP 95) that measures the electric resistivity of the concrete from concrete cylinders/cores [17].

Figure 8 displays a histogram of the electric resistivity measured on cylinders from the two projects. Most of the electric resistivity values for the I-69 project lie within the 12-21 kΩ.cm range which corresponds to moderate chloride ion penetrability (see Figure 8(a)). The electric resistivity values of the US-131 JPCP project, instead, correspond to moderate-to-low chloride ion penetrability (see Figure 8(b)). Ideally, a low 28- or 90-day RCP Coulomb rating (<2000 Coulombs) is necessary to achieve the desired permeability properties. Typically, 20-40% cement replacement by supplemental cementitious material (SCM) is necessary for this purpose. As shown in Table 8 and Table 9, the majority of the concrete used in mainline pavement construction used concrete mixes with 30% SCM (slag).

Table 10 Comparison of chloride penetrability levels established for standards based on electric resistivity (AASHTO TP 95) and charged passed (ASTM C1202) [17]

Chloride ion penetrability	Electric resistivity, kΩ.cm (AASHTO TP 95)	Charge Passed, Coulombs (ASTM C1202)
High	<12	>4000
Moderate	12 to 21	2000 to 4000
Low	21 to 37	1000 to 2000
Very low	37 to 254	100 to 1000
Negligible	>254	<100

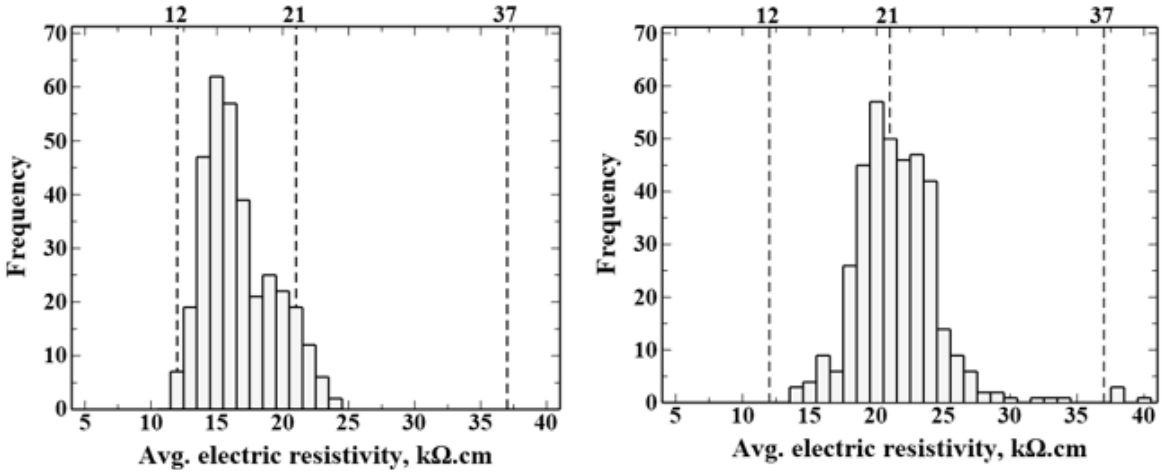

(a) I-69 JPCP (b) US-131 JPCP

Figure 8 Surface resistivity test results

In addition to the SR test data, MDOT used Super Air Meter (SAM) to measure the SAM numbers. The SAM number is an indirect measure of the spacing factor, a measure of the distribution of the air bubbles in the concrete matrix. A spacing factor of 0.008 in, or lower, is recommended by ACI 201 to produce frost-durable concrete. This corresponds to a SAM number of 0.20 psi or below.

Figure 9 summarizes the SAM numbers and air contents (%) of different sublots used in the construction of the mainline I-69 WB (long-life) and EB (standard) pavement sections. These plots are based on the quality assurance (QA) data from the construction record database. The design air content for concrete mix # 527-1 used in the construction of the mainline I-69 was 6.5%. As shown, the required total air content is achieved in most locations. The SAM numbers for the WB long-life sections are between 0.20-0.25 psi (Figure 9(a)), while the SAM number is below the 0.20 psi threshold for most EB standard sections (Figure 9(b)).

Figure 10 shows the SAM numbers and the total air content for the concrete used in the construction of mainline US-131 NB and SB sections at different stations. The design air content (6.5%) and the desired SAM number of 0.20 psi (i.e., spacing factor of 0.008 inches) were achieved in the majority of the locations.

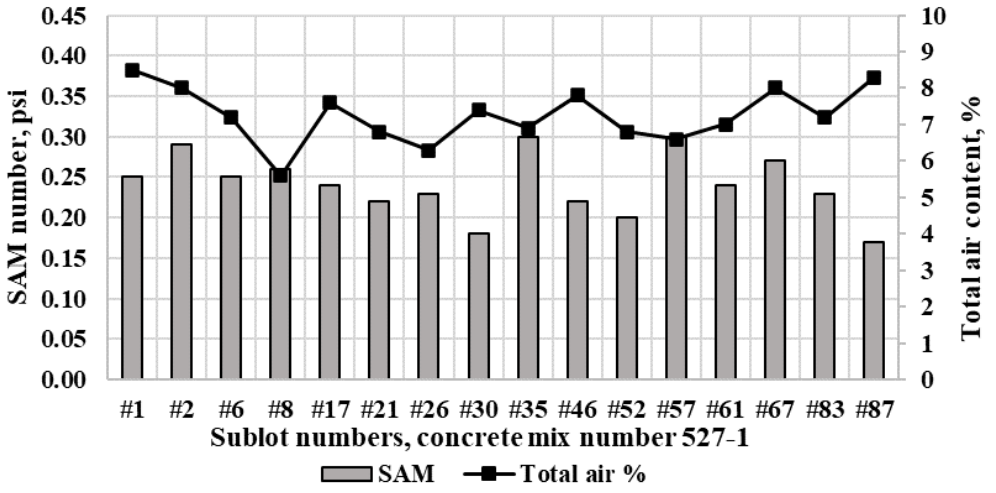

(a) I-69 WB

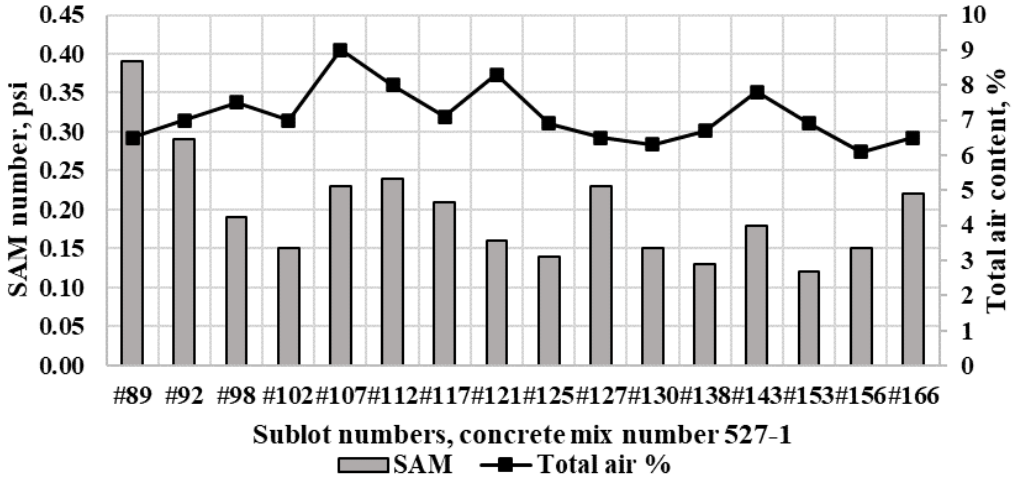

(b) I-69 EB

Figure 9 SAM number and air content for I-69 concrete project, concrete mix # 527-1

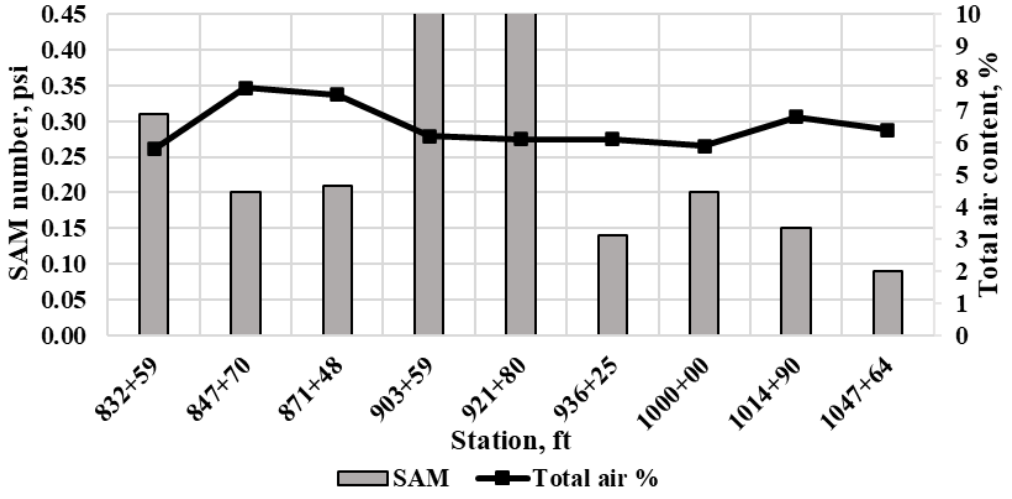

(a) US-131 NB

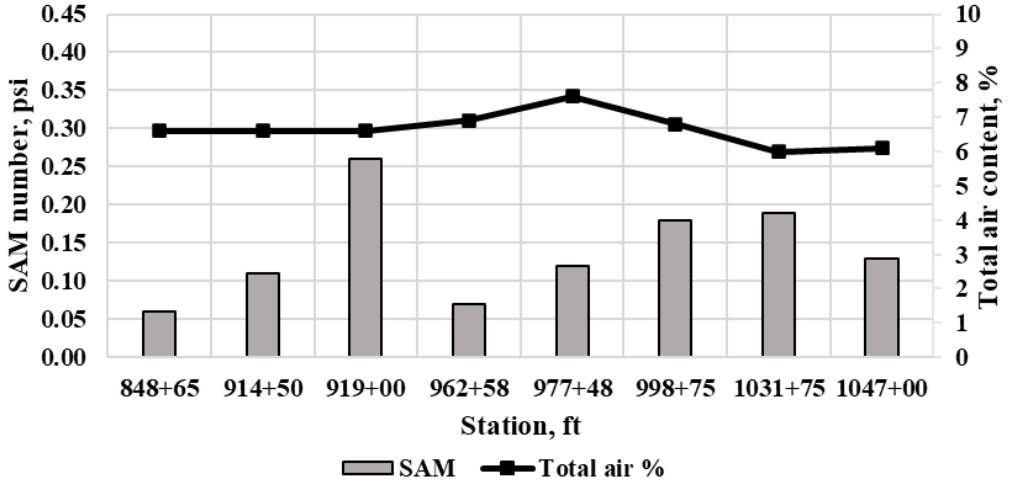

(b) US-131 SB

Figure 10 SAM number and air content for US-131 concrete project, concrete mix # 533-1

Dowel Bar Alignment

The performance of concrete pavements largely depends upon the satisfactory performance of the joints, while the joint's performance depends on adequate load transfer design and appropriate placement of the dowel bars in the case of jointed plain concrete pavement (JPCP). Magnetic Imaging Tools (MIT) scan is one of the methodologies available for checking the misalignment of dowel bars due to either a horizontal translation, longitudinal translation, vertical translation, vertical tilt, and horizontal skew of the bar, or a combination of those. All these misalignments have an impact on the performance of the JPCP i.e., spalling, cracking, or load transfer. Table 11 summarizes the MIT scan results found in the construction database for the US-131 NB pavement. These scans were carried out in two lanes at a time (i.e., 24 dowel bars were scanned at each location). The table shows the number of misaligned dowel bars at the scanned joint.

Table 11 Summary MIT Scan results - US-131 NB pavement

Station	Joint	Date	Number of dowels misaligned			
			Depth (Vertical Translation)	Side shift	Horizontal misalignment	Vertical misalignment
0-00	1	10/31/2018		1	2	
0-14	2	10/31/2018	None			
0-28	3	10/31/2018	None			
0-42	4	10/31/2018	None			
0-56	5	10/31/2018			2	
0-70	6	10/31/2018	2	1	2	
0-84	7	10/31/2018		4		
0-98	8	10/31/2018			3	
1-12	9	10/31/2018		1	1	
1-26	10	10/31/2018		4	1	
842-66	11	10/31/2018			1	
842-80	12	10/31/2018		4		
842-94	13	10/31/2018	None			
843-08	14	10/31/2018			2	
843-22	15	10/31/2018			1	
843-36	16	10/31/2018		4	1	
843-50	17	10/31/2018	None			
843-64	18	10/31/2018		9	1	
843-78	19	10/31/2018		4	2	
843-92	20	10/31/2018	None			
859-40	21	10/31/2018		2	1	
859-54	22	10/31/2018			1	
859-68	23	10/31/2018	None			
859-82	24	10/31/2018			1	
859-96	25	10/31/2018			1	
860-10	26	10/31/2018		1	2	1
860-24	27	10/31/2018			1	
860-38	28	10/31/2018	None			
860-52	29	10/31/2018			1	
860-66	30	10/31/2018			3	
895-47	20	11/2/2018			2	
895-61	21	11/2/2018			1	
896-03	24	11/2/2018			2	
896-17	25	11/2/2018			3	
896-59	28	11/2/2018			1	
896-73	29	11/2/2018			2	
896-87	30	11/2/2018	None			
897-18	0	11/2/2018	None			
884-01	1	11/2/2018		1		
884-15	2	11/2/2018	None			
884-29	3	11/2/2018		1		
884-43	4	11/2/2018			1	
884-57	5	11/2/2018			1	
884-71	6	11/2/2018		12	2	1
884-85	7	11/2/2018			1	
884-99	8	11/2/2018	None			
885-13	9	11/2/2018	None			
885-27	10	11/2/2018			2	

In Table 11, depth means if the dowel was placed deeper or shallower than was required (Dowels are placed at the mid-depth). Different combinations of dowel bar misalignments are shown in Figure 11. Side shift (horizontal translation) is a condition where a dowel is not placed at the required spacing from the surrounding dowels (Dowels are placed 12-inch on center). Horizontal misalignment (skew) mean if the dowel is laid skewed rather than perpendicular to the transverse joint. Vertical misalignment (tilt) corresponds to a dowel that is placed with a vertical tilt (one end of the dowel is deeper than the other).

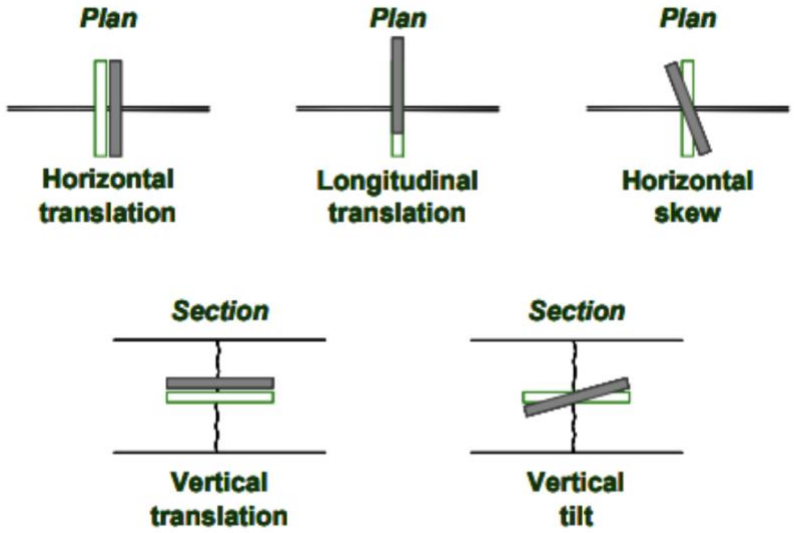

Figure 11 Dowel bar misalignment cases (Tayabji 1986)

It is worth noting that the concrete pavement performance is not heavily impacted unless there is a systematic dowel bar misalignment. The data in Table 11 displays a satisfactory dowel bar alignment with no systematic misalignments. This data can be used in conjunction with FWD data collected over time at these joint locations where the calculated load transfer efficiency (LTE) can be related to the misalignments observed.

Field Tests

The MDOT conducted different field tests on different layers of all four projects to estimate their in-field moduli. The field tests included light weight deflectometer (LWD), dynamic cone penetrometer (DCP), and falling weight deflectometer (FWD). This section presents the analyses of all the available data for each of these field tests.

Light Weight Deflectometer (LWD) Data Analysis

Light weight deflectometer (LWD) tests were conducted on each pavement foundation layer (base, subbase, subgrade layers). Results of LWD tests were analyzed to estimate elastic moduli of each pavement foundation layer. The following equation was used to calculate the force applied during the test (per drop) [18].

$$F_{LWD} = \sqrt{2mghC} \qquad \text{Equation 1}$$

where F_{LWD} is the force applied by the LWD equipment (lb), m is the drop mass (22 lb), g is the acceleration due to gravity (32.17 ft/s^2), h is the drop height (19.7 inches), and C is the spring constant (267290 lb/ft) [18]. The following Boussinesq's elastic half-space equation was used to determine the LWD elastic modulus [18].

$$E_{LWD} = \frac{(1 - v^2)\sigma_0 r}{d_0} f \qquad \text{Equation 2}$$

where E_{LWD} is the LWD elastic modulus; v is the Poisson's ratio [0.35 and 0.40 for tests performed on base and subgrade layers, respectively]; σ_0 is the applied stress (ksi); r is the radius of the plate (12 inches); d_0 is the average deflection (mm); and f is the shape factor [8/3 (rigid plate on granular material) and $\pi/2$ (rigid plate on material with intermediate characteristics) for tests performed on base and subgrade layers, respectively] [18].

I-475 HMA Project

Table 12 presents the descriptive statistics for the elastic moduli of unbound layers that were estimated using the LWD data for the I-475 project. Figure 12 compares the different layer moduli calculated for the inner (IL) and outer lanes (OL) of the various test sections for both the long-life and standard sections. It is observed that the subgrade moduli vary significantly along the NB direction while such differences were not observed between the IL and OL for the same sections. However, it was noticed that the subgrade moduli for both the NB and SB TS-3s are higher and more variable than that of TS-1 and TS-2.

Figure 12 provides a graphical comparison of the elastic modulus of test sections from LWD tests. Except for the TS-1 of the SB pavement, the variability of the subbase is not significant. Base moduli values do not vary much within the NB sections and have higher elastic moduli than the standard design pavement sections. Higher variation is observed for base moduli of the SB standard pavement sections. TS-2 and TS-3 have the highest base moduli among all the standard and long-life sections. The LWD data derived moduli are low owing the small mass used by the device which results in a low stress application and hence, lower moduli are estimated.

Table 12 Descriptive statistics of layer moduli obtained using LWD data – I-475 HMA project

Layer	Test section	Number of drops	Mean	Standard deviation	Minimum	Maximum
Long-life/ Northbound						
Subgrade modulus (ksi)	TS1	20	2.272	0.883	0.680	4.139
	TS2	22	1.107	0.474	0.570	1.913
	TS3	20	4.301	2.091	0.924	8.742
Subbase modulus (ksi)	TS1	22	4.895	0.446	4.020	5.826
	TS2	20	3.898	0.634	2.666	5.534
	TS3	22	4.122	0.498	2.953	4.830
Base modulus (ksi)	TS1	22	12.533	1.826	8.470	16.580
	TS2	22	11.823	1.820	7.997	13.942
	TS3	22	13.271	1.352	10.871	16.390
Standard/ Southbound						

Subgrade modulus (ksi)	TS1	22	1.367	1.112	0.460	3.819
	TS2	22	1.450	0.904	0.431	3.294
	TS3	22	4.603	3.131	0.493	11.262
Subbase modulus (ksi)	TS1	22	6.342	0.850	4.559	8.588
	TS2	22	4.180	0.400	3.378	4.902
	TS3	22	3.966	0.339	3.129	4.868
Base modulus (ksi)	TS1	22	7.279	1.802	3.256	10.603
	TS2	22	14.652	2.386	10.323	20.546
	TS3	22	9.188	0.959	7.808	11.212

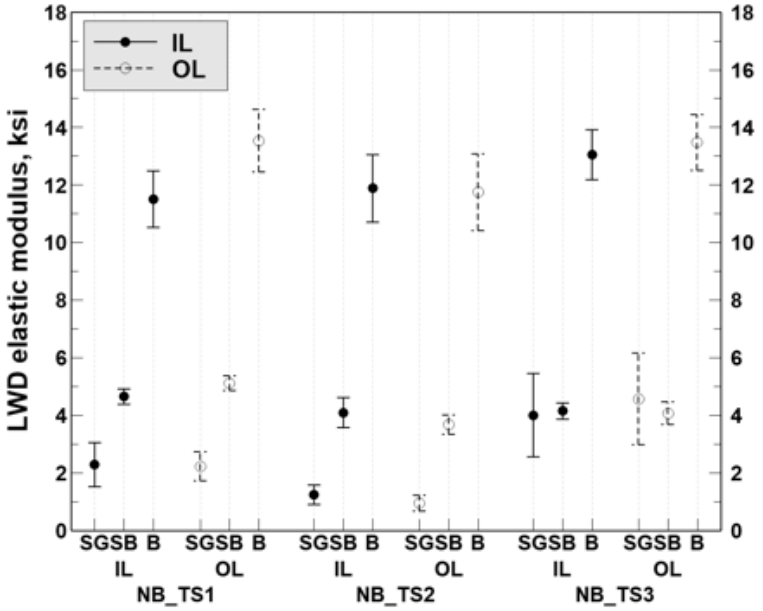

(a) Northbound long-life design

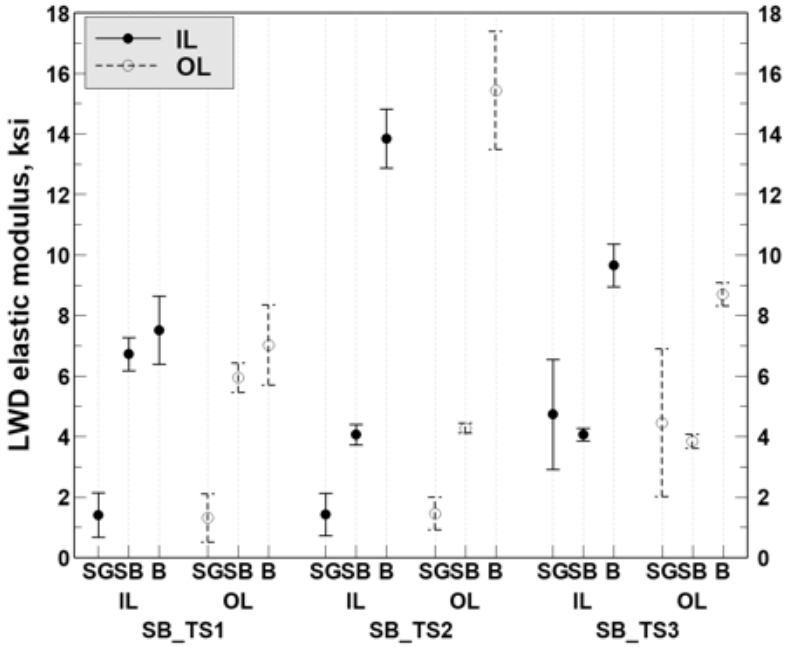

(b) Southbound standard design

Figure 12 Interval plots comparing subgrade (SG), subbase (SB), and base (B) moduli values between different lanes and test sections of the Northbound (NB) long-life and Southbound (SB) standard design pavements – I-475 HMA project

US-131 HMA Project

Subgrade and base layer moduli of test sections in US-131 HMA project calculated using LWD data are reported in Table 13. No records were available for the subbase layer. Figure 13 shows the interval plots for each inner (IL) and outer lane (OL). Subgrade moduli of each test section on the long-life sections do not vary significantly. The base moduli values also exhibit less variation except for the TS-3 (long-life) and TS-4 (standard) where the base moduli are significantly different between the ILs and OLs.

Table 13 Descriptive statistics of layer moduli obtained using LWD data – US-131 HMA project

Layer	Test section	Design	Number of drops	Mean	Standard deviation	Minimum	Maximum
Subgrade modulus (ksi)	TS1	Long-life	7	6.069	1.020	3.957	7.164
	TS2		22	3.874	2.447	0.489	10.764
	TS3		6	3.710	2.096	1.364	7.418
	TS4	Standard	Nil	-	-	-	-
Base modulus (ksi)	TS1	Long-life	22	10.752	2.420	6.971	15.730
	TS2		22	11.695	2.267	7.086	15.846
	TS3		22	13.340	2.422	8.658	16.973
	TS4	Standard	22	12.664	3.068	8.891	19.608

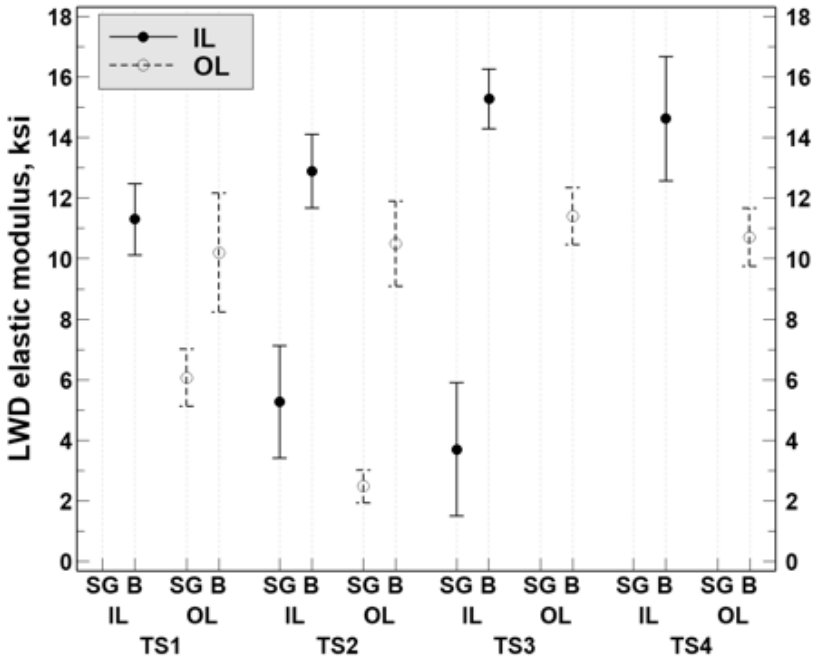

Figure 13 Interval plots comparing subgrade (SG) and base (B) moduli values between different lanes and test sections of the long-life (TS-1 through TS-3) and standard (TS-4) design pavements – US-131 HMA project

I-69 JPCP Project

Table 14 contains the descriptive statistics of the pavement foundation layer moduli (calculated from LWD data) of test sections at I-69 project. A higher variability is observed for the subbase moduli of TS-4 of the long-life WB section. The base layer is also displaying a higher variation for all long-life test sections (see Figure 14).

Table 14 Descriptive statistics of layer moduli obtained using LWD data – I-69 JPCP project

Layer	Test Section	Number of drops	Mean	Standard deviation	Minimum	Maximum
Standard/ Eastbound						
Subbase modulus (ksi)	TS1	61	3.219	1.748	0.920	7.402
Base modulus (ksi)	TS2	60	3.698	1.402	1.035	6.240
Long-life/ Westbound						
Subgrade modulus (ksi)	TS3	37	3.933	2.970	0.582	13.086
Subbase modulus (ksi)	TS4	44	15.030	15.650	1.890	33.281
Base modulus (ksi)	TS3	19	14.200	7.100	8.180	37.990
	TS4	18	15.070	7.120	6.590	30.020
OGDC (ksi)	TS3	18	16.340	8.511	6.940	35.781
Note: OGDC = Open Graded Drainage Course.						

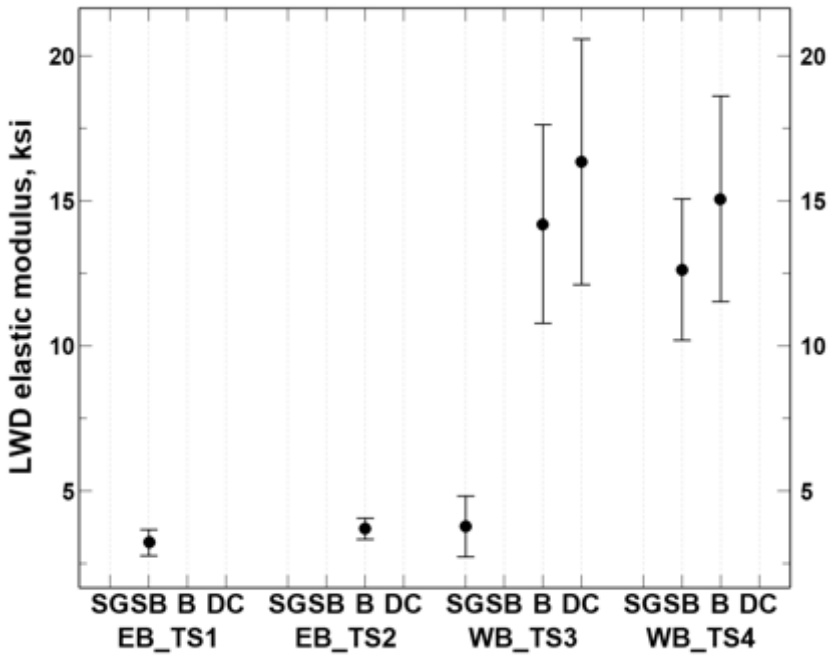

Figure 14 Interval plots comparing subgrade (SG), subbase (SB), base (B), and open-graded drainage coarse (DC) moduli values between different Eastbound (EB) standard and Westbound (WB) long-life design pavements – I-69 JPCP project

US-131 JPCP Project

Table 15 presents the descriptive statistics for the pavement foundation layer moduli (calculated from LWD data) of the test sections at US-131 JPCP project. Figure 15 displays that the subgrade moduli of the NB long-life sections are generally lower than that of the SB standard sections. It is also observed that the subgrade, subbase, and open-graded drainage coarse (OGDC) moduli do not vary significantly for the standard design sections (Figure 15).

Table 15 Descriptive statistics of layer moduli obtained using LWD data – US-131 JPCP project

Layer	Test section	Number of drops	Mean	Standard deviation	Minimum	Maximum
Long-life/ Northbound						
Subgrade modulus (ksi)	TS1	22	4.012	0.910	2.596	6.324
	TS2	22	2.964	0.677	1.506	4.181
Subbase modulus (ksi)	TS1	22	6.349	1.696	3.416	9.541
Base modulus (ksi)	TS1	22	11.327	1.517	8.621	14.456
OGDC (ksi)	TS1	22	10.295	1.264	8.353	13.761
Standard/ Southbound						
Subgrade modulus (ksi)	TS1	12	5.608	1.001	4.450	8.234
	TS2	12	5.057	1.557	1.603	7.938
	TS3	12	4.093	1.590	2.118	6.976
Subbase modulus (ksi)	TS1	22	5.578	1.533	3.617	8.744
	TS1	22	6.874	2.224	1.181	10.523

	TS2	21	6.390	3.013	2.490	11.181
OGDC (ksi)	TS1	22	11.253	1.228	8.834	13.210
	TS2	22	9.591	1.791	7.004	12.554
	TS3	22	9.483	0.913	7.467	10.787

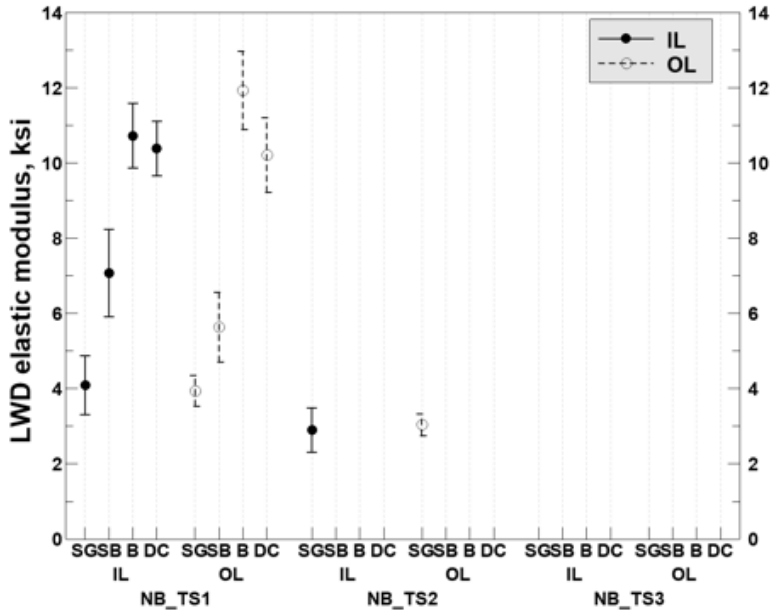

(a) Northbound long-life design

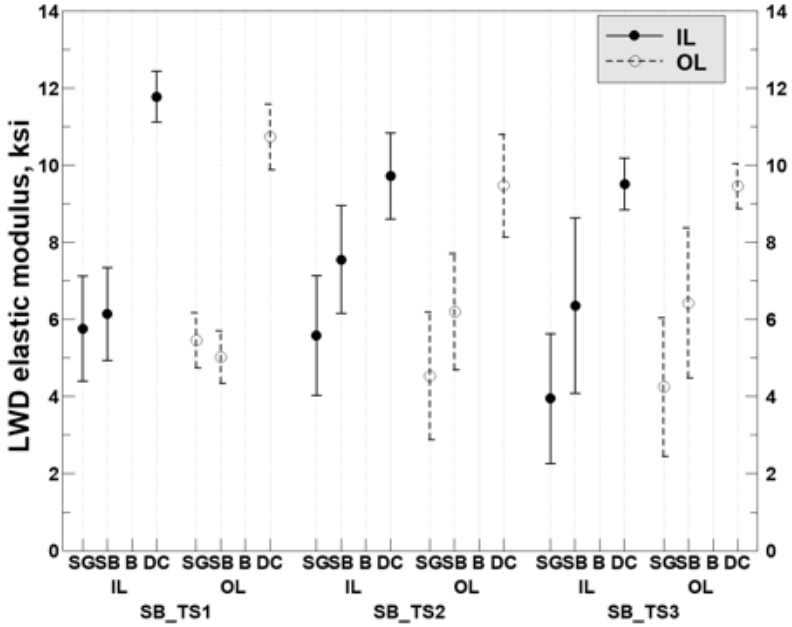

(b) Southbound standard design

Figure 15 Interval plots comparing subgrade (SG), subbase (SB), base (B), and open-graded drainage coarse (DC) moduli values between different lanes and test sections of the Northbound (NB) long-life and Southbound (SB) standard design pavements – US-131 JPCP project

Falling Weight Deflectometer (FWD) Data Analysis

This section summarizes the back-calculated layer moduli for I-475 HMA and US-131 HMA sections and back-calculated layer moduli, LTE and k-values for I-69 JPCP, and US-131 JPCP projects using FWD deflection data. The team used FWD test results on flexible pavement sections (US-131 and I-475) to quantify the spatial variability of the moduli of asphalt, base and subgrade layers. The team could not to make conclusions about the relative performance of long-life and standard sections. This is because FWD tests on long life sections and standard sections were done at different dates (sometimes months apart) and subsurface temperature profiles were not measured. Subsurface temperature profiles can potentially be quite different even if the surface temperatures are the same and subsurface temperature profiles depend on the climatic conditions of previous days. When subsurface temperature profiles are not known, it is not possible to reconcile the differences in the back calculated moduli of AC layers of long life and standard sections.

I-475 HMA Project

For the I-475 HMA project, FWD measurements were available for each of the AC layers (i.e., wearing course (WC), leveling course (LC), and base course (BC)) in both directions (i.e., northbound (NB) for long-life design, and southbound (SB) for standard design). The back-calculation results for the WC only are presented herein, while the results of the LC and BC AC layers can be found in Appendix A. The back-calculation was performed using MODULUS software on a 3-layer pavement structure, where the base and the subbase layers were combined. The descriptive statistics of the results obtained for the I-475 HMA project are summarized in Table 16, while Figure 16 displays the spatial variation within the layer moduli values for TS1 NB. A negligible variation in the AC layer moduli within each lane and between the lanes was observed. On the other hand, base and subgrade layers resulted in considerable differences between their back-calculated moduli at different stations within the section. Similar plots for all the sections of the project can be found in Appendix A.

Figure 17 illustrates the back-calculated AC layer moduli for the I-475 HMA project between different lanes of each test section for both the long-life (NB) and standard (SB) pavement sections. It is observed that moduli of the AC layer in the standard sections are higher than those in the long-life sections. Moreover, high variability was observed in the NB TS-1 and SB TS-2 between the inner and outer lanes. The difference between the NB and SB sections can be attributed to the different pavement temperature conditions during FWD measurements (Figure 17(b)).

As mentioned earlier, a 3-layered structure with combined base and subbase layers was used for moduli back-calculation. Here following, the combined unbound layers will be referred to as ‘Base’. Higher base moduli for the NB TS-1 compared to the other sections (Figure 18), and an overall low variability was observed for both ILs and OLs except for the TS-1 of the SB direction. Generally, the base moduli obtained from the back-calculation are between 25,000 to 40,000 psi. This range is acceptable considering that a base resilient modulus of 33,000 psi is used by MDOT at the design stage in the AASHTOWare Pavement-ME software

Table 16 Descriptive statistics - I-475 HMA project back-calculated layer moduli

Design/ direction	FWD measured on	Lane	Layer	No. of FWD points	Mean (ksi)	Std. Dev. (ksi)	Minimum (ksi)	Maximum (ksi)
Test section 1 (650+00 – 660+00)								
Long-life/ NB	WC	IL	AC	11	577.98	32.41	537.93	644.37
		OL	AC	11	635.68	23.54	608.50	666.80
		IL	Base/SB	11	39.63	7.94	27.50	51.83
		OL	Base/SB	11	42.52	8.53	27.80	52.80
		IL	SG	11	26.51	4.68	17.60	32.20
		OL	SG	11	24.00	4.15	14.80	27.93
Standard/ SB	WC	IL	AC	11	994.7	97.4	890.7	1192.2
		OL	AC	11	932.6	65.7	890.0	1092.6
		IL	Base/SB	11	41.23	7.04	26.93	51.77
		OL	Base/SB	11	27.53	4.28	21.77	35.80
		IL	SG	11	14.49	2.173	12.70	19.53
		OL	SG	11	16.52	2.637	12.53	21.63
Test section 2 (745+00 – 755+00)								
Long-life/ NB	WC	IL	AC	11	579.8	37.5	514.4	633.2
		OL	AC	11	590.12	22.47	552.73	629.20
		IL	Base/SB	11	28.75	3.82	24.20	34.77
		OL	Base/SB	11	31.62	2.69	27.23	35.00
		IL	SG	11	23.82	7.88	13.83	36.07
		OL	SG	11	24.87	4.93	15.30	32.50
Standard/ SB	WC	IL	AC	11	844.7	44.9	754.8	896.0
		OL	AC	11	933.3	70.7	841.2	1037.2
		IL	Base/SB	11	32.23	6.52	19.93	41.27
		OL	Base/SB	11	27.97	6.07	20.10	36.53
		IL	SG	11	13.34	2.83	8.83	17.86
		OL	SG	11	13.34	3.02	8.50	17.36
Test section 3 (770+00 – 780+00)								
Long-life/ NB	WC	IL	AC	11	537.34	25.00	492.20	579.27
		OL	AC	11	549.32	17.44	522.23	574.67
		IL	Base/SB	11	25.28	3.01	20.76	29.96
		OL	Base/SB	11	25.62	2.79	20.06	29.83
		IL	SG	11	22.76	2.43	18.56	28.50
		OL	SG	11	23.72	3.91	20.63	34.67
Standard/ SB	WC	IL	AC	11	995.4	178.7	697.9	1172.7
		OL	AC	11	1094.0	48.4	1008.6	1168.7
		IL	Base/SB	11	37.93	7.32	23.70	48.40
		OL	Base/SB	11	32.56	6.55	20.03	42.23
		IL	SG	11	17.65	2.43	13.66	21.20
		OL	SG	11	17.93	2.57	14.20	22.16

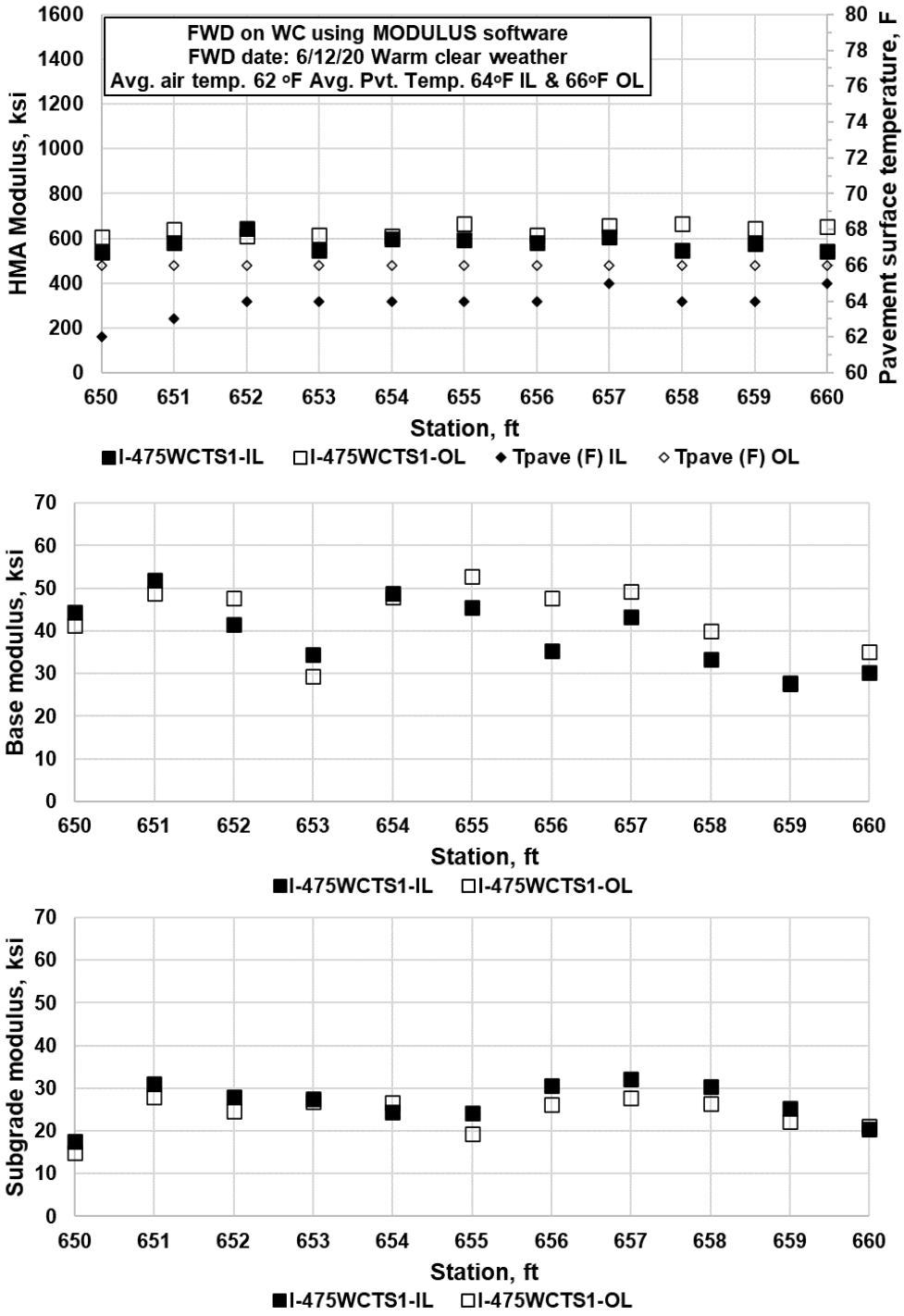

Figure 16 Spatial variation of back-calculated moduli within lanes for I-475 TS1 NB using MODULUS and deflections measured on wearing course

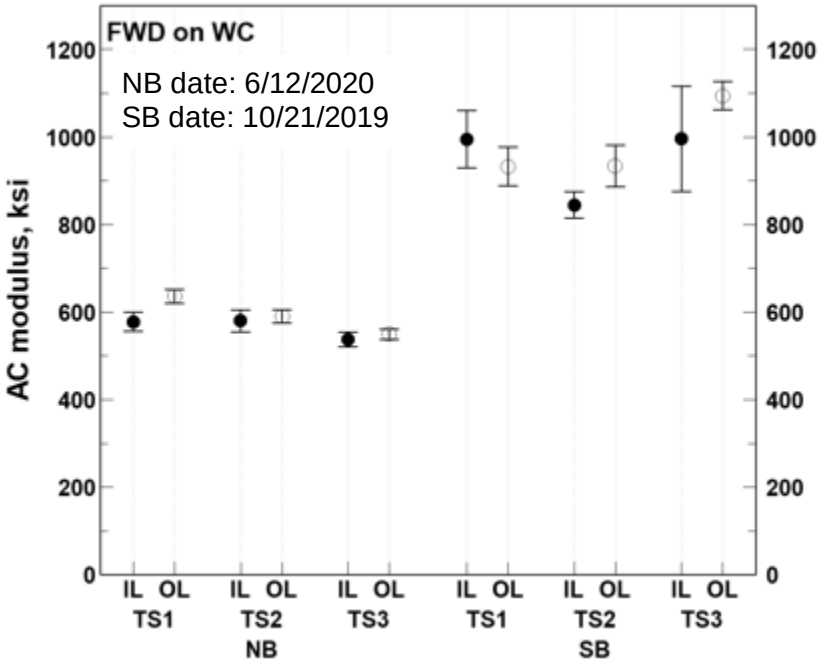

(a) Back-calculated AC moduli values

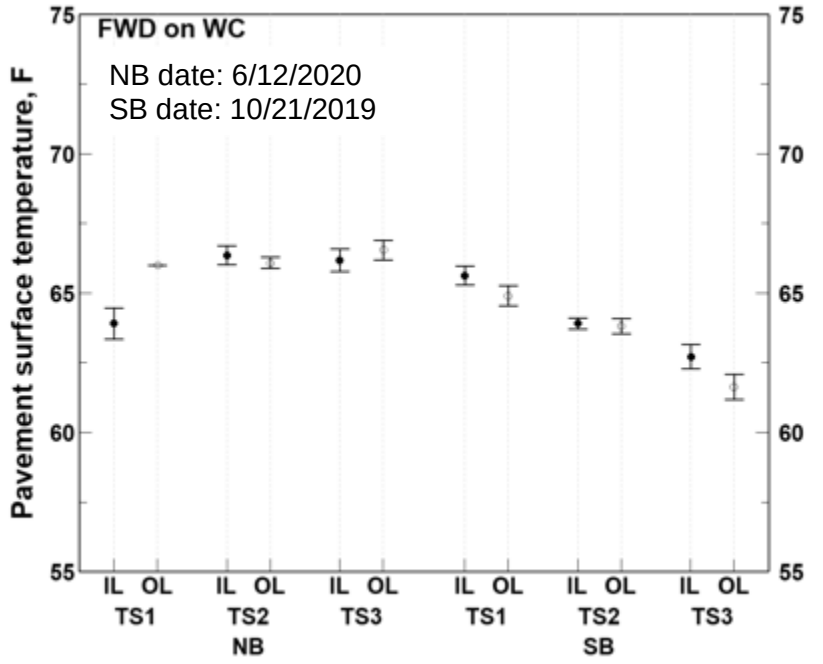

(b) Recorded pavement surface temperatures

Figure 17 Comparison between backcalculated AC moduli values – I-475 HMA standard and long-life pavement sections along with recorded surface temperatures

For subgrade (Figure 18), higher moduli were backcalculated for the long-life NB sections as compared to the standard (SB) sections. However, the NB direction showed also higher variability. The subgrade moduli values for the long-life sections along the NB direction are about 25,000 psi while these are between 14,000 to 18,000 psi for the standard design sections along the

SB direction. Although subgrade values variate spatially within a pavement lane, these are consistent between the inner and outer lanes on each test section.

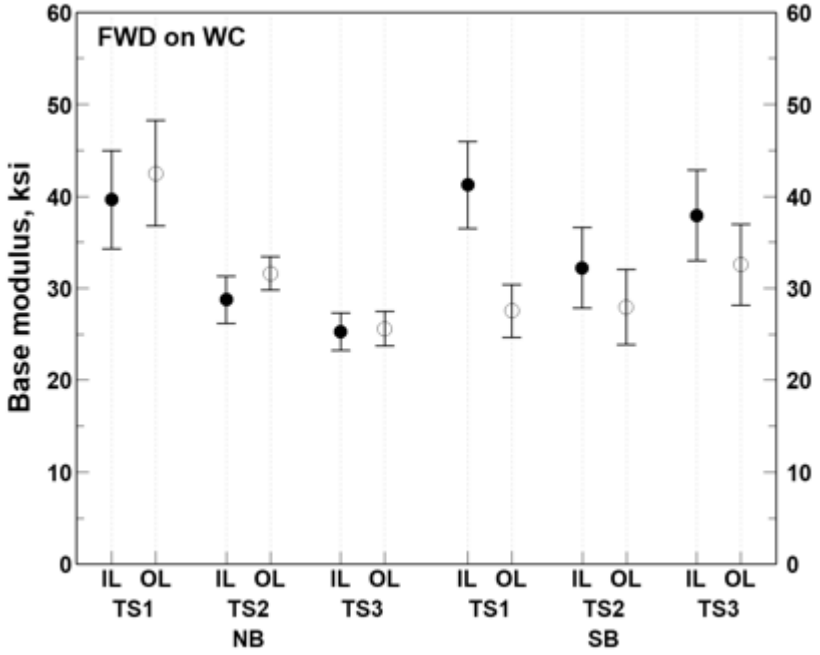

(a) Base moduli values

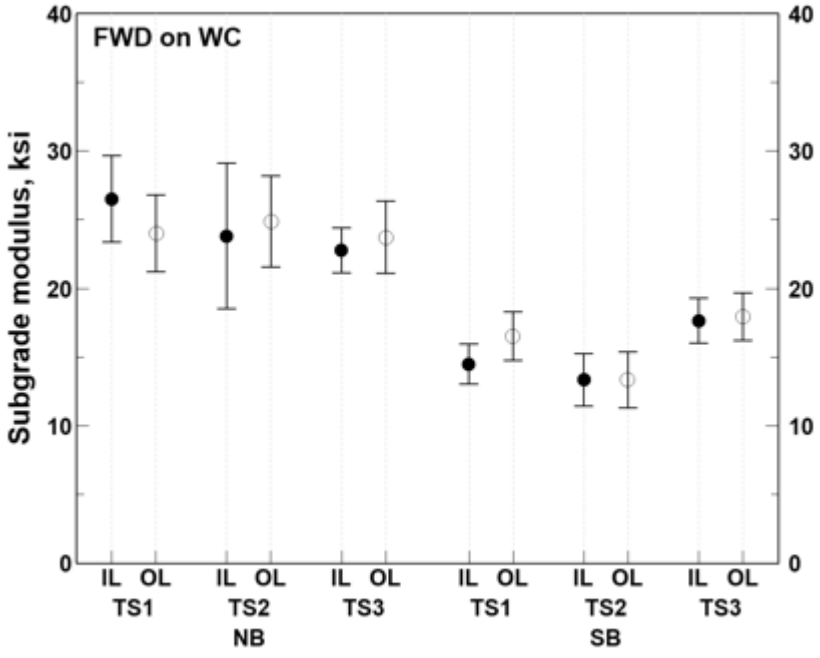

(b) Subgrade moduli values

Figure 18 Comparison between backcalculated base and subgrade moduli values – I-475 HMA standard and long-life pavement sections

US-131 HMA Project

For the US-131 30-year HMA project, FWD measurements were available for each of the AC layers (i.e., WC, LC, and BC) and all sections of the project. The results based on the FWD deflections measured over the WC are summarized herein, and other results are available in Appendix A. Table 17 and Figure 19 illustrate the descriptive statistics of the back-calculated layer. It can be noticed that the moduli for TS-1 and 3 (long-life pavement sections) significantly vary between the inner and the outer lanes. Additionally, outer lanes have higher AC layer moduli as compared to the inner lanes. This may be attributed to the lower surface temperatures recorded at the time of FWD testing at the outer lanes, as displayed in Figure 19b

Table 17 Descriptive statistics – back-calculated layer moduli for US-131 HMA project

Design/ direction	Test section	Lane	Layer	No. of FWD points	Mean (ksi)	Std. Dev. (ksi)	Minimum (ksi)	Maximum (ksi)
Long-life/ NB	TS1	IL	AC	11	1069.6	101.5	938.6	1245.0
		OL	AC	11	1209.7	57.7	1149.1	1335.1
		IL	Base/SB	11	38.84	10.71	24.73	62.03
		OL	Base/SB	11	48.35	13.16	22.80	70.87
		IL	SG	11	22.18	4.71	17.20	31.53
		OL	SG	11	26.21	5.93	21.47	40.87
Long-life/ NB	TS2	IL	AC	11	1112.0	90.8	958.4	1281.4
		OL	AC	11	1160.6	66.4	1057.9	1265.2
		IL	Base/SB	11	38.99	6.10	30.37	51.87
		OL	Base/SB	11	42.11	4.89	36.03	49.30
		IL	SG	11	23.06	8.73	14.27	42.13
		OL	SG	11	23.49	6.76	15.37	37.00
Long-life/ NB	TS3	IL	AC	11	1074.2	73.8	1005.1	1222.4
		OL	AC	11	1173.8	48.9	1086.4	1234.3
		IL	Base/SB	11	32.20	7.34	19.97	40.47
		OL	Base/SB	11	56.25	11.09	33.87	79.10
		IL	SG	11	20.89	4.01	16.47	28.67
		OL	SG	11	22.28	3.91	18.60	32.77
Standard/ NB	TS4	IL	AC	11	1135.9	138.6	1012.5	1479.4
		OL	AC	11	1237.5	126.0	1003.8	1428.0
		IL	Base/SB	11	41.36	5.92	32.30	50.13
		OL	Base/SB	11	45.24	5.97	36.17	54.87
		IL	SG	11	16.47	4.50	10.23	25.70
		OL	SG	11	17.86	5.13	11.93	26.77

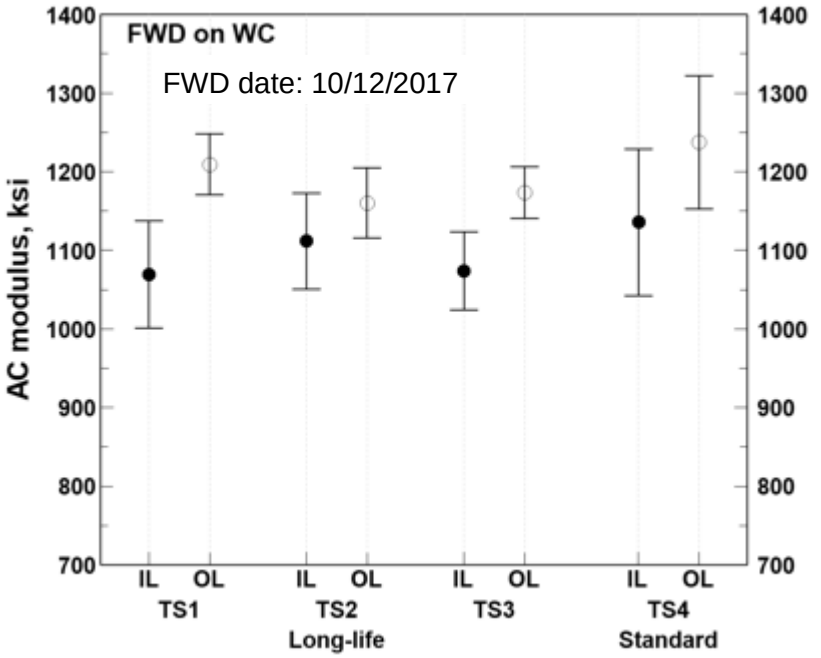

(a) Backcalculated AC moduli values

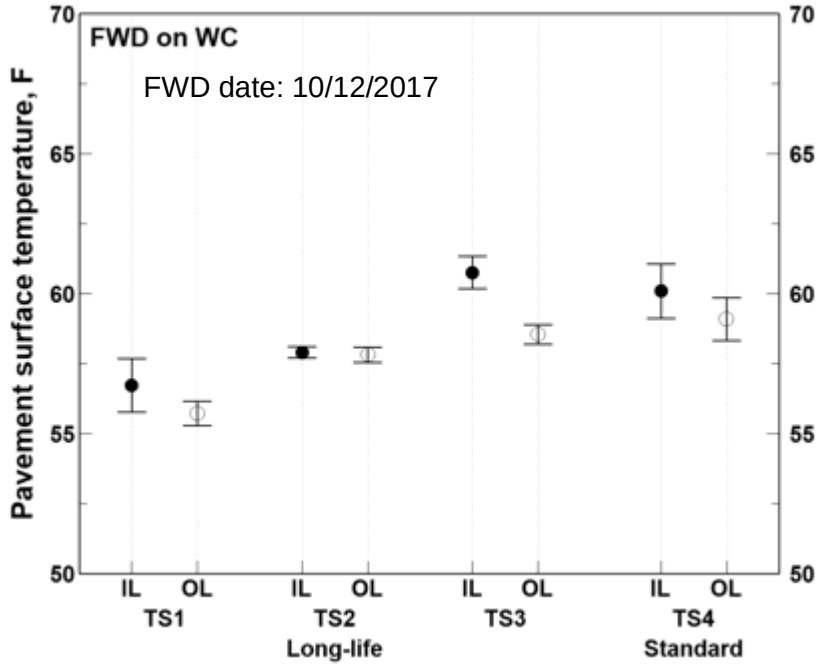

(b) Recorded pavement surface temperatures

Figure 19 Comparison between backcalculated AC moduli values – US-131 HMA standard and long-life pavement sections along with recorded pavement temperatures during FWD testing

Figure 20 illustrates the comparison of the back-calculated base and subgrade layer moduli values for the standard and the long-life pavement sections of the US-131 HMA project. The base moduli values show a significant difference between the inner and outer lanes of TS-3 of the long-life pavement section while they do not vary between the different lanes of the remaining test

sections. The back-calculated base moduli values range between 35,000 to 50,000 psi, higher than the 33,000 psi commonly used by MDOT.

The subgrade moduli display higher variability between the different lanes of TS-1 and 2 as compared to the other two sections as seen in Figure 20. However, the mean subgrade modulus value for either pavement lane of the long-life pavement sections ranges between 22,000 to 26,000 psi while it is around 18,000 psi for TS-4 (standard design section). In all cases, these values are 3 to 4 times higher than the typical subgrade modulus value of 5,000 psi used by the MDOT in the design process. Higher stress application through an FWD device results in higher MR values as compared to the other in-situ tests.

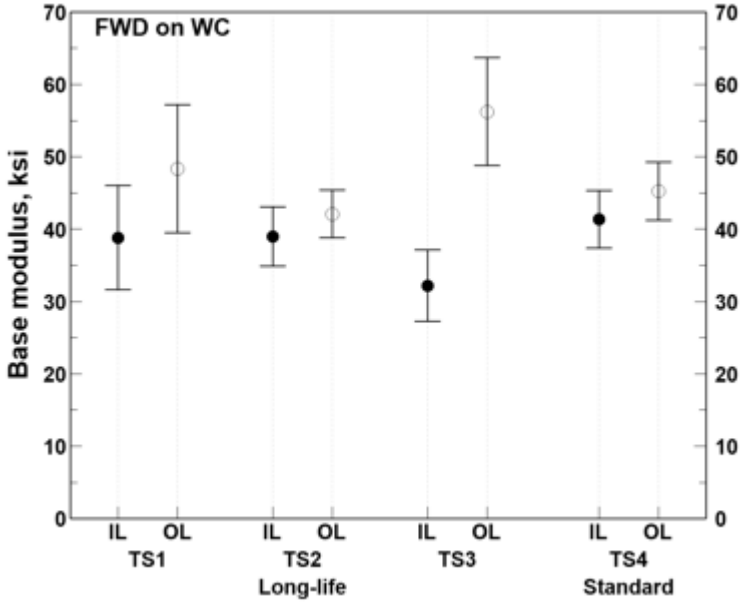

(a) Base moduli values

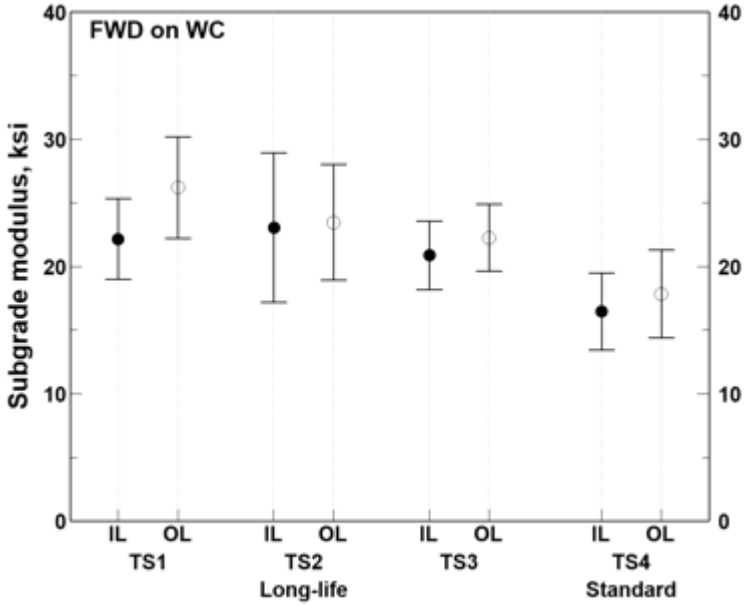

(b) Subgrade moduli values

Figure 20 Backcalculated base and subgrade moduli values - US-131 HMA long-life and standard pavement sections

The AREA method was used for the back-calculation of the PCC layer modulus and the coefficient of subgrade reaction (*k*-value) for the FWD data of the I-69 JPCP project. Descriptive statistics of the calculated PCC slab elastic modulus (Epcc), modulus of subgrade reaction (*k*-value), and load transfer efficiency (LTE) determined from the available FWD mid-slab and joint deflections are available in Table 18. Spatial plots for each of the FWD-related parameters (E, *k*-, and LTE values) for each lane of all the sections of the I-69 JPCP project are instead reported in Appendix A.

The elastic moduli for the PCC slab for the long-life sections are generally higher than those for the standard pavement sections (Figure 21(a)), while the Epcc and *k*-values for all the lanes for the standard pavement sections are comparable. However, there is a significant difference between the PCC slab moduli values for the middle and outer lanes for the long-life TS-4. It was also observed that the *k*-value for the outer lane of the long-life TS-3 and inner lane of TS-4 differs significantly from other lanes of the corresponding pavement sections. Figure 22 shows the estimated load transfer efficiency (LTE) for the standard and long-life pavement sections and the pavement surface temperatures. The LTE values for the standard sections are consistently lower as compared to the long-life sections, and their variability is significantly larger too. This may be explained by the difference in the pavement temperature profiles. Standard sections may have a cooler temperature on the surface than the bottom of the slab. Typically, if the temperatures are cooler on top than the bottom, the slab curls up and the edges may be unsupported. As a result, the deflections may be higher and LTE may be lower than slabs that are flat or curled down.

Table 18 Descriptive statistics for Epcc, *k*-value, and LTE - I-69 JPCP project

Design/ Direction	Test Section	Lane	No. of FWD points	Mean	Std. Dev.	Minimum	Maximum
Epcc (ksi)							
Standard/ EB	TS1	IL	13	5766	386	5070	6506
		ML	13	5627	543	5045	6961
		OL	13	6127	465	5353	6910
Standard/ EB	TS2	IL	13	5854	1108	4435	8080
		ML	12	6619	1199	5302	9851
		OL	13	6331	675	5495	7792
Long-life/ WB	TS3	IL	12	9950	1203	8210	11748
		ML	11	10891	958	9434	12594
		OL	11	8248	1039	6701	9631
Long-life/ WB	TS4	IL	14	7522	621	6604	8344
		ML	14	6979	961	4775	8595
		OL	14	9137	1319	6880	12137
***k*-value (pci)**							
Standard/ EB	TS1	IL	13	338.5	44.1	250.0	417.7
		ML	13	340.4	52.1	250.6	442.3
		OL	13	309.1	30.5	251.1	367.4
Standard/ EB	TS2	IL	13	329.1	69.3	216.8	412.8
		ML	12	330.8	68.8	205.3	426.5
		OL	13	344.7	59.5	265.2	478.5
Long-life/ WB	TS3	IL	12	495.4	73.9	403.3	599.7
		ML	11	498.6	62.9	413.8	589.2
		OL	11	359.2	45.6	285.7	423.0
Long-life/ WB	TS4	IL	14	703.5	156.6	489.9	1076.2
		ML	14	553.5	120.6	390.1	789.7
		OL	14	512.3	118.9	305.4	753.8
LTE (%)							
Standard/ EB	TS1	IL	24	76	14.19	38	93
		ML	26	69	15.44	45	94
		OL	25	70	14.40	48	93
Standard/ EB	TS2	IL	26	76	14.23	50	94
		ML	26	75	11.45	46	93
		OL	26	79	8.86	62	94
Long-life/ WB	TS3	IL	36	88	0.97	86	90
		ML	36	88	1.08	86	90
		OL	22	83	5.69	72	90
Long-life/ WB	TS4	IL	14	86	4.14	77	91
		ML	14	86	3.97	78	92
		OL	40	81	7.26	61	90

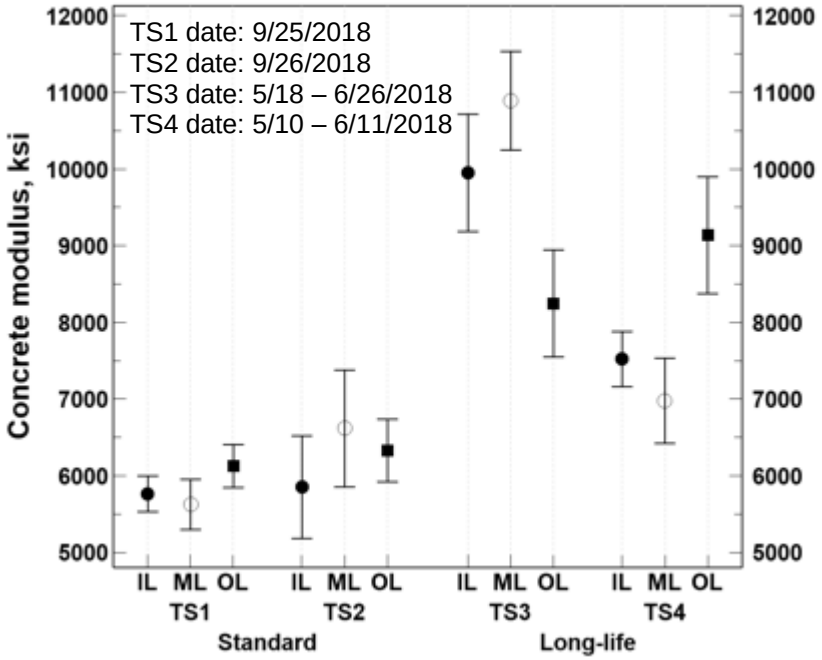

(a) Concrete elastic modulus

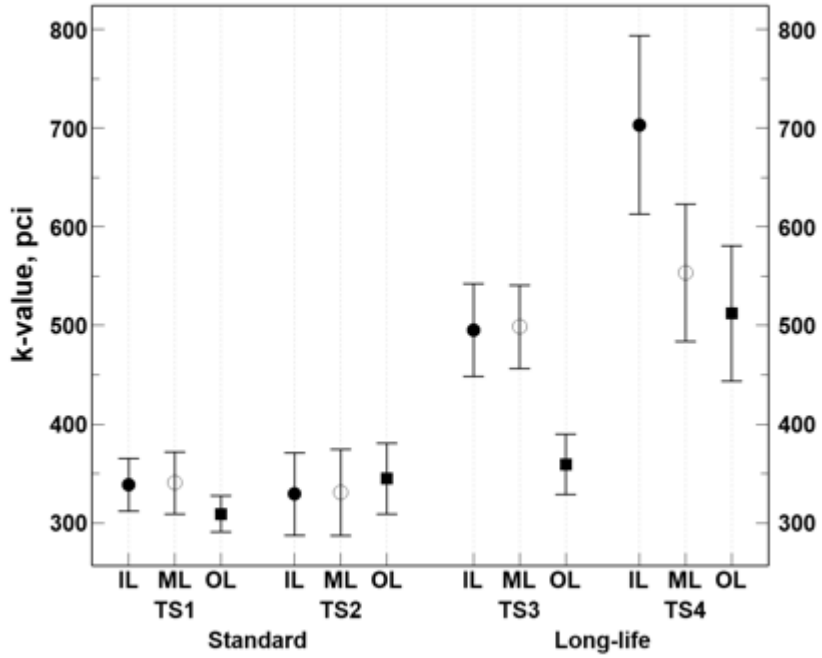

(b) Modulus of subgrade reaction (*k*-value)

Figure 21 Concrete elastic modulus and *k*-values for I-69 JPCP project

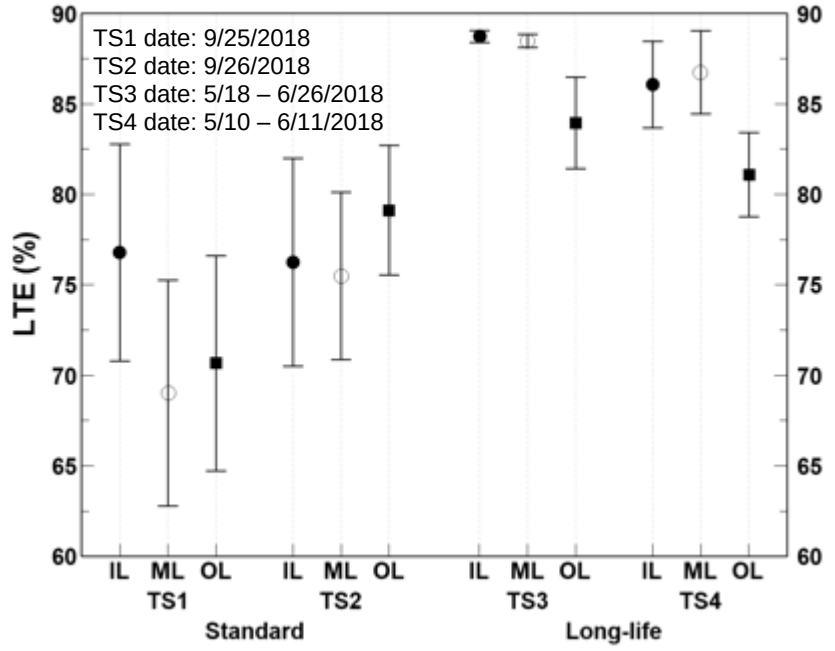

(a) Load transfer efficiency, LTE

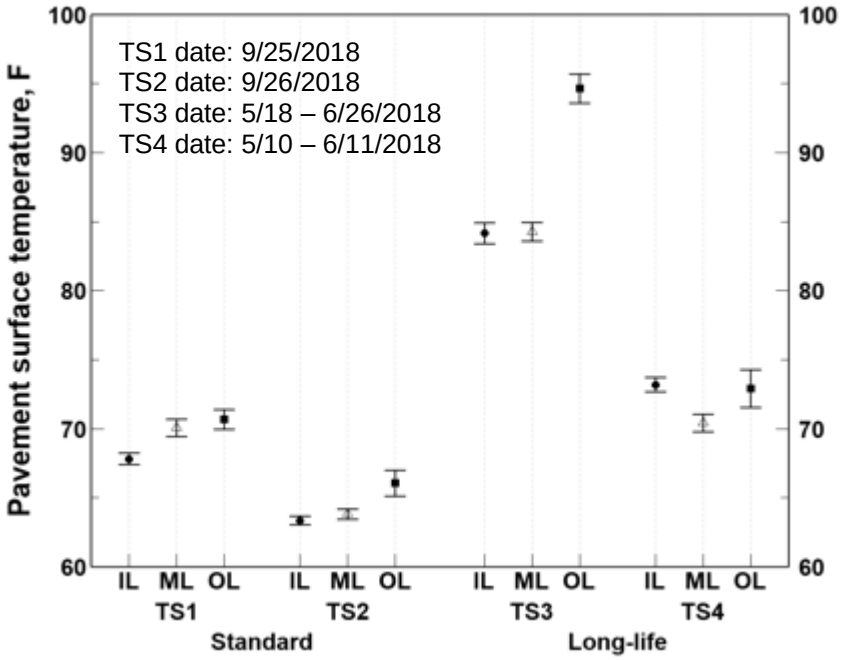

(b) Pavement surface temperature during FWD testing

Figure 22 LTE and pavement surface temperatures recorded during FWD testing: I-69 JPCP project

US-131 JPCP Pavement Project

The FWD deflections data for the US-131 JPCP project was collected on stations between the TS1 and TS2 of the SB, and TS2 only for NB sections two years after the construction. The

FWD testing was conducted in the right lane in two rounds at two different times of the same day. Round 1 was conducted between 9-11 am while Round 2 took place between 12-2 pm. The concrete layer modulus (Epcc), modulus of subgrade reaction (k-value), and load transfer efficiency are summarized in Table 19.

Table 19 Descriptive statistics for Epcc, *k*-value, and LTE – US-131 JPCP project

Design/ Direction	Test Section	Time	No. of FWD points	Mean	Std. Dev.	Minimum	Maximum
Epcc (ksi)							
Long-life/ NB	TS2	am	6	16017	2458	13138	19005
		pm	6	13244	1935	10428	15027
Standard/ SB	n/a	am	8	7839	800	7021	9527
		pm	8	7150	700	6152	8598
***k*-value (pci)**							
Long-life/ NB	TS2	am	6	350	120	200	528
		pm	6	370	64	262	442
Standard/ SB	n/a	am	8	424	24	383	449
		pm	8	380	27	347	417
LTE (%)							
Long-life/ NB	TS2	am	13	92	1.4	90	96
		pm	14	91	1.0	89	92
Standard/ SB	n/a	am	8	92	2.4	86	94
		pm	8	92	0.5	91	93

"n/a" = FWD conducted on stations between TS1 and TS2.

Figure 23 shows a comparison between the elastic modulus of the concrete slab between Round 1 and 2. A significant difference was found between the concrete elastic modulus of the NB TS-2 and SB section regardless of the time of the day. The presence of a CTPB under the concrete slab on the long-life NB section could be a possible reason for such a high Epcc values. Figure 23 also displays the dynamic *k*-values between the two sections, with SB section values higher than those recorded in the NB TS-2. This can be explained by the difference in the pavement surface temperatures during the FWD testing (Figure 24). The lower temperatures may have caused the concrete slab to curl up, ensuring full mid-slab contact with the base, hence reducing the deflections. However, the LTE of either section is comparable, and does not display any considerable difference even though the testing temperatures vary significantly.

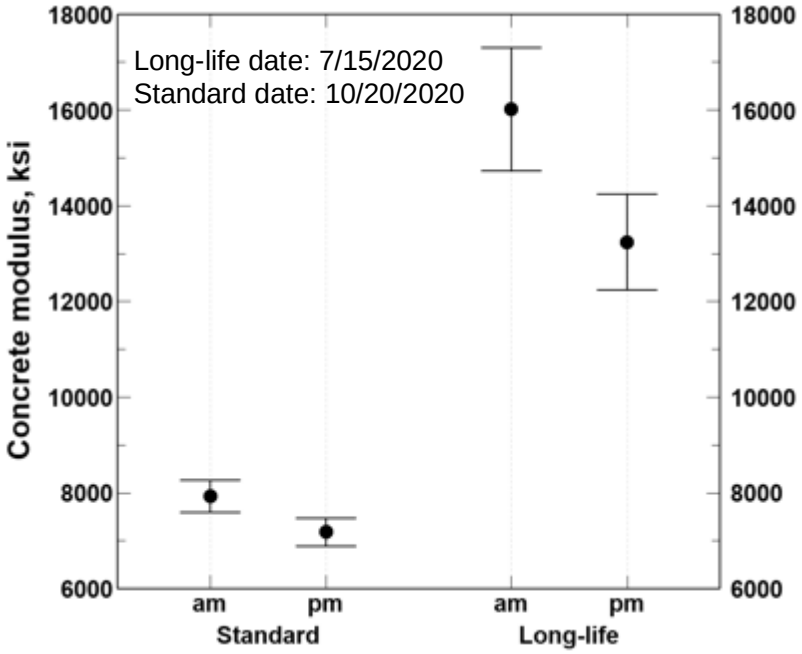

(a) Elastic modulus of concrete slab

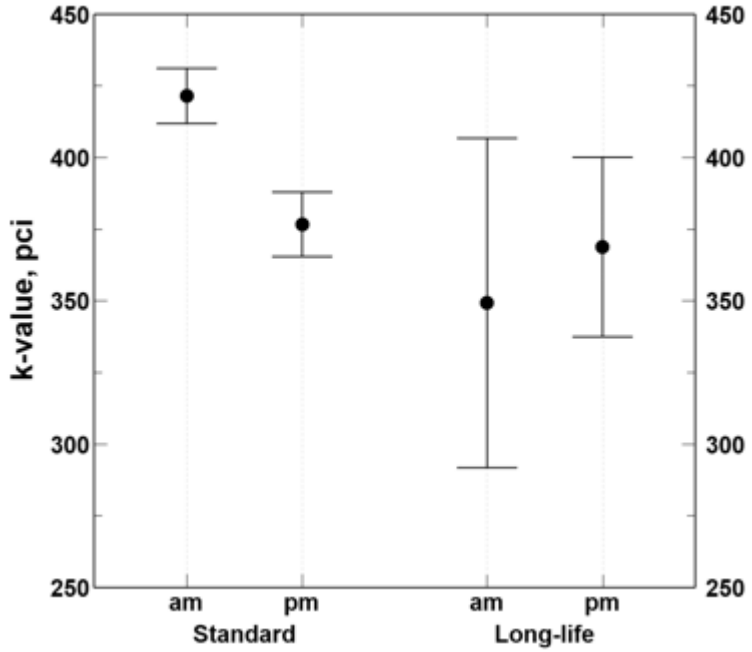

(b) Modulus of subgrade reaction (*k*-value)

Figure 23 Comparison between concrete elastic modulus and *k*-value – US-131 JPCP project

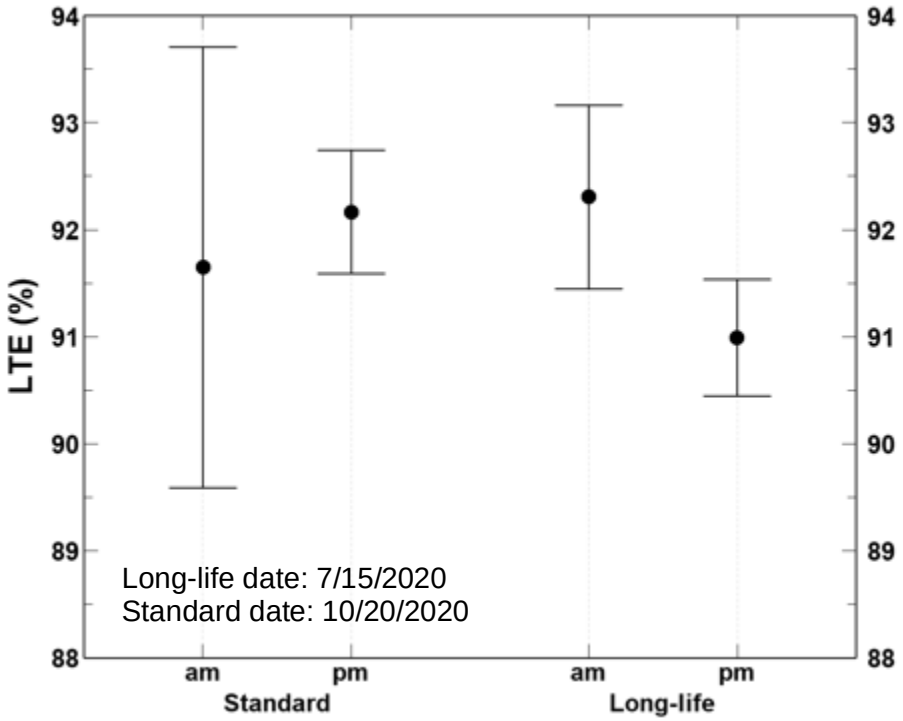

(a) Load transfer efficiency, LTE

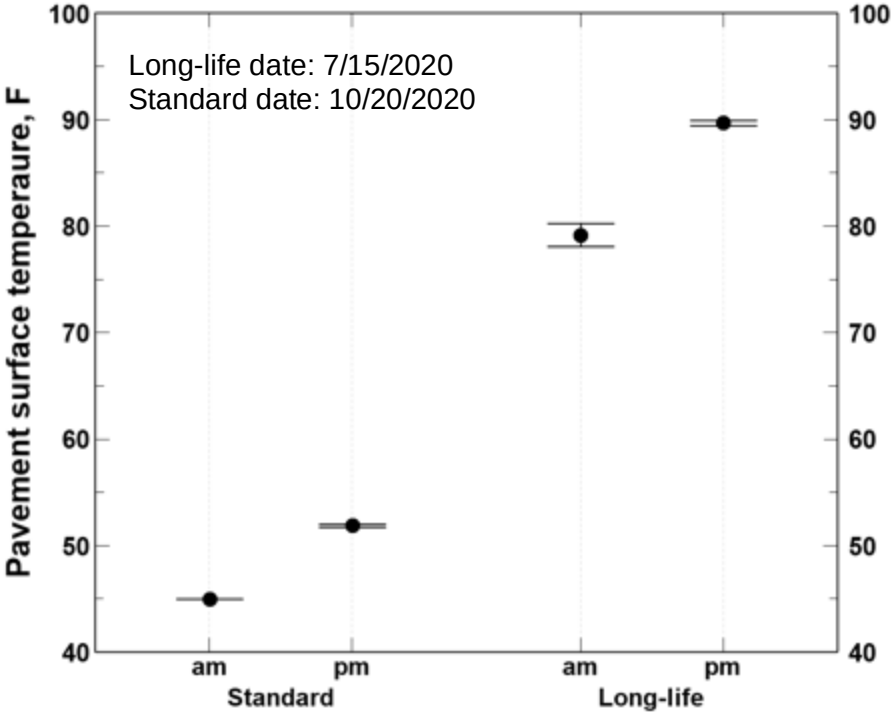

(b) Pavement surface temperature during FWD testing

Figure 24 Comparison between LTE and pavement surface temperatures recorded during FWD testing – US-131 JPCP project

FWD tests conducted on the cement-treated permeable base (CTPB) layer of the ILs and OLs for TS-1 and 2 were analyzed to estimate the in-situ elastic modulus of CTPB, base/subbase (SB), and subgrade (SG) layers for the two test sections. MICHBACK and MODULUS were tried for back calculating layer moduli from FWD data. The difference between predicted values from the two software was not significant. Results obtained using the MICHBACK software are summarized in Table 20. The pavement structure was modeled as a three-layered system with CTPB as the surface layer, base and subbase combined as a middle layer, and the subgrade as the lower semi-infinite layer. It is worth noting that the structure of these two test sections includes a 12-inch stabilized subgrade layer below the subbase. The mean CTPB layer modulus for the two test sections is about one million psi, which correspond to the typical value used in the original Pavement-ME design by the MDOT. Hence, it was concluded that this value is representative for a CTPB layer and it will be utilized in the Pavement-ME analyses presented later in the report.

Table 20 Descriptive statistics for E_{CTPB}, base/SB, and subgrade layers moduli

Parameter	Round	No. of FWD points	Mean	Std.	Minimum	Maximum
E_{CTPB} (ksi)	TS-1	11	978*	369	314	2500
	TS-2	11	1442*	437	500	2455
Base/SB (ksi)	TS-1	11	28	10	11	53
	TS-2	11	23	5	15	31
SG (ksi)	TS-1	11	27	2	23	32
	TS-2	11	30	5	20	42

**Do not include values greater than 2000 ksi.*

Dynamic Cone Penetrometer (DCP) Data Analysis

Dynamic cone penetrometer (DCP) test results for all projects were analyzed to calculate the resilient moduli of the subbase and subgrade layers. The following equations (Equations 3 to 7) were used to estimate the resilient modulus (M_r) of unbound materials from the DCP test results.

$$M_r\,(psi) = 2555 * CBR^{0.64} \quad \text{(NCHRP 1-37A)} \qquad \text{Equation 3}$$

$$M_r\,(psi) = \frac{151.8}{DCP(\frac{mm}{blow})^{1.096}} * 1000 \quad \text{(DCP direct model)} \qquad \text{Equation 4}$$

where Mr = resilient modulus, CBR = California bearing ratio, and DCP = dynamic cone penetrometer. CBR in Equation 3 is computed as follows depending on the classification of soils and subbase materials:

For all soils except for CL soils with CBR < 10 and CH soils:

$$\text{CBR} = 292/\text{DCP}^{1.12} \qquad \text{Equation 5}$$

For CL soils with CBR<10:

$$CBR = \frac{1}{(0.017019 * DCP)^2} \qquad \text{Equation 6}$$

For CH soils:

$$CBR = \frac{1}{0.002871 * DCP} \quad \text{Equation 7}$$

where DCP = DCP index in mm/blow.

I-475 HMA Project

Table 21 and Figure 25 present the descriptive statistics and the layer moduli of the subbase and subgrade layers that are calculated from the DCP data for the I-475 project. It is observed that the trend of DCP-based results is consistent with the LWD results presented above. The subgrade moduli are different in various sections along the NB direction but do not vary between lanes (IL vs OL) of the same section. Similar to the LWD elastic moduli results, the subgrade moduli of the TS-3 for both the NB and SB pavements (in general) are higher than that of other sections. The subbase moduli of pavement foundation layers are consistently lower than that subgrade moduli regardless of project types (Figure 25).

Table 21 Descriptive statistics of layer moduli obtained using DCP data – I-475 HMA project

Layer	Test section	Number of drops	Mean	Standard deviation	Minimum	Maximum
Long-life/ Northbound						
Subgrade modulus (ksi)	TS1	20	10.89	4.05	5.01	20.07
	TS2	22	12.26	4.65	3.77	19.92
	TS3	22	17.14	5.35	6.98	27.35
Subbase modulus (ksi)	TS1	22	7.90	1.85	5.45	13.49
	TS2	22	6.81	0.95	4.61	8.30
	TS3	22	9.02	5.25	6.00	31.70
Standard/ Southbound						
Subgrade modulus (ksi)	TS1	22	14.30	5.93	4.55	26.91
	TS2	22	11.79	2.04	7.51	16.06
	TS3	22	21.90	11.12	6.73	49.71
Subbase modulus (ksi)	TS1	22	8.78	2.39	4.79	13.64
	TS2	22	7.57	1.26	5.45	9.78
	TS3	22	7.63	1.46	5.37	10.34

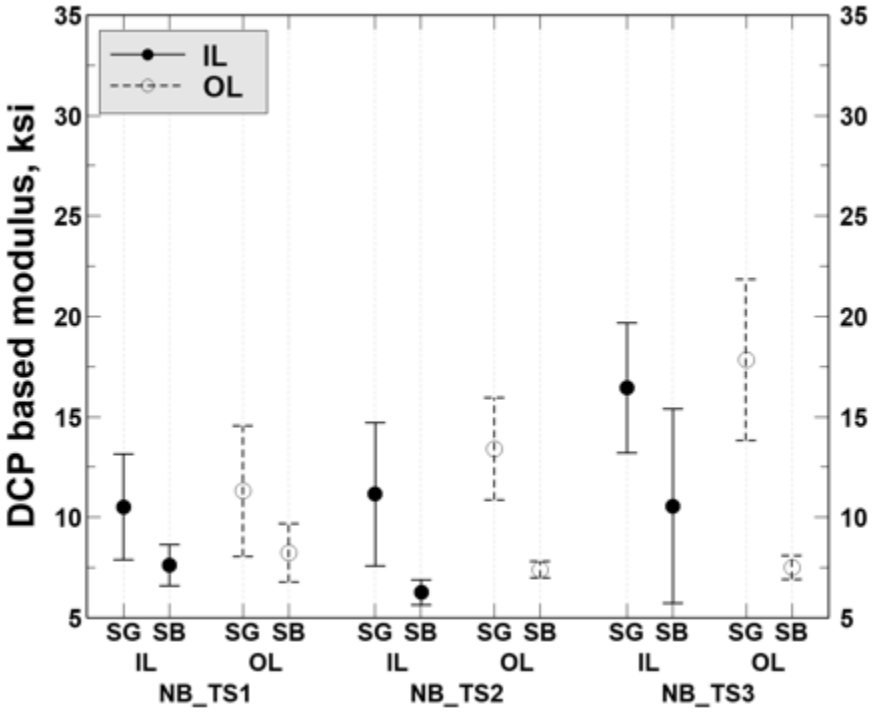

(a) Northbound long-life design

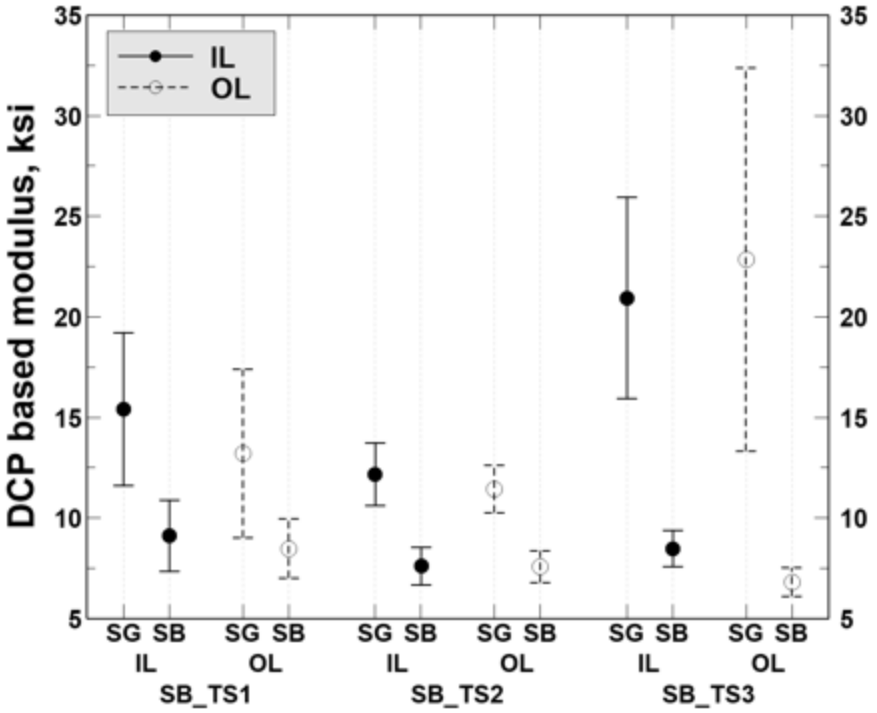

(b) Southbound standard design

Figure 25 Interval plots comparing DCP-based subgrade (SG) and subbase (SB) moduli values between different lanes and test sections of the Northbound (NB) long-life and Southbound (SB) standard design pavements – I-475 HMA project

US-131 HMA Project

The subgrade and subbase layer moduli of the test sections at US-131 HMA project (calculated from DCP data) are summarized in Table 22 and Figure 26. Subgrade moduli of the long-life sections (TS-1 through TS-3) are higher than that of the standard TS-4 even though they show higher variability. The same trend was also observed for the subbase layer moduli of test sections of both long-life and standard test sections.

Table 22 Descriptive statistics of layer moduli obtained using DCP data – US-131 HMA project

Layer	Test section	Design	Number of drops	Mean	Standard deviation	Minimum	Maximum
Subgrade modulus (ksi)	TS1	Long-life	6	59.16	9.26	50.10	73.26
	TS2		6	46.55	23.18	15.29	71.57
	TS3		6	56.65	15.36	39.26	82.03
	TS4	Standard	5	11.49	4.12	5.38	15.56
Subbase modulus (ksi)	TS1	Long-life	6	28.88	6.48	16.42	34.71
	TS2		6	36.22	13.30	22.42	52.88
	TS3		6	45.03	3.28	39.64	49.45
	TS4	Standard	6	17.13	8.39	10.55	32.81

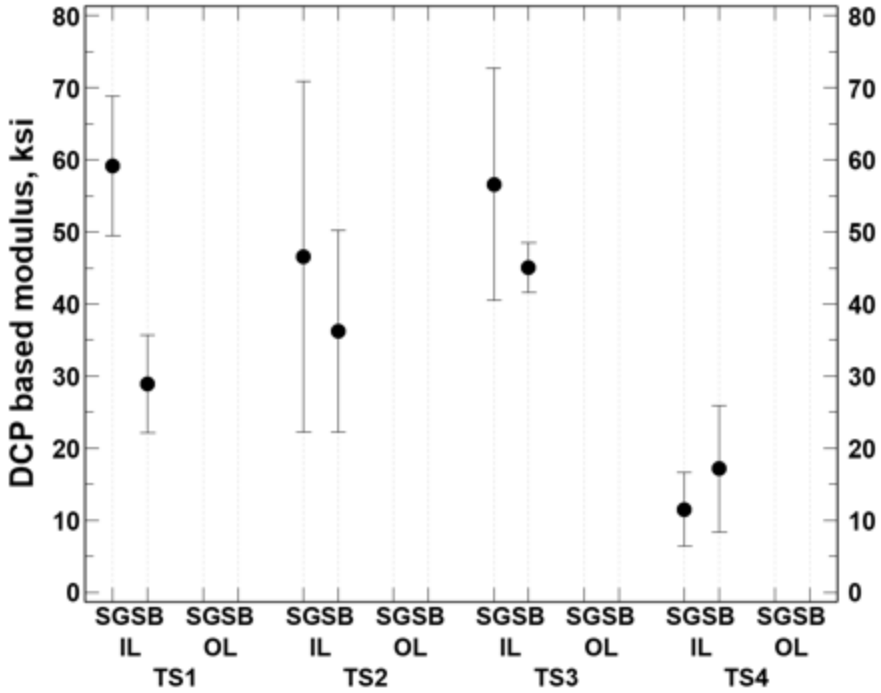

Figure 26 Interval plots comparing DCP-based subgrade (SG) and subbase (SB) moduli values between test sections of the long-life and standard design pavements – US-131 HMA project

Table 23 presents the descriptive statistics of the pavement foundation layer moduli values calculated by using DCP data for I-69 JPCP project. A higher variability is observed for the subgrade and subbase moduli of TS-3 of the long-life WB section (see Figure 27).

Table 23 Descriptive statistics of layer moduli obtained using DCP data – I-69 JPCP project

Layer	Test Section	Number of drops	Mean	Standard deviation	Minimum	Maximum
Standard/ Eastbound						
Subgrade modulus (ksi)	TS1	32	15.44	7.06	6.96	38.60
	TS2	33	8.53	3.53	2.88	21.58
Subbase modulus (ksi)	TS2	33	7.92	2.24	4.39	12.40
Long-life/ Westbound						
Subgrade modulus (ksi)	TS3	10	37.93	24.69	7.45	78.49
Subbase modulus (ksi)	TS3	11	36.8	43.1	9.1	87.059

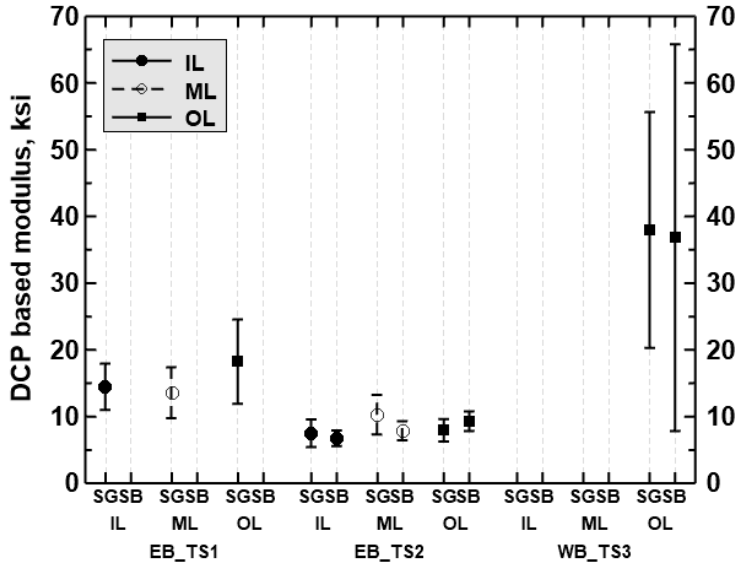

Figure 27 Interval plots comparing DCP-based subgrade (SG) and subbase (SB) moduli values between different lanes of the Eastbound (EB) standard and Westbound (WB) long-life design pavements – I-69 JPCP project

US-131 JPCP Project

Table 24 presents the descriptive statistics of pavement foundation layer moduli of test sections (calculated by DCP data) for the US-131 JPCP project. Figure 28 displays that the subgrade moduli of the NB TS-2 are higher and less variable than that of other NB sections. On the other hand, subgrade modulus of the TS-1 SB section is the highest of all sections but also has noticeable variability. The subbase moduli of the SB sections display some variability and are consistently lower than that of subgrade moduli of these sections.

Table 24 Descriptive statistics of layer moduli obtained using DCP data – US-131 JPCP project

Layer	Test section	Number of drops	Mean	Standard deviation	Minimum	Maximum
Long-life/ Northbound						
Subgrade modulus (ksi)	TS1	5	17.69	7.19	8.68	27.20
	TS2	5	31.642	1.306	29.905	33.306
	TS3	5	17.65	5.80	9.08	23.32
Standard/ Southbound						
Subgrade modulus (ksi)	TS1	11	53.13	24.46	24.99	103.26
	TS2	22	37.50	11.51	11.45	61.75
	TS3	13	24.37	8.37	9.47	35.60
Subbase modulus (ksi)	TS1	11	20.81	11.41	9.05	44.12
	TS1	22	9.052	3.385	1.690	15.839
	TS2	14	10.449	3.435	6.688	17.343

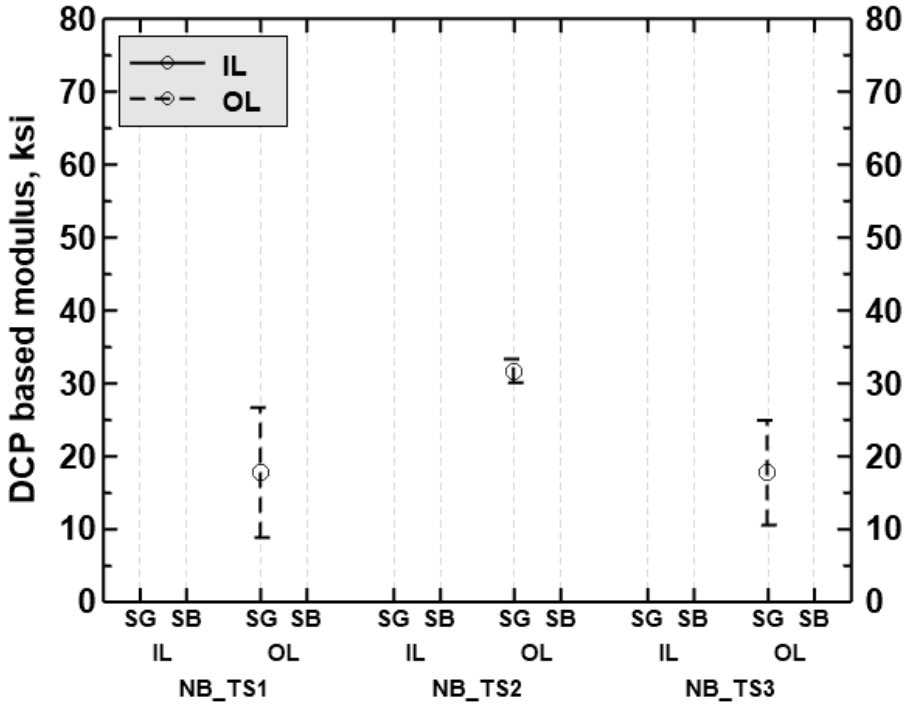

(a) Northbound long-life design

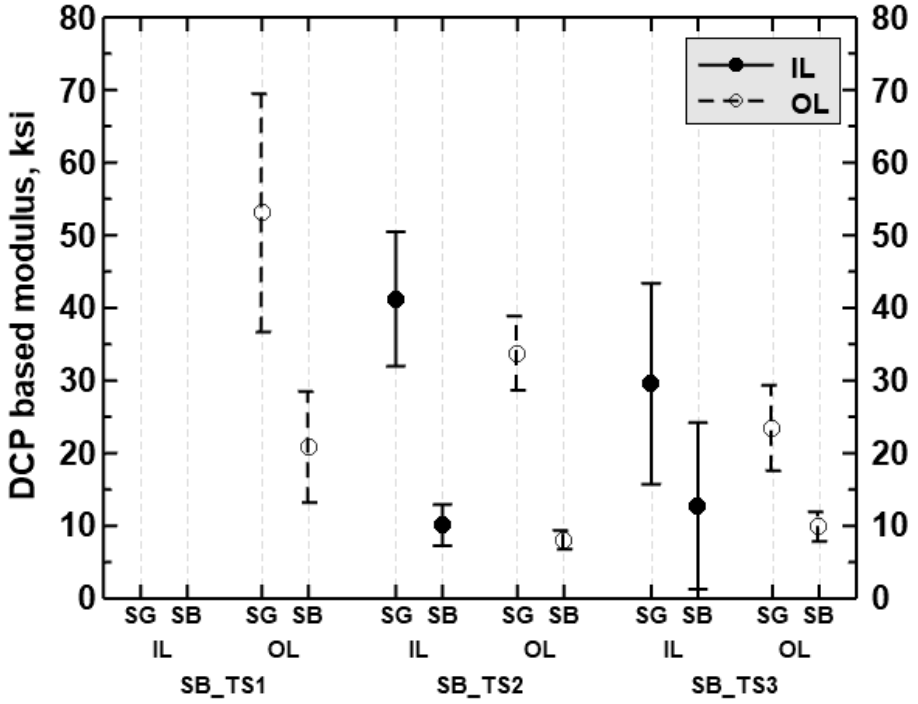

(b) Southbound standard design

Figure 28 Interval plots comparing DCP-based subgrade (SG) and subbase (SB) moduli values between different lanes and test sections of the Northbound (NB) long-life and Southbound (SB) standard design pavements – US-131 JPCP project

Regional Meetings

The project team interviewed the construction staff of the Bay and the Grand regions to learn more about the four long life pilot projects. Some of the salient points of discussion which might have an impact on the pavement performance are reported below.

Bay Region Meeting Notes

- A rain event during the I-69 construction happened before the construction of the drainage structure, which flooded the subgrade and washed away the subgrade under the OGDC layer at some sites. The problem was handled on-site, and the OGDC layer was pulverized and used as a cement-stabilized subgrade.
- The use of RCA (Recycled Concrete Aggregate) in the construction of the cement-treated permeable base (CTPB) layer on the I-69 JPCP project may cause drainage issues in the future.

Grand Region Meeting Notes

- Some portions of the NB pavement sections were paved in November; thus, blankets were used to cover the pavement to maintain temperature overnight.
- The same pavement sections were opened to traffic in December, with the joints unsealed; sealing was undertaken in the following spring.
- Premature spalling of the PCC slab on the outside lane of the NB pavement occurred sometime in Fall of 2019 (almost a year after construction) at these stations: 877+17, 881+65, 884+50, 887+30, 888+95, and 889+68. All these failures had similar offsets transversely, i.e., approximately two feet right of the centerline of the road (within the left wheel track of the lane).
- For the US131 rigid pavement stabilized subgrade construction, the MDOT special provision stated “Immediately following the final grading, cure the compacted subgrade for a minimum of five days before placement of the overlying course. The surface must be protected from rapid drying during this period by placing a curing coat of asphalt emulsion. Other suitable methods of curing the compacted stabilized subgrade may be approved by the Engineer”. The contractor proposed the following: "Toebe proposes to use the sand subbase as the curing method. Once directed by our stabilization subcontractor (Wadel Stabilization, Inc) that their operation is complete able to support the operation, Toebe will cover the stabilized area with the required sand subbase to insulate and retain moisture on the layer. This operation will be done with dozers and it is currently anticipated that the truck traffic would be minimal (the required sand backfill will be stored on the east and west sides of the roadway where it would just need to be pushed back in place. Beyond that, the sand will be kept moist throughout the curing period to minimize moisture loss in the stabilized layer. Toebe would perform this covering operation within 24 hours of Wadel’s direction.". In response, MDOT approved the placement of 8” of sand subbase over the top of the 12” Cement Treated Subgrade section with the contingency that Toebe places the sand on top of the section IMMEDIATELY after Wadels recommendation, not within 24 hours as stated in RFI 001. MDOT agrees that the placement of the sand will assist the curing process of the cement treated subbase.
- For the US131 rigid pavement construction, the underdrains were construction such that the open-graded drainage layer was extended through the subbase layer and the pipe was

installed with a 3-inch notch into the stabilized subgrade. This modification was necessary to avoid storm water drainage conflicts. The modification is shown in Figure 29.

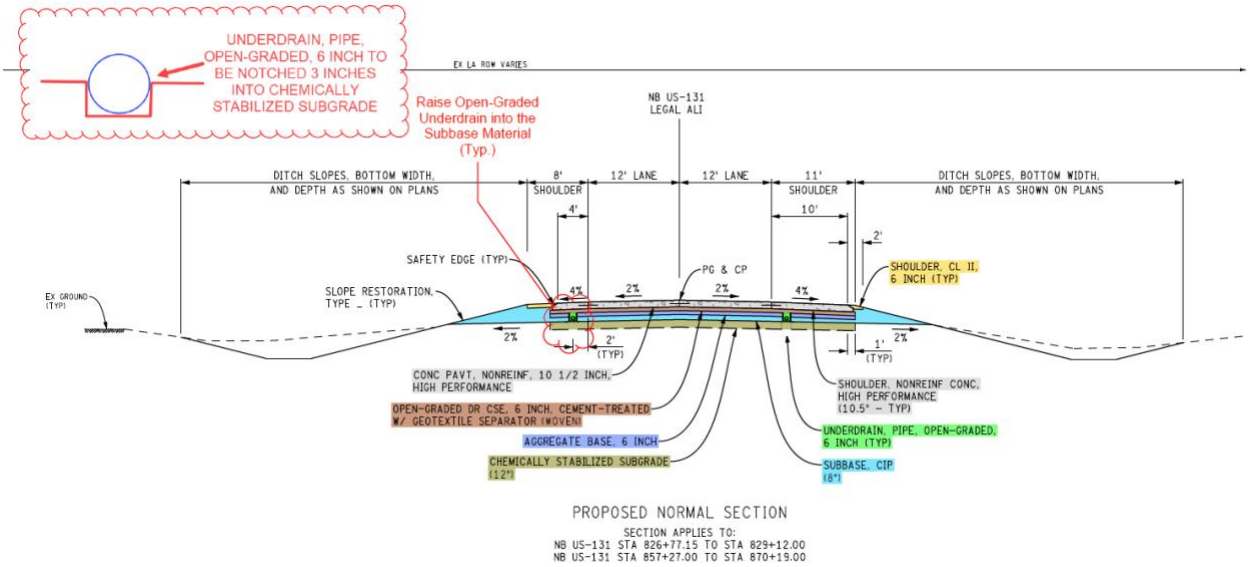

Figure 29 Underdrain installment on US-131 JPCP section

CHAPTER 3: MATERIAL TESTING AND CHARACTERIZATIONS

Linear viscoelastic characterization of asphalt binders

The linear viscoelastic characterization of asphalt binders was conducted in general accordance with AASHTO T 315, Dynamic Shear Rheometer (DSR) test. The bitumen complex modulus (|G*|) and phase angle (δ) were obtained at the same loading frequencies and temperatures as the ones reported in MDOT RC-1593 report to generate the |G*| master curves. Table 25 and Table 26 show the binders provided by MDOT for I-475 and US-131 projects, respectively.

Table 25 List of asphalt binders provided by MDOT, collected from I-475 project.

Date	Direction	Binder Grade	Mix
8/24/2019	SB	52-34	3E10
8/25/2019	SB	52-34	3E10
10/11/2019	SB	58-34	5E10 LV (leveling)
10/13/2019	SB	58-34	5E10 LV (leveling)
10/17/2019	SB	58-34	5E10 TOP
10/18/2019	SB	58-34	5E10 TOP
11/05/2019	NB	58-34	3E30
6/20/2020	NB	70-28p	GGSP
6/04/2020	NB	70-28p	GGSP
5/27/2020	NB	70-28p	4E30
5/26/2020	NB	70-28p	4E30
5/31/2020	NB	70-28p	4E30
5/6/2020	NB	58-34	3E30
5/13/2020	NB	58-34	3E30
5/22/2020	NB	58-34	3E30
6/4/2020	NB	58-34	5E3
6/6/2020	NB	58-34	5E3

Table 26 List of binders provided from US131 project.

Control section	Job number	Asphalt binder	Type of mix
41133	119012A	PG 70-28P	GGSP
41133	119012A	PG 70-28P	4E30
41133	119012A	PG 64-28	3E30
41133	119012A	PG 64-28	5E10
41133	119012A	PG 64-28	3E10
41133	119012A	PG 58-28	2E10

Asphalt binders were tested in their original and short-term aged conditions. Aged bitumen was obtained using the rolling thin-film oven (RTFO) in accordance with AASHTO 240-13. Data at different temperatures for the binders used in long-life and standard sections of I-475 and US-131 are shown in Figure 30 to Figure 33, while complex modulus master curves are provided in the Appendix B. The figures show average and standard deviation of the |G*| of the different binders used in different layers of the standard and the long-life sections. As expected, asphalt

binders with same PG from different HMA layers have similar complex modulus values. Test results also showed a trend between PG and stiffness of the bitumen, as expected. The polymer modification used for the production of the PG 70-28P of the long-life sections in I-475 and the one used in the US-131 resulted in stiffer bitumen compared to both PG 58-34 and PG 64-28 used in the two projects. For both I-475 and US-131, the binder used in the base course of the standard sections (PG 52-34 for I-475 and PG 58-28 for US-131), is softer than the ones used in the top and leveling HMA layers.

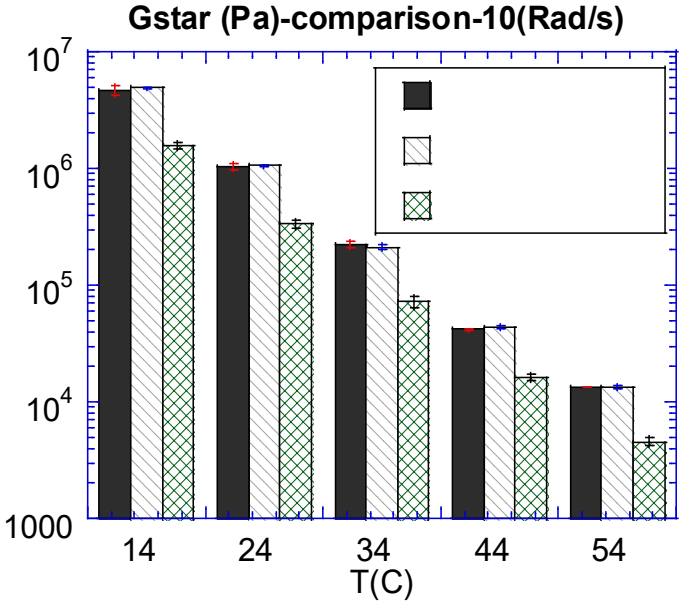

Figure 30 |G*| test raw data comparison – I-475 long-life mixtures binders – RTFO aged

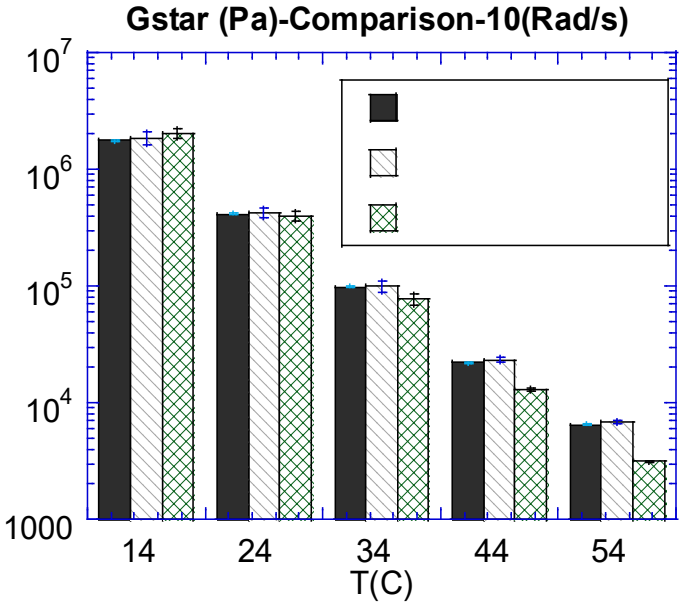

Figure 31 |G*| test raw data comparison – I-475 standard mixtures binders – RTFO aged

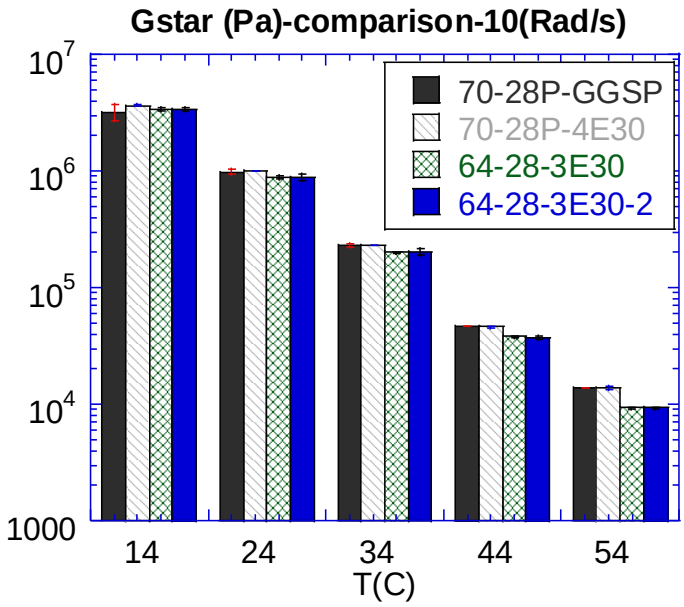

Figure 32 |G*| test raw data comparison – US-131 long-life mixtures binders – RTFO aged

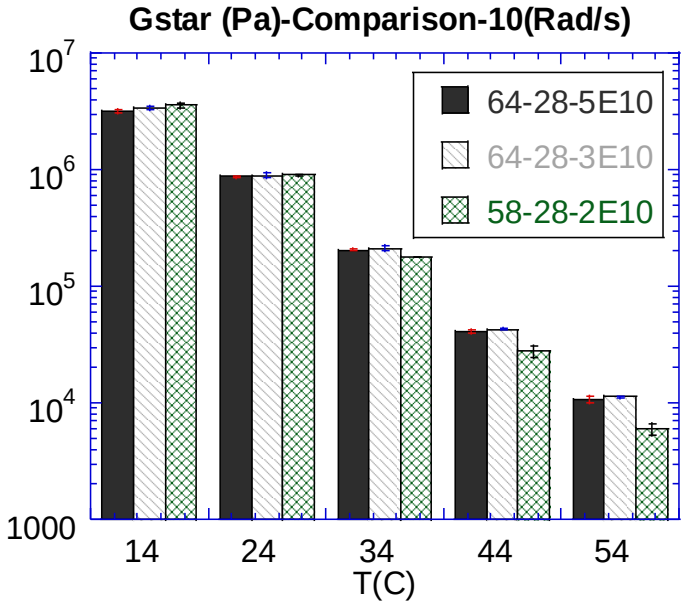

Figure 33 |G*| test raw data comparison – US-131 standard mixtures binders – RTFO aged

Asphalt Binder Multiple Stress Creep Recovery (MSCR) Test

The multiple stress creep recovery (MSCR) test was conducted by using the DSR system in accordance with AASHTO T 350. All binder grades used in the long-life and standard sections of the I-475 and US-131 projects were tested. These binder grades include 70-28P, 58-34 and 52-34 for I-475 and 70-28P, 64-28 and 58-28 for US-131 project. All RTFO-aged binders were tested at 58°C, which corresponds to the high PG temperature required for Michigan's binders before traffic adjustments. Two stress levels of 0.1 and 3.2 kPa were applied and 10 cycles were conducted for each stress level. The test starts with the application of a low stress (0.1 kPa) for 10

creep/recovery cycles then the stress in increased to 3.2 kPa and repeated for an additional 10 cycles. The MSCR test uses two parameters, the percent recovery (%R) and the non-recoverable creep compliance (J_{nr}) at 3.2 kPa, to evaluate their potential to accumulate permanent deformations. The results of MSCR test on I-475 and US-131 projects are shown in Figure 34. The polymer-modified binders (PG 70-28P) used in both projects resulted in %R above the pass-fail threshold. However, differences were noticed in terms of non-recoverable creep compliance. In fact, while the two binders used on the US-131 can be both classified as "E" grade (i.e., suitable for extremely heavy traffic), the two PG70-22P used in the I-475 project belong to two different grades, "E" and "V" for the GGSP and 4E30, respectively. It shall be also noted that the "E" grade of bitumen used in the GGSP mixture of the I-475 has a lower %R and higher Jnr3.2 compared to the "E" grades used in the US-131 project.

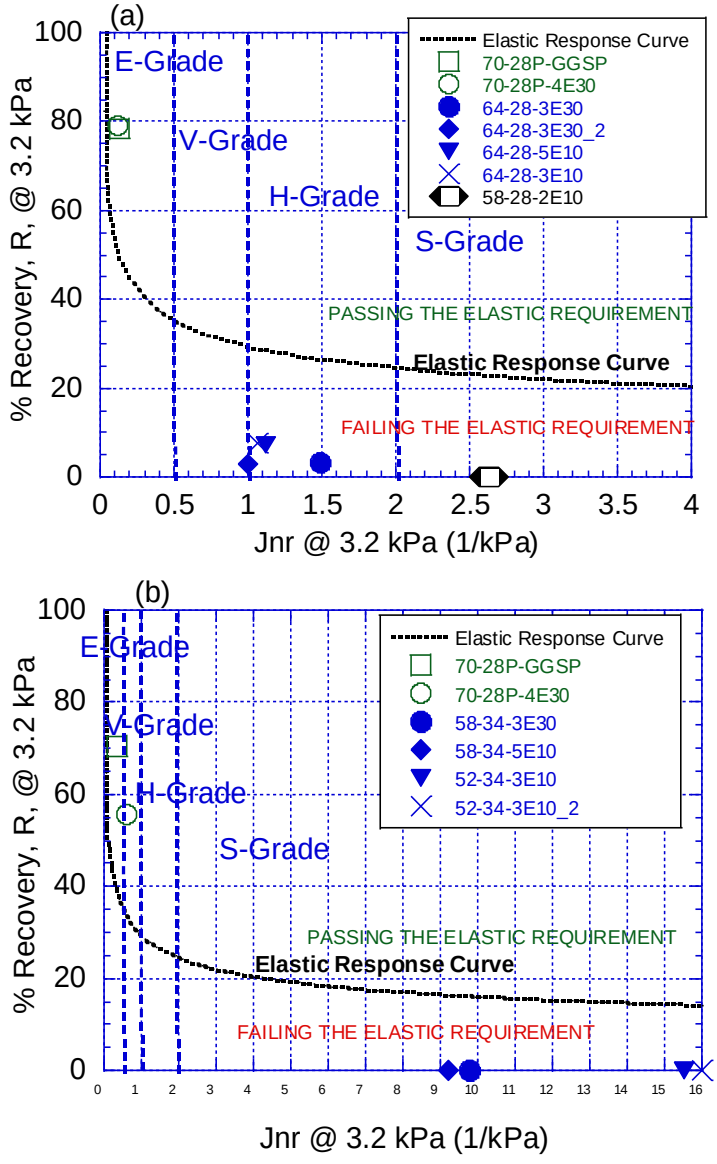

Figure 34 MSCR test results for (a) US-131 and (b) I-475 binders

Asphalt Mixture Dynamic Modulus (|E*|)

Dynamic Modulus (|E*|) tests were conducted on HMA mixtures of I-475 for all six test sections in accordance with AASHTO T342, and their master curves generated in accordance with the AASHTO R84. US-131 mixtures were also tested as part of another project with MDOT. For these tests, 4" diameter and 6" tall samples were prepared by cutting and coring gyratory compactor specimens. Target air voids for the samples was 7%±0.5%. Three replicates for each mixture were tested in uniaxial compression mode at different temperatures (-10°C, 4°C, 21°C, 37°C and 54°C) and loading frequencies (25, 10, 5, 1.0, 0.5, and 0.1 Hz). It is well known that the minimum temperature that the AMPT device is capable of controlling is approximately 0°C. To obtain |E*| data at -10°C, samples were conditioned overnight at -13°C using an external environmental conditioning system. Before each test, samples were quickly transferred into the AMPT chamber (which was kept at 0°C overnight) and tested. This procedure was validated by placing a thermocouple in a dummy sample and running a trial test, during which it was observed that the temperature of the sample was -10°C±0.5°C during the entire test. The duration of each |E*| test was approximately 3 minutes. The stress level is adjusted such that the strain level measured on the sample remains between 75 and 125 microstrains to ensure no damage accumulation during the test.

A summary of results of |E*| tests at the frequency of 10 Hz for I-475 and US-131 mixtures is shown in Figure 35 and Figure 36, respectively. The figures show average and standard deviation of the |E*| of three replicate samples of each layer for each test section of the standard and the long-life pavements. The |E*| master curves are given in Appendix C. As shown in the Figure 35 (a) and (b), the top and levelling courses of the long-life sections (GGSP and 4E30) are generally stiffer than the corresponding layers in the standard sections (5E10-Top and 5E10-Lev). The difference in the stiffness of these layers (GGSP vs 5E10-Top and 4E30 vs 5E10-Lev) is more significant at higher temperatures. These results can only be partially due to the polymer-modified binders. In addition, the gradation of the aggregate's skeleton plays a crucial role. The higher stiffness of the GGSP, for example, can be associated to the high number of stone-to-stone contacts in this Stone Matrix Asphalt – type of HMA, as opposed to the dense-graded mix of the 5E10. It is common understanding that stiffer surface layers are desirable if they are not brittle. A stiffer surface layer can, in fact, reduce the stress transmitted to lower layers and reduce their deformation under loading, hence reducing the potential for fatigue cracking damage. On the other side, the polymer modified binders used on the top layer of the long-life sections is expected to produce a ductile material and reduce the risk of top-down cracking typical of brittle surface HMAs.

It is worth also noting that no performance-related conclusion can be drawn solely based on dynamic modulus test results. These tests are performed in the linear-viscoelastic range of the HMA mechanical response, where damage does not accumulate. Hence, any comments based on |E*| test results would be purely indicative. Damage (e.g., tension-compression fatigue, three-point bending cylinder) as well as plastic strain-inducing (e.g., flow number) tests are needed to fully characterize the asphalt mixture performances.

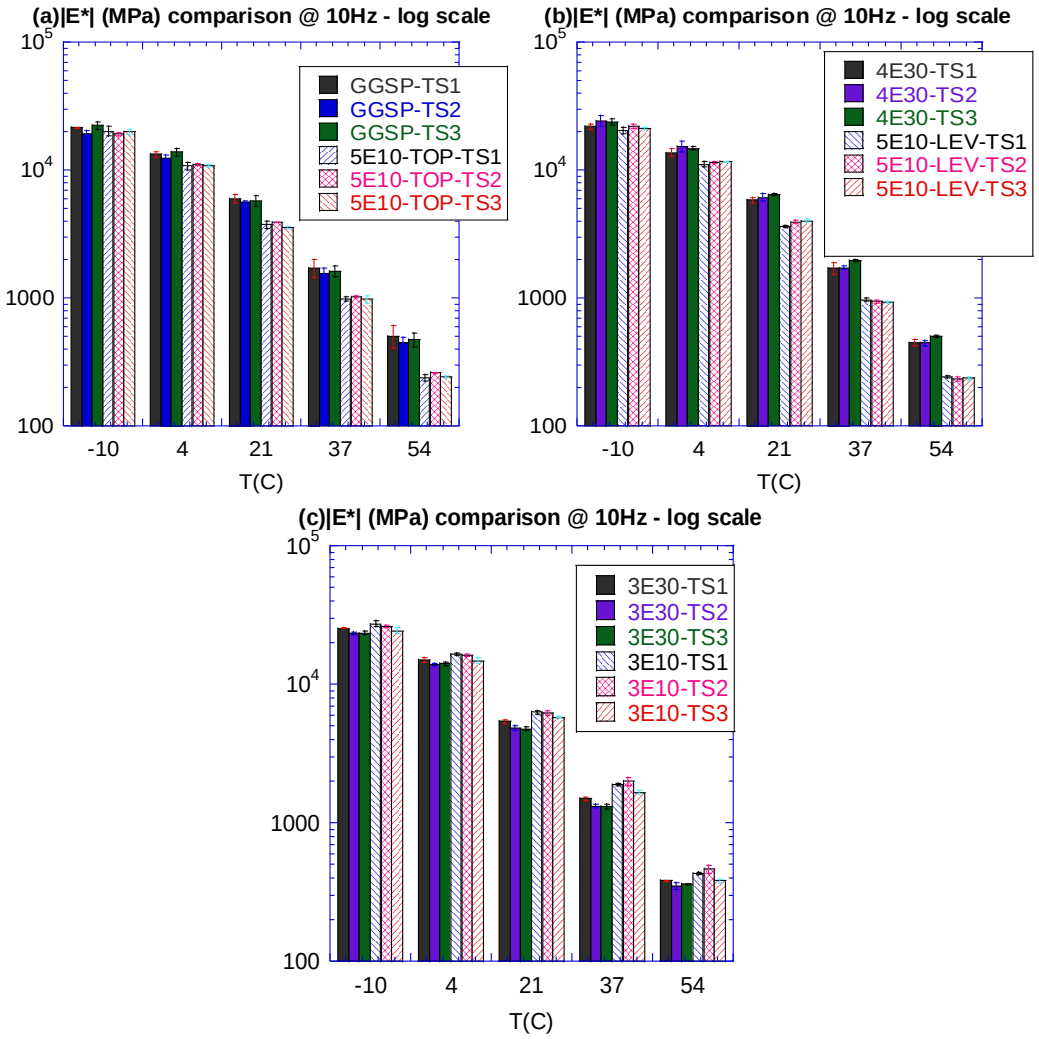

Figure 35 Summary of results of |E*| tests at 10 Hz for I-475 project: (a) GGSP (PG70-28P) vs 5E10-Top (PG58-34), (b) 4E30 (PG70-28P) vs 5E10-Lev (PG58-34) and (c) 3E30 (PG58-34) vs 3E10 (PG52-34)

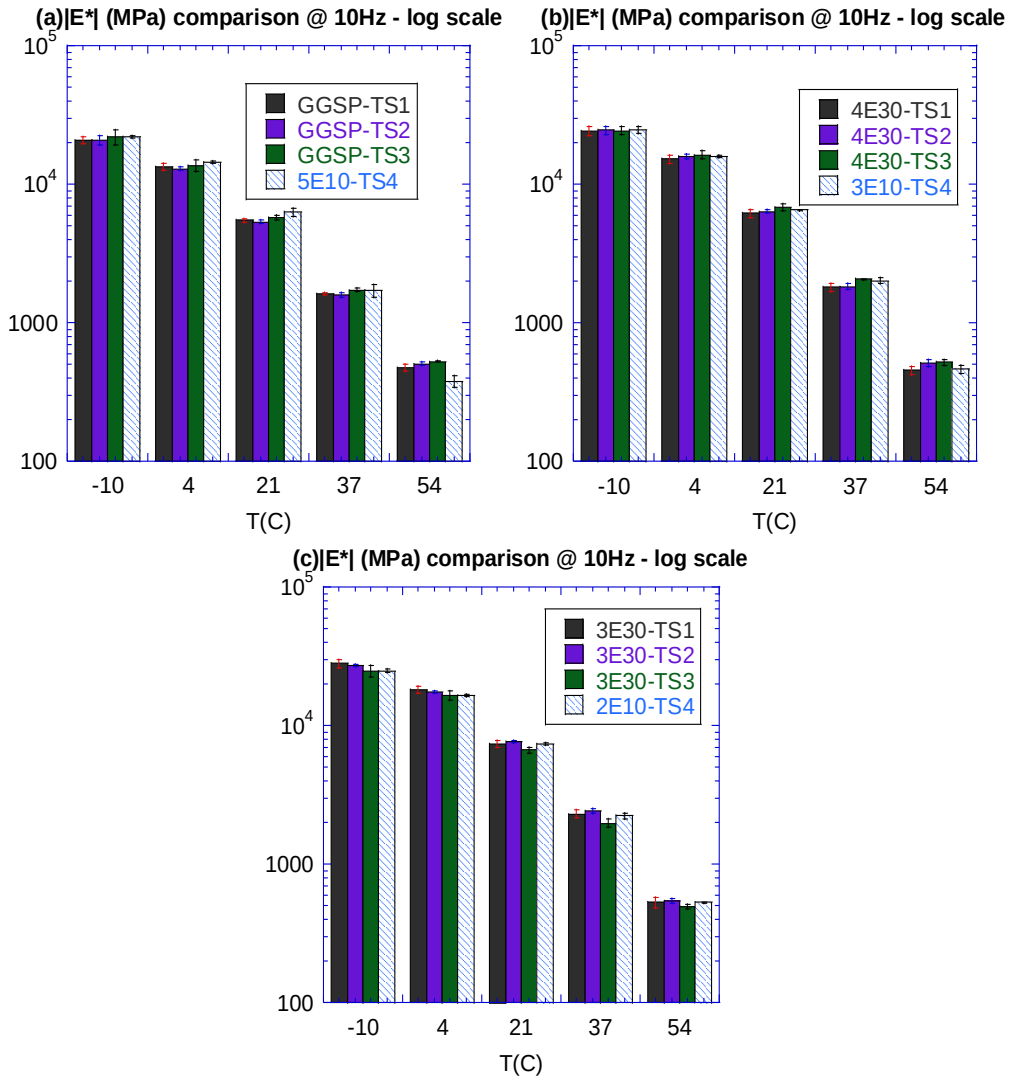

Figure 36 Summary of results of |E*| tests at 10 Hz for project US-131: (a) GGSP (PG70-28P) vs 5E10 (PG64-28), (b) 4E30 (PG70-28P) vs 3E10-LEV (PG64-28) and (c) 3E30 (PG64-28) vs 2E10 (PG58-28)

Asphalt Mixture Confined Dynamic Modulus (|E*|)

Confined dynamic modulus |E*| tests were conducted so that mixture-specific calibration coefficients of the MEPDG HMA rutting model can be computed. Tests were performed on the same samples used for unconfined dynamic modulus tests described above and following the same testing protocol, except for the application of a 10 psi (68.9 kPa) lateral confining pressure. The average of three replicates was used to generate |E*| master curves, in accordance with AASHTO R84. A comparison of confined and unconfined |E*| master curves is shown in Figure 37 and Figure 38 for I-475 and US-131 HMAs, respectively. The effect of lateral confinement can be clearly noticed at high temperatures (i.e., low frequencies).

The effect of confinement, in terms of ratio between confined and unconfined moduli, on different mixtures used in the long-life and standard sections of I-475 and US-131 projects were quantified and plotted in Figure 39 and Figure 40, respectively. The effect of confinement was less

significant on GGSP and 4E30 mixtures of the I-475 compared to 5E10-Top and 5E10-Lev. This was possibly because of the polymer modified binders making the mixtures stiffer (Figure 39). On the other hand, the effect of confinement on the base courses (3E30 and 3E10) were similar. Similar trends have been noticed for the mixtures of the US-131 project (Figure 40). It should be noted that the input required by the AASHTOWare Pavement ME software is the unconfined |E*|. The software, in fact, performs the layered elastic analysis under the assumption of negligible confinement effect, while confinement is actually considered in the HMA rutting model through an empirical variable (k_z).

It is hypothesized that the mixtures that are less affected by confinement are better mixtures. This is because these mixtures do not need confinement to provide a given stiffness (i.e., dynamic modulus). It is well known that unbound materials (base and subbase) need significant confinement to provide sufficient stiffness to withstand traffic loading. If an asphalt mixture is like an unbound material where the confinement affects its stiffness, this means that the binder is not doing its job, or the gradation is not providing sufficient aggregate interlocking. As such, the mixtures whose dynamic moduli are not affected (or affected minimally) by the confinement are better and more stable mixtures. Based on the data provided herein, the GGSP and 4E30 mixtures are much more stable mixtures (not as significantly affected by confinement as other mixtures).

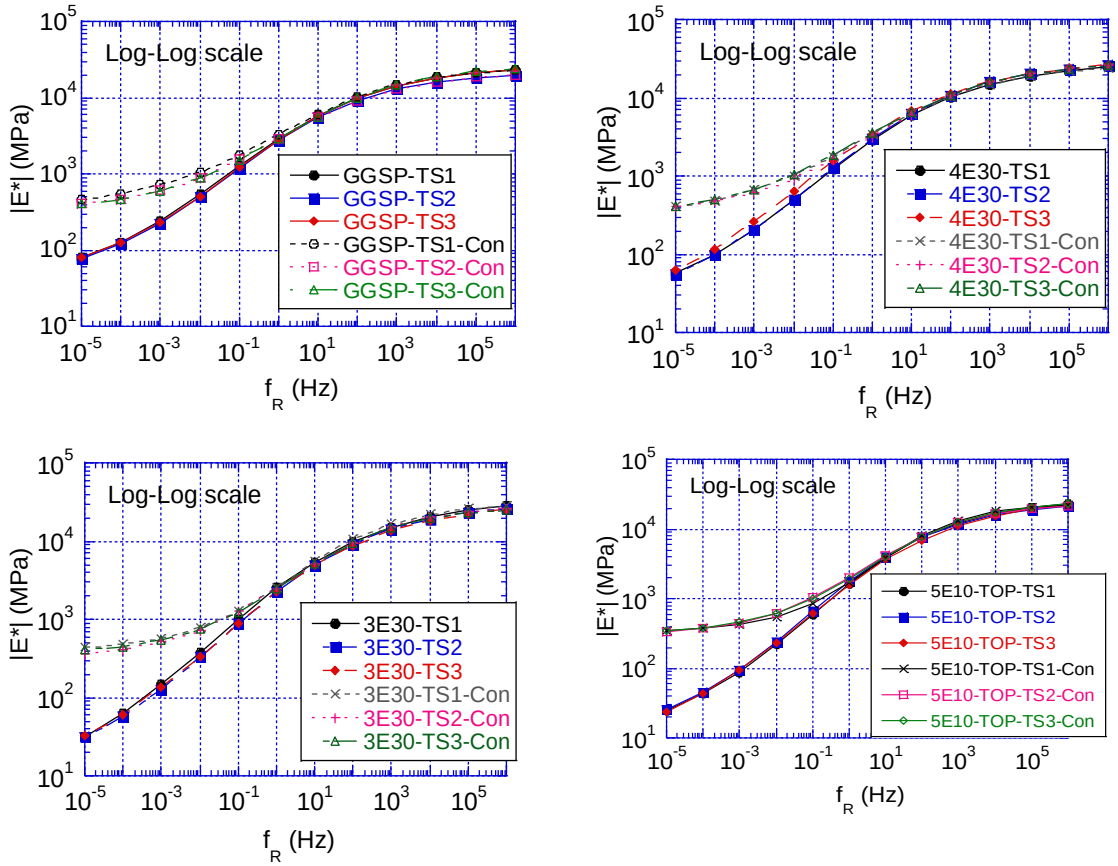

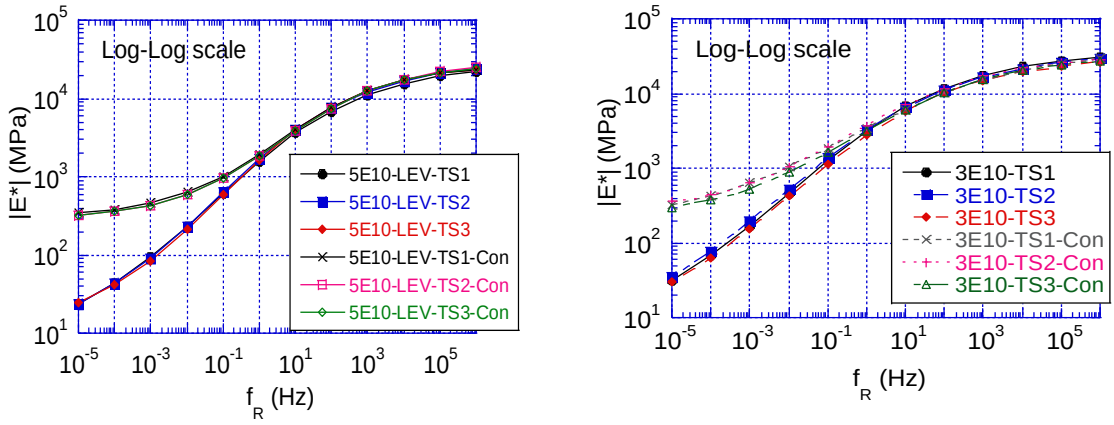

Figure 37 Comparison of confined and unconfined |E*| master curves of the mixtures for the long-life and the standard sections of I-475 project

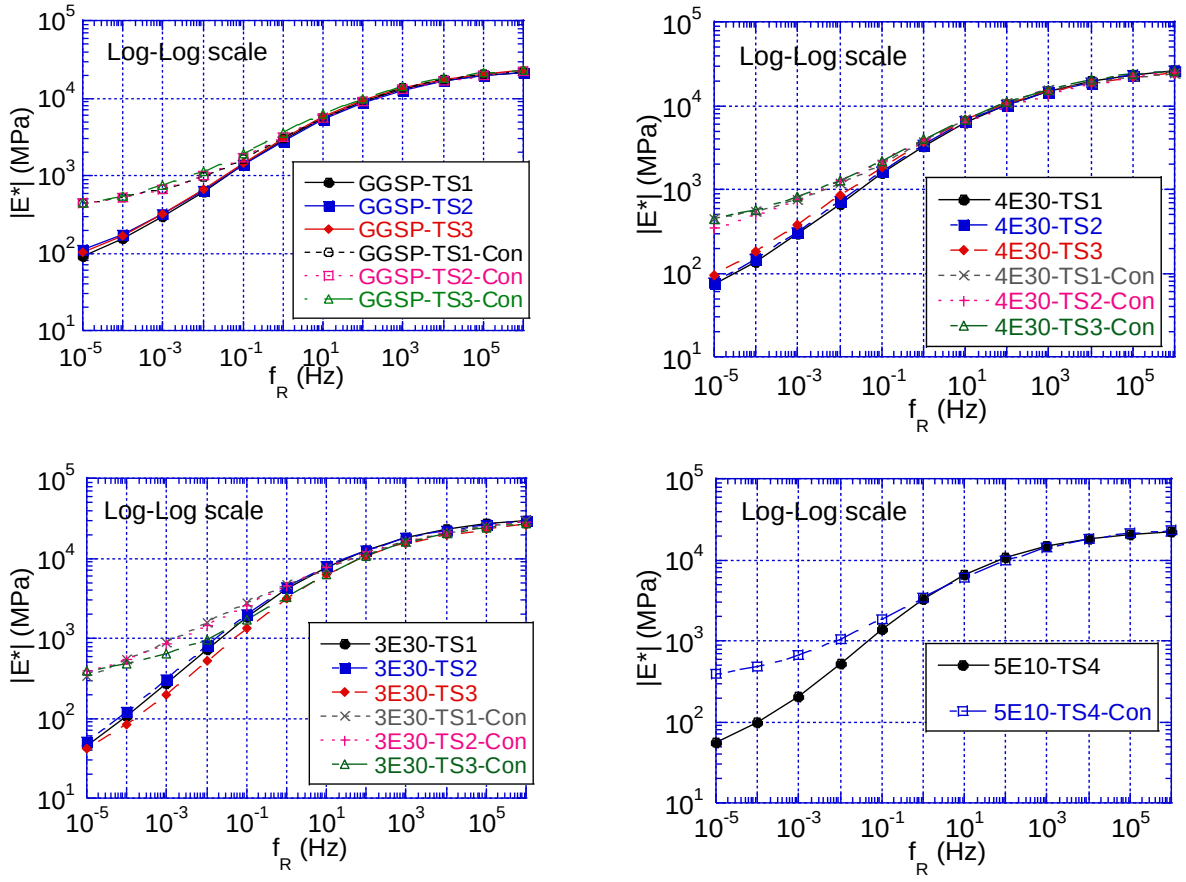

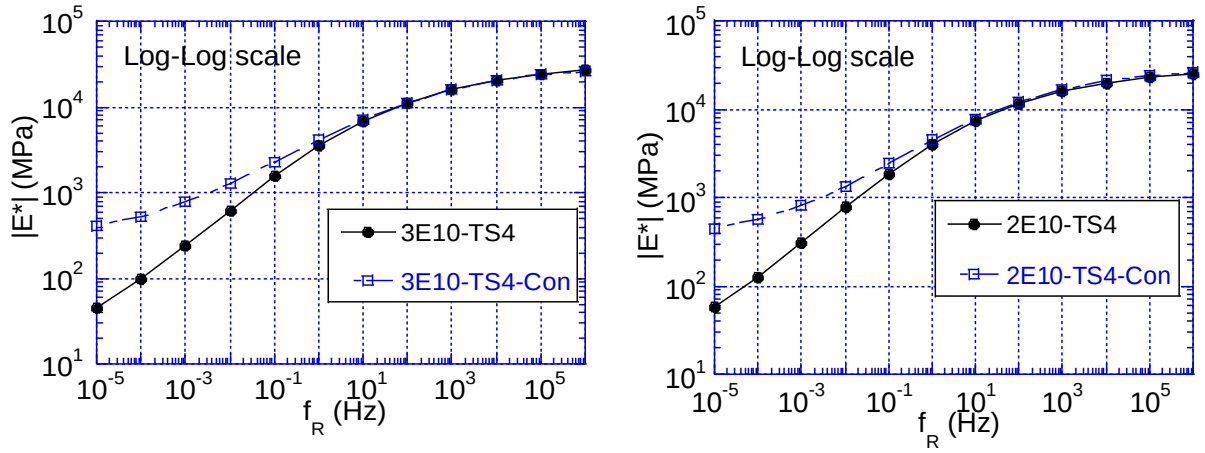

Figure 38 Comparison of confined and unconfined |E*| master curves of the mixtures for the long-life and the standard sections of US-131 project

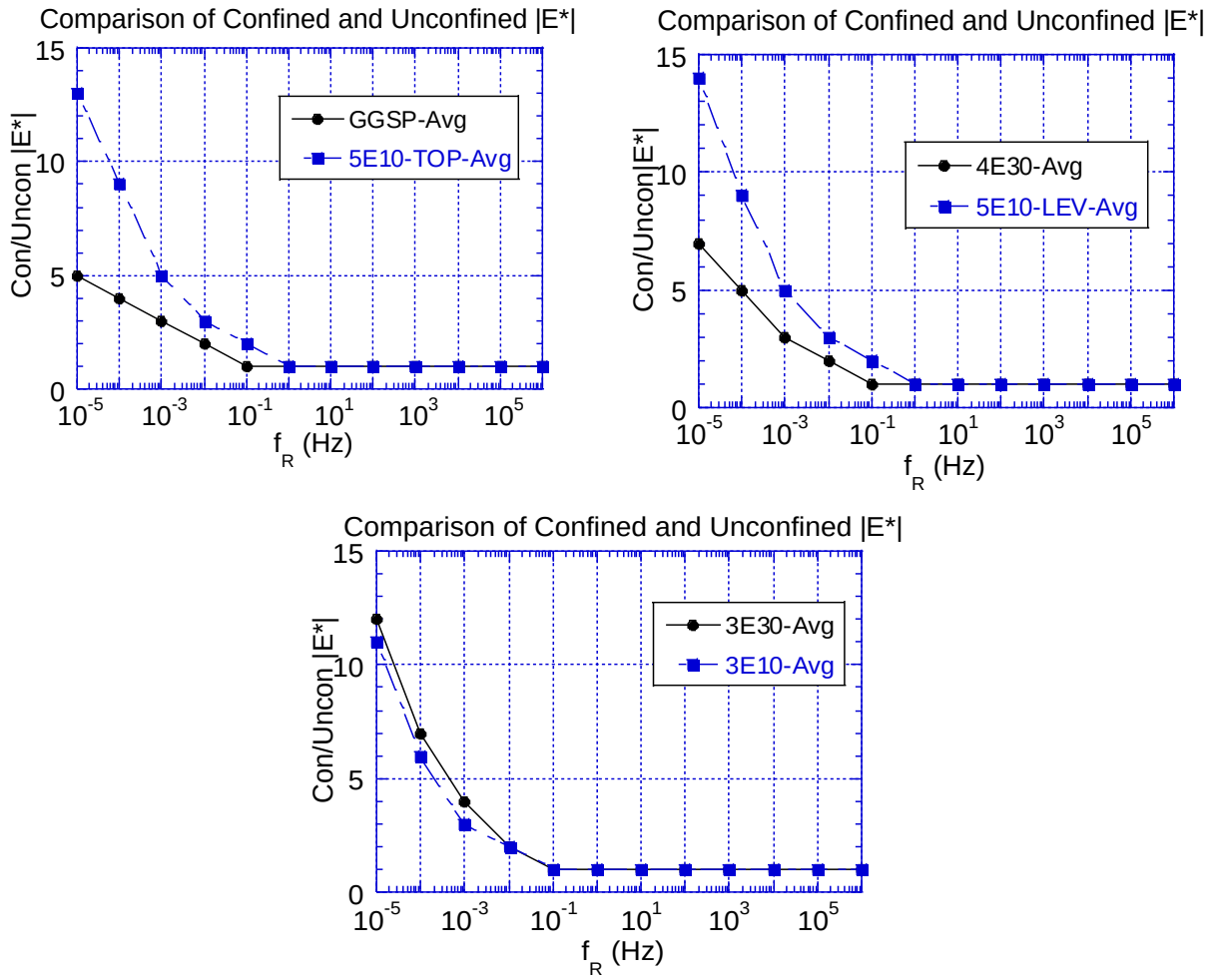

Figure 39 The effect of confinement on long-life and standard mixtures for I-475 project

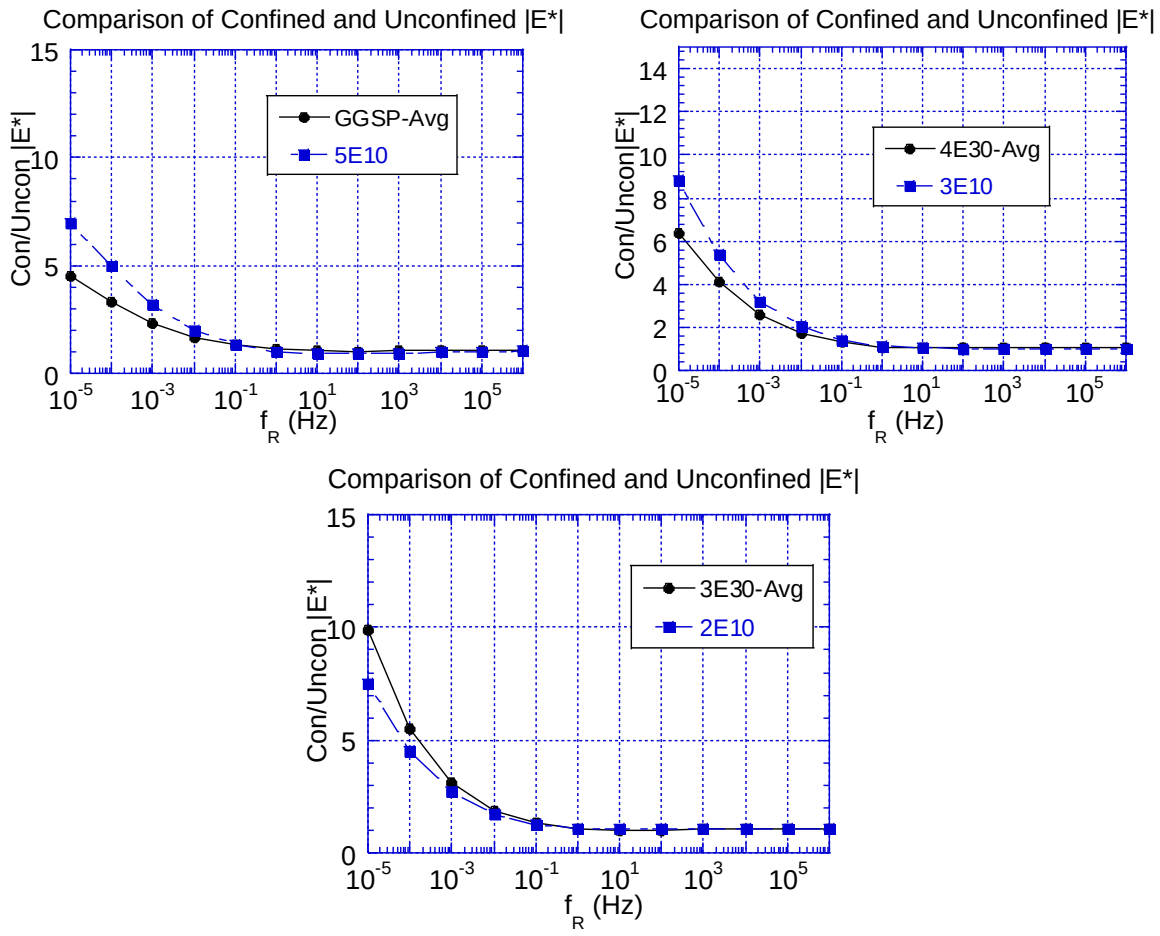

Figure 40. The effect of confinement on long-life and standard mixtures for US-131 project

Asphalt Mixture Repeated Load Permanent Deformation (RLPD) Test

The RLPD tests (also known as Flow Number tests) were conducted in accordance with AASHTO T 378-17 to evaluate the susceptibility of asphalt mixtures to rutting. Laboratory fabricated cylindrical specimens, produced for dynamic modulus test, were subjected to a haversine axial compressive load pulse of 0.1s followed by a 0.9s rest period. The test duration was set equal to 10,000 load repetitions, and samples were tested at repeated deviatoric stress of 482.6 kPa (70 psi), constant confined stress level of 68.9 kPa (10 psi), at a single temperature of 54°C. The results of each individual test are provided in the Appendix D.

None of the mixtures exhibited tertiary flow at the stress state they were tested. A summary of the results obtained on the US-131 HMAs is provided in Figure 41, where the plastic strain accumulated after 10000 cycles is reported. Despite the fact that the |E*| values of the GGSP and 5E10 mixtures were comparable (see Figure 36a), and the GGSP mix had higher binder content than 5E10 (see Table 6), the plastic strain accumulation for the GGSP mix is much less, hence GGSP performed better than 5E10. This confirms that performance indications based solely on dynamic modulus results can be misleading. The |E*| is a nondestructive test run at a very low strain level by design. It only gives stiffness, not necessarily how plastic deformation accumulates in a mix. The RLPD is a 'high strain' test where sample is exposed to large amount of load, and it deforms during testing. Therefore, it better simulates the rutting behavior. GGSP's aggregate

skeleton, combined with polymer modified binder are the two potential reasons for its superior performance. The 4E30 (leveling course, long-life section) also performed better than the material of the corresponding layer in the standard section (3E10), although their stiffnesses were comparable (see Figure 36b). This can be attributed to the fact that the 4E30 mix has been designed using a higher number of gyrations, which probably provides better aggregates' interlocking compared to the one achieved in the 3E10 mix. The accumulated plastic strain in the HMA Base (3E30 and 2E10) were similar on average, with high variability observed between the long-life test sections.

Similar results were obtained on the HMAs of the I-475 (Figure 42). The surface and intermediate layers of long-life sections (GGSP and 4E30) exhibited lower accumulated plastic strain as compared to those of the standard sections (5E10). The two HMAs used for base course, the 3E30 and 3E10, resulted in similar performance.

Based on these results, the overall rutting susceptibility of the structure used in the long-life sections is generally lower than the one of the standard sections in both projects.

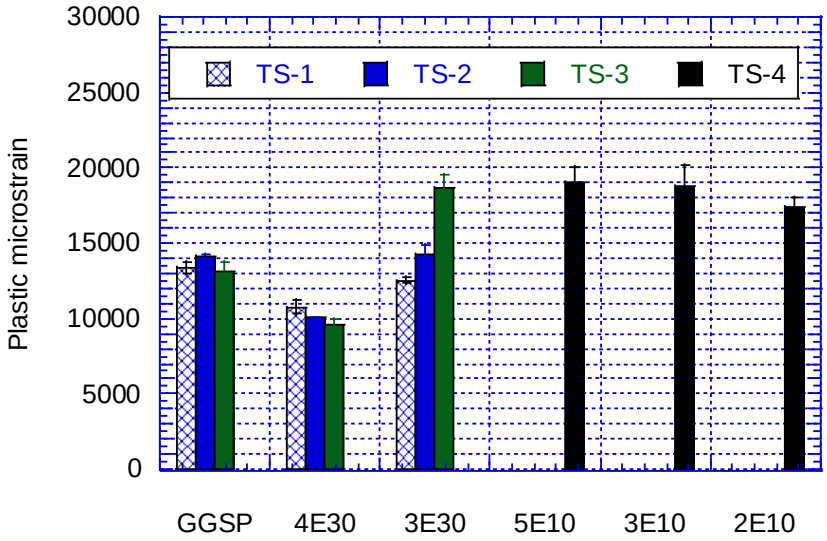

Figure 41. RLPD test results summary for US-131 HMAs.

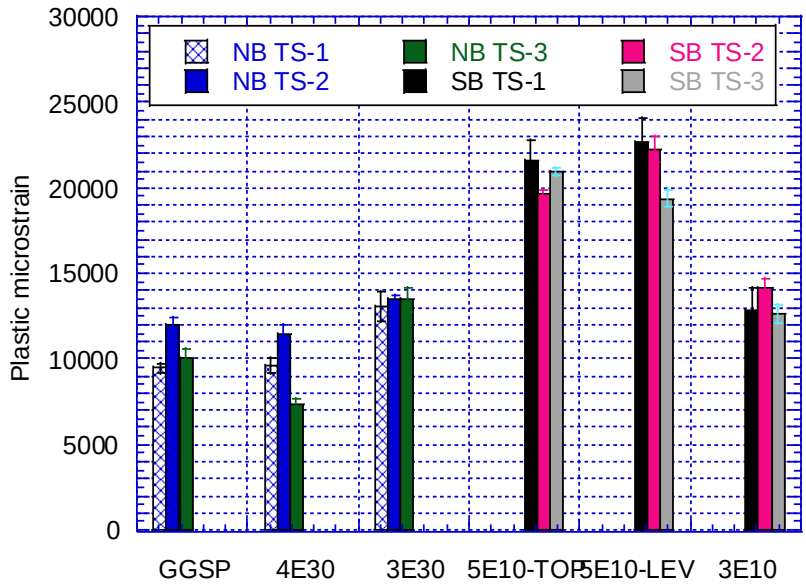

Figure 42. RLPD test results summary for I-475 HMAs.

As mentioned above, results of the RPLD tests were coupled with the confined dynamic modulus test results to calibrate the MEPDG HMA rutting model. The details of the calibration procedure are described in Appendix L and results of the calibration are shown in Table 27 and Table 28.

Table 27 Rutting model calibration coefficients based on the flow number test results US-131

Test section	Mix type	Br1	k1	k2	k3
			-2.4545	3.01	0.22
			Log Br1	Br2	Br3
TS-1	GGSP	118759	5.07	-0.3035	0.7451
TS-1	4E30	17252	4.24	-0.2025	0.8927
TS-1	3E30	2431	3.39	-0.0648	1.0177
TS-2	GGSP	74746	4.87	-0.2730	0.7605
TS-2	4E30	25547	4.41	-0.2268	0.8380
TS-2	3E30	1686	3.23	-0.0405	1.0669
TS-3	GGSP	161450	5.21	-0.3208	0.7328
TS-3	4E30	33769	4.53	-0.2456	0.8145
TS-3	3E30	93	1.97	0.1422	1.1829
TS-4	5E10	655	2.82	0.0296	1.0561
TS-4	3E10	253	2.40	0.0903	1.1505
TS-4	2E10	2208	3.34	-0.0429	1.0598

Table 28 Rutting model calibration coefficients based on the flow number test results I-475

Direction	Test section	Mix type	Br1	k1	k2	k3
				-2.4545	3.01	0.22
				Log Br1	Br2	Br3

NB	TS-1	GGSP	123296	5.09	-0.3294	0.7371
NB	TS-1	4E30	216204	5.33	-0.3711	0.7613
NB	TS-1	3E30	36248	4.56	-0.2466	0.9038
NB	TS-2	GGSP	350143	5.54	-0.3820	0.7211
NB	TS-2	4E30	380887	5.58	-0.3929	0.7433
NB	TS-2	3E30	59863	4.78	-0.2812	0.8827
NB	TS-3	GGSP	652287	5.81	-0.4306	0.6802
NB	TS-3	4E30	198199	5.30	-0.3770	0.7645
NB	TS-3	3E30	34139	4.53	-0.2429	0.8913
SB	TS-1	5E10-TOP	1627	3.21	-0.0541	1.1606
SB	TS-1	5E10-LEV	742	2.87	0.0082	1.1167
SB	TS-1	3E10	14444	4.16	-0.1862	0.9441
SB	TS-2	5E10-TOP	3075	3.49	-0.0889	1.0579
SB	TS-2	5E10-LEV	1998	3.30	-0.0547	1.0658
SB	TS-2	3E10	219257	5.34	-0.3519	0.8493
SB	TS-3	5E10-TOP	2045	3.31	-0.0594	1.0589
SB	TS-3	5E10-LEV	3612	3.56	-0.0986	1.0299
SB	TS-3	3E10	86275	4.94	-0.3085	0.9103

Asphalt Mixture Low-Temperature Indirect Tensile Test (IDT)

The low-temperature indirect tensile tests (IDT) were conducted on mixtures obtained from the I-475 project in accordance with AASHTO T-322-07. The IDT strength tests were performed at -10°C by applying a monotonic displacement-controlled load along the diameter of a cylindrical sample at a rate of 12.5 mm per minute. Samples had a diameter of 150 mm and typical thickness of 38 mm. The maximum load before sample failure is used to calculate the IDT strength of the sample using the following formula:

$$\sigma_s = \frac{2P}{\pi D t_s} \qquad \text{Equation 8}$$

where σ_s is the IDT strength (psi), P the max load (lbs), D is the diameter of the sample (in) and t_s the thickness of the sample (in).

The average of three replicates was used to calculate the IDT strength for each mixture. Typically, for each test section, two samples were in the 7%±0.5% range of air voids, while the third one was slightly out of this range. Tests were performed on all asphalt layers for I-475 Northbound (GGSB, 4E30 and 3E30) and Southbound (5E10 Top, 5E10 Leveling and 3E10 Base) and all test sections (TS1, TS2 and TS3) as part of this project. The US-131 mixtures were instead tested as part of another project with MDOT. The complete set of raw data and volumetrics for all I-475 and US-131 samples are provided in Appendix E. A summary of the IDT test results for I-475 is shown in Figure 43. GGSP and 4E30 show higher IDT strength values compared to 3E30. As expected, 5E10-Top and 5E10-Lev showed similar behavior. The differences of IDT strength values for all of the three mixtures in the standard sections (5E10-Top, 5E10-Lev, and 3E10) are negligible. The raw data of the IDT tests were also used for calculating the Work of Fracture (WOF). The WOF is defined as the area under the IDT load-displacement curve, and it indicates the potential for dissipating energy before failure (Table 29). Mixtures with high WOF typically perform better in the field. Although a direct comparison can be made for all mixtures and among

those of the same layer, it is worth focusing on differences between mixes used for wearing course, since thermal cracking initiates at the surface and then propagate into the pavement structure. The WOF is consistently higher for HMAs used in the long-life sections and, consequently, better thermal cracking performance are expected.

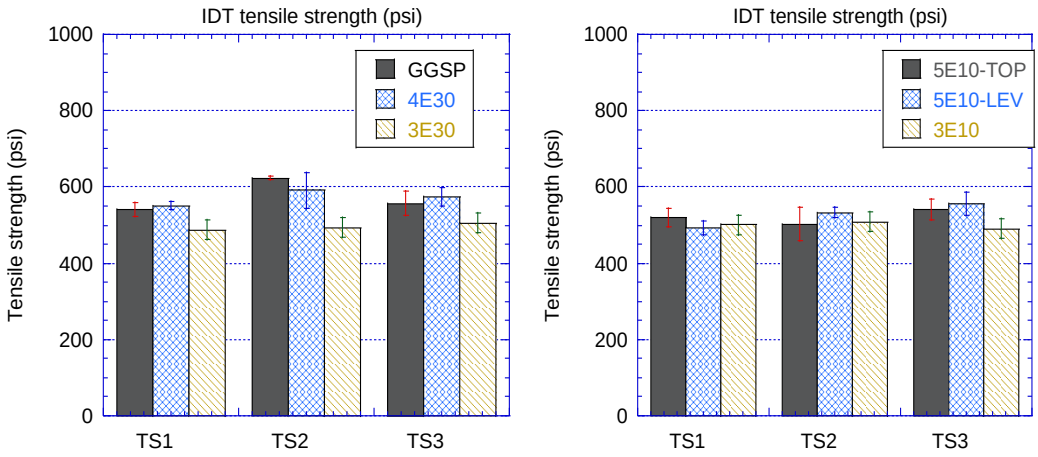

Figure 43 Summary of IDT test results I-475

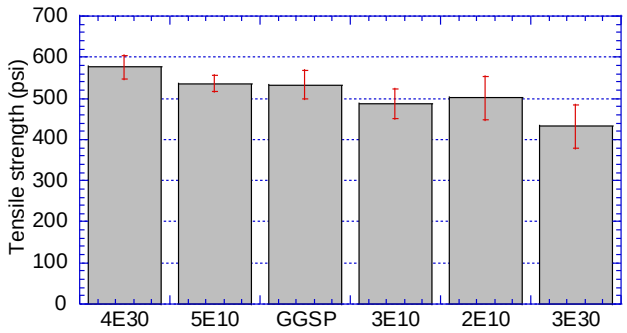

Figure 44 The Indirect Tensile Strength values of the asphalt mixture samples at -10C. (Average of TS1, TS2 and TS3 are shown for GGSP, 4E30 and 3E30)

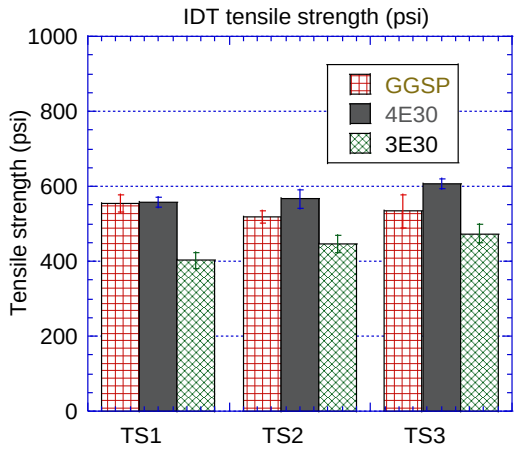

Figure 45 Comparison of US-131 Long-life sections IDT results

Table 29 IDT fracture work summary

Project	Mixtures	GGSP	4E30	3E30	5E10-Top	5E10-Lev	3E10
I-475	Average WOF (Joule)	56.5	39.9	55.2	48.9	45.5	43.5
	Standard deviation	20.3	5.9	10.1	4.0	7.2	10.4
	Mixtures	GGSP	4E30	3E30	5E10	3E10	2E10
US-131	Average WOF(Joule)	64.5	37.3	35.6	32.0	28.5	37.1
	Standard deviation	7.9	6.2	7.2	4.3	1.9	9.9

Asphalt Mixture Three-point Bending Cylinder (3PBC) Test

The 3PBC test was developed as part of NCHRP IDEA 20-30/IDEA 218 project [20]. The 3PBC test is run to determine the fatigue life (i.e., number of cycles to failure, N_f) of asphalt mixtures using cylindrical samples subjected to cyclic three-point bending [19]. A picture of the testing setup is shown in Figure 46. The tests have been conducted on the 68 mm diameter samples obtained by vertically coring a gyratory compactor sample obtained using the loose mixtures collected throughout the project. No further sample preparation (e.g., cutting) was required. The air voids content of each sample was 7±0.5%. The fatigue test was performed in a displacement-controlled mode, and it was conducted at a frequency of 5 Hz. Tests were repeated at two temperatures (10 and 20°C), two replicates at each temperature.

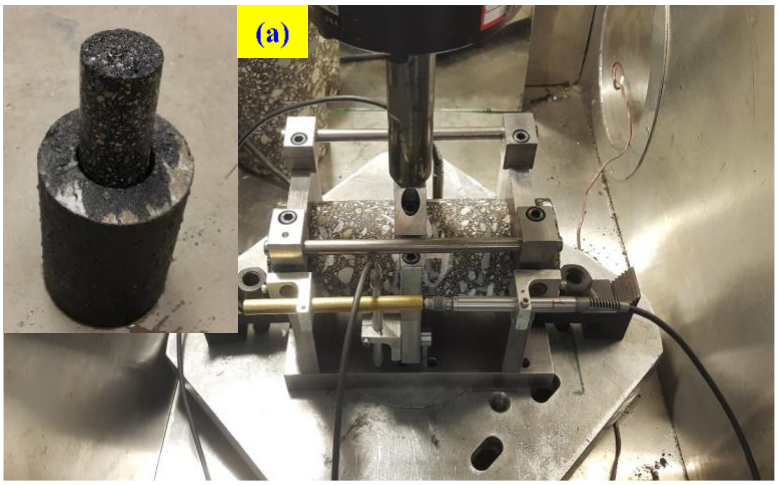

Figure 46 A picture of the 3PBC setup in the material testing system (MTS) with the 68 mm sample

The HMA bottom-up fatigue cracking model implemented in the AASHTOWare Pavement ME software correlates the fatigue life (N_f) to tensile strain (ε_t) and modulus (E) of the asphalt mixture. In this study, first, the raw data of the 3PBC test was analyzed using the Viscoelastic Continuum Damage (VECD) theory [21-23]. The VECD model is based on the elastic–viscoelastic correspondence principle and Schapery's work potential theory to model the mechanical behavior of asphalt mixtures [23]. The application of the VECD formulations allow the prediction of N_f values at different temperatures, strain levels, and frequencies, from a limited set of laboratory data. This eliminates the need to run time consuming fatigue tests at multiple temperatures and strain levels.

The number of cycles to failure (N_f) from the 3PBC tests for surface and base mixes of the I-475 project are displayed in Figure 47 (for 300 micro strain level). As shown, the fatigue cracking performance of the GGSP mixture is, on average, better than any other mixture tested, including the 5E10 mixture used for the surface layer of the traditional section. The HMAs for base layers, 3E30 and 3E10, exhibited a mixed trend. The 3E30 performed better than 3E10 at 10°C but worse at 20°C. This may be an indication of these two mixtures being equivalent. It is worth noting that the long-life sections are designed quite thick so that no bottom-up cracking develops throughout its service life. Therefore, even if 3E30 were to be less resistant that 3E10, the cracks would not develop because of the low strain levels at the bottom of the asphalt due to the additional thickness. On the other hand, top-down cracking is quite possible in thick asphalt pavements. The fact that the GGSP mix performed better in fatigue compared to 5E10 mix is a positive finding and may indicate that the long-life sections will perform better in terms of top-down cracking.

Figure 48 summarizes the results of fatigue tests for US-131 surface and base mixes. Also in this case, the GGSP with polymer-modified binder is performing better compared to the 5E10 mixture at both 10 and 20°C. It is worth mentioning that the 5E10 mix has been produced with 19%-Tier 2 RAP, which might have played a role in the results obtained. The comparison of the 3E30 vs. 2E10 base mixes indicates that the two mixes have similar performance at 20°C while 2E10 has slightly better performance at 10°C.

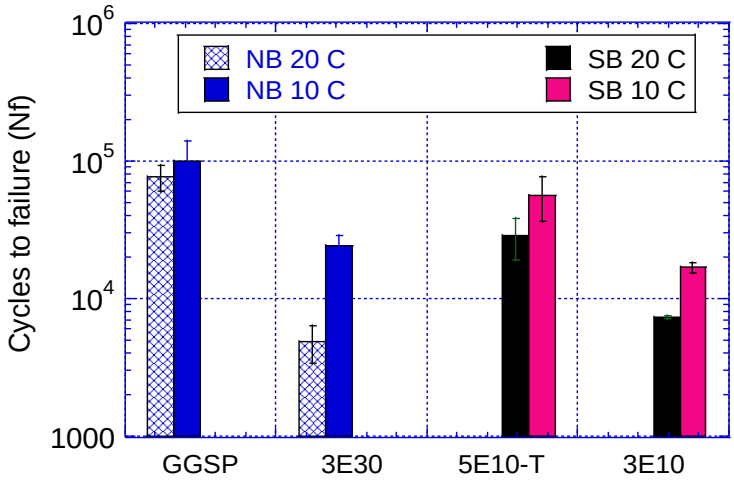

Figure 47 The summary of fatigue testing on surface and base mixtures of I-475 at 300με

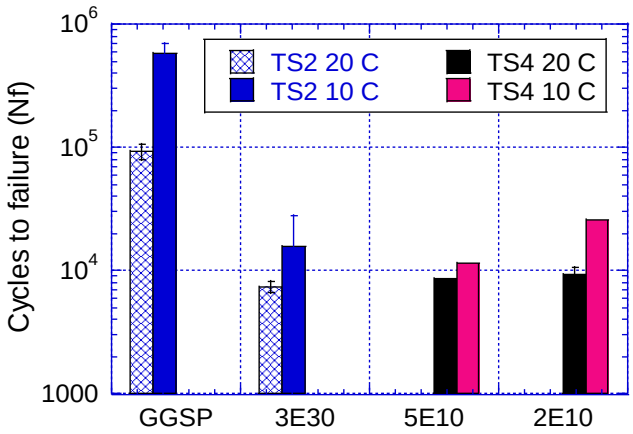

Figure 48 3PBC fatigue testing summary on the surface and base mixtures of US-131 HMA project at 300με

HMA Pavement Core Testing

For each test section of the I-475 project, three cores were provided from the HMA top course, levelling course, and base course. For the long-life test sections separate cores were taken from the 1st lift and 2nd lift of the base course (3E30). Core thicknesses for each of the three core samples of each test section (i.e., TS1-1 means core #1 of TS1) are shown in Table 34 and Table 35 for long-life and standard sections, respectively. As shown, the core thickness variability was about 10% (based on the coefficient of variation - COV) for long-life sections and the average thicknesses were very close to the design thicknesses. Core thickness variability (COV) in standard sections varied from 4.4% to 21.2% and top course was slightly thicker than the design and leveling course was slightly thinner. Overall thickness of the standard sections was slightly lower than the design thickness.

Core air voids of long life and standard sections are shown in Table 32 and Table 40, respectively. As shown, the air voids ranged from 4-5% on average for the long-life sections whereas the air voids for standard sections were slightly above 5% on average. Overall, all these

air voids are quite good and shows good compaction characteristics for both standard and long-life sections.

Core thicknesses of US-131 project are shown in Table 34 and Table 35 for long-life and standard sections, respectively. Overall, the core thickness variability was low in both sections however, standard section thicknesses were a bit lower than the design thickness. Core air voids of US-131 are shown in Table 36 and Table 37. All air voids were about 5-6%, except the GGSP layers where higher air voids were observed (~9% on average).

Table 30 Core thicknesses for I-475 project: Long-life sections

	Thickness (in)													
AC Layer	TS 1-1	TS 1-2	TS 1-3	TS 2-1	TS 2-2	TS 2-3	TS 3-1	TS 3-2	TS 3-3	Avg	COV (%)	Min	Max	Design
GGSP (NB Top)	2.01	2.56	2.20	2.01	1.93	2.05	1.81	2.28	1.77	2.07	11.9%	1.77	2.56	2.00
4E30 (NB Leveling)	2.48	2.40	2.68	2.48	2.60	2.76	1.85	2.68	2.68	2.51	10.9%	1.85	2.76	2.50
3E30 (NB Base, lift 2)	3.58	2.99	3.66	3.15	3.23	2.68	3.07	3.39	3.11	3.21	9.5%	2.68	3.66	3.25
3E30 (NB Base, lift 1)	3.19	3.54	2.48	3.35	2.83	3.46	3.15	3.50	3.23	3.19	10.8%	2.48	3.54	3.25
Total	11.26	11.50	11.02	10.98	10.59	10.94	9.88	11.85	10.79	10.98	5.1%	9.88	11.85	11.00

Table 31 Core thicknesses for I-475 project: Standard sections

	Thickness (in)													
AC Layer	TS 1-1	TS 1-2	TS 1-3	TS 2-1	TS 2-2	TS 2-3	TS 3-1	TS 3-2	TS 3-3	Avg	COV (%)	Min	Max	Design
5E10 (SB Top)	2.0	2.2	2.3	2.1	2.0	2.4	1.7	2.1	2.0	2.08	10.2%	1.65	2.40	1.75
5E10 (SB Leveling)	2.7	2.4	2.7	1.7	1.8	1.9	1.7	1.7	1.9	2.04	21.2%	1.65	2.72	2.50
3E10 (SB Base)	3.7	3.4	3.3	3.6	3.4	3.5	3.2	3.5	3.3	3.44	4.4%	3.19	3.70	3.50
Total	8.35	7.95	8.31	7.32	7.24	7.80	6.50	7.28	7.24	7.55	7.9%	6.50	8.35	7.75

Table 32 Core air voids for I-475 project: Long-life sections

	Core Air Voids (%)												
AC Layer	TS 1-1	TS 1-2	TS 1-3	TS 2-1	TS 2-2	TS 2-3	TS 3-1	TS 3-2	TS 3-3	Avg	COV (%)	Min	Max
GGSP (NB Top)	4.9	4.8	3.3	4.9	5.2	3.1	4.0	3.1	3.5	4.09	20.9%	3.13	5.19
4E30 (NB Leveling)	4.5	4.1	3.7	4.4	5.7	4.6	6.3	4.1	5.1	4.72	17.3%	3.73	6.27
3E30 (NB Base, lift 2)	4.9	5.2	4.9	5.6	5.7	5.3	4.3	4.7	5.5	5.14	9.0%	4.33	5.72
3E30 (NB Base, lift 1)	3.5	4.2	4.4	4.2	5.6	4.7	5.7	4.7	3.8	4.54	16.7%	3.48	5.71

Table 33 Core air voids for I-475 project: Standard sections

	Core Air Voids (%)												
AC Layer	TS 1-1	TS 1-2	TS 1-3	TS 2-1	TS 2-2	TS 2-3	TS 3-1	TS 3-2	TS 3-3	Avg	COV (%)	Min	Max
5E10 (SB Top)	7.0	5.0	5.7	4.7	4.9	5.6	5.5	5.2	4.0	5.28	15.6%	3.97	6.96
5E10 (SB Leveling)	6.1	4.0	5.2	5.1	4.8	4.6	5.1	4.7	4.5	4.89	12.2%	3.97	6.12
3E10 (SB Base)	6.8	6.7	5.3	5.3	5.4	5.7	4.4	3.3	5.1	5.35	20.1%	3.30	6.80

Table 34 Core thicknesses for US-131 project: Long-life sections

	Thickness (in)													
AC Layer	TS 1-1	TS 1-2	TS 1-3	TS 2-1	TS 2-2	TS 2-3	TS 3-1	TS 3-2	TS 3-3	Avg	COV (%)	Min	Max	Design
GGSP (NB Top)	1.50	1.63	1.63	1.63	1.63	1.63	1.50	1.38	1.50	1.56	5.9%	1.38	1.63	1.50
4E30 (NB Leveling)	2.38	2.38	2.38	2.75	3.00	3.00	1.75	2.13	2.50	2.47	16.3%	1.75	3.00	2.50
3E30 (NB Base, lift 2)	3.25	3.75	4.00	3.63	4.38	4.38	3.75	3.75	3.00	3.77	12.2%	3.00	4.38	3.63
3E30 (NB Base, lift 1)	3.88	3.00	2.75	3.13	3.25	3.38	3.00	3.00	4.38	3.31	15.5%	2.75	4.38	3.63
Total	11.01	10.76	10.76	11.14	12.26	12.39	10.00	10.26	11.38	11.11	7.3%	10.00	12.39	11.25

Table 35 Core thicknesses for US-131 project: Standard sections

	Thickness (in)							
AC Layer	TS 4-1	TS 4-2	TS 4-3	Avg	COV (%)	Min	Max	Design
5E10 (NB Top)	1.88	2.00	2.00	1.96	3.5%	1.88	2.00	1.75
3E10 (NB Leveling)	2.75	2.75	2.25	2.58	11.2%	2.25	2.75	3.00
2E10 (NB Base)	4.25	3.88	3.63	3.92	8.0%	3.63	4.25	4.50
Total	8.88	8.63	7.88	8.46	6.1%	7.88	8.88	9.25

Table 36 Core air voids for US-131 project: Long-life sections

	Core Air Voids (%)												
AC Layer	TS 1-1	TS 1-2	TS 1-3	TS 2-1	TS 2-2	TS 2-3	TS 3-1	TS 3-2	TS 3-3	Avg	COV (%)	Min	Max
GGSP (NB Top)	8.70	8.70	8.60	9.20	9.20	7.30	9.60	9.30	10.00	8.96	9%	7.30	10.00
4E30 (NB Leveling)	5.60	6.80	5.30	4.80	5.30	3.90	5.90	6.60	4.30	5.39	18%	3.90	6.80
3E30 (NB Base, lift 2)	5.90	5.10	6.40	5.90	5.80	5.70	4.50	6.20	5.00	5.61	11%	4.50	6.40
3E30 (NB Base, lift 1)	5.20	5.40	4.30	5.50	6.80	6.50	3.80	5.30	5.90	5.41	18%	3.80	6.80

Table 37 Core air voids for US-131 project: Standard sections

	Core Air Voids (%)						
AC Layer	TS 4-1	TS 4-2	TS 4-3	Avg	COV (%)	Min	Max
5E10 (NB Top)	4.80	6.30	4.80	5.30	16%	4.80	6.30
3E10 (NB Leveling)	4.10	6.70	8.20	6.33	33%	4.10	8.20
2E10 (NB Base)	5.20	5.10	5.60	5.30	5%	5.10	5.60

PCC Materials Testing

This section summarizes the laboratory test results performed on concrete samples of the two JPCP projects. The laboratory tests included the determination of the mechanical properties, evaluation of the thermal expansion coefficient, measurement of the electrical resistivity, and durability.

Mechanical Properties

The mechanical properties of concrete including elastic modulus, compressive and flexural strengths were determined in the laboratory using the concrete samples (i.e., cylinders, cores, and beams) for both projects. A summary of the mechanical properties of each JPCP project is presented below.

I-69 JPCP Project

Table 38 summarizes the results of the compressive strength tests for all sections of the I-69 JPCP project. It is noted that concrete samples (cores) from the long-life WB TS-3 and TS-4 were provided by MDOT and tested in the laboratory using the setup shown in Figure 49. The compressive strength values for the standard design sections (i.e., EB TS-1 and TS-2) were retrieved from the MDOT's construction database for the project. The age of the WB TS-3 and TS-4 samples at the time of testing was about 2 years. Since the AASHTOWare Pavement-ME software requires 28-day compressive strength as an input for the PCC layer, the laboratory compressive strengths and the elastic moduli for the WB sections were corrected to their 28-day equivalents using the Pavement-ME equation (Table 38). Figure 50 shows a comparison between the compressive strengths of the standard and long-life pavement materials. The results do not vary since the same non-reinforced high-performance concrete mix was used to construct the PCC slab irrespective of the design of the pavement (i.e., long-life or standard).

Table 38 Compressive strength and elastic modulus test results - I-69 JPCP project

Design/ direction	TS	Sample age	Number of samples	Mean strength (psi)	Std. strength (psi)	Mean elastic modulus (psi)	Std. modulus (psi)
Standard/ EB*	TS-1	30 days	3	6763	378	-	-
Standard/ EB*	TS-2	28 days	3	5847	118	-	-
Long-life/ WB	TS-3	28 days	3[#]	6133	30	3,076,291	314,491
Long-life/ WB	TS-4	28 days	4	5848	270	2,978,928	216,099

*"-" = No data. *Compressive strength values for standard design (EB) sections retrieved from MDOT Report of Test (1854) dated 9/7/2018. [#]Core # 29 was excluded in the mean calculation due to extremely low strength.*

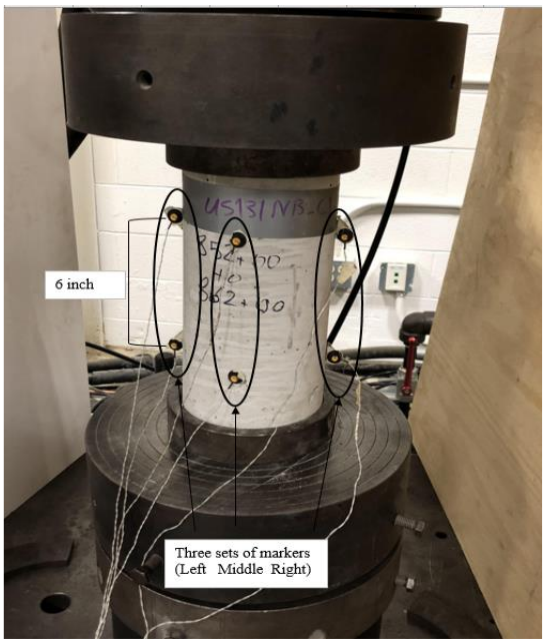

Figure 49 Elastic modulus and compressive strength test setup

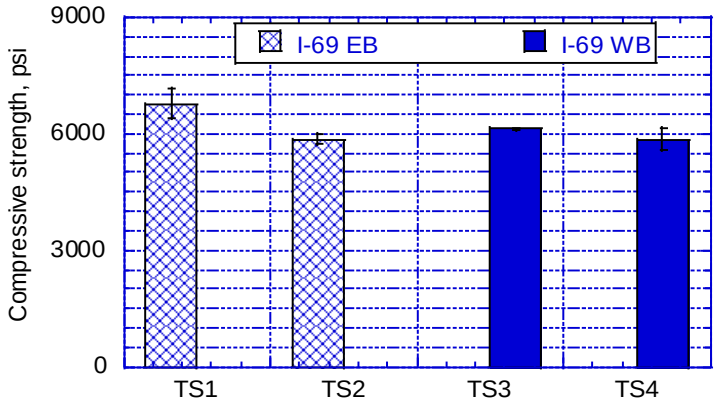

Figure 50 28-day compressive strengths - I-69 JPCP project

Table 39 shows the modulus of rupture (MOR) test results based on third-point loading method using MDOT's portable setup in the Construction Field Services Laboratory. The MOR values for the EB standard design pavement sections were retrieved from the construction records of the project since no beam test data were available. The MOR values for the long-life WB sections were determined in the laboratory. Like in the case of the compressive strength test results, given the age of the samples tested, the 28-days MOR values reported in Table 39 were back-calculated using the AASHTOWare Pavement ME equation. These values are also reported in Figure 51, where negligible difference between all test sections can be observed. Then, the constant k was calculated using the following equation. For the I-69 long-life WB test sections, k was found to be equal to 10 on average, a value in line with the published range of results in the scientific literature.

$$MOR = k \cdot \sqrt{\sigma_c} \qquad \text{Equation 9}$$

Table 39 Modulus of rupture (MOR) - I-69 JPCP project

Design/ direction	TS	Specimen age	Number of specimens	Mean MOR (psi)	Standard deviation (psi)	Minimum MOR (psi)	Maximum MOR (psi)
Standard/ EB*	TS-1	30 days	3	767	27	733	800
Standard/ EB*	TS-2	28 days	3	863	35	817	903
Long-life/ WB	TS-3	2.26 yrs.	6	890	61	800	967
		28 days[#]	6	778	54	-	-
Long-life/ WB	TS-4	2.32 yrs.	3	890	27	862	917
		28 days[#]	3	777	26	-	-

*"-" = No data. *MOR values for EB sections retrieved from MDOT Report of Modulus of Rupture (1160) dated 8/7/2018 & 8/9/2018. [#]Estimated 28-day MOR using Pavement-ME equation.*

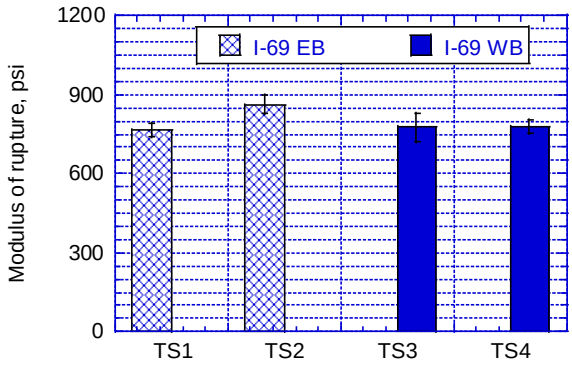

Figure 51 28-day modulus of rupture - I-69 JPCP project

US-131 JPCP Project

Table 40 summarizes the concrete compressive strength results for the US-131 test sections. The strength values shown for the standard (SB) test sections are based on concrete percent-within-limit (PWL) excel sheets from the MDOT's construction records for the project. The strength values for the NB long-life sections displayed in the table are the 28-day back-calculated values using the AASHTOWare Pavement ME equation. The k values of the long-life US-131 NB sections were also estimated to be close to 10. Figure 52 shows a comparison between the 28-day compressive strengths of all the US-131 JPCP project test sections. Despite some variability, compressive strengths are comparable, in line with the fact that the same concrete mix was used to build all test sections.

Table 40 Compressive strength and elastic modulus test results – US-131 JPCP project

Design/ direction	TS	Sample age	Number of samples	Mean strength (psi)	Std. strength (psi)	Mean elastic modulus (psi)	Std. modulus (psi)
Long-life/ NB	TS-1	28 days	2	6570	690	4,351,195	327,232
Long-life/ NB	TS-2	28 days	2	6363	279	3,478,185	6,958
Long-life/ NB	TS-3	28 days	2	7073	218	4,127,731	99,163
Standard/ SB*	TS-1	28 days	10	5808	372	-	-
Standard/ SB*	TS-2	28 days	10	6540	353	-	-
Standard/ SB*	TS-3	28 days	6	5918	209	-	-

*"-" = No data. *SB test results are taken from concrete PWL sheet for US-131.*

Table 41 shows the MOR test results for all the test sections of the US-131 JPCP project. The MOR values for the standard SB test sections are estimated using the MOR equation with a constant k value of 10. Although the value of 10 was estimated from the concrete test results for the NB sections, it was used for MOR estimation of the SB sections as all the sections were built using the same concrete mix. Figure 53 shows the comparison between the MOR values for all the US-131 test sections. NB TS-3 shows the highest concrete MOR as compared to the other sections. The MOR values for all the other test sections are generally comparable.

The results of the compressive strength tests performed on the CTPB cylinders provided from TS-1 and 2 of the long-life NB test sections of the US-131 JPCP project are reported in Table 42. The average value for TS-1 was found to be significantly higher than that of TS-2. Moreover, only one CTPB sample could be tested for elastic modulus determination to prevent damage to the camera sensors of the testing equipment due to the low strength of such material. An ***elastic modulus of 1.3 x 10^6 psi*** was determined for this sample, in agreement with the in-situ elastic moduli determined using the FWD test results. Thus, on average, using a modulus of one million psi for the CTPB layer in the Pavement ME analyses is reasonable.

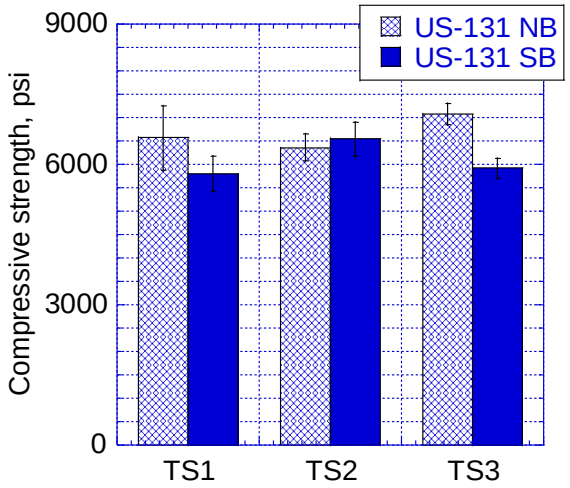

Figure 52 28-day compressive strengths - US-131 JPCP project

Table 41 Modulus of rupture (MOR) – US-131 JPCP project

Design/ direction	TS	Specimen age	Number of specimens	Mean MOR (psi)	Standard deviation (psi)	Minimum MOR (psi)	Maximum MOR (psi)
Long-life/ NB	TS-1	1.79 yrs.	3	833	17	817	850
		28 days#	3	735	15	-	-
Long-life/ NB	TS-2	1.85 yrs.	3	861	17	842	875
		28 days#	3	758	15	-	-
Long-life/ NB	TS-3	1.78 yrs.	3	969	24	942	983
		28 days#	3	855	21	-	-
Standard/ SB*	TS-1	28 days	10	762	24	727	805
Standard/ SB*	TS-2	28 days	10	808	22	775	788
Standard/ SB*	TS-3	28 days	6	769	14	748	788

*"-" = No data. *MOR values for SB sections were calculated using the MOR equation with a constant value of k =10. #Estimated 28-day MOR using Pavement-ME equation.*

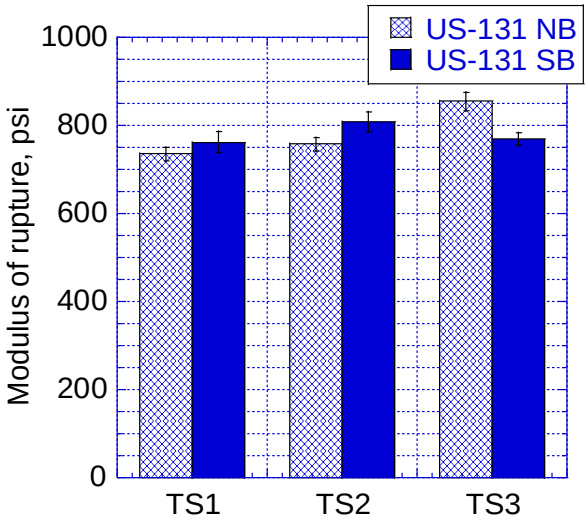

Figure 53 28-day modulus of rupture - US-131 JPCP project

Table 42 CTPB compressive strength test results – US-131 NB JPCP project

Long-life/ NB TS	Specimen age (years)	Failure load (lbs)	Compressive strength (psi)	Average compressive strength (psi)	Standard deviation (psi)
TS-1	2.42	21925	776	740*	36
TS-1	2.42	10395	368		
TS-1	2.42	19892	704		
TS-2	2.41	18283	647	587*	60
TS-2	2.41	11270	399		
TS-2	2.41	14908	528		

**Average calculation excludes the low values highlighted in red.*

Coefficient of Thermal Expansion (CTE) Test

The Coefficient of Thermal Expansion (CTE) measures Portland Cement Concrete (PCC) contraction or expansion caused by temperature changes. As the length changes associated with the thermal expansion are small, it is usually expressed in microstrain (10^{-6}) per degree Celsius (με/ °C) or microstrain per degree Fahrenheit (με/ °F). The typical range of CTE for PCC is about 7.2 to 13 με/ °C (4 to 7.2 με/ °F) [24]. However, the value may vary depending on PCC components, aggregate types, w/c ratio, cement fineness, etc. [25]. The CTE is an essential parameter in the design of concrete pavements. Characterizing the effects of thermal properties on a concrete pavement's structure is to account for its thermal movements. CTE is sometimes represented as an average value rather than a mix-specific input in pavement design. This may lead to erroneous assumptions about the pavement's thermal response and possible distresses. Therefore, conducting CTE tests can help pavement design engineers better predict the impact of mix-specific thermal expansion on pavement behavior.

The AASHTO T 336-15 was adopted to measure the PCC CTE (AASHTO T 336-15 2019). During the test, the specimen is heated in a water bath from 10 to 50°C and then cooled

down to 10 °C. The length and temperature of the specimen at 10°C and 50°C are recorded for CTE calculation for each heating and cooling segment. The CTE value of the test specimen is taken as the average of the heating and cooling segments, provided the two values are within 0.3 microstrain/°C. There are a couple of limitations to the standard method:

- The actual curve of temperature versus length change is unknown within each segment.
- Only the water bath temperature is measured, which may not represent the concrete specimen's temperature.

Therefore, a few modifications were made at the University of Michigan based on AASHTO T336-15 to achieve better accuracy. The modifications are summarized as follows:

- The length change of the specimen vs. temperature is monitored for the entire process.
- Two companion concrete specimens with a thermal couple embedded at the center are introduced to simulate the real temperature change in the test specimens. The average temperature of the two companion concrete specimens was used as the temperature of the test specimen.

Three 6 x 12-inch standard cylinders from US-131 Northbound (NB) sections were used for CTE testing. The surfaces of these cylinders were flat and parallel; thus did not require sawing. However, the three I-69 Westbound (WB) cores had uneven surfaces and were sawn. Their lengths ranged between 9.38 to 9.92 inches after cutting. The prepared specimens from both projects were conditioned by submersion in a limewater bucket for at least 48 hours. Figure 54 and Figure 55 show the CTE test setup.

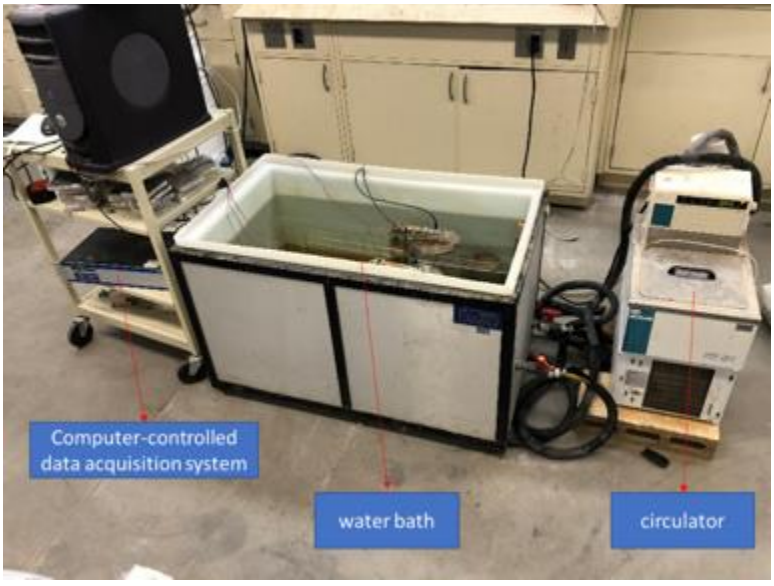

Figure 54 CTE test equipment setup

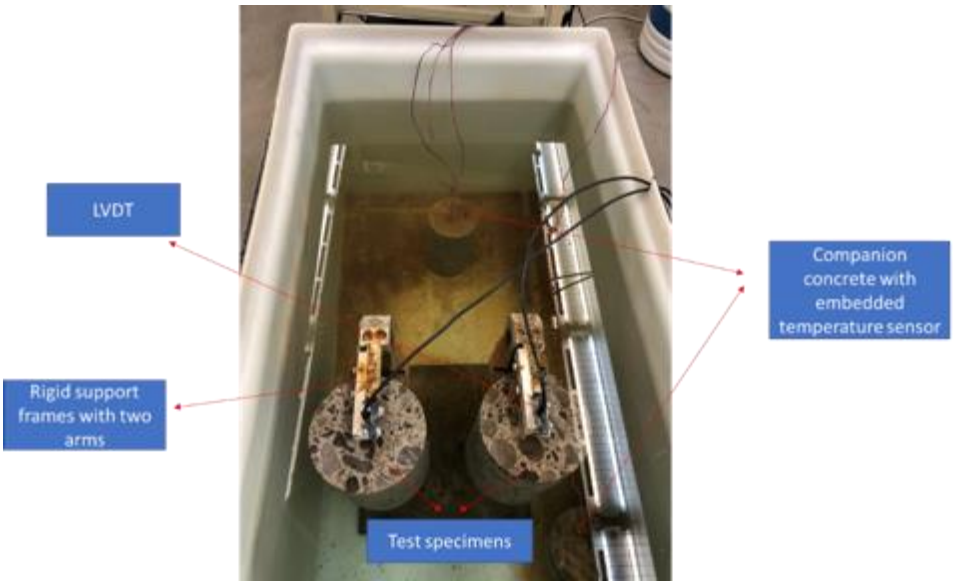

Figure 55 Test specimens connected to the LVDT seating on the frame

Before running the test, calibration is undertaken to measure the correction factor, which can represent the length change of the rigid support frame. Assuming that the length change of the frame varies linearly with temperature, the correction factor is defined as:

$$C_f = \frac{\Delta L_{system}}{L_{CS}} / \Delta T \qquad \text{Equation 10}$$

Where:
L_{CS} = length of the calibration bar at room temperature,
ΔT = temperature change,
ΔL_{system} = change in length of the measuring frame during temperature changes and is given by the equation:

$$\Delta L_{system} = \Delta L_{measured} - \Delta L_a \qquad \text{Equation 11}$$

Where:
$\Delta L_{measured}$ = change in length of the calibration bar during temperature changes,
ΔL_a = actual length change which is obtained by the following equation:

$$\Delta L_a = L_{CS} * \alpha_{invar} * \Delta T \qquad \text{Equation 12}$$

Where:
α_{invar} = CTE of invar.

An Invar 36 with a known coefficient of thermal expansion was used for calibration purposes, shown in Figure 56. The two arms of the support frames were calibrated separately, following the same procedure used for determining the CTE.

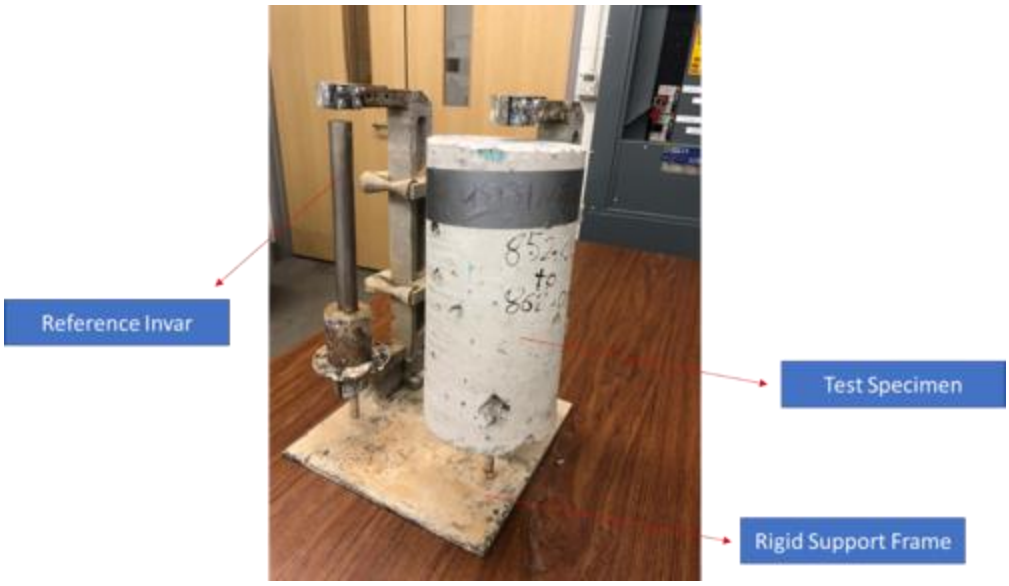

Figure 56 Calibration bar (left) and test specimen (right) seating on the rigid support frame

Table 43 summarizes the dimensions and CTE test results for both the long-life projects. The estimated CTE for cylinders from the US-131 NB project has an average of 7.04 microstrain/°C (3.91 microstrain/°F) after calibration. The CTE estimated using core #61 from the I-69 WB project is much higher than other specimens from the project. Repeated tests on core #61 resulted in similar high CTE values. Therefore, the average CTE estimated using cores from the I-69 WB project is 6.90 microstrain/°C (3.83 microstrain/°F), excluding core #61, which is considered an outlier. The test results showed that the concrete's length changed almost linearly with temperature changes (see Figure 57 and Figure 58). Some nonlinearity is observed as the temperature approaches its lower and higher limits. This non-linear behavior might be caused due to a decrease in the rate of temperature change.

Table 43 Dimensions and CTE results of test specimens

Project	Specimen number	Test section	Length (in)	Diameter (in)	CTE test (AASHTO T336-15)	
					($\times 10^{-6}$ in/in/°C)	($\times 10^{-6}$ in/in/°F)
US-131 NB	C1-3	TS-1	12.035	6.062	8.111	4.506
	C2-3	TS-2	12.047	6.112	6.282	3.490
	C3-3	TS-3	12.046	6.080	6.713	3.729
I-69 WB	#27	TS-4	9.922	5.910	6.733	3.740
	#61	TS-4	9.384	5.906	11.581	6.433
	#61B	TS-4	9.712	5.914	7.033	3.907

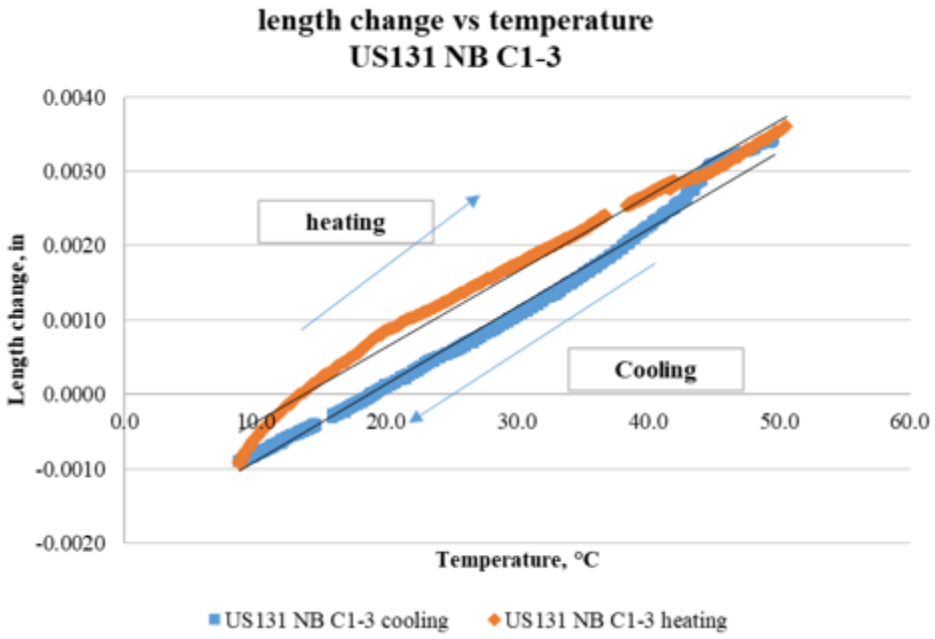

Figure 57 Length change vs. temperature for US-131 NB specimen C1-3

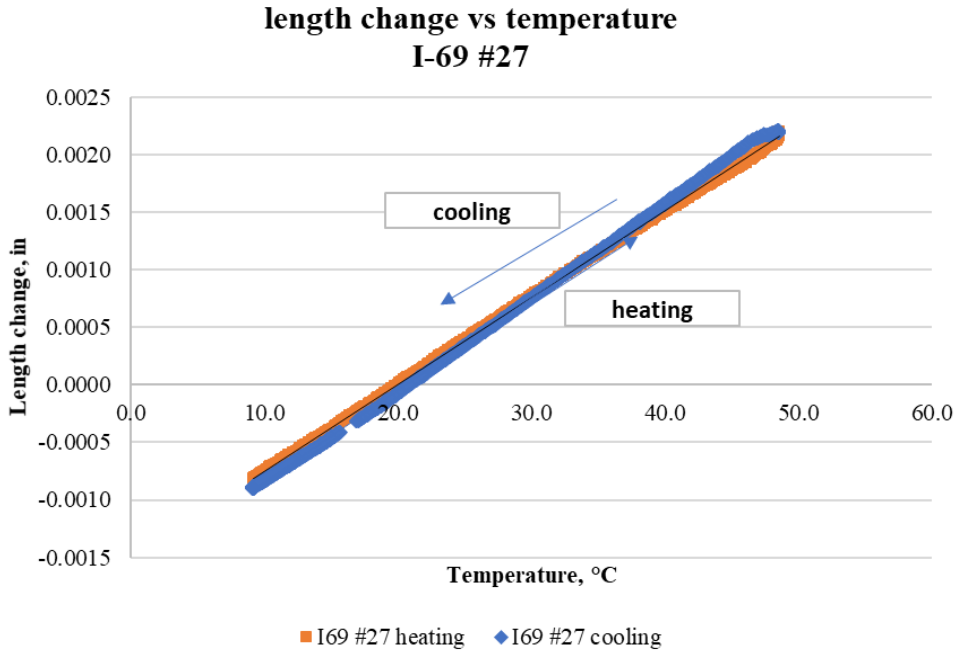

Figure 58 Length change vs. temperature for I-69 WB specimen #27

Concrete Resistivity Testing

Table 10 showed the relationship between the chloride ion penetrability and the SR test (AASHTO TP 95) that measures the electric resistivity of the concrete from concrete cylinders/cores [17]. The SR test results conducted on concrete samples from the long-life pavement sections of I-69 WB and US-131 NB JPCP projects are summarized in Table 44. The

concrete of the US-131 JPCP project falls under very low, while that of the I-69 project falls under low to very low chloride ion penetrability.

Table 44 Resistivity test results

Project	Specimen number	Resistivity (kΩ·cm)	
US-131 NB	1-3	93.2	Mean = 97.7 Std. = 4.90
	2-3	102.9	
	3-3	96.9	
I-69 WB	#27	48.6	Mean = 37.2 Std. = 10.01
	#61	30	
	#61B	32.9	

Water Sorption Test

The water sorption test involved cutting 70mm thick samples with a 100mm width and length from cylinders/cores obtained from the US-131 and I-69 concrete projects. The prepared samples were dried for 2 weeks at 50°C before undergoing a 1-dimentional sorption test for one week according to ASTM C 1585. The sorption test provided a near full water saturation state before freeze-thaw (F-T) testing with the bottom surface continuously in contact with deionized water. Duplicate samples from US-131 and I-69 were moisture conditioned according to the standard procedure and the results are presented in Figure 59 which shows the average values of the tested duplicate specimens.

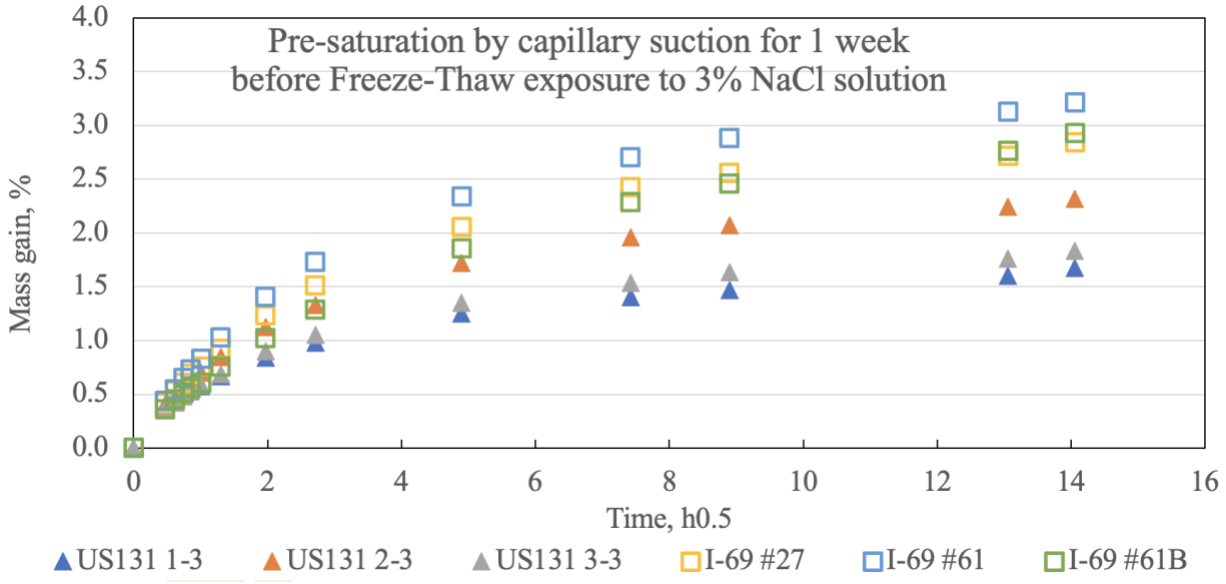

Figure 59 Moisture uptake results according to ASTM C1585

In general, samples from I-69 had a much higher water absorption which indicates a more porous microstructure. The average water absorption after one week for I-69 was about 3.0% while that was about 1.9% for US-131. The denser structure for US-131 led to a decrease in moisture uptake and will potentially increase its F-T resistance.

Freeze-Thaw (F-T) Test

Samples from I-69 had much higher scaling than those from US-131 with I-69 specimen #61B even exceeding the 1500 g/m^2 scaling limit at 28 cycles from RILEM as shown in Figure

60. The scaling development for I-69 showed a bilinear pattern: the deterioration of samples accelerated after about 26 cycles. However, the scaling for US-131 was insignificant with an average of about 500 g/m^2 after 80 cycles. This was consistent with the results from the moisture uptake. The samples from US-131 and I-69 after the F-T testing can be compared are displayed in Figure 61. It is visible in the figure that the I-69 concrete has performed worse as compared to the US-131 in terms of F-T resistance, a durability concern.

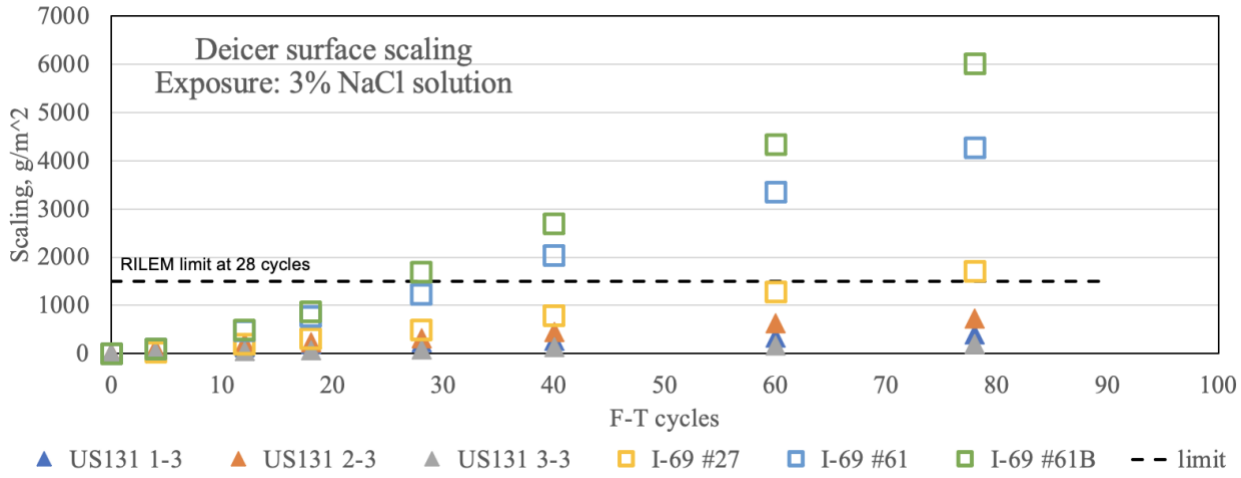

Figure 60 Deicer scaling results

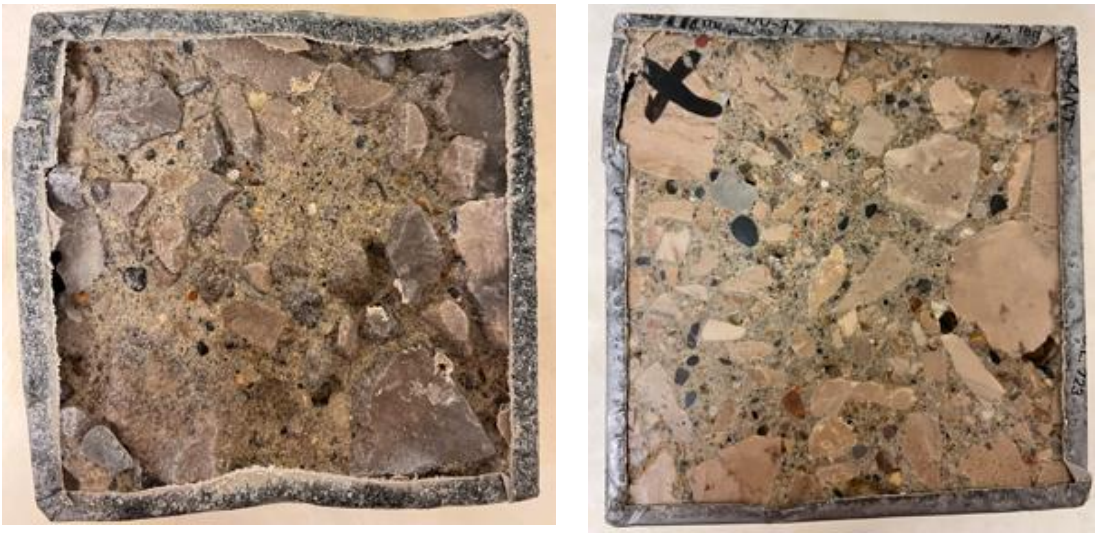

(a) I-69 specimen #61 (b) US-131 specimen 3-3

Figure 61 Samples after the F-T test

The Relative Dynamic Modulus (RDM) of elasticity is the ratio of dynamic modulus of the concrete determined at a certain number of F-T cycles over its initial value (i.e., before the F-T conditioning begins). The samples from US-131 had no internal cracking as the Relative Dynamic Modulus (RDM) remains above 95% during the test periods (Figure 59). The I-69 specimen #27 had less moisture uptake during the sorption test and had no obvious decrease in RDM as well. I-

69 specimens #61 and #61B show different levels of internal cracking. Specimen #61B had a greater drop in RDM which had the largest scaling as well.

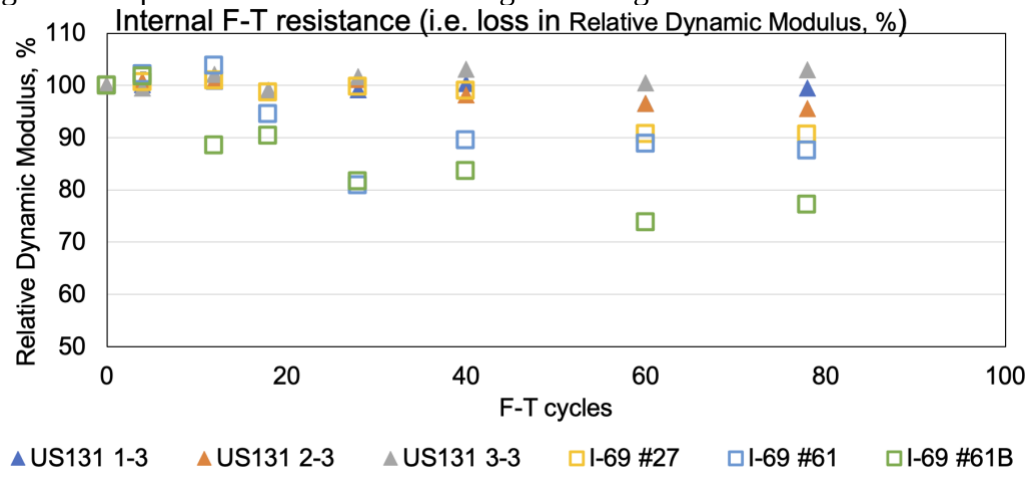

Figure 62 Relative Dynamic Modulus (RDM) results

Concrete Air Void Analysis

Based on ASTM C457, an air void analyzer is used to assess the air-void system in hardened concrete, using both point count procedures and the linear traverse method. 20mm thick square specimens with 100mm width and length are cut from the same beam specimens used for the F-T test. The specimens are first polished using silicon carbide abrasives to obtain a smooth surface. The point count procedure is to determine the volume fractions of air voids, paste and aggregate on the polished surface by recording the number of stops over each phase under the crosshair of a microscope. The same scanned surface is used for the linear traverse test. Before the start of the linear test, the surface was treated by coating it with barium sulfate to fill all the air voids, and the rest of the surface was painted black with caution so that the air voids could form a sharp contrast to the concrete matrix. The RapidAir 457 automatic image analyzer was used to scan the prepared surface for which the air void characteristics report was obtained.

Table 45 shows the air void analysis results. The average hardened air content of samples from US-131 is 5.5% based on the point count results which falls within the range of specified air (5.0% - 8.0%). The average spacing factor is 134 microns which is way below the upper limit of 200 microns recommended by ACI. The average hardened air content of samples from I-69 is 5.9% with an average of 141 microns in spacing factor.

Table 45 Air void analysis based on ASTM C 457

Project	Sample	Station	Point count			Linear traverse test			
						Air content, %		Spacing factor, µm	Specific surface, 1/mm
			Air	Paste	Aggregate	Entrained air <500 µm	Total air <4000 µm		
US-131	1-3	852-862	5.3	27.3	67.4	4.1	5.8	147	31
	2-3	885-895	5.6	22.7	71.7	4.8	5.6	114	36
	3-3	970-980	5.6	22.3	72.1	3.5	4.7	142	32
I-69	#27	404+00	5.9	23.3	70.8	4.3	6.7	134	26
	#61	403+50	6	30.8	63.2	3.8	5.1	161	31
	#61B	405+71	5.9	26.5	67.6	4.4	5.3	128	36

Unbound Material Testing

Unbound material testing included forty-one (41) samples that were collected from I-69, I-475, and US 131 projects. These included 14 granular samples for base course, 13 for subbase, and 14 for subgrade layers. A summary of the material information is provided in Table 46.

Table 46 Unbound material samples information

Location	Pavement Type	TS	Direction	Start Location	End Location	Type of Layer Tested
I-69	Rigid	1	EB	0340+00	0350+00	Base, Subbase, Subgrade
		2	EB	0367+00	0377+00	Base, Subbase, Subgrade
		3	WB	0340+00	0350+00	Base, Subbase, Subgrade
		4	WB	0396+00	0406+00	Base, Subbase, Subgrade
I-475	HMA	1	NB	0650+00	0660+00	Base, Subbase, Subgrade
		2	NB	0745+00	0755+00	Base, Subbase, Subgrade
		3	NB	0770+00	0780+00	Base, Subbase, Subgrade
		1	SB	0650+00	0660+00	Base, Subbase, Subgrade
		2	SB	0745+00	0755+00	Base, Subbase, Subgrade
		3	SB	0770+00	0780+00	Base, Subbase, Subgrade
US 131	HMA	1	NB	1090+00	1100+00	Base, Subbase, Subgrade
		2	NB	1127+52	1137+81	Base, Subbase, Subgrade
		3	NB	1170+00	1180+00	Base, Subbase, Subgrade
		4	SB	1210+10	1220+00	Base, Subbase, Subgrade
	Rigid	1	NB	0852+00	0862+00	Base, Subbase, Subgrade
		2	NB	0885+00	0895+00	Base, Subbase, Subgrade
		3	NB	0970+00	0980+00	Base, Subbase, Subgrade
		1	SB	0850+00	0860+00	Base
		2	SB	0895+00	0905+00	Subbase, Subgrade
		3	SB	0977+00	0987+00	Base, Subbase

HMA = hot mix asphalt; TS = test section; EB = east bound; WB = west bound; NB = north bound; SB = south bound.

Index Properties and Compaction Characteristics

This section presents the index properties of all unbound materials including gradation, soil classification, Atterberg limits and compaction characteristics of the pavement foundation materials.

Material Classification

The particle size distribution of the granular materials was determined in accordance with ASTM C136, D6913, and D7928 and the Atterberg limits were determined in accordance with ASTM D4318. The material classification was performed according to the Unified Soil Classification System (USCS) (ASTM D2487) and the American Association of State Highway and Transportation Officials (AASHTO) soil classification system (AASHTO M 145). Materials collected from each test section layer were mixed together thoroughly and representative samples were taken from each mix and reported. Furthermore, the materials in different section with very similar/identical gradation characteristics were reported using the average value of their combined gradations. Then, hydrometer test and wet sieve and dry sieve analyses were performed on the representative sample to obtain the index properties of that material. Even though the hydrometer tests, sieve analyses, and Atterberg limits tests were performed on all the materials, the results of these tests were combined for the materials showing very similar index properties for simplicity.

Figure 63, Figure 64, and Figure 65 show the gradation curves of the base, subbase, and subgrade materials, respectively. Table 47, Table 48, and Table 49summarize the index properties

of the base, subbase, and subgrade materials, respectively. For some of the test sections, due to the similarity of the material, the materials were combined across the test sections. Raw particle size distribution data is included in Appendix F, while the effective particle size, D_{10}, particle sizes at which 30% and 60% of the particles are finer, D_{30} and D_{60}, are included in Appendix G.

According to the AASHTO classification, all samples collected for the base layers were classified as to A-1-a (stone fragments, gravel and sand). There were three different USCS groups for the base materials: (1) GW (well-graded gravel with or without sand), (2) GW-GM (well-graded gravel with silt and sand), and (3) GP-GM (poorly graded gravel with silt and sand). The subbase materials were classified into three AASHTO groups: (1) A-2-4 (silty or clayey gravel and sand), (2) A-1-b (stone fragments, gravel and sand), and (3) A-3 (fine sand). According to USCS, these materials were either SW-SM (well-graded sand with silt or with silt and gravel), SP-SM (poorly graded sand with silt or with silt and gravel), or SP (poorly graded sand with or without gravel). Finally, the samples of the subgrade layers, were classified as A-1-b (stone fragments, gravel and sand), A-2-4 (silty or clayey gravel and sand), A-3 (fine sand), A-4 (silty soil), and A-6 (clayey soil) groups according to AASHTO, and SM (silty sand), SW-SM (well-graded sand with silt and gravel), SP-SM (poorly graded sand with silt), SP (poorly graded sand with or without gravel), CL-ML (sandy silty clay), and CL (sandy lean clay) following the USCS groups.

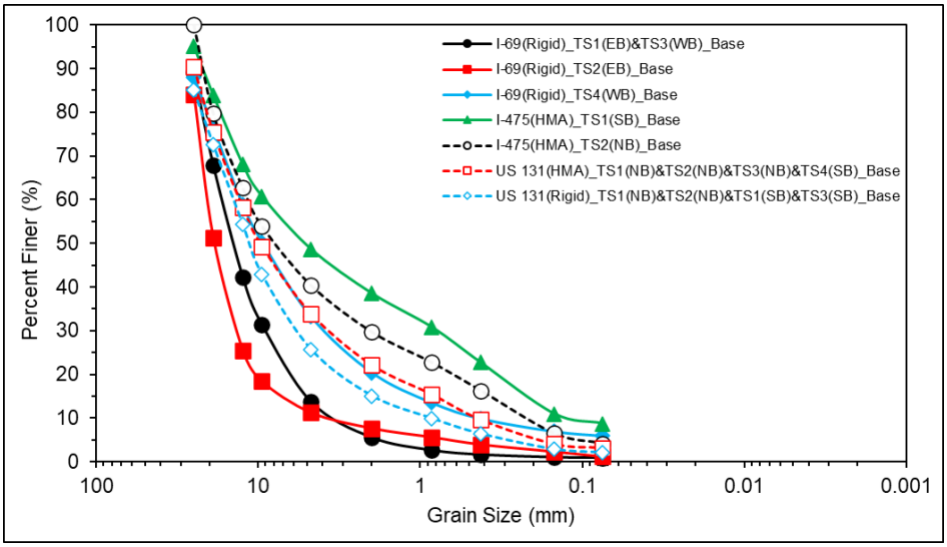

Figure 63 Particle size distributions of base materials

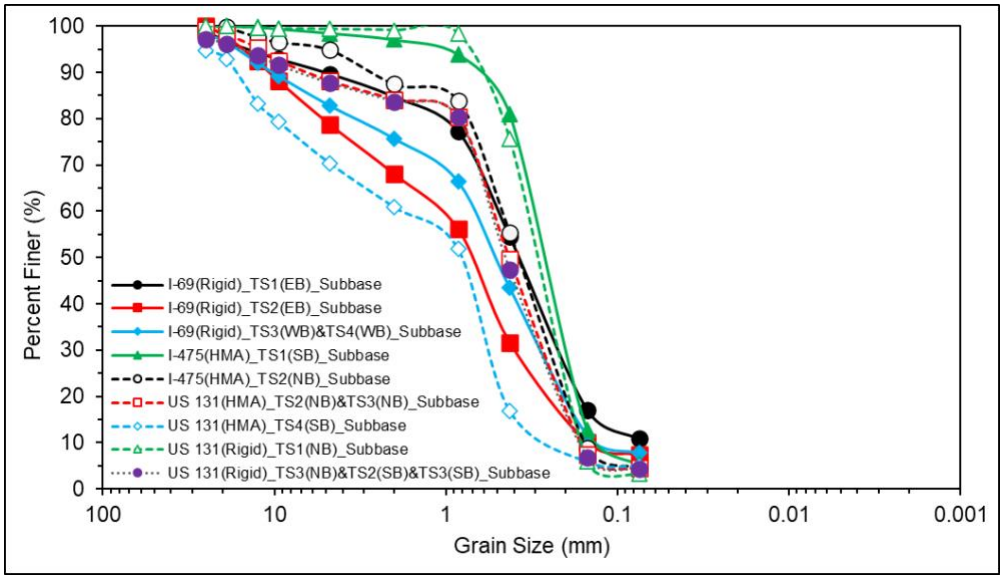

Figure 64 Particle size distributions of subbase materials

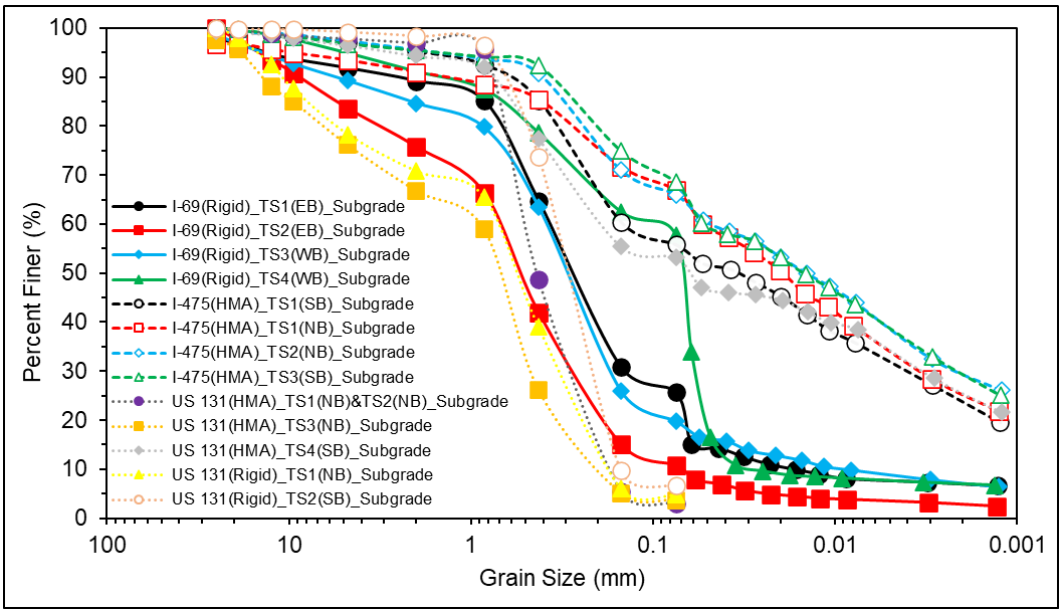

Figure 65 Particle size distributions of subgrade materials

Table 47 Index properties of base materials

Base Material	Gravel (%)	Sand (%)	Fines (%)	C_u	C_c	LL	PI	AASHTO	USCS
I-69(Rigid)_TS1(EB) &TS3(WB)_Base	86.3	12.8	0.9	4.8	1.4	NA	NP	A-1-a	GW
I-69(Rigid)_TS2(EB)_Base	88.7	10.1	1.2	5.5	2.5	NA	NP	A-1-a	GW
I-69(Rigid)_TS4(WB)_Base	66.8	27.3	5.9	29.3	2.8	NA	NP	A-1-a	GW-GM
I-475(HMA)_TS1(SB)_Base	51.3	40.0	8.7	80.0	0.6	NA	NP	A-1-a	GP-GM
I-475(HMA)_TS2(NB)_Base	59.6	36.2	4.2	47.8	1.5	NA	NP	A-1-a	GW

US 131(HMA)_TS1(NB) &TS2(NB)&TS3(NB) &TS4(SB)_Base	66.1	30.7	3.2	29.2	2.4	NA	NP	A-1-a	GW
US 131(Rigid)_TS1(NB)& TS2(NB)&TS1(SB) &TS3(SB)_Base	74.3	23.7	2.1	16.5	2.8	NA	NP	A-1-a	GW

Fines = silt and clay; C_u = uniformity coefficient; C_c = coefficient of curvature; LL = liquid limit; PI = plasticity index; AASHTO = American Association of State Highway and Transportation Officials; USCS = Unified Soil Classification System; NP = non-plastic; NA = not available.

Table 48 Index properties of subbase materials

Subbase Material	Gravel (%)	Sand (%)	Fines (%)	C_u	C_c	LL	PI	AASHTO	USCS
I-69(Rigid)_TS1(EB)_Subbase	10.3	78.8	10.8	7.2	1.8	15.7	NP	A-2-4	SW-SM
I-69(Rigid)_TS2(EB)_Subbase	21.2	71.4	7.3	7.1	1.0	NA	NP	A-1-b	SW-SM
I-69(Rigid)_TS3(WB) &TS4(WB)_Subbase	17.2	75.0	7.7	5.6	1.1	NA	NP	A-1-b	SP-SM
I-475(HMA)_TS1(SB)_Subbase	1.5	93.2	5.3	2.5	1.3	NA	NP	A-3	SP-SM
I-475(HMA)_TS2(NB)_Subbase	5.1	90.3	4.6	2.9	1.0	NA	NP	A-3	SP
US 131(HMA)_TS2(NB) &TS3(NB)_Subbase	11.9	83.7	4.4	2.9	1.0	NA	NP	A-1-b	SP
US 131(HMA)_TS4(SB)_Subbase	29.6	65.4	5.0	6.5	0.6	NA	NP	A-1-b	SP
US 131(Rigid)_TS1(NB)_Subbase	0.6	96.1	3.2	2.0	1.1	NA	NP	A-3	SP
US 131(Rigid)_TS3(NB) &TS2(SB)&TS3(SB)_Subbase	12.3	83.3	4.4	3.4	1.0	NA	NP	A-1-b	SP

Fines = silt and clay; C_u = uniformity coefficient; C_c = coefficient of curvature; LL = liquid limit; PI = plasticity index; AASHTO = American Association of State Highway and Transportation Officials; USCS = Unified Soil Classification System; NP = non-plastic; NA = not available.

Table 49 Index properties of subgrade materials

Subgrade Material	Gravel (%)	Sand (%)	Fines (%)	C_u	C_c	LL	PI	AASHTO	USCS
I-69(Rigid)_TS1(EB)_Subgrade	8.2	66.0	25.8	22.1	3.0	16.8	2.1	A-2-4	SM
I-69(Rigid)_TS2(EB)_Subgrade	16.4	72.8	10.8	9.8	1.9	13.7	NP	A-1-b	SW-SM
I-69(Rigid)_TS3(WB)_Subgrade[a]	10.8	69.4	19.8	43.1	9.7	12.6	1.0	A-2-4	SM
I-69(Rigid)_TS4(WB)_Subgrade[a]	5.2	37.1	57.8	3.5	1.2	22.6	7.6	A-4	CL
I-475(HMA)_TS1(SB)_Subgrade	2.9	41.3	55.8	NA	NA	21.4	10.1	A-4	CL
I-475(HMA)_TS1(NB)_Subgrade	6.6	26.5	66.9	NA	NA	24.7	12	A-6	CL
I-475(HMA)_TS2(NB)_Subgrade	2.7	31.3	66.0	NA	NA	24.7	11.6	A-6	CL
I-475(HMA)_TS3(SB)_Subgrade	3.3	28.2	68.5	NA	NA	22.9	10.1	A-4	CL
US 131(HMA)_TS1(NB) &TS2(NB)_Subgrade	2.2	94.8	3.0	2.6	1.1	NA	NP	A-1-b	SP
US 131(HMA)_TS3(NB)_Subgrade	23.9	72.5	3.6	3.8	1.0	NA	NP	A-1-b	SP
US 131(HMA)_TS4(SB)_Subgrade	3.5	43.3	53.2	NA	NA	22.0	6.6	A-4	CL-ML
US 131(Rigid)_TS1(NB)_Subgrade[a]	21.7	73.6	4.8	3.5	0.9	NA	NP	A-1-b	SP
US 131(Rigid)_TS2(SB)_Subgrade[a]	0.9	92.5	6.6	2.3	1.2	NA	NP	A-3	SP-SM

Fines = silt and clay; C_u = uniformity coefficient; C_c = coefficient of curvature; LL = liquid limit; PI = plasticity index; AASHTO = American Association of State Highway and Transportation Officials; USCS = Unified Soil Classification System; NP = non-plastic; NA = not available.

[a]There are unstabilized and cement-stabilized (with 5% cement) subgrade materials. However, for the determination of the index properties, only the unstabilized subgrade materials were used.

Proctor Compaction

The maximum dry unit weight (MDU) and optimum moisture content (OMC) of all unbound materials were determined in accordance with the ASTM D1557-12 (method C) technical standard for the base materials (except the I-69(Rigid)_TS2(EB)_Base), ASTM D698-12 (methods A and B) for the subbase and unstabilized subgrade materials, ASTM D558/D558M-19 (method A) for the cement-stabilized subgrade materials), and ASTM D7382-20 (method 2A) for I-69(Rigid)_TS2(EB)_Base material. No corrections (ASTM D4718/D4718M-15) were applied to the materials containing oversized particles.

The application of the ASTM D1557-12 methodology to the sample "I-69(Rigid)_TS2(EB)_Base" was not possible due to the size limitations of the compaction testing standard.-This material contained more than 30% oversized particles, which exceeded the limit percentage mentioned in ASTM D1557-12 to apply the correction factor for oversized particles. . Therefore, another compaction testing method using a vibrating hammer (ASTM D7382-20) was performed on this material. This method covers the dry unit weight of unbound material with more than 30% oversized particles. Figure 66, Figure 67, and Figure 68 show the compaction curves for the unbound base, subbase, and subgrade, respectively. The raw data are included in Appendix I. The MDU and OMC values of the materials are reported in Table 50, Table 51 and Table 52 for base, subbase, and subgrade, respectively.

The MDU values of the unbound base materials ranged from 133.1 pcf to 136.6 pcf. For the same materials, the OMCs were between 8.3% and 10.2%. For I-69(Rigid)_TS2(EB)_Base, the MDU value was 116.4 pcf, and there was no OMC value since this material was very coarse (gravel content ~>90%) and relative density test is conducted instead of compaction test. For subbase samples, the MDU values varied between 131.5 pcf and 107.4 pcf, while the OMCs were between 6.3% to 12.1%. In both cases, the range of variation of the subbase properties were higher than that of the base materials. Finally, for the subgrade materials (both unstabilized and cement-stabilized materials), the MDU values ranged between 115.3 pcf and 134.8 pcf, and the OMCs were between 6.9% and 13.0%.

US 131(Rigid)_TS1(NB)_Subbase showed the lowest maximum dry unit weight (MDU) (107.4 pcf) and the lowest optimum moisture content (OMC) (6.3%) compared to the other subbase materials (the second lowest MDU add OMC values were 117.1 pcf and 7.4%, respectively). Based on the particle size distribution, US 131(Rigid)_TS1(NB)_Subbase had the lowest amount of gravel (0.6%), the highest amount of sand (96.1%), and the lowest amount of fines (silt and clay) (3.2%). In addition, the uniformity coefficient (C_u) value of US 131(Rigid)_TS1(NB)_Subbase (2) was the lowest value among the subbase materials, which may indicate that this material was more poorly graded than the other subbase materials. The differences in the particle size distribution and the uniformity may be the reasons for the lowest MDU and OMC for US 131(Rigid)_TS1(NB)_Subbase compared to other subbase materials.

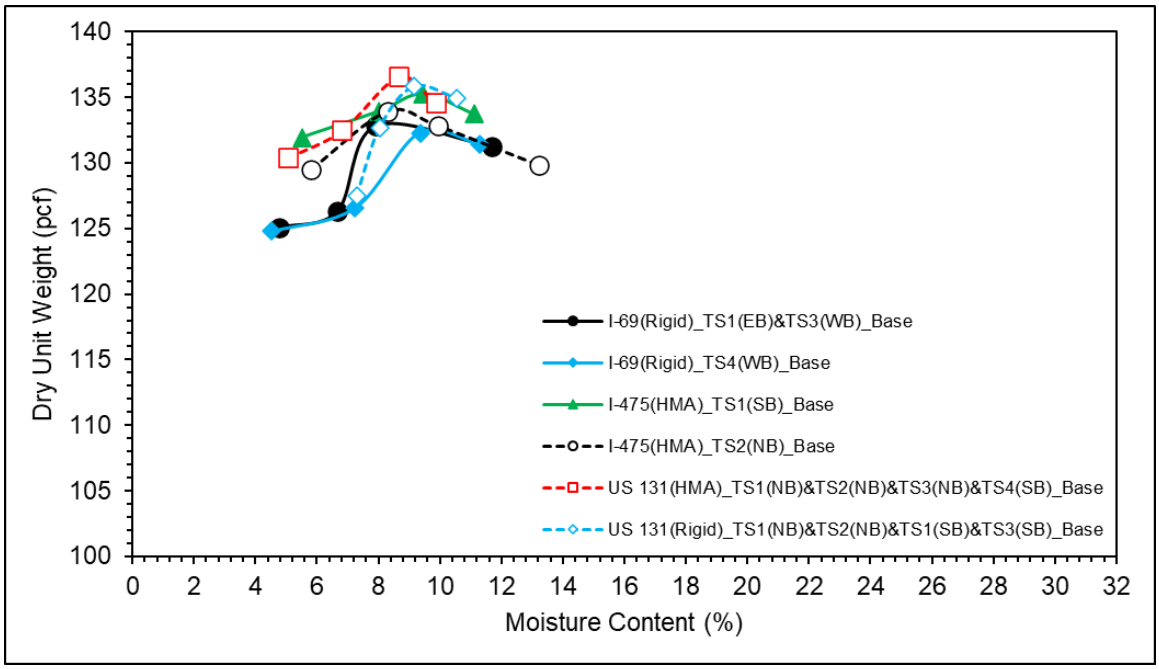

Figure 66 Compaction curves for base materials

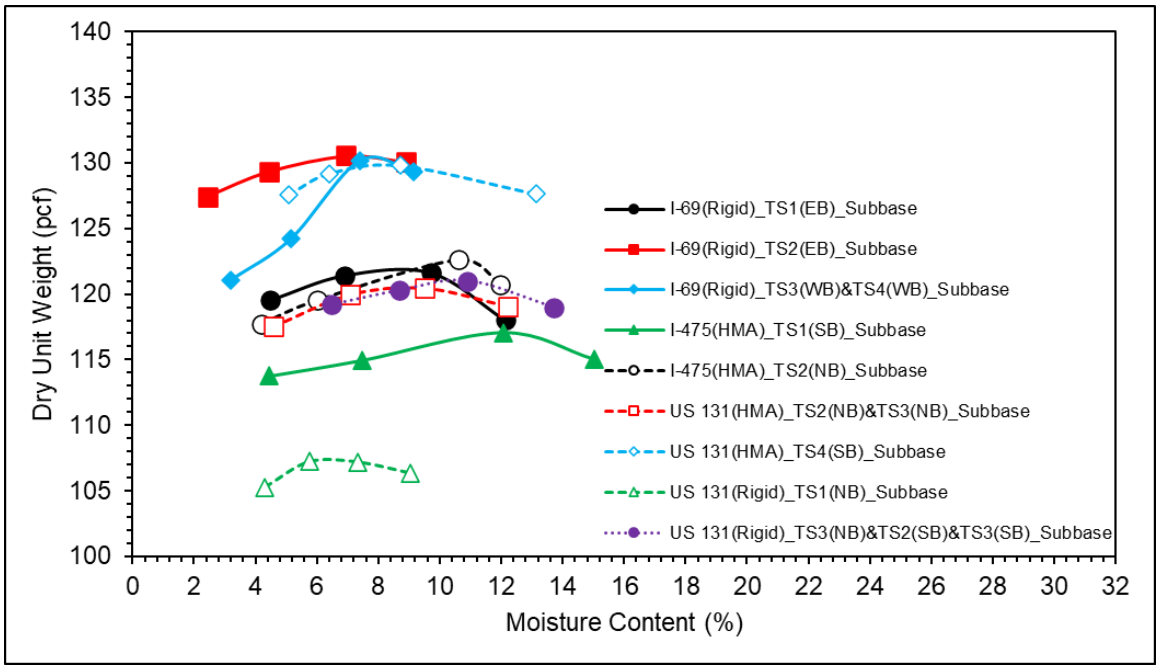

Figure 67 Compaction curves for subbase materials

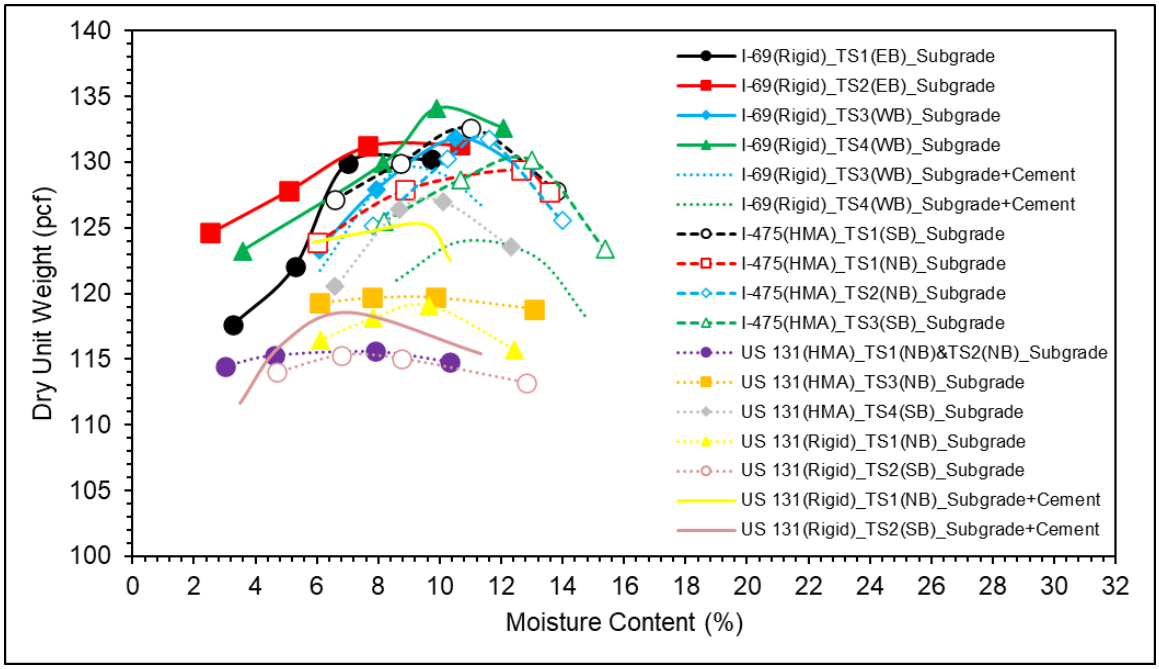

Figure 68 Compaction curves for subgrade materials

Table 50 Compaction test results for base materials

Base Material	MDU (pcf)	OMC (%)
I-69(Rigid)_TS1(EB)&TS3(WB)_Base	134.6	9.9
I-69(Rigid)_TS2(EB)_Base[a]	116.4	NA
I-69(Rigid)_TS4(WB)_Base	133.1	10.2
I-475(HMA)_TS1(SB)_Base	135.3	9.5
I-475(HMA)_TS2(NB)_Base	133.9	8.3
US 131(HMA)_TS1(NB)&TS2(NB)&TS3(NB)&TS4(SB)_Base	136.6	8.7
US 131(Rigid)_TS1(NB)&TS2(NB)&TS1(SB)&TS3(SB)_Base	135.9	8.8

MDU = maximum dry unit weight; OMC = optimum moisture content; NA = not available.
[a]The compaction test was performed on an oven-dry sample per ASTM D7382-20 (method 2A). Therefore, there is no OMC value for this material.

Table 51 Compaction test results for subbase materials

Subbase Material	MDU (pcf)	OMC (%)
I-69(Rigid)_TS1(EB)_Subbase	122.0	8.6
I-69(Rigid)_TS2(EB)_Subbase	130.8	7.4
I-69(Rigid)_TS3(WB)&TS4(WB)_Subbase	131.5	8.4
I-475(HMA)_TS1(SB)_Subbase	117.1	12.1
I-475(HMA)_TS2(NB)_Subbase	122.8	9.8
US 131(HMA)_TS2(NB)&TS3(NB)_Subbase	120.4	9.5
US 131(HMA)_TS4(SB)_Subbase	129.8	8.3
US 131(Rigid)_TS1(NB)_Subbase	107.4	6.3
US 131(Rigid)_TS3(NB)&TS2(SB)&TS3(SB)_Subbase	121.0	10.9

MDU = maximum dry unit weight; OMC = optimum moisture content.

Table 52 Compaction test results for subgrade materials

Subgrade Material	MDU (pcf)	OMC (%)
I-69(Rigid)_TS1(EB)_Subgrade	133.4	8.6

I-69(Rigid)_TS2(EB)_Subgrade	132.1	9.3
I-69(Rigid)_TS3(WB)_Subgrade	131.9	10.8
I-69(Rigid)_TS4(WB)_Subgrade	134.8	10.6
I-69(Rigid)_TS3(WB)_Subgrade+Cement	130.0	9.2
I-69(Rigid)_TS4(WB)_Subgrade+Cement	124.3	11.4
I-475(HMA)_TS1(SB)_Subgrade	130.1	9.8
I-475(HMA)_TS1(NB)_Subgrade	132.6	11.2
I-475(HMA)_TS2(NB)_Subgrade	131.7	11.6
I-475(HMA)_TS3(SB)_Subgrade	130.2	13.0
US 131(HMA)_TS1(NB)&TS2(NB)_Subgrade	115.7	6.9
US 131(HMA)_TS3(NB)_Subgrade	119.8	9.0
US 131(HMA)_TS4(SB)_Subgrade	127.1	9.8
US 131(Rigid)_TS1(NB)_Subgrade	119.1	9.7
US 131(Rigid)_TS2(SB)_Subgrade	115.3	7.4
US 131(Rigid)_TS1(NB)_Subgrade+Cement	125.7	8.6
US 131(Rigid)_TS2(SB)_Subgrade+Cement	118.5	7.1

MDU = maximum dry unit weight; OMC = optimum moisture content.

Resilient Modulus (M_R) Testing

Resilient modulus (M_R) tests were performed on all samples at room temperature following the methodology described in the AASHTO T 307 using SPAX-3000 equipment to measure the stiffness of the materials. Figure 69 shows the SPAX-3000 device with its lower, middle, and upper cells fully assembled.

After the calculation of the quantity of material needed for each cylindrical test specimen (6-inch by 12-inch), the testing procedure consists of preparing six separate oven-dry batches with the original gradation of the corresponding material. Figure 70 shows the six batches prepared for I-69(Rigid)_TS1(EB)_Subbase as an example. The gradation of each lift was kept identical to reduce inhomogeneity occurring during specimen preparation.

Figure 69 SPAX-3000 device (fully assembled)

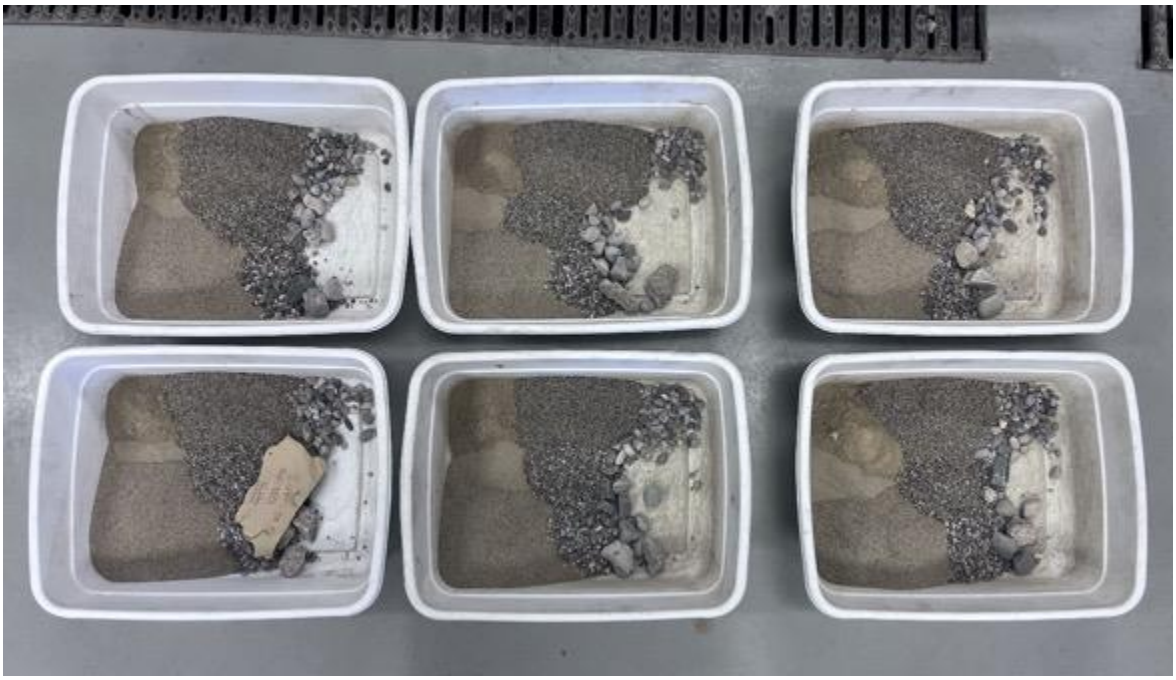

Figure 70 Batches prepared for I-69(Rigid)_TS1(EB)_Subbase

A latex membrane (0.025-inch thick) was folded into a split compaction mold and secured with O-rings. Vacuum was applied to keep the membrane tight against the mold. The mold setup was then placed on the bottom platen having a porous stone in its center to compact the specimen.

A filter paper was placed on top of the platen to prevent clogging of the porous stone by fine particles. Figure 71 presents the compaction mold setup on the bottom platen and the internal view of the mold setup. One of the oven-dry batches prepared previously was mixed with water to reach to the desired OMC, and the wet batch was put into the mold. Compaction was performed using a vibrating hammer until the target thickness of 2 inches was achieved. After the compaction of the first lift, the surface was trimmed to ensure specimen integrity with the upper layer, and the second batch (i.e., lift) was placed on the top and compacted. These steps were repeated until a total specimen height of 12 inches was reached (6 lifts in total). Figure 72 shows the compaction procedure with the vibrating hammer and the compacted specimen at its final height. Duplicate specimens were prepared for each material.

Figure 71 (a) Compaction mold setup and (b) inside of the mold

Figure 72 (a) Compaction with vibrating hammer and (b) compacted specimen

The mold containing the compacted specimen was then transferred to the testing chamber. After disconnecting the vacuum pump from the mold, it was connected to the bottom platen to apply vacuum to the specimen. Then, a second membrane (0.012-inch thick) was placed on top of the first one (0.025-inch thick) to cover all the membrane punctures caused by the sharp edges of coarse aggregate particles. Another filter paper was placed on top of the specimen, and a top platen was placed on top of the filter paper. The membranes were folded back on the top and bottom platens and then sealed with O-rings. The vacuum pump was then switched to the top platen. During the assembly, the specimen was kept under vacuum through a vacuum line connected to the top platen until confining pressure was applied. Figure 73 shows a specimen placed in the test chamber and ready to be tested.

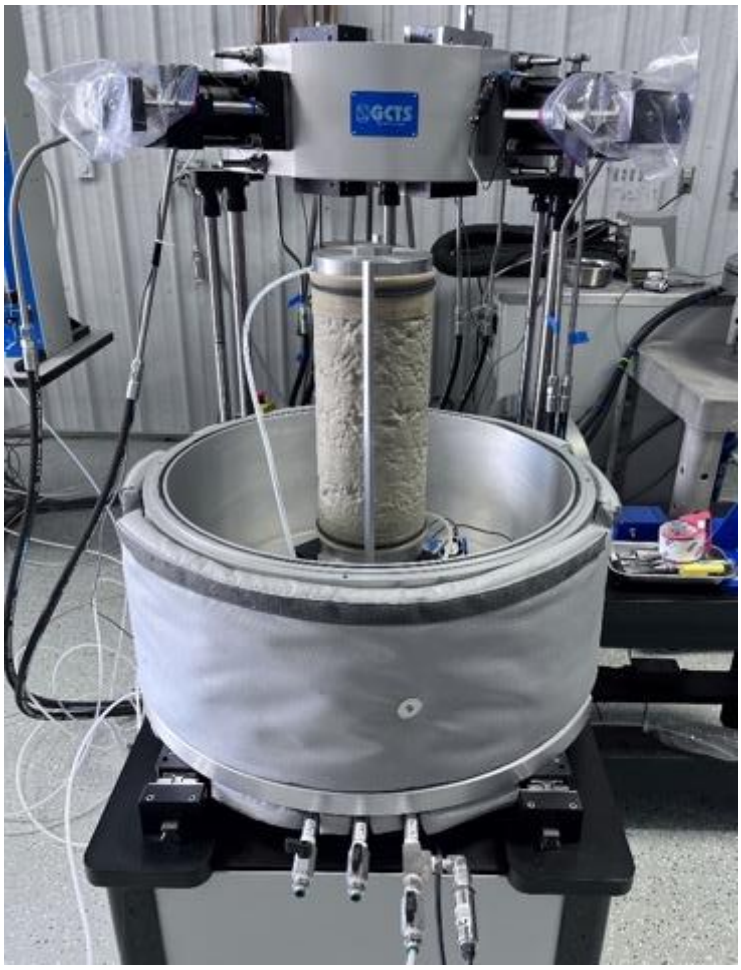

Figure 73 Specimen placed in the test chamber and ready to be tested

The mid and upper cells were placed on top of the lower cell where the specimen was placed, and then the top plate was placed on the top of the upper cell. The upper cell was lifted and secured. Two internal linear variable displacement transducers (LVDTs) were placed to directly measure the specimen deformations during testing. Figure 74 shows the lifted and secured upper cell. The SPAX-3000 assembly was completed by lowering the upper cell and installing the sealing ring (Figure 69).

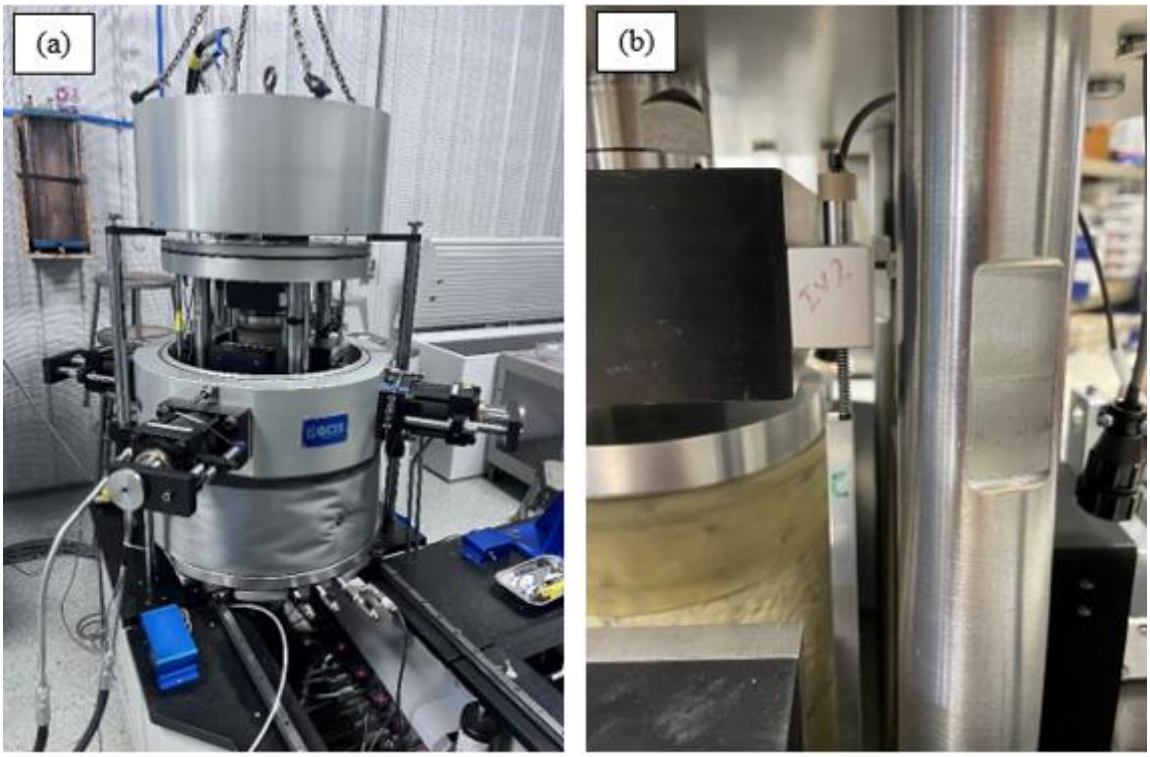

Figure 74 (a) Lifted and secured upper cell and (b) installed internal LVDT

For all the samples for the unbound base materials, the testing sequence provided in the AASHTO T 307 was used (called the base/subbase testing sequences hereinafter). Some of the subbase materials were not stiff enough to withstand the base/subbase testing sequence; therefore, the testing sequences provided for subgrade soils were used instead (called the subgrade testing sequences hereinafter) for these subbase materials. Table 53 summarizes the subbase materials and the type of testing sequences used. For all the subgrade samples, the subgrade testing sequences were used. Details of the testing sequences can be found in Appendix I.

Table 53 Subbase materials and type of testing sequences

Material	Testing Sequence (AASHTO T 307)[a]
I-69(Rigid)_TS1(EB)_Subbase	Subgrade Testing Sequences
I-69(Rigid)_TS2(EB)_Subbase	Base/Subbase Testing Sequences
I-69(Rigid)_TS3(WB) &TS4(WB)_Subbase	
I-475(HMA)_TS1(SB)_Subbase	Subgrade Testing Sequences
I-475(HMA)_TS2(NB)_Subbase	Base/Subbase Testing Sequences
US 131(HMA)_TS2(NB) &TS3(NB)_Subbase	Subgrade Testing Sequences
US 131(HMA)_TS4(SB)_Subbase	
US 131(Rigid)_TS1(NB)_Subbase	
US 131(Rigid)_TS3(NB)& TS2(SB)&TS3(SB)_Subbase	

Data Analysis and Test Results

The conventional Mechanistic-Empirical Pavement Design Guide (MEPDG) model shown in Equation 13 was used to determine the M_R characteristics of the materials using the elastic deformations recorded during the last five cycles of each testing sequence [26, 27].

$$M_R = k_1 P_a \left(\frac{\theta}{P_a}\right)^{k_2} \left(\frac{\tau_{oct}}{P_a} + 1\right)^{k_3} \quad \text{Equation 13}$$

where k_1, k_2, and k_3 are the fitting parameters, P_a is the atmospheric pressure (ksi), θ is the bulk stress ($\theta = \sigma_1 + \sigma_2 + \sigma_3 = \sigma_1 + 2\sigma_3$) (ksi), σ_1, σ_2, and σ_3 are the principal stresses (ksi), and τ_{oct} is the octahedral shear stress [$\tau_{oct} = 1/3\sqrt{(\sigma_1 - \sigma_2)^2 + (\sigma_1 - \sigma_3)^2 + (\sigma_2 - \sigma_3)^2}$] (ksi).

Summary M_R (SM_R) values were determined based on the NCHRP Project 1-28A [28]. The summary MR (SM_R) value represents the M_R value to be used for pavement design. During M_R testing, 1 conditioning sequence and 15 loading sequences are applied. Each loading sequence has different stress combinations. During data analysis, one M_R value is calculated per each loading sequence. Since there are 15 loading sequences, there will be 15 different M_R values. Among those 15 M_R values, a representative value, which is the summary resilient modulus (SM_R) value, is chosen for pavement design. Per NCHRP 1-28A study recommendations, for the base materials and some of the subbase materials, the bulk stress (θ) and the octahedral shear stress (τ_{oct}) values corresponding to the 6th sequence of the base/subbase testing sequences were used to calculate SM_R (θ = 30 psi and τ_{oct} = 7 psi, per NCHRP 1-28A recommendation). For the subgrade materials and some of the subbase materials, the stresses corresponding to the 13th sequence of the subgrade testing sequences were used to calculate SM_R (θ = 12 psi and τ_{oct} = 3 psi, per NCHRP 1-28A recommendation). It is noted that the NCHRP 1-28A study is the most comprehensive study to test unbound materials under different stress conditions for different pavement foundation layers.

Summaries of the M_R test results of the base, subbase, and subgrade materials are provided in Table 54, Table 55, and Table 56, respectively. Figure 75, Figure 76, and Figure 77 show the SM_R values of the base, subbase, and subgrade materials, respectively. Detailed M_R test results are provided in Appendix J. Overall, the base materials showed an average SM_R value of 37.72 ksi, more than two and three times higher than those observed for subbase and unstabilized subgrade samples which have average values of 15.78 ksi and 11.33 ksi, respectively. The average SM_R value of the subbase materials (15.78 ksi) was slightly higher than ones obtained from the unstabilized subgrades (11.33 ksi). The cement-stabilized subgrade materials exhibited higher average SM_R value (26.78 ksi) than the subbase materials (15.78 ksi); however, this value was still lower than the average SM_R value of the base materials (37.72 ksi).

For the base materials, the highest and the lowest SM_R values were observed on the US 131 (Rigid)_TS1(NB)&TS2(NB)&TS1(SB)&TS3(SB)_Base and I-475(HMA)_TS1(SB)_Base. Among the subbase samples, I-475(HMA)_TS2(NB)_Subbase showed the highest SM_R value (30.06 ksi) while I-69(Rigid)_TS1(EB)_Subbase yielded the lowest SM_R value (11.90 ksi). Finally, within the subgrade materials, the highest SM_R values (ranging from 21.61 ksi to 35.80 ksi) were observed in the cement-stabilized subgrade materials. US 131(HMA)_TS4 (SB)_Subgrade showed the lowest SM_R value (5.09 ksi) among the subgrade samples.

Table 54 Resilient modulus (MR) test results for base materials

Base Material	Fitting Parameters			R^2	SM_R (ksi)	SD (ksi)
	k_1	k_2	k_3			
I-69(Rigid)_TS1(EB)&TS3(WB)_Base	2103.26	0.64	-0.13	0.95	46.54	2.40
I-69(Rigid)_TS2(EB)_Base	1645.50	0.75	-0.7	0.93	31.46	1.95
I-69(Rigid)_TS4(WB)_Base	1635.78	0.78	-0.51	0.97	34.52	2.84
I-475(HMA)_TS1(SB)_Base	1422.31	0.93	-0.78	0.95	30.07	0.51
I-475(HMA)_TS2(NB)_Base	1326.10	0.76	-0.11	0.91	32.21	0.62
US 131(HMA)_TS1(NB) &TS2(NB)&TS3(NB)&TS4(SB)_Base	1900.74	0.63	-0.13	0.93	41.70	2.38
US 131(Rigid)_TS1(NB) &TS2(NB)&TS1(SB)&TS3(SB)_Base	2322.56	0.65	-0.35	0.96	47.52	8.34

k_1, k_2, and k_3 = fitting parameters in Equation (1); SM_R = summary M_R; SD = standard deviation.
Note: SM_R values were determined at the bulk stress (θ) and the octahedral shear stress (τ_{oct}) corresponding to the 6th sequence of the base/subbase testing sequences (AASHTO T 307) (θ = 30 psi and τ_{oct} = 7 psi).

Table 55 Resilient modulus (M_R) test results for subbase materials

Subbase Material	Fitting Parameters			R^2	SM_R (ksi)	SD (ksi)
	k_1	k_2	k_3			
I-69(Rigid)_TS1(EB)_Subbase	1096.63	0.56	-1.09	0.88	11.90[a]	0.00
I-69(Rigid)_TS2(EB)_Subbase	880.07	0.61	-0.37	0.95	17.28[b]	3.36
I-69(Rigid)_TS3(WB)&TS4(WB)_Subbase	848.05	0.38	-0.20	0.77	15.12[b]	0.69
I-475(HMA)_TS1(SB)_Subbase	1152.86	0.51	-1.2	0.86	12.38[a]	2.94
I-475(HMA)_TS2(NB)_Subbase	1376.23	0.62	-0.12	0.88	30.06[b]	0.84
US 131(HMA)_TS2(NB)&TS3(NB)_Subbase	1556.20	0.80	-1.10	0.96	16.07[a]	0.55
US 131(HMA)_TS4(SB)_Subbase	1480.30	0.90	-2.00	0.91	12.80[a]	0.53
US 131(Rigid)_TS1(NB)_Subbase	1525.38	0.89	-2.00	0.92	13.21[a]	4.16
US 131(Rigid)_TS3(NB) &TS2(SB)&TS3(SB)_Subbase	1332.65	0.64	-1.50	0.93	13.23[a]	1.54

k_1, k_2, and k_3 = fitting parameters in Equation (1); SM_R = summary M_R; SD = standard deviation.
[a]SM_R values were determined at the bulk stress (θ) and the octahedral shear stress (τ_{oct}) corresponding to the 13th sequence of the subgrade testing sequences (AASHTO T 307) (θ = 12 psi and τ_{oct} = 3 psi).
[b]SM_R values were determined at θ and τ_{oct} corresponding to the 6th sequence of the base/subbase testing sequences (AASHTO T 307) (θ = 30 psi and τ_{oct} = 7 psi).

Table 56 Resilient modulus (M_R) test results for subgrade materials

Subgrade Material	Fitting Parameters			R^2	SM_R (ksi)	SD (ksi)
	k_1	k_2	k_3			
I-69(Rigid)_TS1(EB)_Subgrade	1772.24	0.98	-2.80	0.96	13.12	2.43
I-69(Rigid)_TS2(EB)_Subgrade	1043.15	0.75	-2.10	0.94	9.13	0.53
I-69(Rigid)_TS3(WB)_Subgrade	1096.63	0.58	-1.60	0.82	10.83	1.37
I-69(Rigid)_TS4(WB)_Subgrade	1556.20	0.48	-2.80	0.98	12.70	0.14
I-69(Rigid)_TS3(WB)_Subgrade+Cement	3568.85	0.50	-1.60	0.95	35.80	4.29
I-69(Rigid)_TS4(WB)_Subgrade+Cement	2208.35	0.36	-1.90	0.96	21.61	4.40
I-475(HMA)_TS1(SB)_Subgrade	1480.30	0.49	-4.00	0.93	9.77	0.30
I-475(HMA)_TS1(NB)_Subgrade	2115.57	0.35	-3.83	0.94	14.78	2.04
I-475(HMA)_TS2(NB)_Subgrade	2540.64	0.41	-4.11	0.94	16.71	4.74
I-475(HMA)_TS3(SB)_Subgrade	1276.40	0.44	-3.86	0.92	8.73	2.34
US 131(HMA)_TS1(NB)&TS2(NB)_Subgrade	1512.23	0.69	-1.17	0.81	15.78	2.92
US 131(HMA)_TS3(NB)_Subgrade	1719.86	1.00	-3.30	0.89	11.61	0.16
US 131(HMA)_TS4(SB)_Subgrade	549.40	0.34	-2.23	0.87	5.09	0.00
US 131(Rigid)_TS1(NB)_Subgrade	992.27	0.75	-2.00	0.73	8.84	0.72
US 131(Rigid)_TS2(SB)_Subgrade	812.41	0.45	-0.35	0.87	10.24	0.05
US 131(Rigid)_TS1(NB)_Subgrade+Cement	2835.57	0.65	-2.00	0.96	25.75	4.16
US 131(Rigid)_TS2(SB)_Subgrade+Cement	2440.60	0.70	-1.50	0.94	23.96	0.93

k_1, k_2, and k_3 = fitting parameters in Equation (1); SM_R = summary M_R; SD = standard deviation.
Note: SM_R values were determined at the bulk stress (θ) and the octahedral shear stress (τ_{oct}) corresponding to the 13th sequence of the subgrade testing sequences (AASHTO T 307) (θ = 12 psi and τ_{oct} = 3 psi).

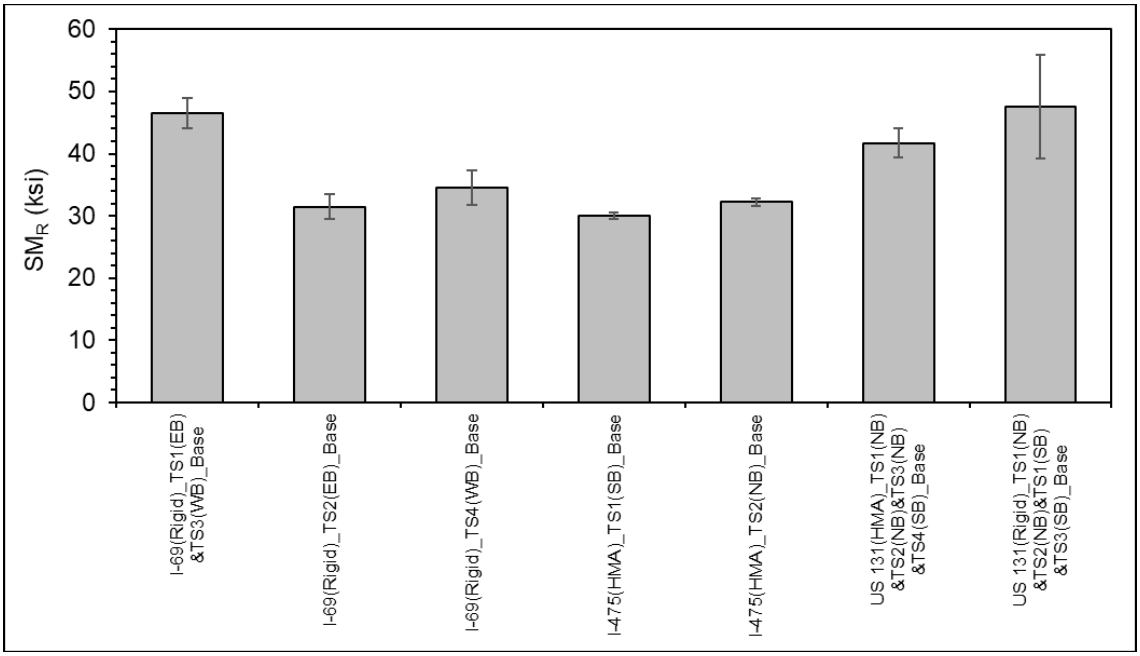

Figure 75 Summary resilient modulus (SM_R) values for base materials

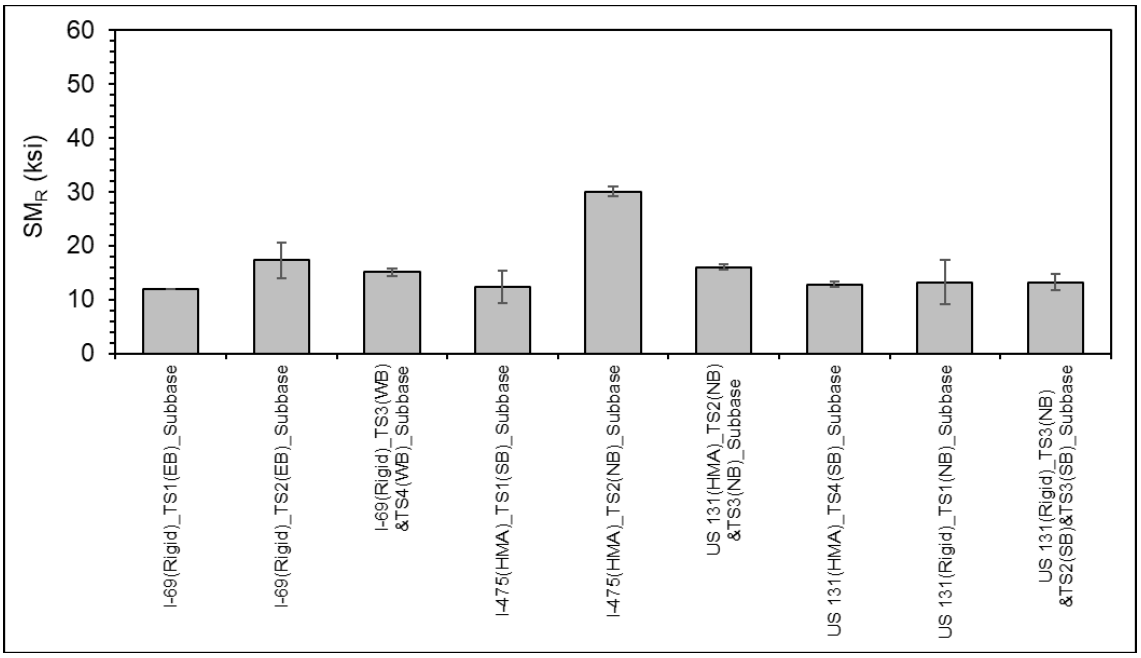

Figure 76 Summary resilient modulus (SM_R) values for subbase materials

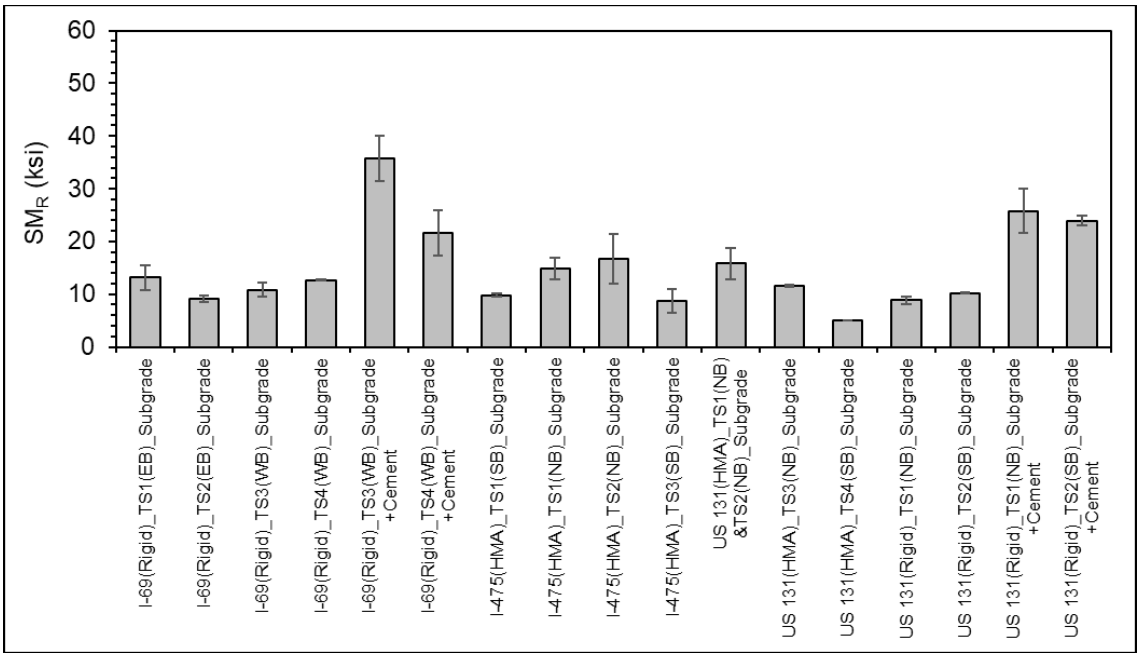

Figure 77 Summary resilient modulus (SM_R) values for subgrade materials

Table 57 and Figure 78 report the SM_R values for the pavement foundation layers at different locations. Tests performed on the base layer of the US 131 (rigid) resulted in the highest average SM_R value (47.52 ksi) among all base layers. Within the samples collected from the subbase layers, the ones from the I-475 (HMA) and US 131 (rigid) projects provided the highest and the lowest average SM_R values (21.22 ksi and 13.22 ksi), respectively. The subbase layers of the I-69 (rigid) and US 131 (HMA) showed similar average SM_R values (14.76 ksi and 14.43 ksi,

respectively). Among the unstabilized subgrade layers, the highest and lowest average SM_R values were observed in I-475 (HMA) and US-131 (rigid), respectively. The unstabilized subgrade in I-69 (rigid) showed a slightly higher average SM_R value (11.44 ksi) than that of the US 131 (HMA) (10.83 ksi). The cement-stabilized subgrade layer in I-69 (rigid) exhibited a higher average SM_R value (28.70 ksi) than that in US 131 (rigid) (24.86 ksi).

Table 57 Summary resilient modulus (SM_R) values for pavement foundation layers at different locations

Foundation Layer	I-69 (Rigid)		I-475 (HMA)		US 131 (HMA)		US 131 (Rigid)	
	SM_R (ksi)	SD (ksi)	SM_R (ksi)	SD (ksi)	SM_R (ksi)	SD (ksi)	SM_R (ksi)	SD (ksi)
Base	37.51	7.97	31.14	1.51	41.70	NA	47.52	NA
Subbase	14.76	2.71	21.22	12.50	14.43	2.31	13.22	0.01
Subgrade	11.44	1.84	12.50	3.85	10.83	5.39	9.54	0.99
Subgrade+Cement	28.70	10.04	NA	NA	NA	NA	24.86	1.27

SD = standard deviation.

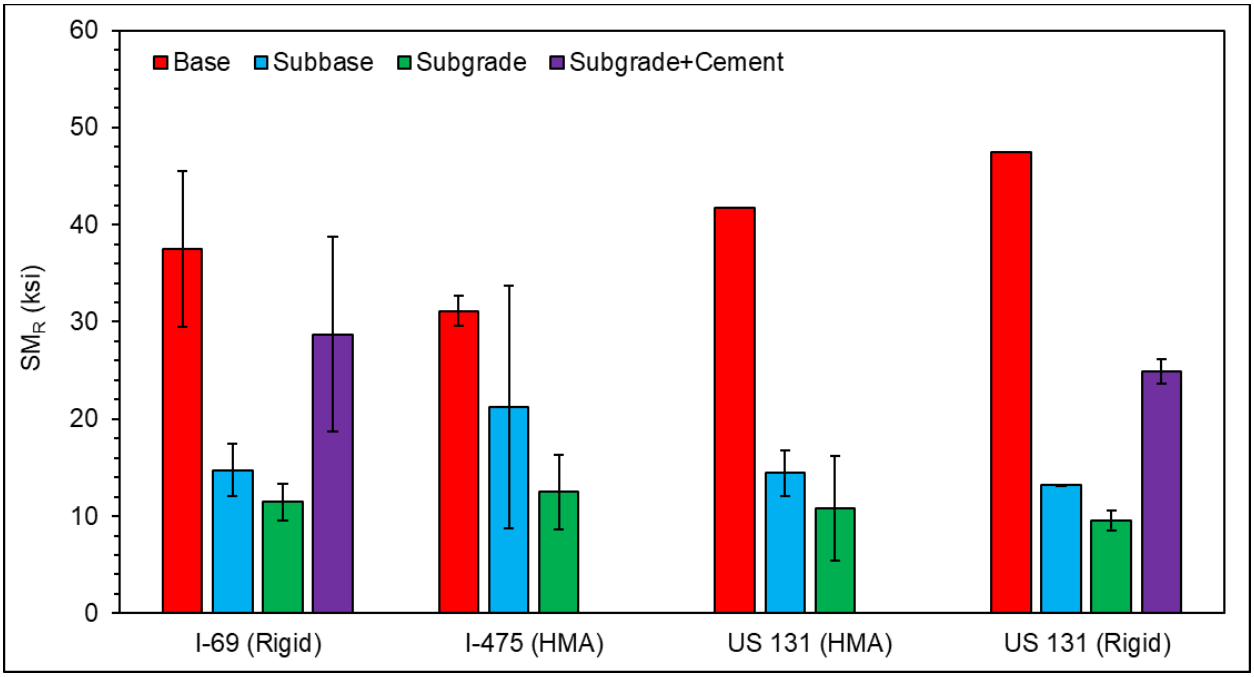

Figure 78 Summary resilient modulus (SM_R) values for pavement foundation layers at different locations

Correlations

An effort was made to find linear correlations between the SM_R values and the index properties of the materials. The base, subbase, and subgrade materials were evaluated separately due to differences in the compaction method and the testing sequences applied during M_R tests. Only correlations with R^2 values higher than 0.50 were here reported. Other correlations can be found in Appendix K.

Base Materials

For the base materials, I-69(Rigid)_TS2(EB)_Base was not considered in the correlations since the MDU value of this material was determined by using a different methodology to accommodate the size limitations of the Proctor compaction (ASTM D1557-12). For the other base layers, ASTM D1557-12 was performed. Figure 79 shows the correlations between the SM_R values and some index properties of the base materials. There were direct relationships between SM_R and gravel content, D_{30}, D_{60}, and gravel/sand ratio. On the other hand, SM_R was inversely proportional to sand content, fines content, and C_u.

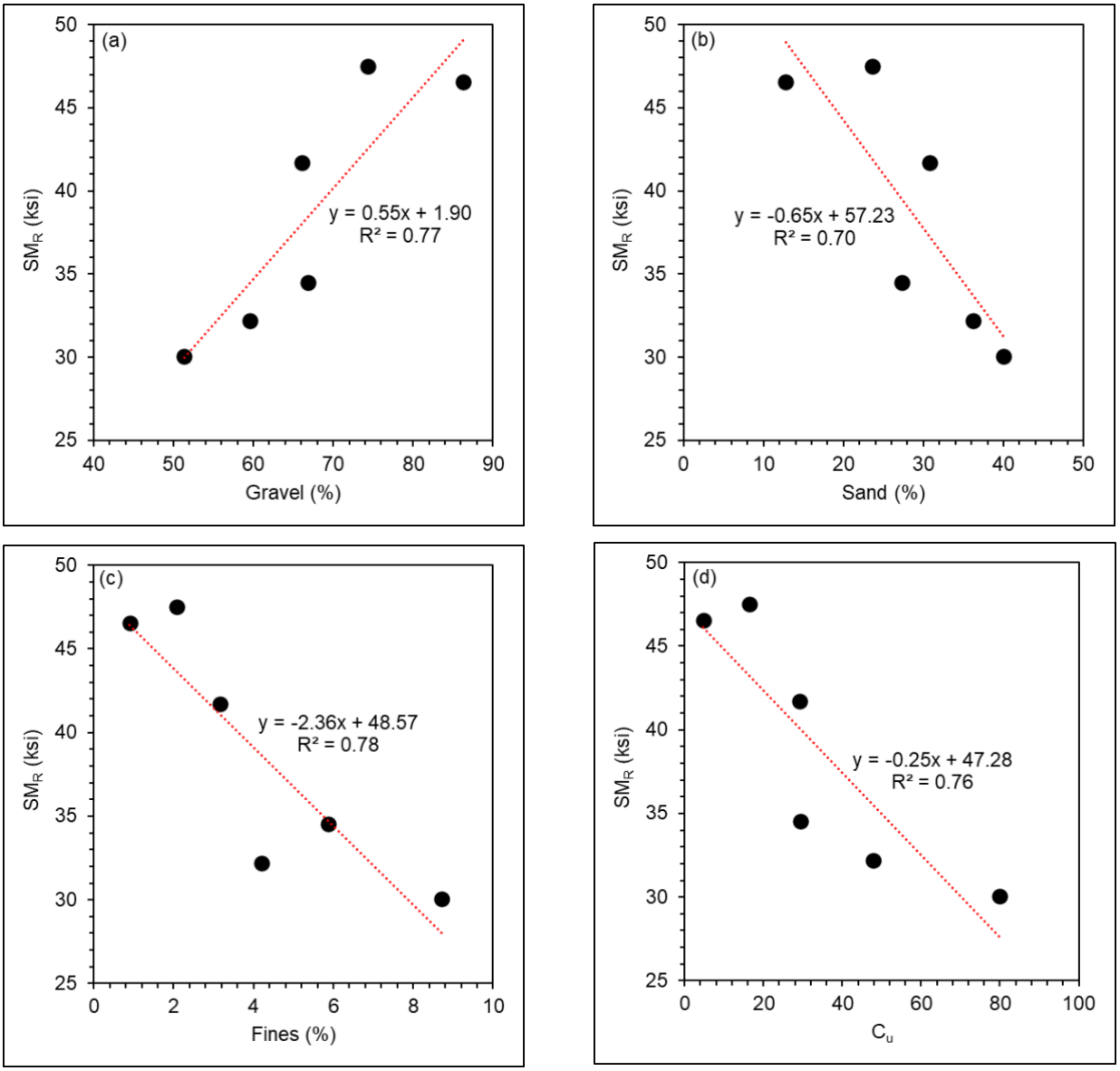

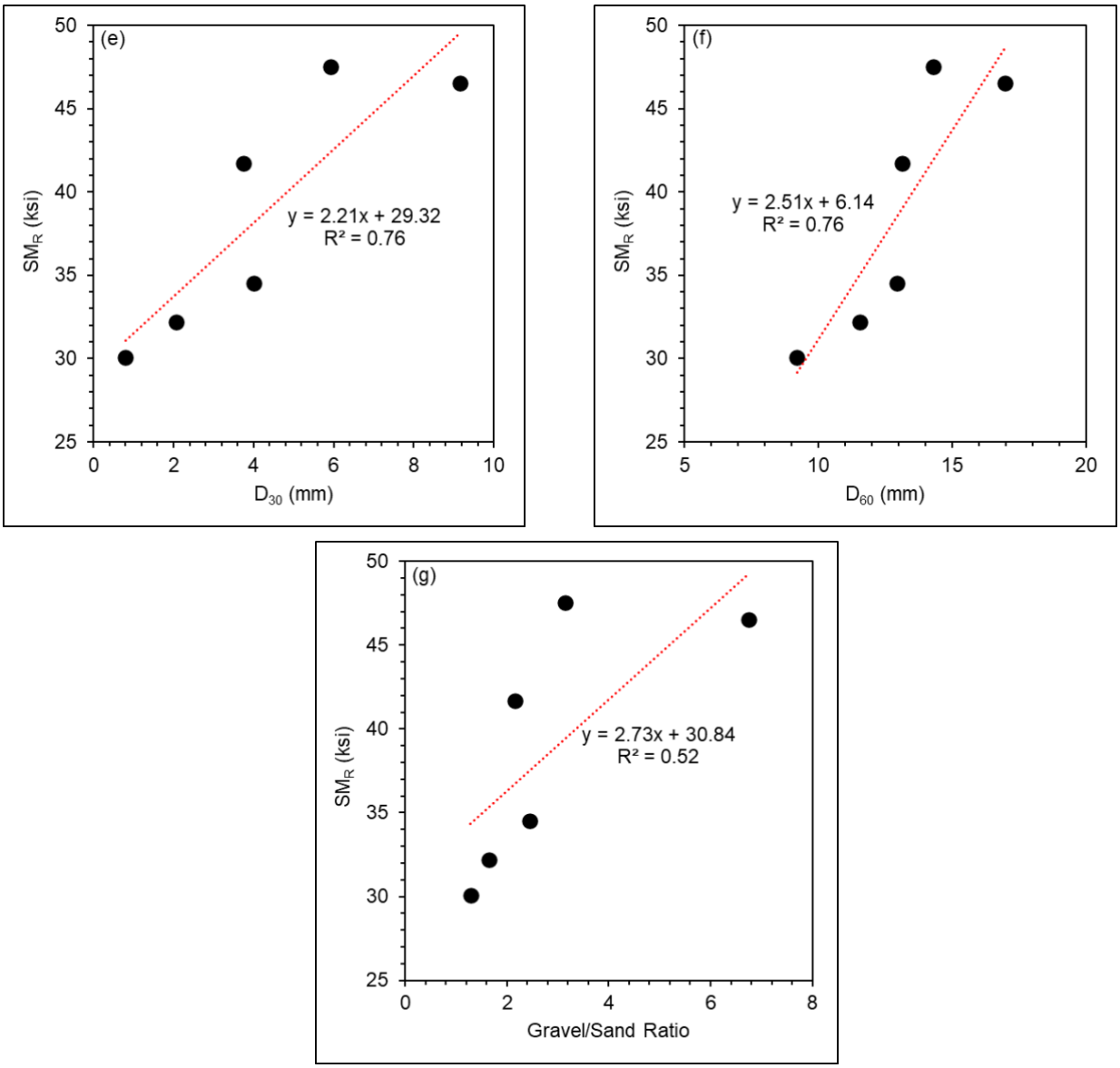

Figure 79 Linear correlations between summary resilient modulus (SM_R) and (a) gravel content, (b) sand content, (c) fines (silt and clay) content, (d) uniformity coefficient (C_u), (e) particle size at which 30% of the particles are finer (D_{30}), (f) particle size at which 60% of the particles are finer (D_{60}), and (g) gravel/sand ratio for base materials

Subbase Materials (*materials tested at base/subbase testing sequences*)

In this section, only the subbase materials tested at the base/subbase testing sequences (AASHTO T 307) were used in the correlations. Figure 80 exhibits the correlations between the SM_R values and some index properties of the subbase materials. While SM_R of subbase materials was inversely proportional to gravel content, fines content, C_u, MDU, and gravel/sand ratio, there were direct relationships between SM_R and sand content, D_{10}, and OMC.

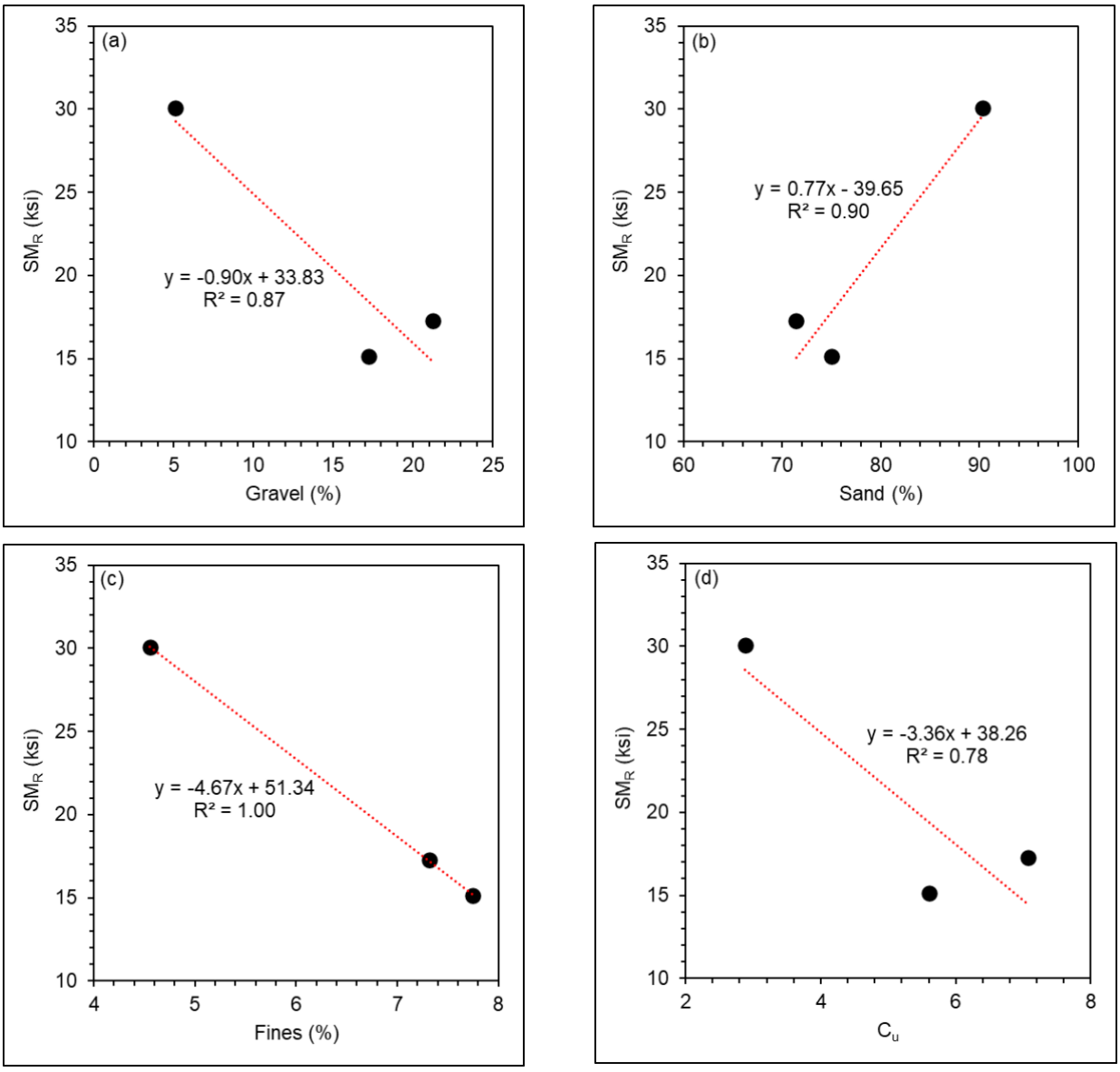

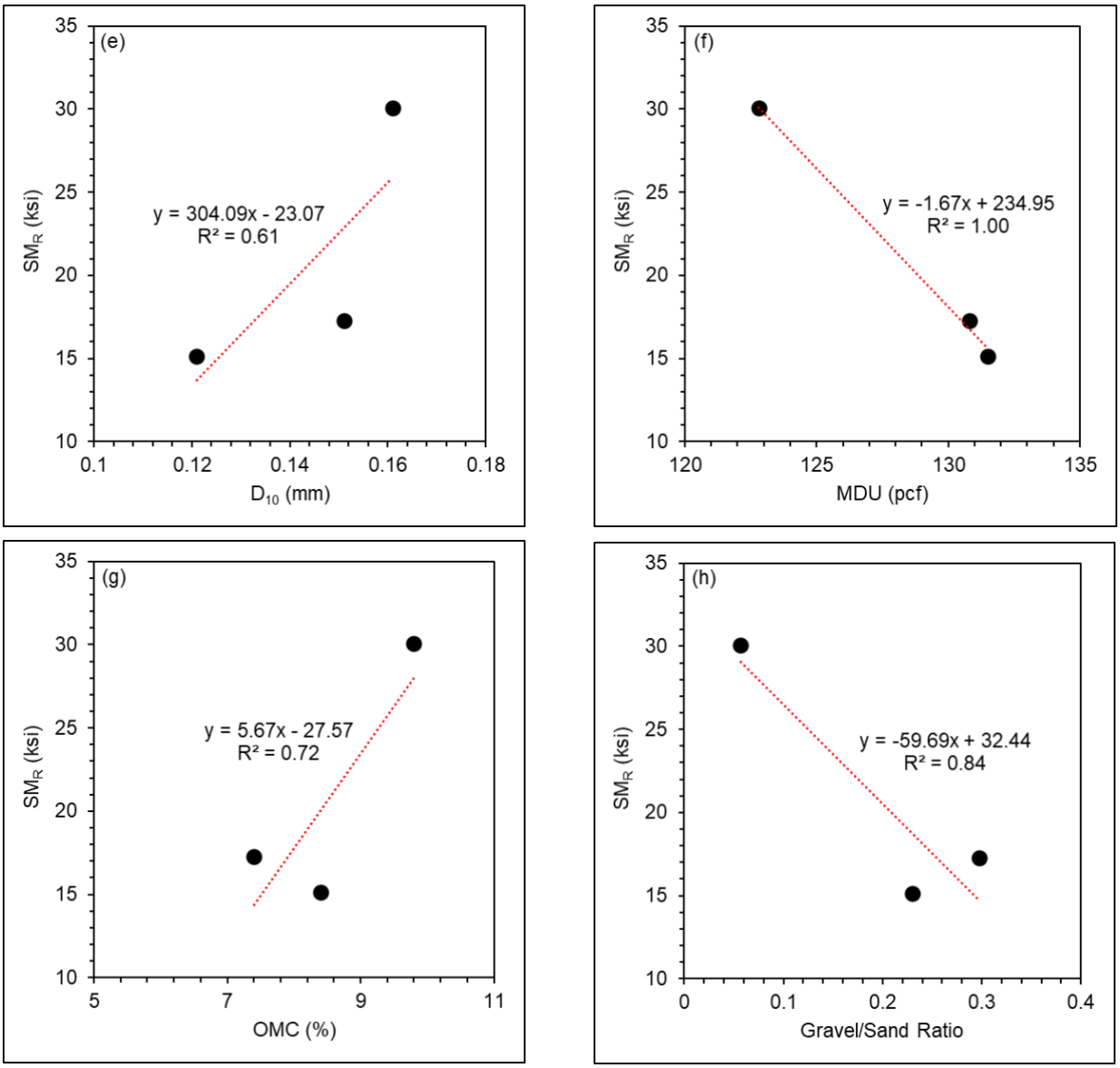

Figure 80 Linear correlations between summary resilient modulus (SMR) and (a) gravel content, (b) sand content, (c) fines (silt and clay) content, (d) uniformity coefficient (Cu), (e) effective particle size (D10), (f) maximum dry unit weight (MDU), (g) optimum moisture content (OMC), and (h) gravel/sand ratio for subbase materials

Subbase Materials (*materials tested at subgrade testing sequences*)

In this section, only the subbase materials tested at the subgrade testing sequences (AASHTO T 307) were used in the correlations. After comparing the SM_R values with the index properties, no correlation satisfied the threshold of R^2 (0.5). All the correlations obtained for these subbase materials are provided in Appendix K.

Subgrade Materials

For the subgrade materials, no correlations were found to satisfy the R^2 threshold set (0.50). All the correlations obtained during the study are reported in Appendix K.

Discussion on Various Modulus Values Obtained from Different Tests

Unbound Layers

As part of this project, several methods (laboratory, FWD, LWD and DCP) were used to estimate the modulus of sublayers of standard and long-life pavement sections. This section includes a brief discussion on comparisons of moduli obtained from different methods and the values selected for mechanistic-empirical (ME) analyses.

A comparison of unbound layer moduli for I475I-475 flexible pavement project is shown in Figure 81. The following observations can be made from these figures:

- Subgrade moduli obtained from lab Mr tests and DCP tests were relatively close to each other, except the standard section. On the other hand, the LWD tests revealed unreasonably low moduli values for typical subgrade soils. FWD backcalculated modulibackcalculations for both standard and long-life sections were higher than laboratory measurements, which is consistent with the literature. It is typical for lab Mr results to be 2-5 times lower than the FWD results, and it is a common practice to reduce FWD backcalculated values by a factor and use them in design and analyses. Therefore, it was decided to use the lab Mr tests results for subgrade in ME analyses.

- Subbase moduli obtained from DCP and LWD tests were simply too low, and they did not make sense. FWD backcalculation could only provide an 'average' base/subbase moduli, but they were not too far from the lab Mr values. Therefore, lab Mr was thought to be the most representative subbase moduli to be used in ME analyses.

- Base moduli from lab and FWD were very close, which makes sense because although FWD-based modulus is for base/subbase combination, it is affected more by the base modulus because it is closer to the surface load. LWD data was too low and did not make sense. Therefore, lab Mr was used in the ME analyses.

Figure 82 shows a comparison of unbound layer moduli for the US-131 flexible pavement project. The following observations can be made from these figures:

- Again, the LWD tests revealed unreasonably low moduli, and DCP results for long life sectionssection resulted in unreasonably high moduli for subgrade soils. Lab Mr results were lower than FWD backcalculated valuesbackcalculations (as expected). It was decided to use the lab Mr tests results for subgrade in ME analyses.

- Subbase moduli obtained from lab and DCP tests agreed reasonably well for the standard section. However, the DCP modulus from long life section was unreasonably high for a subbase. Therefore, lab Mr of subbase was used in ME analyses.

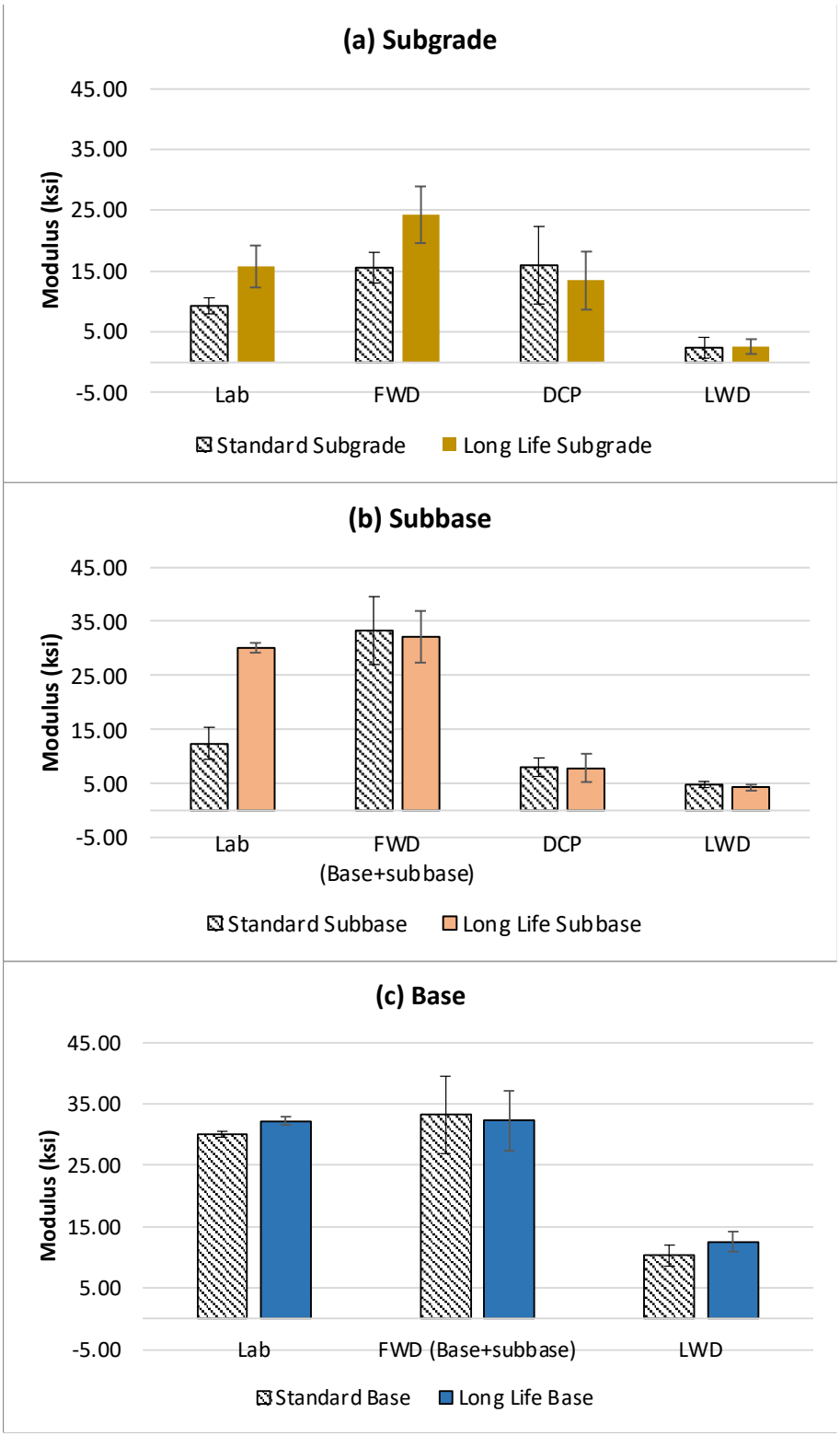

Figure 81. Comparison of unbound layer moduli for I475 flexible pavement. Note: DCP data was not available for the base layer.

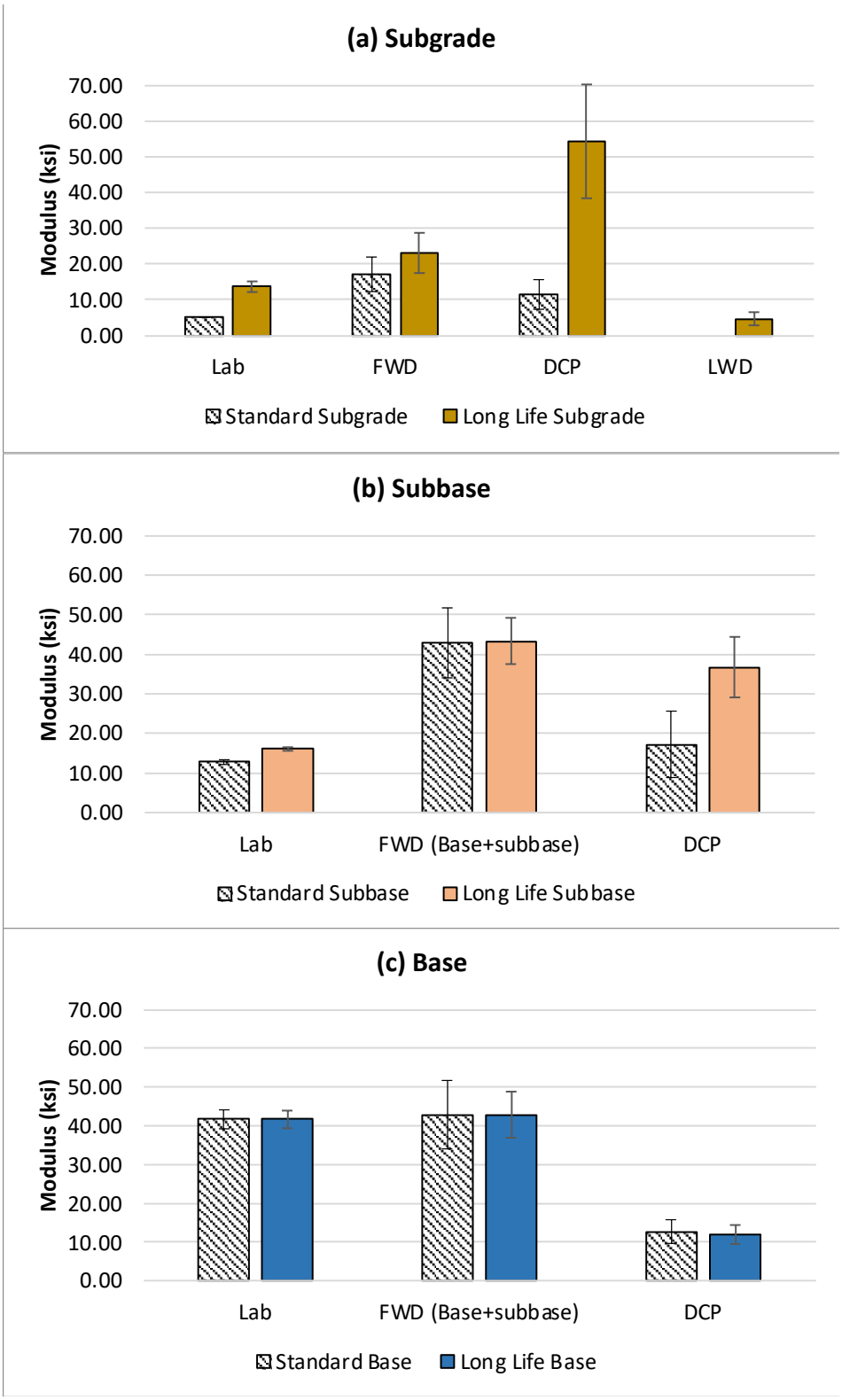

Figure 82. Comparison of unbound layer moduli for US-131 flexible pavement. Note: There was no LWD data available for subgrade of standard section, subbase and base of both sections.

- Base moduli from lab and FWD were very close, and DCP data was too low and did not make sense. Therefore, lab Mr was used in the ME analyses

Unbound layer moduli for the I-69 rigid pavement are summarized in Figure 83. Based on these figures, the following general observations can be made:

- Subgrade moduli measured in the lab were lower than the FWD-based values, which is expected. It is noted that the FWD backcalculation method for rigid pavements assumes Winkler foundation (PCC over springs) and a modulus of subgrade reaction represents the stiffness of all unbound layers (base, subbase, and subgrade) combined. The FWD Mr shown in Figure 83a was computed with the following formula: Mr = 19.4*4*k/1000. DCP results were close to the lab values, and LWD results were too low to be reasonable. Lab Mr was used for the subgrade in ME analyses because it is measured using actual subgrade samples.

- Similar observations were made on the modulus of the subbase where lab Mr values were lower than FWD (which is the modulus of the combined unbound layers). DCP-based and LWD-based modulus for long life section was too variable, and standard section values for DCP and LWD were too low. Lab test results seemed the most reasonable results to be used in ME analyses.

- Base moduli obtained from lab and FWD-based results were very close, possibly because of the same reason mentioned before, i.e., the base is closer to the surface load, and it affects the overall response more than the subbase and subgrade. DCP results were just too low and unreasonable. Therefore, the lab Mr values were used in the ME analyses.

Figure 84 shows a summary of the moduli values measured using different methods. The following general conclusions can be made by looking at the graphs in Figure 84:

- As mentioned before, the FWD-based moduli are the combined modulus of base/subbase/subgrade, and they are greater than the lab measured subgrade moduli. This is certainly expected. LWD-based moduli were too low to be reasonable, and DCP-based results for the standard section were too high (given that the subgrade of long life section is stabilized). DCP-based and lab Mr values for the long life section agreed reasonably well with each other. It was decided that the lab Mr values are most reasonable to be used in ME analyses.

- Subbase Mr values measured in the lab were a bit lower than expected, but they agreed with DCP results. Since FWD-based results are for the combined unbound layer, they were expected to be higher than lab values. It appears the most reasonable moduli for the subbase is lab Mr since it is for the subbase layer and agrees with the DCP, and FWD is for combined layers.

- Base moduli from the lab measurement for the US-131 were quite high, which is not unreasonable for this type of unbound material. Also, given the FWD-based moduli for the combined unbound layers is about 30 ksi, it is expected to have a large base Mr because the subbase Mr was quite low (Figure 84b) and subgrade Mr (lab-based) was lower than FWD-based values. It appears lab-based Mr values were the most reasonable values to use.

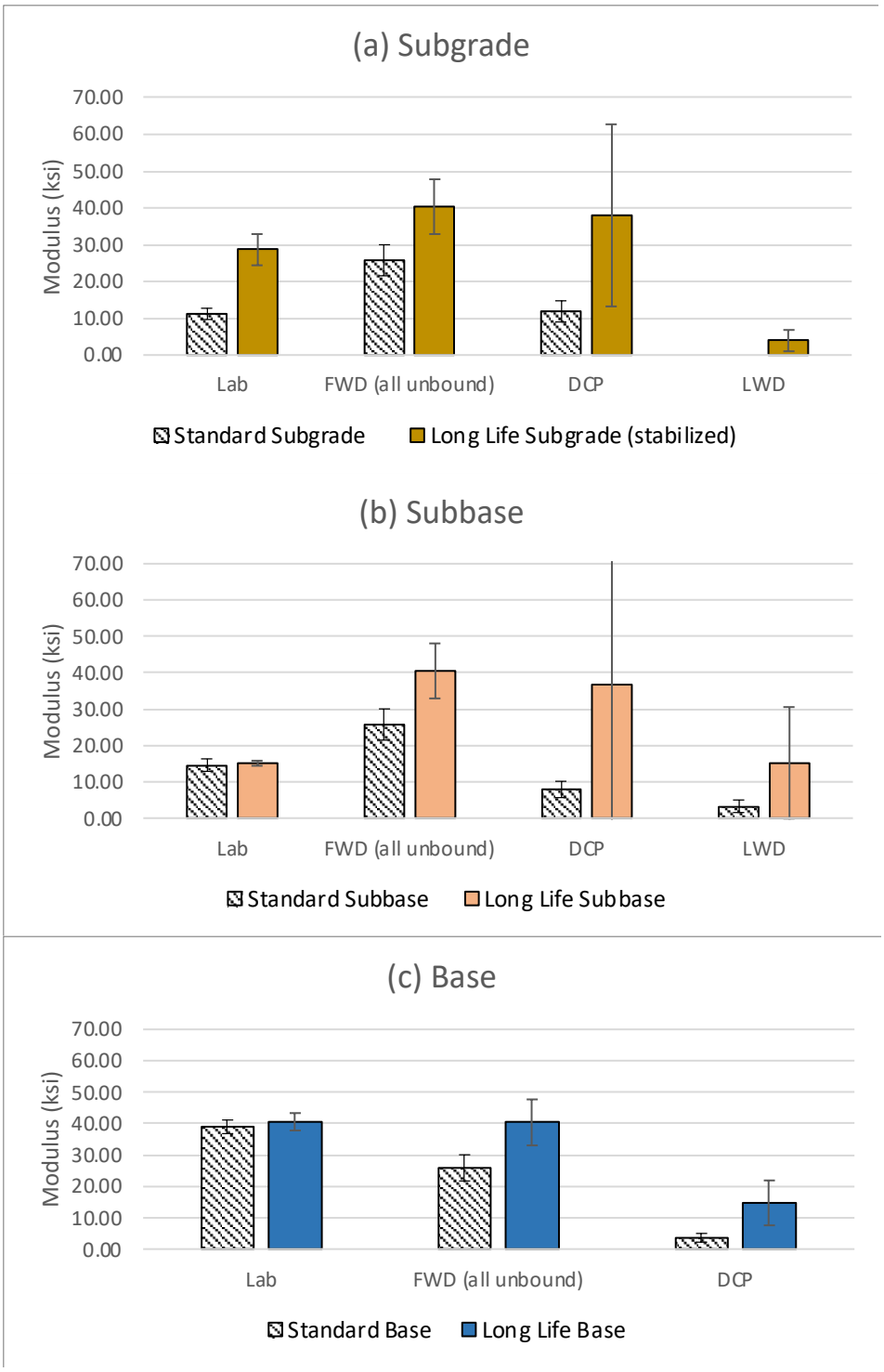

Figure 83. Comparison of unbound layer moduli for I-69 rigid pavement. Note: LWD data was not available for base of both long life and standard sections.

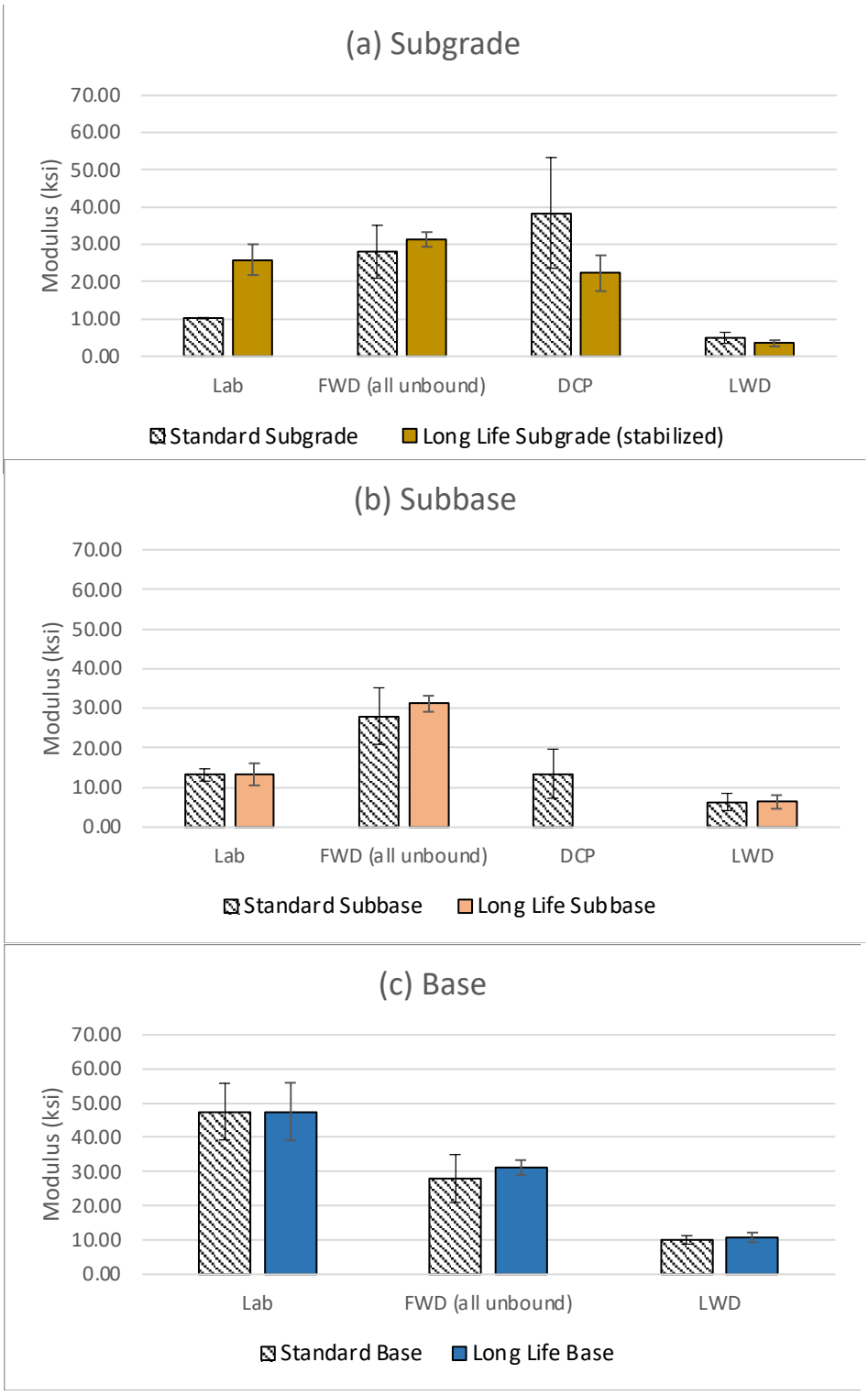

Figure 84. Comparison of unbound layer moduli for US-131 rigid pavement. Note: DCP data was not available for subbase of long-life section and both long life and standard sections.

Asphalt Mixture Layers

Dynamic modulus (|E*|) test results for the asphalt mixture layers (top, leveling, and base layers) could not be directly compared with the field FWD backcalculations. There are several reasons for this:

- Traditional FWD backcalculation algorithms (MODULUS, MODCOMP, etc.) works reliably with three combined layers, i.e., HMA, base, and subgrade. Therefore, the backcalculated HMA modulus representes the modulus of a combination of top, intermediate, and base HMA layers.

- There are advanced algorithms (e.g., BackLAVA, ViscoWave, etc.) to backcalculate dynamic modulus master curve of multiple layers, but they require temperature profile (variation of temperature with depth). Although the surface temperature was measured during the FWD tests, the temperature profile was not measured. Depending on the time of the year, temperature profiles can be very different, even when the surface temperature is the same. Sunshine, wind, air temperature fluctuations, and even precipitation during the preceding days can affect the temperature profile in a given day. Without the temperature profile measurements, dynamic modulus cannot be accurately backcalculated.

Since |E*| is widely accepted to be the most fundamental 'modulus' parameter for HMA, team used the |E*| master curve in ME analyses.

Concrete Layers

Comparison of concrete layer moduli for US-131 and I-69 rigid pavements are shown in Figure 85 and Figure 86, respectively. Concrete cores or cylinders were not provided to the team from the standard sections; therefore, lab results are not available. The team had compressive strength values measured during the construction for both US-131 and I-69 projects and used the following equation (same equation used by the Pavement ME in Level 3 analysis) to estimate the modulus of elasticity (Ec) of concrete:

$$E_c = 33\rho^{3/2}(f_c)^{1/2} \qquad \text{Equation 14}$$

where E_c = concrete modulus of elasticity (psi), ρ=unit weight of concrete (lb/ft^3) and f_c = concrete compressive strength (psi).

As shown in Figure 85 and Figure 86, the Ec values backcalculated from FWD deflections were unrealistically high, especially long-life section of US-131. Laboratory Ec values and Ec values computed from strength were relatively close. Since the Ec values computed from strength were somewhere between the lab measured and FWD-based Ec values, it was decided that Ec values computed from strength should be used in the ME analyses. Besides, Level 1 ME inputs for concrete requires Ec values measured at different days (7 days, 20 days ...etc.), which we could not do.

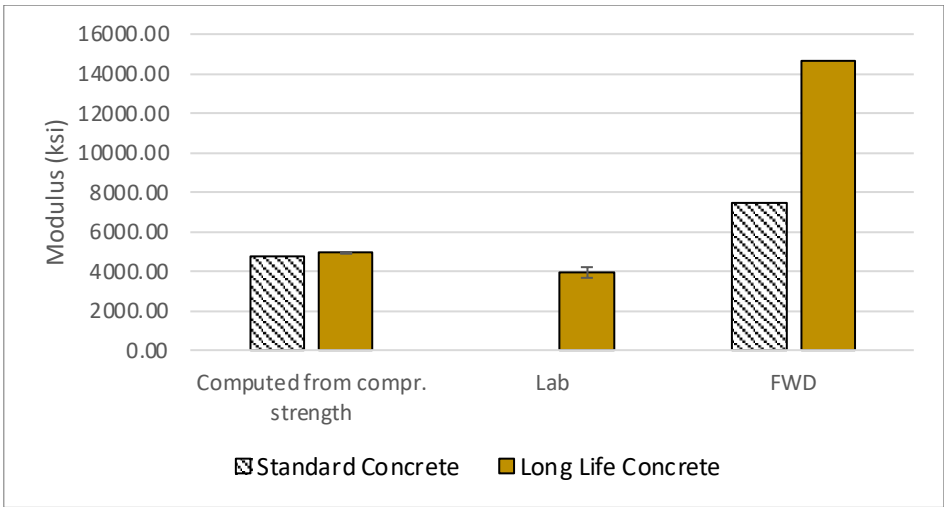

Figure 85. Comparison of concrete layer moduli for US-131 rigid pavement.

Figure 86. Comparison of concrete layer moduli for I-69 rigid pavement.

CHAPTER 4: MATERIAL DATABASE AND DYNAMOD UPDATE

The research team updated the DynaMOD software database with |E*|, |G*|, D(t) and IDT data collected as part of this project. DynaMOD is a standalone software that serves as a database for the test results conducted under MDOT research projects. DynaMOD helps engineers to easily reach the material testing data and generate inputs that can directly be used by mechanistic empirical pavement analysis tools.

Regarding the HMA testing, the results of all of the |E*|, |G*| and IDT tests conducted on 6 HMA mixtures (GGSP, 4E30, 3E30, 5E10-TOP, 5E10-LEV and 3E10) and 3 different binders (70-28P, 58-34 and 52-34) for long-life and standard test sections of I-475 project were used for this task. The research team had updated the DynaMOD database with US-131 test results as part of another project with MDOT. Table 58, Table 59 and Table 60, respectively, show the mixture |E*|, binder |G*| and mixture IDT data added to the DynaMOD database.

The following equations are used to compute mixture |E*| from the coefficients in Table 58:

$$\log(|E^*|) = b_1 + \frac{b_2}{1 + \exp(-b_3 - b_4 \log(f_R))} \quad \text{Equation 15}$$

$$\phi = d_1 e^{-\frac{(d_2 - \log(f_R))^2}{2d_3^2}} \quad \text{Equation 16}$$

$$f_R = f\ a(T) \quad \text{Equation 17}$$

where b_1, b_2, b_3 and b_4 are the |E*| master curve data to obtain coefficients, ϕ is the phase angle, d_1, d_2, and d_3 are the Gaussian fit coefficients, f is the frequency of the load and $a(T)$ is the shift factor coefficient, which is a function of temperature (T). Same equations are used to compute binder |G*| from the coefficients in Table 59.

The results of concrete tests and unbound material tests are readily accessible through the structured folders created and submitted for each project until a database is created for these test results.

Table 58 Mixture |E*| master curve data added to the DynaMOD database

HMA_ID	a1 (for deg F)	a2(for deg F)	Tref (F)	b1 (psi)	b2	b3	b4	d1	d2	d3	Binder PG
GGSP-US-131	0.000187938	-0.094041953	69.8	3.662	2.916	0.720	0.476	29.57	-1.44	3.43	PG70-28P
4E30-US-131	0.000156578	-0.093410593	69.8	3.352	3.294	0.963	0.424	31.12	-1.93	3.66	PG70-28P
3E30-US-131	0.000180488	-0.090483873	69.8	2.726	3.952	1.120	0.437	32.14	-1.78	3.51	PG64-28
5E10-US-131	0.000130835	-0.08370529	69.8	3.481	3.071	0.920	0.550	32.40	-1.87	3.41	PG64-28
3E10-US-131	0.000166614	-0.088461404	69.8	2.941	2.761	0.787	0.581	32.29	-1.55	3.20	PG64-28
2E10-US-131	0.000176022	-0.093493151	69.8	3.099	3.537	1.122	0.458	31.94	-1.87	3.40	PG58-28
GGSP-US-131	0.000184257	-0.093525515	69.8	3.805	2.916	0.720	0.476	29.57	-1.44	3.43	PG70-28P
GGSP-US-131	0.000195193	-0.095438319	69.8	3.678	2.916	0.720	0.476	29.57	-1.44	3.43	PG70-28P
GGSP-TS1-I475-NB	0.000191411	-0.090038891	69.8	3.671	2.917	0.715	0.519	29.58	-1.40	3.26	PG70-28P
GGSP-TS2-I475-NB	0.000175045	-0.088121441	69.8	3.742	2.769	0.714	0.554	30.39	-1.47	3.24	PG70-28P
GGSP-TS3-I475-NB	0.000210029	-0.093695454	69.8	3.712	2.874	0.666	0.531	29.95	-1.22	3.24	PG70-28P
4E30-TS1-I475-NB	0.000130361	-0.079129686	69.8	3.440	3.183	0.790	0.506	30.53	-1.59	3.45	PG70-28P
4E30-TS2-I475-NB	0.000168887	-0.087077791	69.8	3.449	3.191	0.794	0.513	31.34	-1.34	3.16	PG70-28P
4E30-TS3-I475-NB	0.00014073	-0.083594598	69.8	3.361	3.291	0.903	0.480	31.13	-1.68	3.28	PG70-28P
3E30-TS1-I475-NB	0.000198321	-0.090014181	69.8	2.952	3.761	0.821	0.458	31.67	-0.96	3.22	PG58-34
3E30-TS2-I475-NB	0.00021242	-0.091858332	69.8	3.079	3.589	0.746	0.483	32.77	-0.99	3.12	PG58-34
3E30-TS3-I475-NB	0.000228353	-0.094904681	69.8	3.085	3.580	0.742	0.473	31.68	-0.77	3.09	PG58-34
5E10-TOP-TS1-I475-SB	0.000169143	-0.082627906	69.8	3.152	3.471	0.573	0.514	34.23	-0.84	2.99	PG58-34
5E10-TOP-TS2-I475-SB	0.000185639	-0.086408591	69.8	3.121	3.447	0.683	0.516	33.74	-0.95	3.01	PG58-34
5E10-TOP-TS3-I475-SB	0.000198789	-0.089578853	69.8	3.007	3.614	0.631	0.473	33.79	-0.93	3.18	PG58-34
5E10-LEV-TS1-I475-SB	0.000198789	-0.089578853	69.8	3.007	3.614	0.631	0.473	33.80	-0.97	3.16	PG58-34
5E10-LEV-TS2-I475-SB	0.000203547	-0.090984955	69.8	3.056	3.584	0.625	0.494	34.03	-0.97	3.21	PG58-34
5E10-LEV-TS3-I475-SB	0.000194807	-0.087631132	69.8	3.165	3.447	0.588	0.529	33.86	-1.09	3.29	PG58-34
3E10-TS1-I475-SB	0.000171659	-0.086352833	69.8	2.868	3.870	0.960	0.464	32.50	-1.37	3.20	PG52-34
3E10-TS2-I475-SB	0.000176369	-0.087636925	69.8	2.851	3.869	0.997	0.450	32.25	-1.42	3.19	PG52-34
3E10-TS3-I475-SB	0.000206963	-0.093487969	69.8	2.889	3.782	0.941	0.465	33.10	-1.23	3.12	PG52-34

Table 59 Binder |G*| master curve data added to the DynaMOD database

Excel filename	a1 (for deg C)	a2 (for deg C)	Tref (C)	b1 (Pa)	b2	b3	b4	d1	d2	d3
PG58-28-US-131 - 2E10-MAINLINE.xlsx	0.00062386	-0.139	21.0	-6.59	15.54	1.44	0.26	138.60	-24.22	20.28
PG70-28P-US-131 - GGSP.xlsx	0.00062103	-0.143	21.0	-5.95	15.37	1.24	0.19	76.69	-235.44	367.91
PG64-28-US-131 - 3E30.xlsx	0.00051168	-0.129	21.0	-6.67	15.55	1.48	0.25	138.56	-24.54	19.92
PG64-28-US-131 - 5E10.xlsx	0.00043380	-0.121	21.0	-6.45	15.47	1.41	0.24	137.57	-26.81	21.60
PG70-28P-US-131 - 4E30.xlsx	0.00061203	-0.142	21.0	-5.53	15.54	1.06	0.19	76.73	-235.44	367.91
PG64-28-US-131 - 3E10-MAINLINE.xlsx	0.00054616	-0.134	21.0	-6.77	15.41	1.58	0.25	138.52	-24.85	19.61
PG64-28-US-131 - 3E30-W.xlsx	0.00036564	-0.113	21.0	-6.42	15.71	1.32	0.24	140.33	-24.24	19.59
PG70-28P-I475-GGSP.xlsx	0.00067414	-0.148	21.0	-6.46	18.07	0.81	0.15	61.94	-81.66	354.68
PG70-28P-I475-4E30.xlsx	0.00062874	-0.141	21.0	-5.78	17.37	0.76	0.16	102.51	-151.46	149.64
PG58-34-I475-3E30.xlsx	0.00047868	-0.119	21.0	-8.69	18.19	1.29	0.21	139.90	-21.31	16.97
PG58-34-I475-3E30-2.xlsx	0.00041848	-0.114	21.0	-8.33	18.02	1.25	0.21	158.38	-26.33	19.02
PG58-34-I475-3E30-3.xlsx	0.00041436	-0.113	21.0	-6.47	15.43	1.32	0.24	139.57	-22.17	17.17
PG52-34-I475-3E10.xlsx	0.00056411	-0.128	21.0	-6.11	15.26	1.22	0.26	140.48	-18.68	15.44

Table 60 Mixture Indirect Tensile (IDT) Strength data added to the DynaMOD database

Mix_ID	Avg IDT strength (psi)	S.D of IDT
GGSP-TS1-US-131	554.4	24.0
4E30-TS3-US-131	607.1	13.1
3E30-TS3-US-131	473.5	8.5
5E10-TS4-US-131	536.0	20.0
3E10-TS4-US-131	486.0	36.4
2E10-TS4-US-131	501.0	53.0
GGSP-TS2-US-131	519.7	18.5
GGSP-TS3-US-131	533.1	34.9
4E30-TS1-US-131	557.4	12.7
4E30-TS2-US-131	566.7	24.3
3E30-TS1-US-131	402.0	64.2
3E30-TS2-US-131	447.0	49.0
GGSP-TS1-I475-NB	541.0	18.0
GGSP-TS2-I475-NB	624.0	5.0
GGSP-TS3-I475-NB	557.0	32.0
4E30-TS1-I475-NB	551.0	11.0
4E30-TS2-I475-NB	592.0	47.0
4E30-TS3-I475-NB	574.0	23.0
3E30-TS1-I475-NB	488.0	13.0
3E30-TS2-I475-NB	494.0	44.0
3E30-TS3-I475-NB	506.0	38.0
5E10-TOP-TS1-I475-SB	521.0	24.0
5E10-TOP-TS2-I475-SB	503.0	43.0
5E10-TOP-TS3-I475-SB	541.0	27.0
5E10-LEV-TS1-I475-SB	493.0	19.0
5E10-LEV-TS2-I475-SB	533.0	14.0
5E10-LEV-TS3-I475-SB	556.0	30.0
3E10-TS1-I475-SB	501.0	15.0
3E10-TS2-I475-SB	508.0	37.0
3E10-TS3-I475-SB	491.0	6.0

CHAPTER 5: PAVEMENT PERFORMANCE PREDICTIONS AND ANALYSIS

The MDOT has currently adopted Pavement ME V2.3 for pavements design. MDOT uses coefficients that were calibrated for Michigan conditions for the design of flexible pavements. However, global coefficients are used for the design of JPCP in Pavement ME V2.3. The Pavement ME V2.6 calibration was not completed at the time of this report, therefore, the results of Pavement ME V2.3 should be more reliable for flexible pavements (since they were calibrated). For rigid pavements, since Pavement ME V2.3 and V2.6 are identical when global calibration coefficients are used, either one could be used.

Pavement performance analysis on the flexible projects

Since as-built material properties and their variability during construction and other structural design elements have significant impacts on achieving the long-life purpose of the four pilot projects, it is essential to evaluate the long-term performance of the pavement structures using tools like the AASHTOWare Pavement ME using the as-built input data collected throughout the project. Therefore, tor evaluation of the two flexible pavement pilot projects, I-475 and US-131, the AASHTOWare Pavement ME V.2.3 and V.2.6 and PerRoad were used for performance prediction. Pavement ME V.2.3 is currently adopted by MDOT and Michigan calibration coefficients are available for this version. Pavement ME V.2.6 uses the latest version of the distress models which mainly differ from the previous one for the new HMA top-down cracking mode. PerRoad is a flexible perpetual pavement design software that has been developed at Auburn University in collaboration with the Asphalt Pavement Alliance (APA), the National Asphalt Pavement Association (NAPA), and the State Asphalt Pavement Associations (SAPA). The software is based on layered elastic analysis and a statistical analysis procedure (Monte Carlo simulation) to predict the responses within the pavement structure. Pass/fail criteria can be selected based on the pavement response or using transfer functions to convert the responses to different distresses within the pavement. The main advantage of this software is that it can compare the distribution of the tensile strain at the bottom of the HMA layers resulting from different load, climatic condition, and material stiffnesses with a predefined criterion for this distribution. The default values for the strain distribution criteria were developed based on the NCAT (National Center for Asphalt Technology) test track experiment results.

Table 61 shows the inputs used in AASHTOWare Pavement ME simulations for I-475 and US-131, respectively. Pavement structures were evaluated in AASHTOWare Pavement ME for a design life of 50 and 30 years for the I-475 and US-131, respectively. A new flexible pavement project type with an initial International Roughness Index (IRI) of 67 in/mi and 95% reliability level were used for the analysis. Average annual daily truck traffic (AADTT), vehicle class distribution, growth factors, monthly adjustment factors were provided by MDOT.

Table 61 Pavement ME inputs for I-475 project

Section	ID	PG	Layer	|E*|	|G*|	IDT strength	Air voids (%)	Layer thickness (in)	Creep compliance	Unbound layers properties
Long-life sections	GGSP	70-28P	Top	LM	LM	LM	LM	LM	Calculated from |E*|	LM
	4E30	70-28P	Lev	LM	LM	LM	LM	LM	Calculated from |E*|	LM
	3E30	58-34	Base	LM	LM	LM	LM	LM	Calculated from |E*|	LM

Standard sections	5E10-top	58-34	Top	LM	LM	LM	LM	LM	Calculated from |E*|	LM
	5E10-leveling	58-34	Lev	LM	LM	LM	LM	LM	Calculated from |E*|	LM
	3E10	52-34	Base	LM	LM	LM	LM	LM	Calculated from |E*|	LM

Notes: GGSP = Gap Graded Superpave, LM= Lab measured, DV=Design values

Table 62 Pavement ME inputs for US-131 project

	ID	PG	Layer	|E*|	|G*|	IDT strength	Air voids (%)	Layer thickness (in)	Creep compliance	Unbound layers properties
Long-life sections	GGSP	70-28P	Top	LM	LM	LM	LM	LM	Calculated from |E*|	LM
	4E30	70-28P	Lev	LM	LM	LM	LM	LM	Calculated from |E*|	LM
	3E30	64-28	Base	LM	LM	LM	LM	LM	Calculated from |E*|	LM
Standard section	5E10	64-28	Top	LM	LM	LM	LM	LM	Calculated from |E*|	LM
	3E10	64-28	Lev	LM	LM	LM	LM	LM	Calculated from |E*|	LM
	2E10	58-28	Base	LM	LM	LM	LM	LM	Calculated from |E*|	LM

Notes: GGSP = Gap Graded Superpave, LM= Lab measured, DV=Design values

The results of the simulations using the AASHTOWare Pavement ME 2.6 using global coefficients are shown in Figure 87 and Figure 88, and observations can be summarized as follows:

- The predicted bottom-up cracking for both projects is minimal, as observed in Figure 87 and Figure 88. Although the predicted top-down cracking of the long-life sections starts earlier than standard sections, the final distress magnitude for all sections of both the I-475 and US-131 is below the pass-fail threshold at the end of 50 years.
- Two of the I-475 long-life sections and all the US-131 test sections fail for thermal cracking.
- The rutting performance of all the test sections is acceptable, with the long-life sections slightly outperforming the standard sections.
- Regarding IRI, all of the test sections of I-475 and US-131 fail relatively early in the design life. This might be partially due to the early thermal and top-down cracking developed. It also may be because of the significant vertical shift due to the 95% reliability calculations. The authors do not think the IRI predictions of Pavement ME V2.6 are reasonable and local calibration is needed.

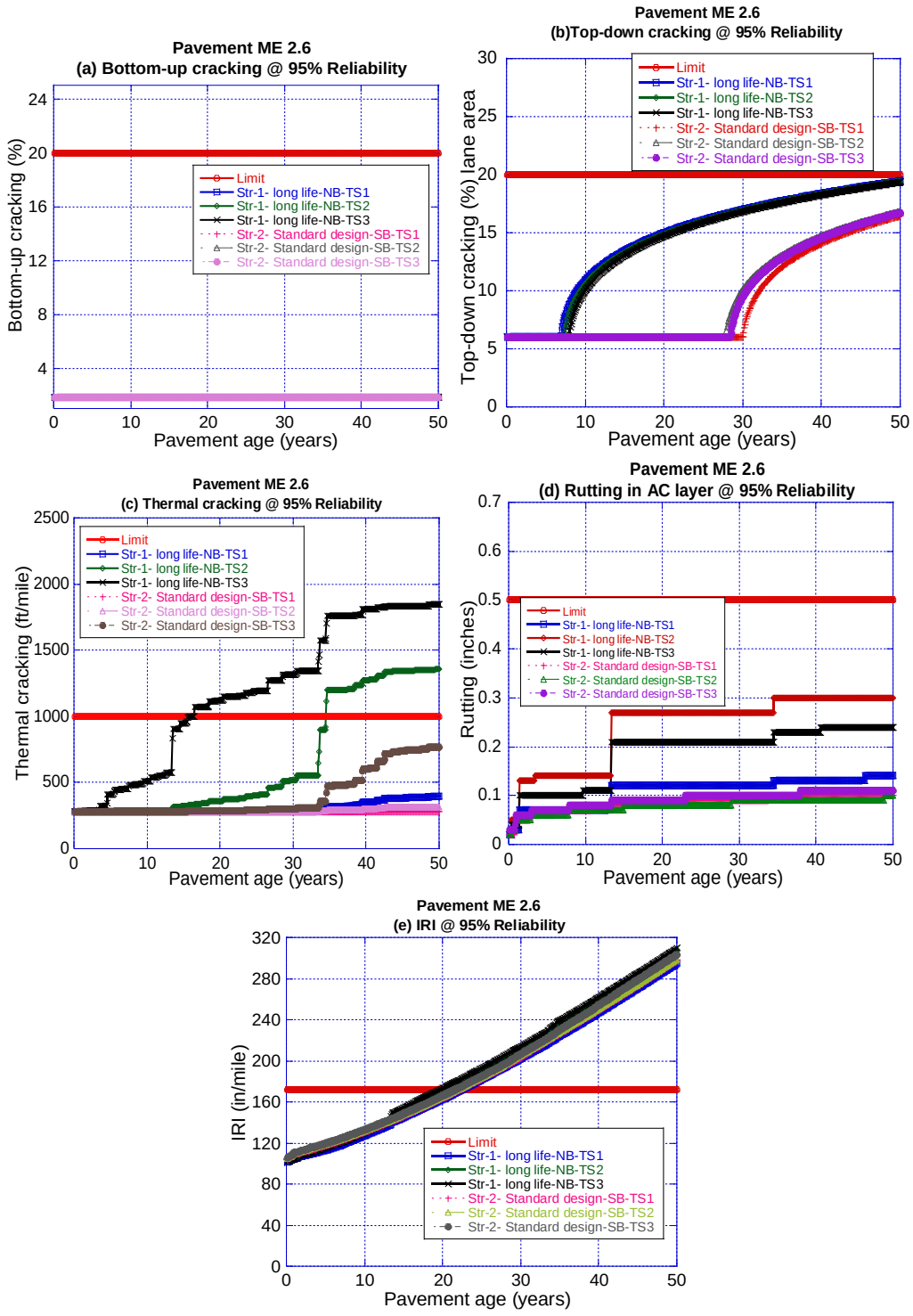

Figure 87 I-475 Pavement ME 2.6 predicted distresses (a)bottom-up cracking, (b) top-down cracking, (c)thermal cracking, (d) rutting in AC, (E) IRI

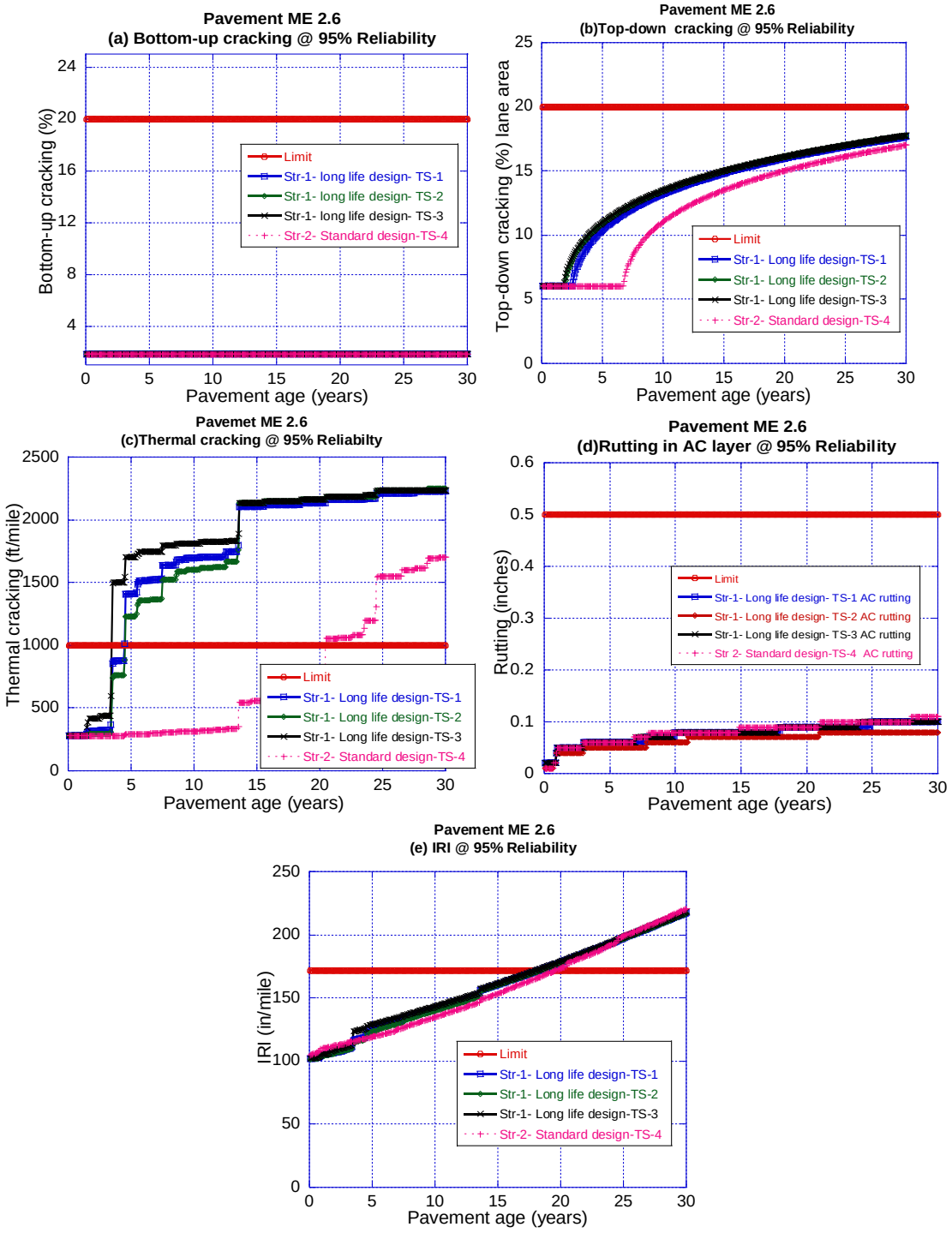

Figure 88 US-131 Pavement ME 2.6 predicted distresses (a) bottom-up cracking, (b) top-down cracking, (c)thermal cracking, (d) rutting in AC, (e) IRI

The results of the simulations using the AASHTOWare Pavement ME 2.3 using MDOT local calibration coefficients are shown in Figure 89 and Figure 90, and observations can be summarized as follows:

- The predicted bottom-up cracking for both projects is acceptable with the long-life sections outperforming the standard sections. The standard sections of the I-475 project fail for top-down cracking, while no failure was predicted for the long-life pavement structures. It is noted that MDOT does not currently use v2.3 top-down cracking for design decisions
- The predicted thermal cracking is negligible regardless of the project and sections analyzed.
- The standard sections of the I-475 project fail for HMA rutting, while all other pavement sections analyzed do not.
- The predicted IRI of all I-475 sections exceed the pass-fail threshold between 30-40 years of service life. On the contrary, all the US-131 test sections are below the limits until end of the design life.
- Overall, the long-life sections perform better than the standard sections.

In order to calculate seasonal pavement moduli for the PerRoad simulations, 52 weeks of the year were divided into four 13-weeks period representing the four seasons. Average monthly air temperatures were extracted from the corresponding AASHTOWare Pavement ME climatic files. Seasonal pavement moduli for HMA layers were calculated based on dynamic modulus master curves for the seasonal temperatures and frequency of 10 Hz. The COV (coefficient of variation) used in these simulations is the highest COV observed for each mixture in the dynamic modulus test. Due to the limited number of layers that can be implemented in the software, base and subbase layers were combined into one layer using Odemark's equivalent thickness method. The lab measured resilient modulus values for unbound layers were used for these calculations. The resilient modulus values for unbound layers were considered constant in different seasons. The thicknesses and variation in the thicknesses for HMA layers is based on the analysis of cores described in the previous chapter. An example of seasonal and structural inputs for I-475 NB test section 1 is shown in Figure 91.

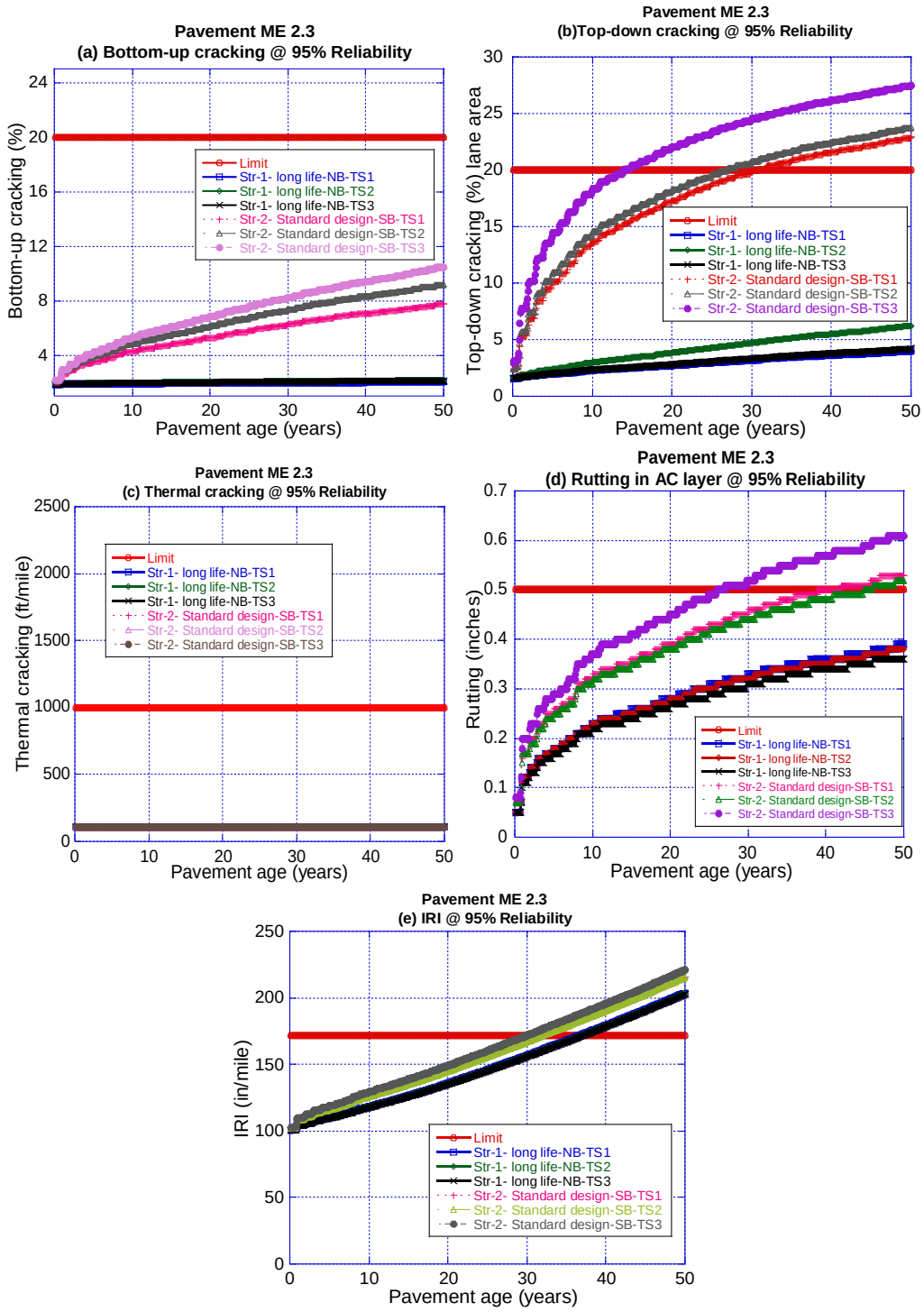

Figure 89 I-475 Pavement ME 2.3 predicted distresses (a)bottom-up cracking, (b) top-down cracking, (c)thermal cracking, (d) rutting in AC, (e) IRI

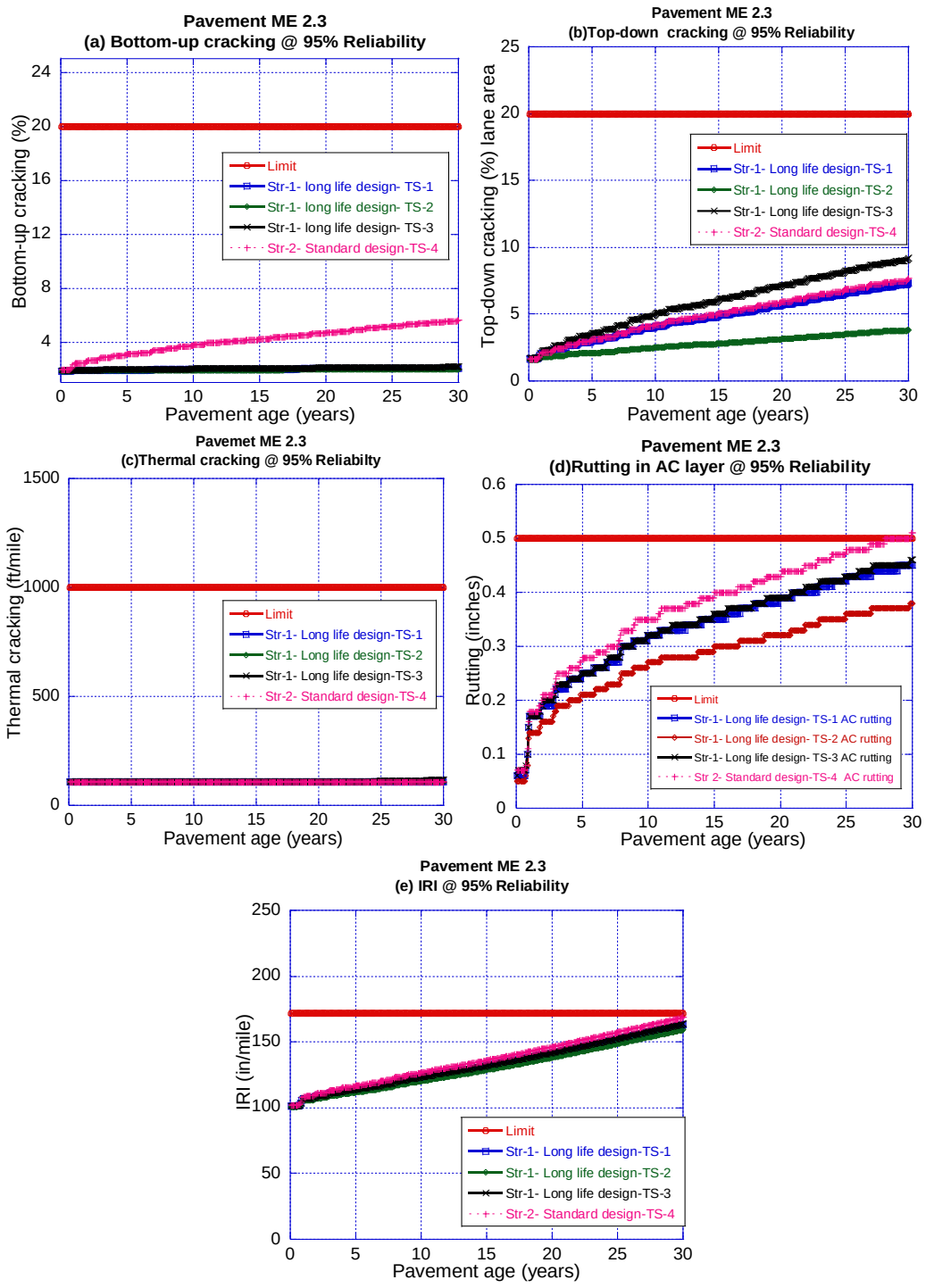

Figure 90 US-131 Pavement ME 2.3 predicted distresses (a)bottom-up cracking, (b) top-down cracking, (c)thermal cracking, (d) rutting in AC, (e) IRI

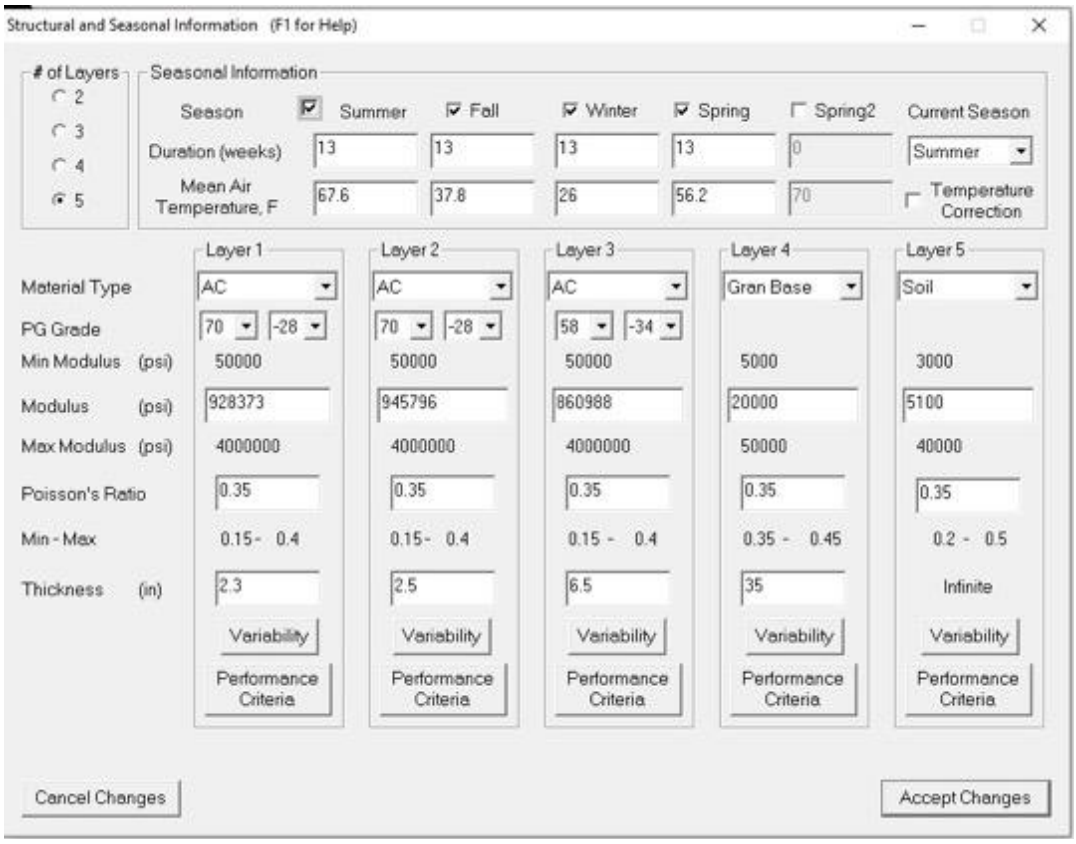

Figure 91 PerRoad structural and seasonal inputs- I-475 NB test section 1

The performance criteria for evaluation of the performance of the long-life and standard test sections of US-131 and I-475, were defined at 4 locations in the pavement structure:

- Principal strain at the top of the top HMA course (indication of top-down cracking)
- Horizontal strain distribution at the bottom of the base HMA course (indication of bottom-up cracking)
- Vertical strain at the middle of the combined base and subbase layer (indication of rutting)
- Vertical strain at the top of the subgrade layer (indication of rutting)

Pavement performance criteria and values used in this study are summarized in Table 63.

Table 63 Pavement performance criteria for PerRoad simulations

Location		Performance criteria	Threshold limit	
Layer	Position			
Top HMA layer	Top	Principal strain	-100 με	
Base HMA layer	Bottom	Horizontal strain distribution	Percentile	με
			95th	-257
			85th	-194
			75th	-158
			65th	-131
			55th	-110
Combined base and subbase	Middle	Vertical strain	150 με	
Subgrade	Top	Vertical strain	200 με	

Based on the above performance criteria, all the long-life and standard test sections resulted in acceptable performance and passed the PerRoad criteria. The results for I-475 NB test section-1 are listed in Table 64. As shown, the strain distribution at the bottom of the HMA layer is significantly lower than the failing criteria. Additionally, vertical strains at the middle of the combined base and subbase layer and top of the subgrade layer are also significantly lower than the target values. This can be an indication of acceptable performance in terms of rutting in the unbound layers. Similarly, all the predicted principal strains at the top of the top HMA layer are below the defined target value. This prediction could be an indication of good performance in top-down cracking. Similar results were obtained for all long-life and standard test sections of the US-131 and I-475 projects.

Table 64 PerRoad analysis results- I-475 NB test section 1

Perpetual Pavement Design Results: Percentile Responses							
Layer	Location	Criteria	Target	Units	Target percentile	Actual percentile	Pass/Fail?
1	Top	Principal Strain	-100	microstrain	50	100	Pass
1	Bottom	Tensile Strain	-257	microstrain	95	100	Pass
			-194	microstrain	85	100	Pass
			-158	microstrain	75	100	Pass
			-131	microstrain	65	100	Pass
			-110	microstrain	55	100	Pass
4	Middle	Vertical Strain	150	microstrain	50	100	Pass
5	Top	Vertical Strain	200	microstrain	50	100	Pass

The cumulative distribution of the defined performance criteria (strains) for I-475 and US-131 are shown in Figure 92 and Figure 93, respectively. As shown in these figures, all the predicted principal strains at the top of the HMA surface layer are below the defined target value. This prediction could be an indication of good performance in top-down cracking. The cumulative distribution of the horizontal strains at the bottom of the AC layer shows that all the long-life and standard section pass the PerRoad horizontal strain distribution criteria, since all of them are on the left side of the PerRoad limits. Additionally, the predicted values for the long-life sections are less than standard sections for a given percentile. There is a similar trend in the vertical strain response at the middle of the base layer. This can be an indication of acceptable performance in terms of rutting in the unbound layers. Similar results were obtained for all long-life and standard test sections of the US-131 and I-475 projects.

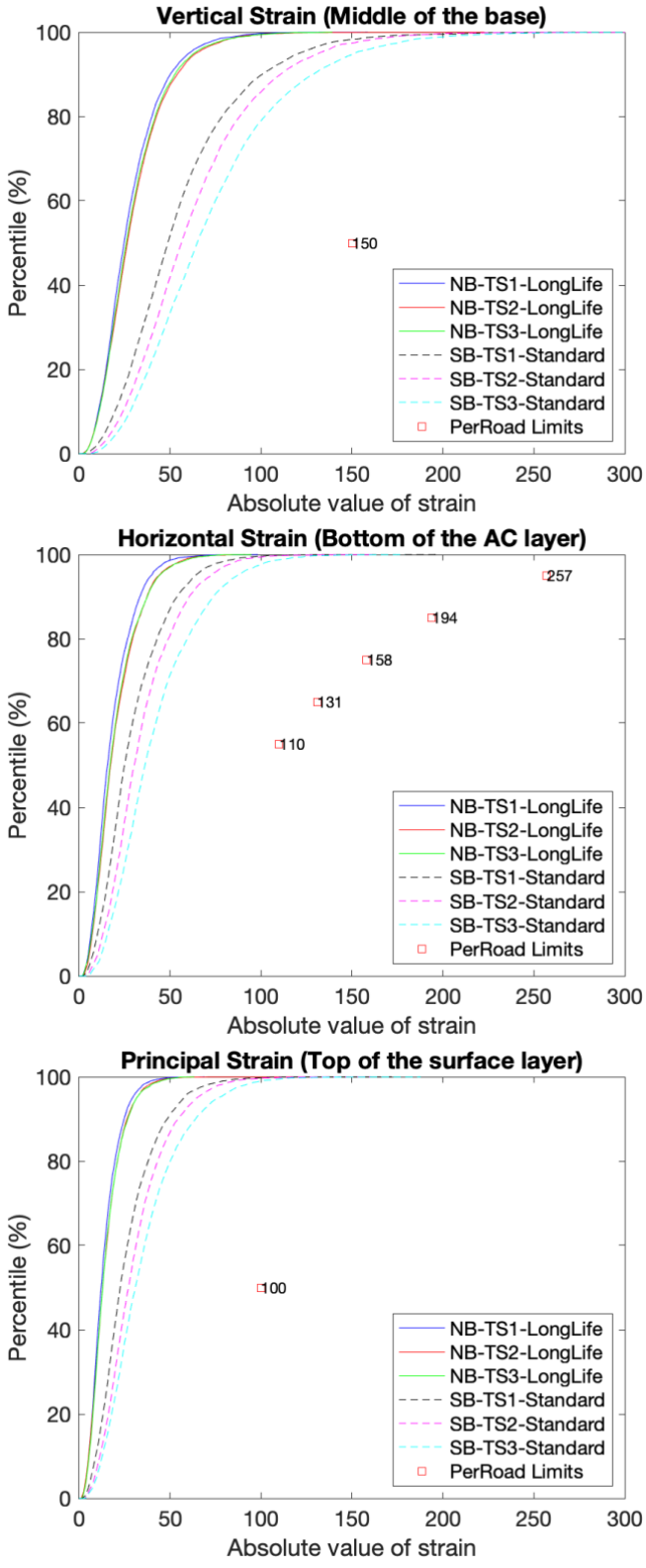

Figure 92 Cumulative distribution of defined performance criteria in PerRoad – I-475

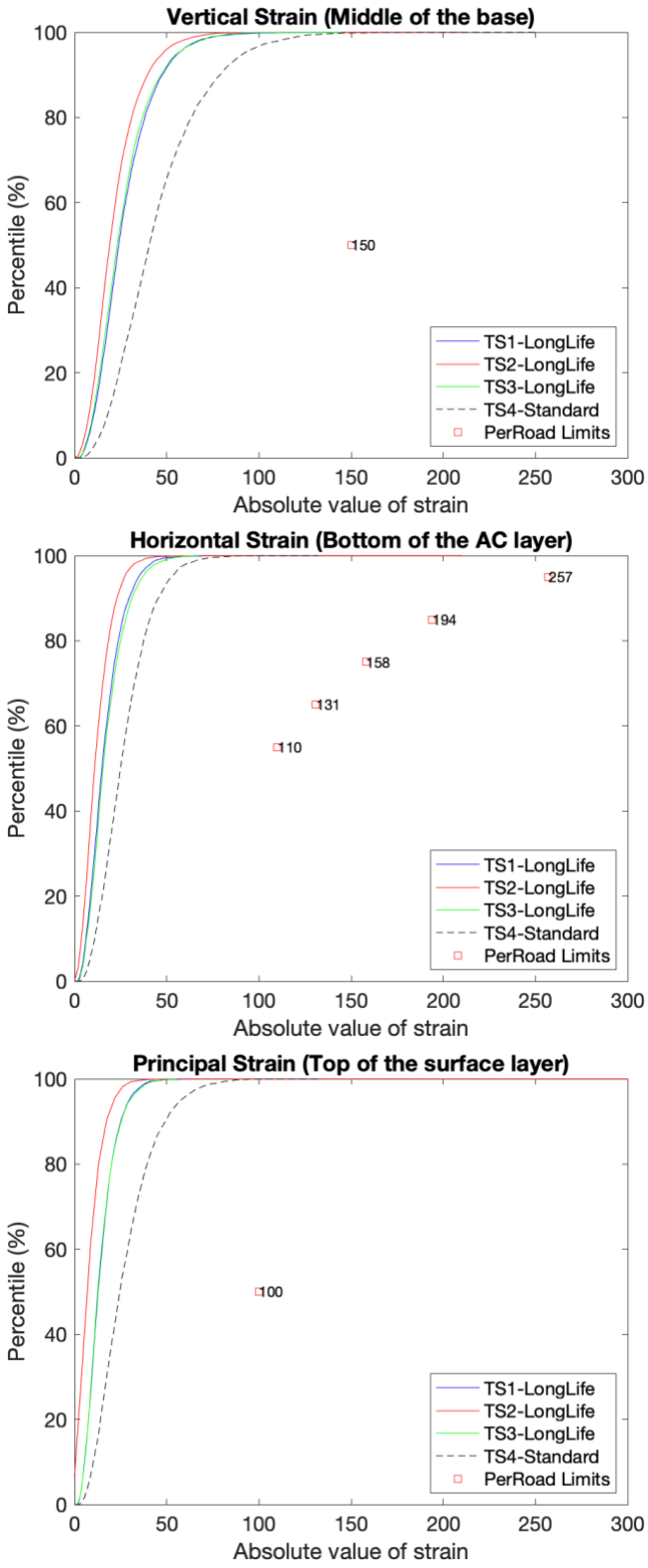

Figure 93 Cumulative distribution of defined performance criteria in PerRoad – US-131

Pavement ME analyses on the I-69 JPCP project

The structural inputs used to compare performances between the long-life and standard sections of the I-69 project are reported in Table 65. EB TS-1 and 2 are the standard 20-year design pavements while WB TS-3 and 4 are the 30-year long-life pavements. The base and subbase moduli values were estimated at 30 psi bulk stress as per guidelines recommended in NCHRP 1-28A using laboratory test data for the mentioned layers. Laboratory-determined stabilized and non-stabilized subgrade layer moduli values were utilized in the AASHTOWare Pavement ME analyses. A CTPB modulus value of one million psi was used in the Pavement-ME analysis since the FWD backcalculation and laboratory test resulted in a similar modulus for the layer. Coefficients of thermal expansion are the lab measured values from the samples from standard and long-life test sections. In addition, soil gradations determined in the laboratory for the base and subbase materials were utilized.

Table 65 Pavement ME inputs for I-69 pavement sections

Layer/ parameter		Standard - Eastbound (EB)		Long-life - Westbound (WB)	
		TS-1	TS-2	TS-3	TS-4
PCC slab	Thickness, in	9.5	9.5	10.2*	10.4*
	Strength, psi	6,763	5,847	6,133	5,848
CTPB	Thickness, in	-	-	6	6
	Modulus, psi			1,000,000	1,000,000
Base, A-1-a	Thickness, in	6 (OGDC)	6 (OGDC)	6	6
	Modulus, psi	46,000	31,000	46,000	32,000
Subbase, A-1-a	Thickness, in	10	10	8	8
	Modulus, psi	12,000	15,000	14,000	14,000
Subgrade, A-6	Stabilized	No	No	Yes	Yes
	Modulus, psi	13,000	9,000	22,000	35,000
Joint spacing, ft		14			
Coefficient of thermal expansion, in/in/°F		4.5×10^{-6}		3.83×10^{-6}	
Dowel diameter, in		1.25		1.5	
Slab width, ft		12			
Initial IRI, in/mile		73	73	71	71

* Average thickness determined from the cores.

Average annual daily truck traffic (AADTT), vehicle class distribution, growth factors, and monthly adjustment factors were used from the initial ME design files provided by the MDOT. The average annual daily truck traffic (AADTT) used was 4,788, the percentage of trucks in the design direction was 51%, the percentage of trucks in the design lane was 77%, and the number of lanes in the design direction was three. The MDOT climate station data were used for the city of Flint, MI.

An initial International Roughness Index (IRI) of 73 inches/mile and 71 inches/mile was used in the standard and long-life sections analyses, respectively as opposed to 65 inches/mile in the original ME design. This value was extracted from the 2019 PMS sensor data, as illustrated in Figure 94. This plot shows the overall mean IRI (MRI) along the pavement sections measured every 0.1-mile for the control section (CS) 25085. Most MRI values fall between the range of 60 to 80 inches/mile. The EB TS1 MRI values are recorded between CS beginning milepost (BMP) of 0.6-0.8, EB TS2 from BMP: 1.3-1.5, WB TS3 from BMP: 0.7-0.9, and WB TS4 from BMP: 1.7-1.9.

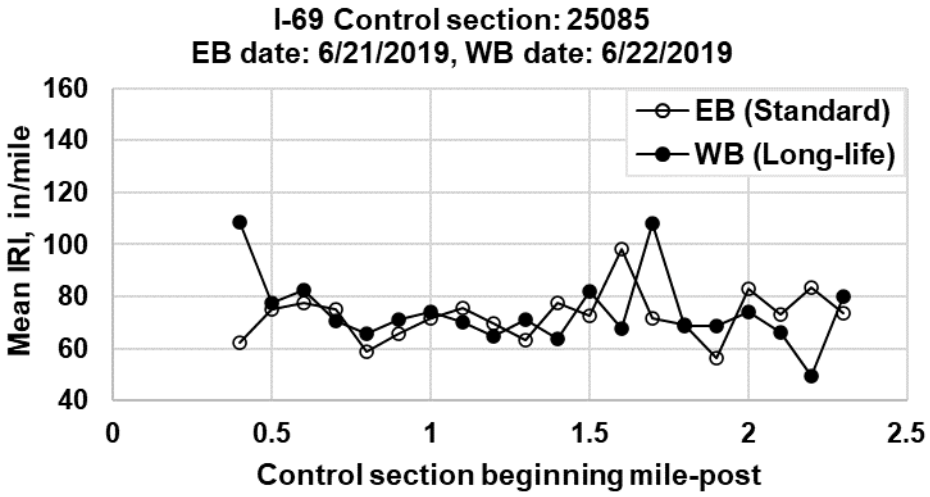

Figure 94 Mean IRI measured at I-69 projects

Figure 95 displays the predicted IRI values for the standard and the long-life sections at 95% reliability.. Pavement-ME software v2.6 was used for analyzing the as-built performance using global calibration coefficients for new rigid pavement. It is noted that the models and the corresponding global coefficients of both the Pavement-ME versions (i.e., V.2.3 and V.2.6) are the same. It is observed that the long-life sections are outperforming the standard sections. The standard designed TS-1 and 2 are meeting the IRI threshold of 172 inches/mile at an age of about 18 years. On the contrary, the 30-year long-life design TS-3 and 4 are well below the IRI threshold at the end of the 50-year analysis period. Also, there is no considerable section-to-section variation in the performance within the standard or the long-life designs.

Figure 96 shows the mean joint faulting and transverse cracking predictions for the I-69 project. Figure 96(a) shows that the mean joint faulting for the standard section is higher than the long-life sections; however, it is considerably lower than the threshold value of 0.125 inches at the end of the 20 years; their intended design life. It is noted that the EB TS-1 and 2 have a 9.5-inch thick PCC slab that incorporates a 1.25-inch dowel bar as compared to the long-life design sections, TS-3 and 4. The transverse cracking predicted by ME is 1.23% for all the sections at 95% reliability irrespective of the design used, which is far below the threshold of 15% slabs cracked over the entire design life, as shown in Figure 96(b).

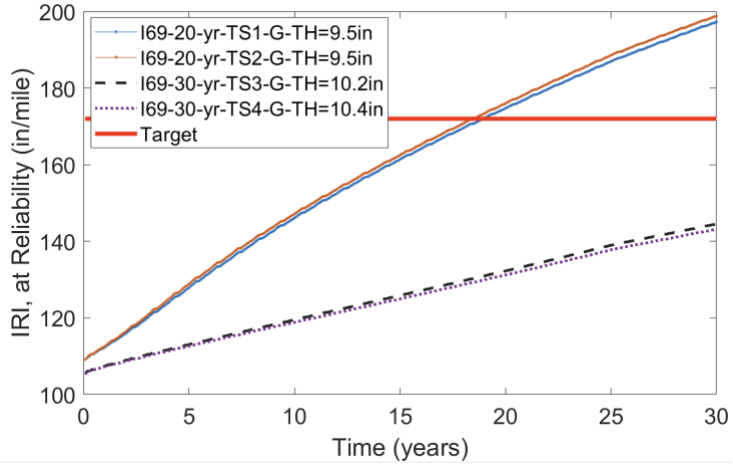

Figure 95 Pavement ME predicted IRI: I-69 project

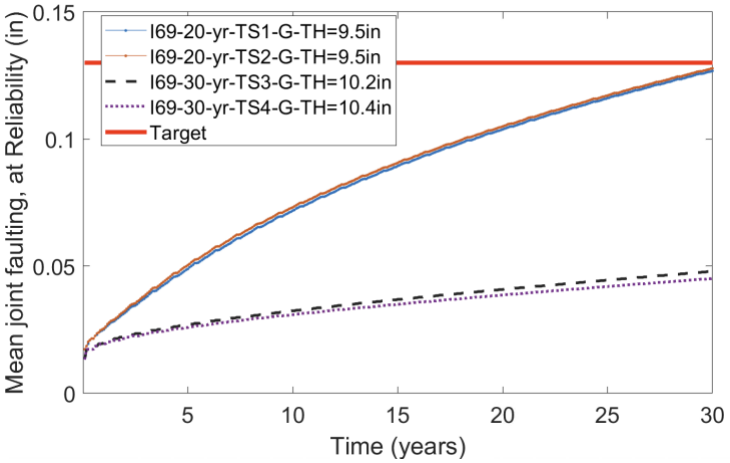

(a) Mean joint faulting

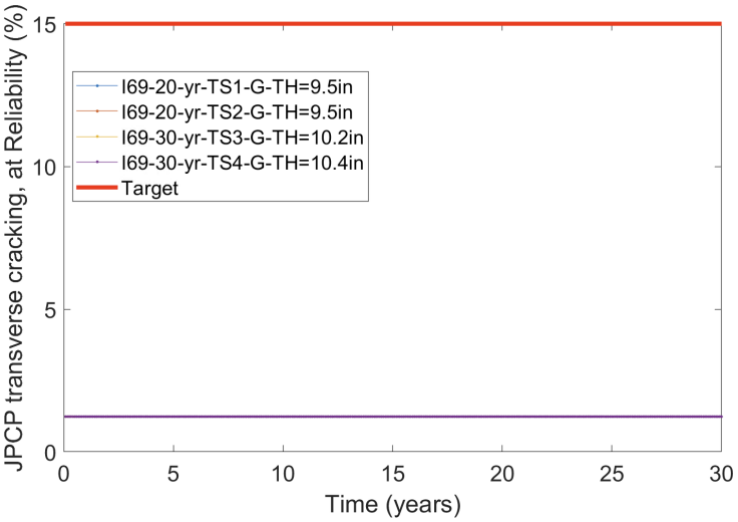

(b) Transverse cracking

Figure 96 Pavement ME faulting and transverse cracking predictions: I-69 project

Pavement ME analyses on the US-131 JPCP project

Table 66 displays the structural inputs used to compare performances between the long-life and standard sections of the US-131 project. The NB sections are the 50-year design (long-life) while Southbound (SB) sections are the 20-year (standard) design pavements. The PCC slab compressive strength values used in the analyses for the long-life test sections were determined in the laboratory (from cylinders). The PCC compressive strength values for the standard sections were extracted from the construction records. A modulus of one million psi was used for the CTPB layer since the FWD backcalculation and laboratory test resulted in a similar modulus for the layer while the base moduli values were estimated at 30 psi bulk stress as per guidelines recommended in NCHRP 1-28A using laboratory test data for the mentioned layers. The analyses also incorporate subbase and subgrade layer moduli values determined in the laboratory. Coefficients of thermal expansion are the lab measured values from the samples from standard and long-life test sections.

Average annual daily truck traffic (AADTT), vehicle class distribution, growth factors, and monthly adjustment factors were used from the initial ME design files provided by the MDOT. The average annual daily truck traffic (AADTT) used was 3683, the percentage of trucks in the design direction was 50%, the percentage of trucks in the design lane was 96%, and the number of lanes in the design direction was 2. The MDOT's climate station data were used for the city of Grand Rapids, MI.

Table 66 Pavement ME inputs for US-131 pavement sections

Layer/ parameter		Long-life (NB) design			Standard (SB) design		
		TS-1	TS-2	TS-3	TS-1	TS-2	TS-3
PCC slab	Thickness, in	10.5	10.5	10.5	10.5	10.5	10.5
	Strength, psi	6,570	6,363	7,073	5,808	6,540	5,918
CTPB	Thickness, in	6	6	6	-	-	-
	Modulus, psi	1,000,000	1,000,000	1,000,000			
Base, A-1-a	Thickness, in	6	6	6 (OGDC)	6 (OGDC)	6 (OGDC)	6 (OGDC)
	Modulus, psi	50,000	50,000	50,000	50,000	50,000	50,000
Subbase, A-1-a	Thickness, in	8	8	20	10	10	10
	Modulus, psi	10,000	10,000	10,000	10,000	10,000	10,000
Subgrade, A-6	Stabilized	Yes	Yes	No	No	No	No
	Modulus, psi	25,000	25,000	10,000	10,000	10,000	10,000
Joint spacing, ft		14					
Coefficient of thermal expansion, in/in/°F		3.91×10^{-6}			4.5×10^{-6}		
Dowel diameter, in		1.5					
Slab width, ft		12					
Initial IRI, in/mile		72	72	72	66.5	66.5	66.5

An initial IRI of 66.5 inches/mile and 72 inches/mile was used in the analyses for the standard and the long-life sections, respectively instead of the 55 inches/mile used in the original ME design. This data was extracted from 2019 sensor data, as displayed in Figure 97. The plot displays the overall MRI values along the pavement sections measured every 0.1-mile for CS 41132. The long-life design NB TS1 is covered by the MRI values recorded between CS BMP of 9.2-9.4, NB TS2 from BMP: 9.8-10.0, and NB TS3 from BMP: 11.4-11.6. The standard design SB TS1 is covered by the MRI values recorded between CS BMP of 9.3-9.5, SB TS2 from BMP: 10.1-10.3, and SB TS3 from BMP: 11.7-11.9.

The MRI values for the SB sections are consistently lower than the NB sections, and the majority fall between the range of 55 to 80 inches/mile. The NB sections are rougher, with some MRI values approaching and even higher than 100 inches/mile. The profile measurement time can be a possible explanation for such variability and high MRI values. It is well known that a profile variation of 10% is expected between morning and afternoon timings on the rigid pavements. The average MRI value for the NB pavement is estimated at 76 inches/mile, but 72 inches/mile is used in the ME analyses. This is to offset the effect of time and the rougher sections' MRI values on average for the NB pavement.

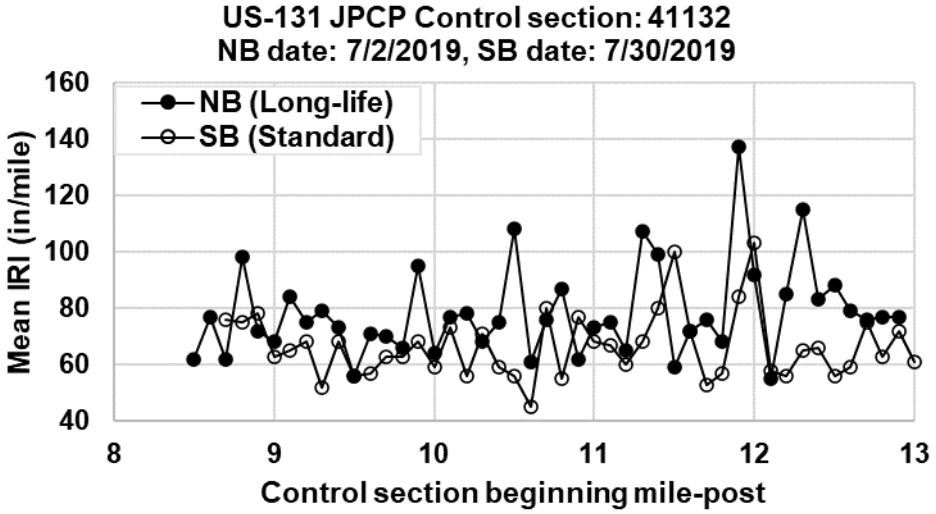

Figure 97 Mean IRI measured at US-131 projects

Figure 98 displays the predicted IRI values for the standard and the long-life sections at 95% reliability. The standard design sections were analyzed for a 75-year design for comparison. It is observed that the long-life sections are performing slightly better than the standard sections at the end of the 50-year design period. However, at 20 years, the IRI predictions (using V.2.6 with global coefficients) were very similar for the standard and long-life sections. There is no section-to-section variation in the performance within the standard or the long-life designs. The SB standard design test sections cross the IRI threshold of 172 inches/mile at around 50 years of age while the long-life TS-1 and 2 meet the threshold at an age of 67 years. The NB long-life design TS-3 hits the threshold IRI value at about 63 years.

Figure 99 shows the mean joint faulting and transverse cracking predictions for the US-131 projects. Figure 99(a) shows that the mean joint faulting for the standard section is almost twice as compared to the long-life sections; however, it is considerably lower than the threshold value of 0.125 inches even at the end of 75 years analysis period. Also, the section-to-section variability in either design is negligible. The standard design sections also have higher faulting even at the end of their 20-year design period than the long-life sections. Figure 99(b) displays that the transverse cracking predicted by ME is 1.23% for all the sections at 95% reliability irrespective of the design used, which is far below the threshold of 15% slabs cracked over the entire design life.

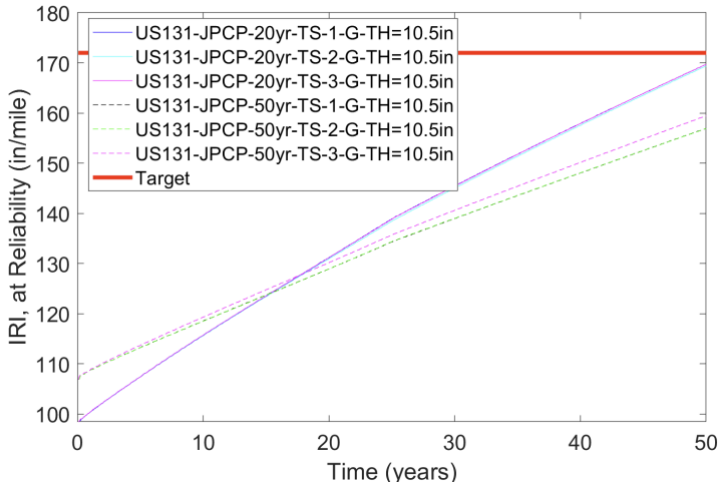

Figure 98 Pavement ME predicted IRI – US-131 projects

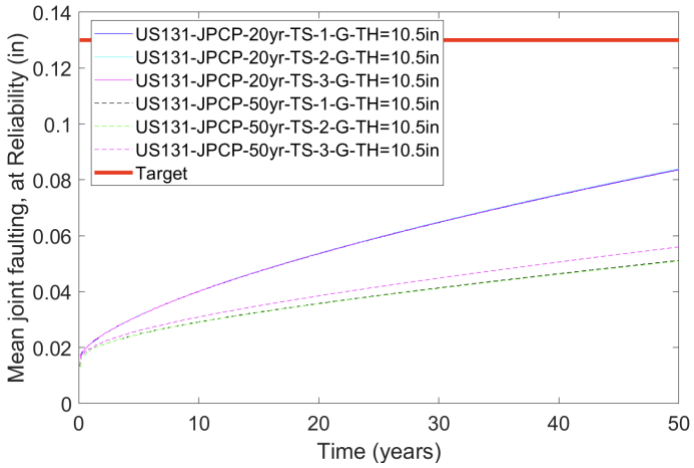

(a) Mean joint faulting

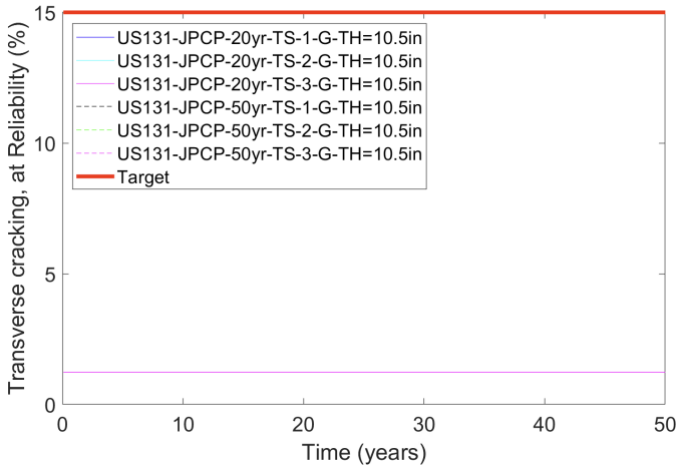

(b) Transverse cracking

Figure 99 Pavement ME faulting and transverse cracking predictions – US-131 projects

CHAPTER 7: CONCLUSIONS & RECOMMENDATIONS

A list of general conclusions based on the data and observations gathered during this project are summarized in the subsections below.

Structural design improvements

Flexible long-life pavements (I-475 and US-131)

Long life pavements were designed as thick pavements with no potential for bottom-up cracking. This goal was indeed achieved because the Pavement ME software predicted no bottom-up cracking. In addition, the strain distribution predicted by PerRoad software was significantly lower than the thresholds. Therefore, it is highly unlikely that any bottom-up cracking will develop in these pavements during their service lives.

Rigid long-life pavements (I-69 and US-131)

The long-life sections of both projects were thick enough to have no predicted transverse cracking (either top-down or bottom-up) during their service lives. It is noted the concrete layer thicknesses of standard and long-life sections were very similar (or the same in the case of US-131) and no transverse cracking was predicted for the standard section as well. The IRI values exhibited a significant difference in I-69 (standard versus long-life). This was because of a combination of reasons such as larger dowel diameter, lower CTE, JPCP thickness, and differences in lower layers properties. Among all these, dowel diameter was the most influencing factor, and it is recommended to use a dowel diameter of 1.5" or higher in long-life pavements.

One observation regarding the US 131 project is that there was not much difference between the standard and long-life sections. The differences were mainly on the base/subbase/subgrade layer properties and thicknesses, which did not make significant difference on the predicted performances of standard and long-life sections. The PCC thicknesses were the same (10.5"),") and 1.5" diameter dowel was used in both standard and long-life sections. Both of these parameters are significant inputs to the Pavement ME analyses. In fact, standard section was predicted to perform exceptionally well (50-year design life without any preventive maintenance), although it was supposed to be designed to last 20 years (without any preventive maintenance). The team did not have access to the original design files for the standard sections of the US-131 rigid pavements.

Another observation regarding the long-life sections of US-131 (50-year design) and I-69 (30-year design) is that their cross sections were very similar and predicted performances by Pavement ME were similar. It appears I-69 may be overdesigned in terms of structural design because both US-131 and I-69 were predicted to last more than 50 years (by Pavement ME). However, historically, the main problem in Michigan is joint spalling. Therefore, the real life difference between I-69 and US-131 can be due to the joint spalling (which may be seen in the future).

Material improvements

Flexible long-life pavements (I-475 and US-131)

Laboratory dynamic modulus, fatigue, rutting and indirect tensile strength experiments all showed better performance of the GGSP and 4E30 mixtures, over their standard counterparts (5E10 and 3E10). The main reasons for this superior performance are probably the use of the polymer modified binder, limiting the amount of recycled materials and high film thickness

(>9microns) in GGSP and 4E30. Another reason could be the use of higher quality aggregates that are specified in E30 and GGSP mixtures. In future long-life projects, in surface layer, it is strongly recommended to use polymer modified binder, limit the RAP/RAS to Tier 1, and specify high film thickness (>9microns)

In RITF report, it was recommended to have fines/effective binder ratio < 1.2. However, the GGSP performed exceptionally well in lab tests (fatigue, rutting, and low-temperature cracking) even though its fines/effective binder ratio was greater than 1.2. Therefore, this RITF report recommendation probably does not apply to GGSP (or similar Stone Matrix Asphalt) mixtures.

Rigid long-life pavements (I-69 and US-131):

In the RITF report, the use of 20-40% supplementary cementitious materials (SCMs) were recommended and in both long-life projects, 30% SCM was used. The SCM was used in both standard and long-life sections, so its effect could not be quantified. On the other hand, the slag was used as SCM in US-131, and fly ash was used in some parts of I-69. Durability tests revealed potential concerns for the concrete material from I-69, which may be due to the fly ash. Therefore, it is preferrable to use slag as SCM instead of fly ash in future long-life projects. However, this observation is based on limited set of data and more research is needed to investigate the true effects of different kinds of SCMs on the concrete performance.

Construction-related improvements

Flexible long-life pavements (I475 and US-131):

In-place HMA density was recommended in the RITF report to be greater than 93% Gmm. This was achieved in all layers of I-475 but only leveling and base layers of US-131. The top GGSP layer had an in-place density of 91.6% (i.e., air voids of 8.4%) on average. It is recommended to monitor the performance of the top GGSP layer in US-131 and potentially consider one of the pavement preservation treatments (e.g., spray-on rejuvenator, micro-surfacing, etc.) to minimize the potential effect of high air voids.

It appeared that sufficient joint density was achieved in both I-475 and US-131 projects, probably because of the echelon paving of the surface (GGSP) layer. Echelon paving of the surface layer is strongly recommended to be implemented in future long-life projects.

Designing outside lane at 14 ft instead of 12 ft would potentially have increased wheel wander standard deviation and reduce the rate of damage accumulation. However, the impact of wheel wander standard deviation in Pavement ME simulation results is not very significant (see Figure 100 and Figure 101). Therefore, the wider outside lane is probably not needed. So, keeping the I-475 and US-131 pavement lanes 12' wide was a good decision.

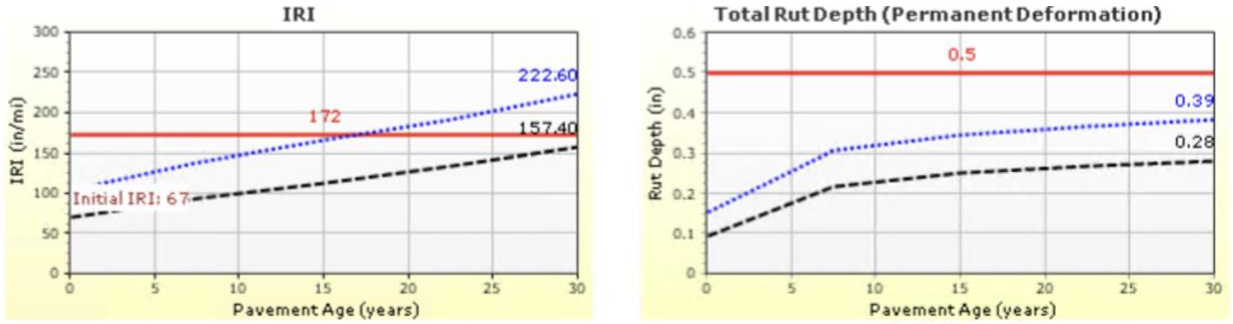

Figure 100. STR1-long-life-TS1: wheel wander standard deviation = 10"

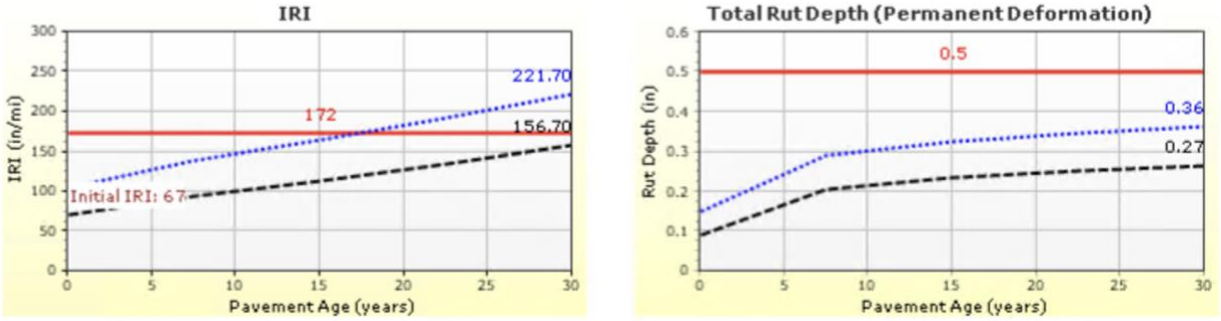

Figure 101. STR1-long-life-TS1: wheel wander standard deviation = 20"

Intelligent compaction was not used in any of the projects. Intelligent compaction would have probably reduced the variability of in-place air voids. In I-475 and US-131 projects, coefficient of variation (COV = standard deviation/mean) of core air voids ranged from 9% to 21%. While these COV values are not very large, potentially lower COV of air voids (i.e., more uniformity) could have been achieved with intelligent compaction.

Rigid long-life pavements (I-69 and US-131):

The RITF report had recommended an initial IRI less than 65 in/mile and 55 in/mile for 30-year and 50-year design long life pavements. However, this was not achieved where the average IRI was 71 in/mile and 72 in/mile for I-69 and US-131, respectively. It is important to mention that these projects were subject to the MDOT's standard ride quality requirements.

QC/QA improvements for both flexible and rigid long-life pavements

The RITF report recommended tightening Percent Within Limits (PWL) requirements for QC/QA testing. For long life pavements, it was recommended to specify remove/replace when PWL<75 and when PWL<90 for 30- and 50-year design, respectively. Although this was not done in these projects and MDOT's standard PWL specs were used, QC/QA data reviewed by the team did not lead to a specific concern regarding the QC/QA data.

Initial Costs

The initial costs per mile of the long-life pavements and their standard counterparts are shown in Table 67. As shown, based on cross-section cost only, long-life pavements were more expensive by 27.2% to 59.4%. However, focusing on cross-section costs may be misleading. Based on the total project cost (per lane mile), the difference ranged from 6.6% to 15.5%. Total project

cost can be considered cross-section costs plus the "other costs" needed to construct that cross section. Since a pavement cannot be constructed without the "other costs", "other costs" will be paid regardless of whether long-life or standard cross sections are selected. Since the "other costs" are quite significant, selecting a long-life cross-section over a standard cross-section does not change the overall cost significantly.

Table 67 also shows the expected lives without maintenance (fix life) based on Pavement ME simulations. As shown, the difference in expected life is significantly higher than the difference in the total project costs. Therefore, long-life pavements are expected to be more cost-effective than the standard counterparts. An accurate life cycle cost analysis cannot be performed because of a lack of actual performance data, when the maintenance treatments would be applied to these pavements, and how those treatments would extend their lives.

Table 67. Long-life pilot projects initial costs per lane mile

Project	Design (yr.)	Cross-Section Cost1	% Difference (Cross-Section Cost1)	Total Project Cost2	% Difference (Total Project Cost)	Expected Life Pavement ME* (yr.)	% Difference (Expected Life)
US-131 30 Year HMA	20	$436,550	42.5%	$1,338,765	13.9%	27	22.2%
	30	$622,195		$1,524,410		33	
I-69 30 Year Concrete	20	$514,836	59.4%	$1,973,633	15.5%	18	177.8%
	30	$820,829		$2,279,626		50	
I-475 50 Year HMA	20	$510,354	59.3%	$1,892,846	16.0%	26	42.3%
	50	$812,875		$2,195,367		37	
US-131 50 Year Concrete	20	$565,857	27.2%	$2,335,515	6.6%	52	21.2%
	50 A3	$720,015		$2,489,673		63	
	50 B3	$796,107	40.7%	$2,565,765	9.9%	-	-

Notes: All costs are per lane-mile of mainline pavement and are from the as-bid results using the bid amounts for the winning bidder.

It should be noted that these cost increases are project specific and should not be used for network analysis. For example, specification enhancements that resulted in increased costs may vary from contractor to contractor depending on their material sources, quality control measures, etc. In particular, the total project costs can vary significantly from project to project depending on the full scope of work involved for each project. Furthermore, the actual performance life of these long-life pavements will not be known until sometime in the future and thus we can only assume that the percentage increase in cost will result in longer life pavement.

1 - Cost for the pavement and shoulder cross-section pay items. I-475 is the only one that includes ramps - all other projects built all the ramps as 20-year designs.

2 - Total project costs include everything but pay items for structures work and lane rental bids. Calculated as: Total bid amount - structures bid amount (if part of the contract) - lane rental bid amount (if part of the contract) - total cross-section costs (all designs). This was then divided by total pavement lane miles. This is the "other costs" amount that is then added to each cross-section cost.
3 - 50 yr. design A did not have stabilized subgrade, design B had stabilized subgrade

4 - The expected lives shown in this table are predicted values and it is too early to determine if these are accurate estimates.

Comments on Future Testing

The LWD data did not provide useful information regarding modulus of the layers, therefore, running this test is not recommended. The DCP data provided reasonable results only in certain sections, and in other sections, the DCP results were not useful to derive the modulus of the layers. While these tests may be useful to assess the relative variability at different locations along a project length, they are not very useful to estimate moduli of unbound layers, especially for the purpose of using ME analyses.

FWD backcalculations did provide reasonable moduli, but, because of limitations of existing backcalculation algorithms, sublayer (HMA top, HMA intermediate, HMA base, unbound base, subbase and subgrade, etc.) moduli could not be obtained. Therefore, FWD is also not very useful to obtain moduli of individual sublayers, for the purpose of performing ME analyses. But FWD may be very useful tool to identify the variations on the structural capacity of different spatial locations along a pavement project.

Because of inconsistencies in test results with the LWD, DCP and FWD, MDOT may consider collecting material samples from different layers and perform laboratory testing for characterizing properties of the materials provided on the project. These tests include HMA |E*|, unbound layer M_R, concrete compressive strength, modulus of rupture and CTE. Alternatively, FWD testing protocol and data analysis methodology could be improved to obtain layer moduli that are more consistent with the laboratory measurements.

REFERENCES

1. Newcomb, D. *Perpetual Pavements - A Synthesis*. 2002.
2. Ferne, B., *Long-life pavements—a European study by ELLPAG.* International Journal of Pavement Engineering, 2006. **7**: p. 91-100.
3. Association, E.A.P., *Long-Life Asphalt Pavements–Technical version*. 2007, Belgium.
4. Hall, K., et al., *Long-life concrete pavements in Europe and Canada*. 2007.
5. Mahoney, J.P., *Study of long-lasting pavements in Washington State.* Transportation Research Circular, 2001. **503**: p. 88-95.
6. Tarefder, R.A. and D. Bateman, *Design of optimal perpetual pavement structure.* Journal of transportation engineering, 2012. **138**(2): p. 157-175.
7. Romanoschi, S.A., et al., *First findings from the Kansas perpetual pavements experiment.* Transportation Research Record, 2008. **2068**(1): p. 41-48.
8. St Martin, J., et al., *Long-life rehabilitation design and construction: I-710 Freeway, Long Beach, California.* Transportation Research Circular, 2001(503).
9. Thompson, M.R. and S.H. Carpenter. *Considering hot-mix-asphalt fatigue endurance limit in full-depth mechanistic-empirical pavement design*. in *Proc., International Conference on Perpetual Pavement*. 2006. Citeseer.
10. Timm, D.H. and D.E. Newcomb, *Perpetual pavement design for flexible pavements in the US.* International Journal of Pavement Engineering, 2006. **7**(2): p. 111-119.
11. Walubita, L.F. and T. Scullion, *Texas perpetual pavements: new design guidelines*. 2010, Texas Transportation Institute.
12. Tayabji, L. and S. Lim, *Long Life Concrete Pavements: Best Practices and Directions from the States*. 2007, Washington: Federal Highway Administration US Department of Transportation.
13. Harm, E., *Illinois extended-life hot-mix asphalt pavements.* Transportation Research Circular, 2001. **503**: p. 108-112.

14. Newcomb, D.E., M. Buncher, and I.J. Huddleston, *Concepts of perpetual pavements.* Transportation Research Circular, 2001. **503**: p. 4-11.
15. Bleech, C., *Roads Innovation Task Force Report*. 2016, Michigan Department of Transportation.
16. Rupnow, T.D. and P.J. Icenogle, *Surface resistivity measurements evaluated as alternative to rapid chloride permeability test for quality assurance and acceptance.* Transportation research record, 2012. **2290**(1): p. 30-37.
17. Tanesi, J. and A. Ardani, *Surface resistivity test evaluation as an indicator of the chloride permeability of concrete*. 2012, United States. Federal Highway Administration.
18. Vennapusa, P.K. and D.J. White, *Comparison of light weight deflectometer measurements for pavement foundation materials.* Geotechnical Testing Journal, 2009. **32**(3): p. 1-13.
19. Seitllari, A. and M. Kutay, *Development of 3-point bending beam fatigue test system and implementation of viscoelastic continuum damage (VECD) theory.* Journal of the Association of Asphalt Paving Technologists, 2019. **88**: p. 783-810.
20. Seitllari, A., M. Hasnat, and M.E. Kutay, *Development of Three Point Bending Cylinder (3PBC) Asphalt Mixture Fatigue Test System*. 2022.
21. Kim, Y.R., H.-J. Lee, and D.N. Little, *Fatigue characterization of asphalt concrete using viscoelasticity and continuum damage theory (with discussion).* Journal of the Association of Asphalt Paving Technologists, 1997. **66**.
22. Kutay, M.E., N.H. Gibson, and J. Youtcheff, *Conventional and viscoelastic continuum damage (VECD)-based fatigue analysis of polymer modified asphalt pavements (with discussion).* Journal of the Association of Asphalt Paving Technologists, 2008. **77**.
23. Kutay, M.E. and M. Lanotte, *Viscoelastic continuum damage (VECD) models for cracking problems in asphalt mixtures.* International journal of pavement engineering, 2018. **19**(3): p. 231-242.
24. Buch, N. and S. Jahangirnejad, *Quantifying coefficient of thermal expansion values of typical hydraulic cement concrete paving mixtures*. 2008, Michigan. Dept. of Transportation. Construction and Technology Division.
25. Chung, Y. and H.-C. Shin, *Characterization of the coefficient of thermal expansion and its effect on the performance of Portland cement concrete pavements.* Canadian Journal of Civil Engineering, 2011. **38**(2): p. 175-183.
26. Witczak, M.W., *Harmonized test methods for laboratory determination of resilient modulus for flexible pavement design* 2003.
27. Witczak, M.W., et al., *Laboratory Determination of Resilient Modulus for Flexible Pavement Design*. 2004: Transportation Research Board.
28. Nazarian, S., et al., *Evaluating mechanical properties of earth material during intelligent compaction*. 2020.
29. Walls, J. and M.R. Smith, *Life-cycle cost analysis in pavement design: Interim technical bulletin*. 1998, United States. Federal Highway Administration.
30. Zimmerman, K.A., K.D. Smith, and M.G. Grogg, *Applying economic concepts from life-cycle cost analysis to pavement management analysis.* Transportation research record, 2000. **1699**(1): p. 58-65.
31. Chan, A., G. Keoleian, and E. Gabler, *Evaluation of Life-Cycle Cost Analysis Practices Used by the Michigan Department of Transportation.* Journal of Transportation Engineering, 2008. **134**(6): p. 236-245.

32. Rangaraju, P.R., S. Amirkhanian, and Z. Guven, *Life cycle cost analysis for pavement type selection*. 2008.
33. Ang, A.H. and W.H. Tang, *Probability concepts in engineering planning and design, basic principles*. Vol. 1. 1975: John Wiley & Sons Incorporated.
34. Zayed, T.M., L.-M. Chang, and J.D. Fricker, *Life-cycle cost analysis using deterministic and stochastic methods: Conflicting results.* Journal of Performance of Constructed Facilities, 2002. **16**(2): p. 63-74.
35. Tighe, S., *Guidelines for Probabilistic Pavement Life Cycle Cost Analysis.* Transportation Research Record, 2001. **1769**(1): p. 28-38.
36. FHWA, *Life cycle cost analysis in pavement design-interim technical bulletin*. 1998, FHWA.
37. MDOT, *Pavement Selection Manual*. 2021, Michigan Department of Transportation.